Identifying Novel Mediators of Adipose Tissue and Skeletal Muscle Crosstalk and Their Role in Mediating Muscle Metabolic Phenotype and Insulin Sensitivity

By

Thomas Andrew Nicholson

A Thesis Submitted to the University of Birmingham for the Degree of DOCTOR OF PHILOSOPHY

Supervisors

Dr Simon Wyn Jones

Dr Leigh Breen

Dr Christopher Church

Dr David Baker

Institute of Inflammation and Ageing

College of Medical and Dental Sciences

University of Birmingham

February 2020

Abstract

Type II diabetes is a chronic metabolic disorder that carries a significant and increasing economic burden. Unfortunately, there is no cure for type II diabetes and treatments are limited. Adipose tissue cross talk with skeletal muscle and adipose-secreted cytokines (adipokines) have been implicated in driving skeletal muscle insulin resistance typical of type II diabetes; although this is largely based on evidence from animal models and rodent cell lines.

The aim of this thesis was to investigate the role of novel adipose/skeletal muscle cross talk mechanisms in mediating human skeletal muscle insulin signalling. This thesis demonstrates that the novel adipokine vaspin is secreted from human subcutaneous adipose tissue, and is more highly expressed in obese older individuals compared to lean older individuals. Furthermore, using primary human myotubes derived from lean and obese donors, vaspin was demonstrated to induce activation of the PI3K/AKT axis, promote both GLUT4 expression and translocation, and sensitise older obese human skeletal muscle to insulin-mediated glucose uptake.

This thesis also presents the first evidence of differential secretion of extracellular vesicles from lean and obese subcutaneous adipose tissue. Such vesicles were capable of increasing skeletal muscle inflammation, in addition to upregulating both atrophic and metabolic skeletal muscle gene expression, supporting the notion that extracellular vesicles are novel mediators of adipose tissue and skeletal muscle crosstalk in humans.

Acknowledgements

First and foremost I would like to thank every person who volunteered to take part in this study, as without them I would not be writing this acknowledgements section. On a similar note, I would like to express my gratitude to the BBSRC and Medimmune for funding this PhD. Next, I have to thank my supervisors; Dr Simon Jones, Dr David Baker and Dr Christopher Church for all their support, advice and encouragement throughout this project. I would like to extend a special thankyou to Simon for all his time, patience and guidance over the years. I couldn't have asked for a better supervisor- if not just to laugh at your stories of misfortune and injuries.

I would also like to thank all the members of the Jones Group, past and present. Especially Dr Mary O'Leary, for teaching me pretty much everything I know in the lab. Although you did terrify me at first, I will be forever grateful. Throughout my PhD, I have also been lucky enough to share a lab with the Lord Group. Jon, Rob, Kirsty, Sam, Ahsan, Hema, Jack, Josh and Christos 'The Greek Stallion' Ermogenous, thank you for all your help and more importantly, the laughs and Jokes that made each day enjoyable (excluding the many times I was ambushed with 'are you ok to give me some blood', before sitting down at my desk in the morning). A special mention must go to Dr Jon Hazeldine, who has been like an extra supervisor during this PhD. Thanks for your endless help in and out of the lab and I look forward to bombarding you with WhatsApp messages in the years to come.

Closer to home, Mom, Dad, Grandma, Grandpa and Joe, thank you for everything. I definitely would not have got to this point, or be the person I am today without you. Thank you for all the sacrifices you have made to give me the best life possible and more importantly, instilling self-belief in me. Grandpa, you've shown me that no matter where you start, you can accomplish anything as long as you're determined and willing to work hard enough and reminding myself of this has helped me no end during these last few years. Finally, thank you to my girlfriend Hollie. You have been a constant

source of love and support and now I don’t know what I’d do without you. Thank you for always making me laugh and reminding me that on the days when Western blots don’t work, there is still a life full of fun and adventure outside the lab.

For Grandma and Grandpa

Publications arising during the completion of this thesis

Nicholson T, Church C, Baker DJ, Jones SW. The role of adipokines in skeletal muscle inflammation and insulin sensitivity. J Inflamm (Lond). 2018; 15:9.

Nicholson T, Church C, Tsintzas K, Jones R, Breen L, Davis ET, et al. Vaspin promotes insulin sensitivity of elderly muscle and is upregulated in obesity. J Endocrinol. 2019; 241:1.

Pearson MJ, Herndler-Brandstetter D, Tariq MA, **Nicholson TA**, Philp AM, Smith HL, et al. IL-6 secretion in osteoarthritis patients is mediated by chondrocyte-synovial fibroblast cross-talk and is enhanced by obesity. Sci Rep. 2017; 7(1): 3451.

O'Leary MF, Wallace GR, Davis ET, Murphy DP, **Nicholson T**, Bennett AJ, et al. Obese subcutaneous adipose tissue impairs human myogenesis, particularly in old skeletal muscle, via resistin-mediated activation of NFkappaB. Sci Rep. 2018; 8(1): 15360.

Murphy DP, **Nicholson T**, Jones SW, O'Leary MF. MyoCount: a software tool for the automated quantification of myotube surface area and nuclear fusion index. Welcome Open Res. 2019; 4:6.

Pearson MJ, Philp AM, Haq H, Cooke ME, **Nicholson T**, Grover LM, et al. Evidence of Intrinsic Impairment of Osteoblast Phenotype at the Curve Apex in Girls With Adolescent Idiopathic Scoliosis. Spine Deform. 2019;7(4): 533-42.

Awards

Best Poster presentation**.** Federation of European Physiological Societies. Vienna, 2017.

Table of Contents

List of Figures

Chapter 1

Chapter 2

Chapter 3

Chapter 4

Chapter 5

Chapter 6

List of Tables

Chapter 1

Chapter 2

Chapter 4

List of Abbreviations

°C	Degrees Celcius
μM	Micromolar
4EBP-1	Eukaryotic translation initiation factor 4E-binding protein 1
ADP	Adenosine diphosphate
AKT	Protein kinase B
AMPK	5' AMP-activated protein kinase
AS160	AKT substrate of 160 kDa
ATP	Adenosine triphosphate
BAT	Brown adipose tissue
BMI	Body mass index
CCL2	Chemokine ligand 2
CEBPA/B	CCAAT Enhancer Binding Protein α/β
CMKLR1	Chemokine like receptor 1
COA	Coenzyme A
Ct	Cycle threshold
DAG	Diacylglycerol
DGK	Diacylglycerol kinase
DMSO	Dimethyl sulfoxide
eIF4E	Eukaryotic translation initiation factor 4E
ELISA	Enzyme-linked immunosorbent Assay
EV	Extracellular Vesicle
EWAT	Epididymal white adipose tissue

FA-1	Foetal antigen 1
FABP4	Fatty acid binding protein 4
FACS	Fluorescence activated cell sorting
FAS	Fatty acid synthase
FBP1	Fructose bisphosphatase 1
FBS	Foetal bovine serum
FFA	Free fatty acid
FGF-21	Fibroblast growth factor 21
FOXO	Forkhead box protein O
FOXO1	Forkhead box protein O1
FSTL1	Follistatin-related protein 1
GAP	GTPase-activating protein
GDP	Guanosine diphosphate
GEF	Guanine nucleotide exchange factor
GPCR	G-protein coupled receptor
GSK3ß	Glycogen synthase kinase 3 beta
GTP	Guanosine triphosphate
HGF	Hepatocyte growth factor
HIF1A	Hypoxia inducible factor 1
HIIT	High intensity interval training
IF	Immunofluorescence
IFN	Interferon gamma
IGF-1	Insulin-like growth factor 1
IKKβ	IκB-kinase-β
IL	Interleukin

IL-15	Interleukin 15
IL-1β	Interleukin 1 beta
IL-6	Interleukin 6
IL-8	Interleukin 8
IMAT	Intramuscular adipose tissue
IMCL	Intramyocellular lipid
IR	Insulin resistance
kg	Kilogram
l	Litre
LAT1	Large neutral amino acid transporter
LDL	Low density lipoprotein
LNC14	Lipocalin 14
m	Metre
MAFbx	Muscle atrophy F-box protein
MCP-1	Monocyte chemoattractant protein 1
MHC	Myosin Heavy Chain
mmol	Millimolar
MPS	Muscle protein synthesis
mTORC1	Mammalian target of rapamycin complex 1
MTORC2	Mammalian target of rapamycin complex 2
MuRF-1	Muscle RING finger 1 protein
MYF5	Myogenic factor 5
MyoD	Myogenic differentiation 1 protein
NFκB	Nuclear factor-κB
nM	Nanomolar

NTC	Non targeting control
OLETF	Otsuka Long-Evans Tokushima Fatty
OP	Obese prone
OR	Obese resistant
p38	MAPK p38 mitogen-acivated protein kinases
P70S6K	Ribosomal protein S6 kinase beta-1
PAT1	Proton-Assisted amino acid transporter
PAX3	Paired box protein 3
PAX7	Paired box protein 7
PBS	Phosphate-buffered saline
PCG-1α	Peroxisome proliferator-activated receptor gamma coactivator 1-alpha
PDK1	Pyruvate Dehydrogenase Kinase 1
PI3k	Phosphoinositide 3-kinase
PKB	Protein kinase B
PKC	Protein kinase C
PPARδ	Peroxisome proliferator-activated receptor delta
PREF-1	Preadipocyte factor 1
PVDF	Polyvinylidene difluoride
RER	Rough endoplasmic reticulum
RHEB	Ras homolog enriched in brain
RIPA	Radioimmunoprecipitation assay buffer
RNA	Ribonucleic acid
ROS	Reactive oxygen species
RT	Resistance training
SAT	Subcutaneous adipose tissue

SDS	Sodium dodecyl sulphate
SDS PAGE	SDS polyacrylamide gel electrophoresis
SHC	SHC homology
siRNA	Small interfering RNA
SNAT2	Sodium-coupled neutral amino acid transporter 2
SREBP1	Sterol regulatory element-binding protein 1
SREBP2	Sterol regulatory element-binding protein 2
SUnSET	Non-Radioactive Surface Sensing of Translation
SWAT	Subcutaneous white adipose tissue
T2D	Type II diabetes
TAG	Triacylglycerols
TBS-T	Tris buffered saline with Tween 20
TMB	Tetramethylbenzidine
TNFα	Tumour necrosis factor alpha
Tris-HCL	Tris hydrochloride
TSC1/2	Tuberous sclerosis complex 1/2
UCP1	Uncoupling protein 1
UDP	Uridine diphosphate
UK	United Kingdom
ULK-1	Unc-51 like autophagy activating kinase
USF	Upstream stimulatory factor 1
ZDF	Zucker diabetic fatty

CHAPTER 1: Introduction

1.1 General Introduction

Improved healthcare systems, living conditions and vaccinations, coupled with a decline in birth rates have resulted in an ageing population within many developed countries. In the UK, 18% of the population were aged 65 or older in 2016. Over the next 50 years this demographic is predicted to increase to 26% of the population, equating to an additional 8.6 million people. Greater increases still are expected in older age groups, with the number of residents over 85 expected to increase 3-fold over the same time period (1). Importantly such increases in lifespan do not directly correlate with increases in health span, as highlighted by the UK average healthy life expectancy being just 65, despite an average life expectancy of approximately 80 (2). Consequently, many elderly individuals are living with chronic, age-associated morbidities such as coronary artery disease, arthritis, chronic kidney disease, sarcopenia and diabetes during the last decades of life. Not only does this have an impact on the person's quality of life, it is likely to have a considerable future economic impact, with a proportionally reduced workforce having to fund an increased cost of healthcare (3). Additionally, decreased physical activity and alterations in metabolism typically lead to an accumulation of adipose tissue mass with age, particularly in countries with a Western diet (4-6). As a result, there is a significant positive association between age and the proportion of the population that are over-weight (having a body mass index (BMI) greater than 25 kg/m^2) and importantly, clinically obese (BMI >30 kg/m^2) (7).

Critically, the prevalence of obesity is becoming worryingly high. The World Health Organisation (WHO) estimated that, globally; 300 million people were clinically obese in 2005 (8). By 2016, revised estimates indicated that this figure had risen to 650 million adults worldwide, which equates to approximately 10% of the global population (8). In the UK, the most recent Government statistics indicated that 63% of adults and 28% of children aged 2-15 were overweight or obese in 2015 (9).

Obesity is associated with increased mortality and the development of a number of diseases including cancer (10), osteoarthritis (11), chronic obstructive pulmonary disease (12), obstructive sleep apnoea (13) and type 2 diabetes (T2D).

Over 3 million people in the UK were living with T2D in 2014 (4.5% of the total population) (14) and it is estimated that between 2010 and 2011 T2D cost the NHS £21.8 billion (15). If diagnosis and treatment options remain unchanged, it is projected that this cost will increase to £35.6 billion by 2035-2036 (15). To put this into perspective, the annual spend on the treatment of T2D in the UK is currently greater than the budgets for the police, judicial system and fire service combined (9). Therefore, T2D is a significant problem that carries a growing economic burden, particularly in developed countries (9, 16).

It is now known that skeletal muscle is responsible for the majority of insulin stimulated glucose uptake in humans (17). Therefore, skeletal muscle is not only central to the regulation of blood glucose in healthy individuals, but is also the primary site of insulin resistance in individuals presenting with T2D. As a result, significant efforts have been made to determine how increasing adiposity impacts skeletal muscle function, in order to better understand the causal link between obesity and the development of T2D. Ultimately, such mechanistic knowledge is critical for the identification of novel targets for therapeutic intervention.

1.2 Skeletal muscle structure and function

1.2.1 Skeletal muscle function

Skeletal muscle is the most abundant tissue type in the human body, accounting for approximately 40-50% of total body mass and up to 75% of total body proteins in adults (18). Primarily, skeletal muscle facilitates voluntary movement and locomotion via the contraction and relaxation of antagonistic muscle pairs, innervated by the somatic nervous system. Additionally, skeletal muscle has important autonomic functions such as facilitating spontaneous breathing, via innervation of the diaphragm by cervical nerves 3-5 (19) and providing postural support, through contraction of muscles such as the lumbar multifidus, which runs along the spine (20). Skeletal muscle also provides important physical protection of vital internal organs and is central to thermoregulation, contracting involuntarily to enable shivering when cold (21). Importantly, recent evidence has also demonstrated that skeletal muscle secretes a plethora of cytokines (myokines), thereby establishing skeletal muscle as a vital endocrine organ, regulating numerous whole body functions through tissue crosstalk, particularly following exercise (22).

Adult skeletal muscle is a very plastic tissue and responds rapidly to exercise and dietary nutrients to increase in size (hypertrophy), force production and aerobic capacity, ultimately leading to increased performance. On the other hand, disuse of skeletal muscle leads to rapid muscle wasting (atrophy). Indeed, it appears that as little as 5 days of bed rest can result in a significant loss on skeletal muscle mass of around 4%, which translates to a decline in skeletal muscle strength of 9% (23). Following longer time periods, this trend continues, with 2 weeks of muscle disuse causing a loss of isometric strength of approximately 30% (24). Such disuse atrophy has been shown to be a predictor of morbidity, particularly following hospitalisation and therefore has significant implications for patient outcome, especially for the elderly and those with debilitating conditions such as cancer and traumatic injury (25, 26).

1.2.1 Skeletal muscle structure

Embryonically, skeletal muscle begins do develop from the mesoderm by 10-13 weeks of gestation, with mature structures typically observed by 25 weeks (27). In adult humans, the organisation of skeletal muscle is complex and the exact number of individual skeletal muscles is not definitive, with estimations ranging from 520 -700 muscles.

Skeletal muscles are composed of many individual skeletal muscle fibres (Figure 1.1). A skeletal muscle fibre (myofiber) is formed when muscle cells (myocytes) fuse, forming multinucleated structures that are typically between 10-100 µm in diameter and around 3 cm in length, but remarkably may reach up to 40 cm in the case of the satorious muscle (28). Each individual myofibre is surrounded by a basement membrane (endomysium) consisting of an inner basal lamina which has direct contact with the skeletal muscle fibre's sarcolemma and an outer reticular lamina (29). This structure is predominantly formed of laminins and type IV collagen and plays an important role in myogenesis, the protection and maintenance of myofibre structure and facilitating regeneration following injury by acting as a scaffold (29).

Furthermore, bundles of individual skeletal muscle fibres are surrounded by the perimysium, a collagenous (predominantly thought to be type I collagen) structure, forming a fascicle (30). In turn, multiple fascicles are themselves surrounded by an epimysium, formed from a mix of large bundles of collagens type I and III and this collectively forms a muscle (Figure 1.1) (30). Finally, the endomysium, perimysium and epimysium extend beyond muscle fibres forming tendons, facilitating the muscle-bone connection.

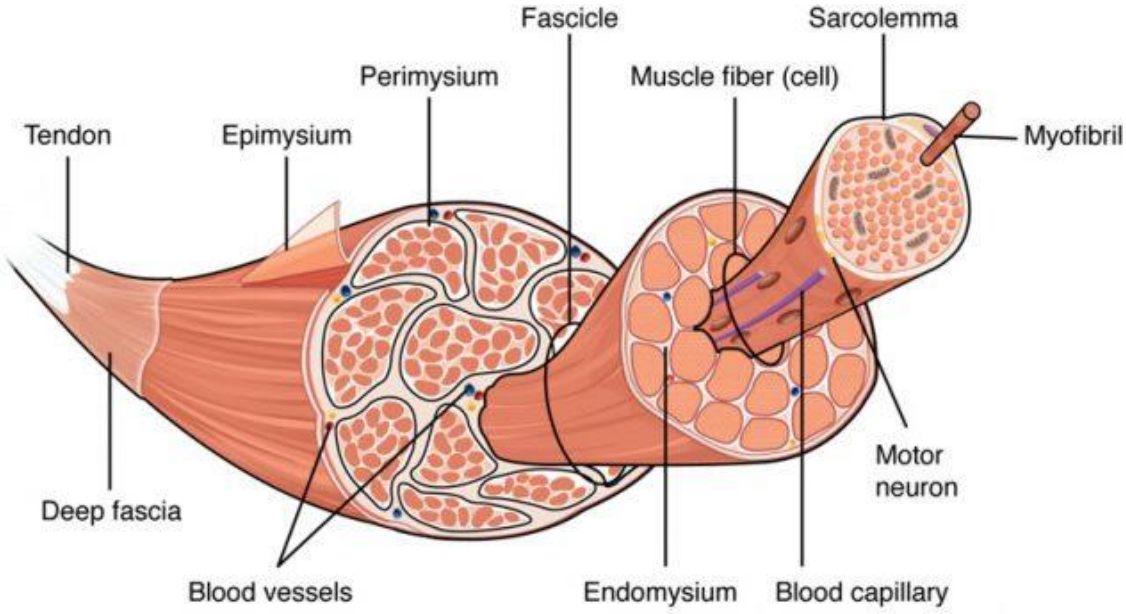

Figure 1. 1. Skeletal muscle structure.

Multiple skeletal muscle cells (myocytes) fuse to form a multinucleated muscle fibre, each enclosed by the endomysium. Muscle fibres are collectively bundled together by the perimysium, forming a fascicle. Fascicles are encapsulated by the outermost epimysium forming the complete muscle fibre structure. Skeletal muscle fibres are innervated by motor neurones and have an extensive capillary network. Image adapted from Betts et al (31).

Importantly, skeletal muscle also has a population of satellite cells, located between the muscle plasma membrane and the basal lamina (32), identifiable by a number of cell surface markers, with paired box proteins 7 (Pax7) (present in both quiescent and proliferative states) typically the most specific (33). These are skeletal muscle specific stem cells, capable of differentiation into mitotic muscle cells termed myoblasts. In turn, myoblasts fuse generating new myofibres, allowing regeneration of skeletal muscle following injury.

Activation of quiescent satellite cells from the G_0 stage of the cell cycle is multifaceted. Firstly, physical damage (e.g. injury) results in disruption of the basal lamina which consequently frees satellite cells via disruption of α7/β1 integrin mediated adhesion and thus increases their mobility (34, 35). Additionally, damage to the extracellular matrix also causes release of hepatocyte growth factor (HGF) from extracellular matrix proteins including versican, fibrillin-2, and glypicans (36). Furthermore, damage to muscle fibres and blood vessels, coupled with infiltration of macrophages, B-cells and T-cells leads to the additional release of nitric oxide and cytokines, including Interleukin-6 (IL-6) and Interferon-γ (IFN). Collectively these signalling molecules promote quiescent satellite cells to enter into the cell cycle, leading to commitment to the skeletal muscle cell lineage (35, 37-39).

Initially in this process, the expression of Pax3/7 on satellite cells decreases, which in turn permits the increase of the transcription factor MYF_5 (40). Upregulation of MYF_5 is followed by upregulation of the additional transcription factors; myogenic regulatory factor 4 (MRF4), MyoD and myogenin. Evidence suggests that following MYF_5 upregulation, the order in which the expression of subsequent myogenic factors increase is not critical. Indeed these factors appear to possess the ability to activate each other, indicating the presence of redundancy (41). Ultimately the activation of these transcription factors in turn induces the upregulation of a plethora of muscle specific genes and thus commitment to the skeletal muscle cell lineage (42).

1.2.3 Skeletal muscle fibre types

Human skeletal muscle fibres can be sub-classified as either type I (slow twitch) or type II (fast twitch) based on their myosin heavy chain (MHC) expression (Table 1.1). Type I fibres contract slowly, with little force, but have a high resistance to fatigue as they primarily depend on oxidative phosphorylation. In contrast, type II fibres contract quickly and with greater force, but rapidly fatigue due to being heavily reliant on anaerobic glycolysis (43).

Type I fibres appear red in colour due to having a dense capillary network and high myoglobin content necessary to support oxidative phosphorylation. Conversely, type II fibres have a lower oxygen demand and so have less myoglobin and a smaller capillary network, pertaining to a white appearance. Human type II fibres can be further divided into type II A and type II X, depending on MHC gene expression (Table 1.1), while it has also become apparent that some fibres co-express different isoforms of MHC, giving rise to intermediate or hybrid fibres (44). Therefore it is now apparent that a spectrum of fibre types exists, with the proportion of each in a muscle group determining its functional ability. For example, muscles with a high proportion of type I fibres better facilitate endurance exercise, while greater heterogeneity of type II fibres enables explosive movements such as sprinting (45).

Due to the plastic nature of skeletal muscle, muscle fibre types can shift, to an extent, in response to regular training, leading to either increased muscular endurance or power (46). Additionally, different disease states often associate with the loss of specific fibre types. For example, elderly individuals with sarcopenia primarily present with a loss of type II fibres, while chronic obesity or muscle unloading following injury is primarily associated with type I fibre atrophy (47-49). Recent evidence also suggests that such specific fibre type loss may differentially impact whole body metabolism, with type I fibre atrophy having a greater association with reduced insulin sensitivity (50).

Fibre type	Speed of contraction	Metabolism	MHC Isoform	Myosin gene
I	Slow	Oxidative	MHC-I	MYH7
IIA	Fast	Oxidative/glycolytic	MHC-II	MYH2
IIX	Fast	Glycolytic	MHC-II	MYH1

Table 1. 1 Characteristics of the main human skeletal muscle fibre types

1.3 The role of insulin and skeletal muscle in glucose homeostasis

1.3.1 The mechanism of insulin production

In a healthy individual, plasma glucose is maintained within the range of 4.0-6.1 mmol/L. If blood glucose is elevated, for example following a meal, glucose uptake in various cell types increases. Glucose uptake is a process driven by the hormone insulin, a 5.8 KDa anabolic peptide hormone. In response to elevated plasma glucose, beta cells of the pancreas secrete insulin into the blood, which is then able to bind to its complementary insulin receptor in target tissues, initiating the insulin signalling pathway (51). Importantly, approximately 20% of intracellular insulin is transported along a microtubule network in order to associate with the cell membrane. Thus, beta cells are primed for rapid insulin release when stimulated (52).

The Initial step in the production of insulin involves the translation of the insulin gene *INS,* resulting in the production of preproinsulin. Next, a signal sequence present on preproinsulin is cleaved in the rough endoplasmic reticulum (RER) to produce proinsulin. Then, semi-helical A and helical B domains of proinsulin are linked via disulphide bonds, stabilising its structure. Finally, in the Golgi apparatus, the enzymes prohormone convertase 1/3 and prohormone convertase 2 cleave a c-peptide chain which links the A and B domains of proinsulin, generating the final insulin structure.

Intracellular insulin couples to Zn^{2+} resulting in the formation of hexameric crystal structures which are predominantly stored in cytoplasmic granules, of which there are approximately 10,000 per β-cell (53, 54). This is a very efficient and swift production process, with up to 99% of translated RNA yielding mature insulin protein molecules, within approximately 2 hours (53).

1.3.2 The mechanism of insulin secretion

Upon increased extracellular glucose concentrations, glucose diffuses down its concentration gradient into pancreatic β-cells by facilitated diffusion, mediated by membrane spanning GLUT1 channels (55). In turn, uptaken glucose enters the glycolysis pathway, rapidly generating ATP. Subsequently the intracellular ATP:ADP ratio increases, which inhibits membrane ATP-sensitive K^+ channels (56). Inhibition of such channels in turn elicits depolarisation of the β-cell membrane. If depolarisation surpasses a membrane potential of -50 mV, then voltage gated Ca^{2+} channels are activated enabling an influx of Ca^{2+} ions (56). Critically, increased intracellular calcium initiates fusion of the insulin containing granule (described above) with the plasma membrane, resulting in insulin secretion via exocytosis.

In the pancreas, ß-cells are organised into structures called islets. Importantly, it appears that complex communication occurs between ß-cells within an islet and also between islets themselves (57). This allows insulin to be released in controlled, rhythmic waves, at approximately 5 minute intervals (58, 59). It is thought that the purpose of such a phenomenon is to maintain insulin sensitivity in target tissues, by preventing insulin receptor internalisation and down regulation due to a sustained presence of insulin (58). Such intercellular communication appears to be multifaceted; firstly, the protein connexin-36 forms gap junctions between ß-cells, allowing Ca^{2+} transfer and thus depolarisation to rapidly spread throughout adjacent cells (60). Further, paracrine signalling is also likely to be an important regulator of insulin secretion, with ß-cells releasing signalling molecules such as ATP to drive insulin release in surrounding cells (61). Emerging data suggests that insulin secretion may also be regulated by even more sophisticated mechanisms. For example, Johnston et al. recently described a subset of pancreatic ß-cells with pacemaker properties. These cells were demonstrated to function as ‘hubs’, communicating with numerous ‘follower’ cells in order to regulate their insulin release (62). Additionally, Tang et al. recently reported the novel neuronal

innervation of β-cells via 3D histology, suggesting that regulation of insulin release is not just local between adjacent cells and islets, but universal throughout the pancreas (63).

1.3.3 The insulin signalling pathway

The extracellular binding of insulin to the insulin receptor (IR) causes a conformational change in the receptor that enables auto-phosphorylation of intracellular tyrosine domains within its activation loop region. Following phosphorylation of the activation loop, the insulin receptor is further phosphorylated in additional regions, including Tyrosine-960 (64). This provides a site for a family of membrane localised proteins known as insulin receptor substrate (IRS) proteins (IRS1-6) to associate with, forming an IR-IRS complex (64, 65). Numerous other proteins have since been demonstrated to associate with the insulin receptor, including DOCK1 and-2, APS, CBL, GAB1 and SH2B, although such interactions are less well studied. Association of IRS, (predominantly IRS1 and IRS2) with the insulin receptor facilitates phosphorylation of up to 20 residues within their central C-terminal domain. In turn, this allows signalling proteins containing a src-homology 2 (SH2) domain to bind and initiate downstream signalling (66). One such protein is Phosphoinositide 3-kinase (PI3K), which contains 2 regulatory subunits (P55 and P85). Binding of PI3K to IRS results in phosphorylation of these regulatory subunits, which in turn promotes activation of P110, the catalytic subunit of PI3K. Activated PI3K functions to phosphorylate phosphatidylinositol 4,5-bisphosphate (PIP_2), generating phosphatidylinositol-3,4,5-triphosphate (PIP3). PIP3 is localised to the membrane and provides a docking site for the recruitment and activation of Phosphoinositide-dependent kinase-1 (PDK-1), in turn allowing PDK-1 to phosphorylate the threonine-308 (Thr^{308}) residue of protein kinase B (PKB)/AKT, leading to its partial activation. Additional phosphorylation of serine residue-473 (Ser^{473}) within the hydrophobic motif of AKT is needed for its full activation (67). Such phosphorylation is necessary to stabilize Thr^{308} phosphorylation and is mediated by a downstream target of AKT, the

mechanistic target of rapamycin complex 2 (mTORC2), in a positive feedback process (Figure 1.2) (68, 69).

There are 3 known subtypes of AKT, of which AKT2 is reported to have the highest expression in human insulin sensitive tissues such as skeletal muscle. Thus AKT2 is thought to be the most important subtype for transduction of insulin signalling in such tissue types (70). In support of this, Cho et al. demonstrated that AKT2 knock out mice display insulin resistance and a diabetic phenotype, while AKT1 or AKT3 selective knock out mice are unaffected in this regard (71). Critically, AKT acts to phosphorylate various effector proteins causing either upregulation or downregulation of a number of cellular processes (discussed in detail below and depicted in Figure 1.2) and is therefore central to the cellular effects driven by activation of the insulin signalling pathway. Therefore, it is critical that AKT activation is tightly regulated. In order to achieve this, negative feedback mechanisms are initiated following activation of AKT. For example, AKT facilitates activation of mechanistic target of rapamycin complex 1 (mTORC1), in turn, mTORC1 facilitates the dephosphorylation of AKT, via degradation of IRS1/2 (Figure 1.2) (72, 73). Dysregulated AKT activation has been identified as a key driver of many diseases such as cancer (74, 75) immune cell dysfunction, atherosclerosis (76) as well as insulin resistance and T2D (77).

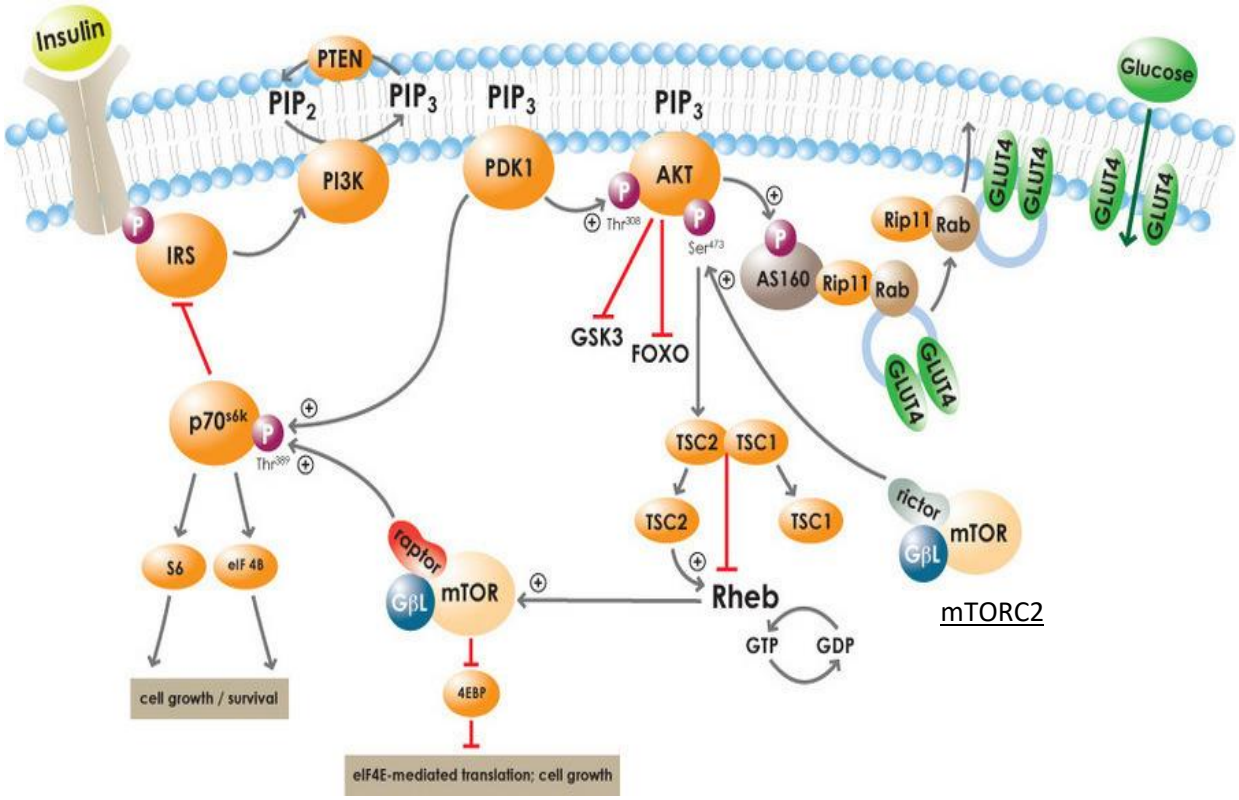

Figure 1. 2. The insulin signalling pathway.

IRS proteins recognise and bind to the activated insulin receptor, resulting in phosphorylation of IRS. Phosphorylated IRS proteins are then able to phosphorylate and activate PI3K. In turn PI3K activation leads to the downstream phosphorylation of AKT (protein kinase B) at 2 sites, namely Thr^{308} and Ser^{473}. In its active form, p-AKT is able to phosphorylate various effector proteins that upregulate a number of cellular processes. Firstly phosphorylation of AS160 mediates insertion of GLUT4 into the plasma membrane and thus glucose uptake, while activation of mTORC1 drives skeletal muscle hypertrophy and regulation of proteins such as GSK3B and FOXO, which modulate cellular metabolism and gene transcription respectively.

Adapted from May, 2005 (78).

1.3.4 The effect of insulin on skeletal muscle glucose uptake

Skeletal muscle is responsible for up to 80% of insulin stimulated plasma glucose uptake in healthy individuals and is therefore critical for the maintenance of glucose homeostasis (17). Insulin stimulated activation of AKT causes increased translocation and insertion of glucose transporter 4 (GLUT4) from intracellular vesicles to the cell membrane. GLUT4 is a protein consisting of 12 transmembrane domains that facilitates the movement of plasma glucose down its concentration gradient into the cell (79). Importantly, only approximately 5% of cellular GLUT4 is localised at the plasma membrane during rest, but increases to around 50% in response to insulin (80).

The trafficking of GLUT4 and insertion into the plasma membrane is a complex process that is yet to be fully elucidated. Current evidence indicates that a target of AKT, the AKT Substrate 160 (AS160), also known by its gene name TBC1D4, plays an important role. AS160 is thought to be a GTPase activating protein (GAP), a family of proteins that act to hydrolyse guanine triphosphate (GTP) bound to Rab proteins (81). Rab proteins have an important role in vesicle trafficking and are active in their GTP bound state (82, 83). Following knockdown of AS160 in 3T3-L1 adipocytes, an up to 6-fold increase in membrane bound GLUT4 is observed, thus in unstimulated conditions AS160 acts to maintain its target Rab protein in an inactive guanine diphosphate (GDP) bound state, holding GLUT4 vesicles within the cytoplasm (84, 85).

Phosphorylation of AS160 inhibits its GTPase function and in turn prevents GTP hydrolysis of Rab proteins (86). The simultaneous exchange of RabGDP for RabGTP mediated by guanine exchange factors (GEFs) promotes a net increase in RabGTP. GLUT4 vesicle associated Rab proteins are now active and free to facilitate translocation of GLUT4 vesicles to the plasma membrane (Figure 1.2) (86, 87). Such a mechanism is demonstrated by overexpression of AS160, which prevents substantial GLUT4 translocation and so limits insulin stimulated GLUT4 translocation and glucose uptake.

Importantly, Consitt et al. demonstrated that insulin stimulated phosphorylation of AS160 in skeletal muscle is negatively associated with insulin sensitivity (88). Similarly, blunted AS160 phosphorylation is reported in the skeletal muscle of subjects with T2D and insulin resistant women with Polycystic Ovary Syndrome (89, 90). *In vitro* studies investigating insulin stimulated activation of AS160 are limited. However, treatment of primary human myotubes with palmitate, replicating an obese microenvironment, elicited a similar reduction in insulin stimulated AS160 phosphorylation (91). Whether such blunting of AS160 occurs directly or is simply due to dysregulation upstream in the insulin signalling pathway requires further study.

The precise mechanism of how intracellular vesicles associate with the membrane to increase GLUT4 insertion is currently not well understood, although SNARE proteins are thought to be involved in this process (92). Additionally recent evidence suggests that, in skeletal muscle, PI3K also activates the signalling protein rac1 and this protein facilitates GLUT4 translocation through inducing reorganisation of the intracellular cytoskeleton (93).

1.3.5 Effect of insulin on skeletal muscle metabolism.

In addition to driving glucose uptake in skeletal muscle, insulin also directly increases glycogen synthesis. Following increased transport into skeletal muscle, glucose is first phosphorylated to glucose-6-phosphate by hexokinase and then further converted to UDP-glucose. Increased glucose-6-phosphate drives an increase in glycogen synthase activity by inducing allosteric changes in glycogen synthase (94). Additionally, insulin further augments glycogen synthase activation through AKT-mediated phosphorylation and thus inhibition of glycogen synthase kinase-3 beta (GSK3ß), an inhibitor of glycogen synthase (95). Further, insulin inhibits the opposing enzyme, glycogen phosphorylase, to limit glycogen breakdown. Collectively, these effects facilitate the conversion of UDP-glucose to glycogen, promoting net glycogen synthesis.

In addition to glucose, insulin also has a profound effect on skeletal muscle protein metabolism. Firstly, numerous studies have shown insulin augments amino acid uptake by skeletal muscle (96). McDowell et al. demonstrated that such insulin stimulated amino acid uptake may be due to both the direct activation and membrane insertion of the Sodium-coupled neutral amino acid transporter-2 (SNAT2) (97). More recently, Walker et al. showed insulin is also able to increase the mRNA expression of SNAT2, in addition to large neutral amino acid transporter-1 (LAT1) and Proton-Assisted Amino Acid Transporter (PAT1) in C2C12 myotubes (98). Surprisingly, further mechanistic studies of insulin stimulated amino acid uptake, particularly in human cells, are limited.

Insulin also has a major anabolic effect on skeletal muscle and it appears such an effect is achieved through multiple mechanisms. Firstly, following its activation (described above), pAKT phosphorylates and inhibits Forkhead box protein O1 (FOXO1). FOXO1 is a positive regulator of the muscle specific ubiquitin E3 ligases MAFbx and MuRF-1 and therefore its inhibition reduces proteasomal mediated protein degradation, promoting net protein synthesis (99, 100).

Additionally, pAKT mediates phosphorylation of the tuberous sclerosis complex (TSC1/2) (101). In unstimulated conditions, TSC1/2 acts as a GAP, which functions to hold the effector protein Ras homolog enriched in brain (RHEB) in its inactive GDP bound state. Phosphorylation of TSC1/2 inhibits its GAP function, therefore allowing activation of RHEB. In turn, RHEB facilitates activation of mTORC1. Importantly mTORC1 is the central regulator of a number of cellular processes which collectively promote skeletal muscle hypertrophy (102).

Firstly, mTORC1 activates ribosomal P70 S6 kinase 1 (p70S6K1), a key step in driving protein synthesis (103, 104). Simultaneously, mTORC1 also phosphorylates and consequently inhibits 4E-binding protein 1 (4EBP1) (105). This releases 4EBP1 from its inhibitory binding to eukaryotic initiation factor 4E (eIF4E). Once free from 4EBP1, eIF4E can facilitate protein translation, thus further increasing protein synthesis. Conversely, mTORC1 also phosphorylates and inhibits unc-51-like kinase 1 (ULK1)

(106). This is the key protein involved in activation of the autophagy pathway, therefore its inhibition prevents muscle protein breakdown and contributes to net protein synthesis (106).

In vivo, it appears that insulin only directly increases muscle protein synthesis in humans when amino acid delivery to the skeletal muscle is also increased, often above physiological levels (107, 108). Indeed, a recent meta-analysis of studies investigating the anabolic effect of insulin indicated that such an effect is more likely attributable to reducing muscle protein breakdown (107). Importantly, in the absence of sufficient stimuli such as regular resistance exercise, skeletal muscle mass declines from approximately 35 years of age, with rates of muscle mass and strength loss accelerating to 1% and 5% per year respectively from the age of 60 (109). One of the primary causes for such muscle wasting with age is the development of anabolic resistance (110). As insulin is a key anabolic hormone, a reduction in the anabolic response to insulin is likely an important contributory factor to the decline in skeletal muscle mass with age. Critically this may lead to the development of sarcopenia, frailty, decreased quality of life and ultimately increased mortality (111, 112).

Similarly, insulin resistance is also associated with a reduction in both muscle mass and quality. Muscle mass is reported to decline up to 2-fold faster in individuals with T2D in comparison to non-diabetic controls, while the incidence of sarcopenia in T2D patients is up to 3-fold higher in comparison to non-diabetic controls, even when adjusting for additional risk factors such as BMI (113-115). It is likely that a reduction in insulin-stimulated muscle protein synthesis and increased muscle protein breakdown is an important contributing factor to such declines in muscle loss, particularly with progression of the T2D.

1.3.6 The effect of insulin on adipose tissue and liver metabolism

In adipose tissue, insulin has the same effects on glucose metabolism as observed in skeletal muscle. Insulin directly increases glucose uptake via the translocation of GLUT4, while driving increased glycogen synthesis and decreased glycolysis (116). Importantly, insulin also regulates adipose tissue lipid metabolism and this is essential for maintaining whole body energy balance (116). In times of nutrient depletion, lipids that are predominantly stored in adipose tissue as triglycerides, are hydrolysed to free fatty acids by the enzyme hormone-sensitive lipase (117). In turn, such free fatty acids are able to enter the circulation and are taken up by tissues such as skeletal muscle, where they are then oxidised to provide energy.

In contrast, during times of nutrient excess, insulin directly prevents such lipolysis and subsequent mobilization of fatty acids by inhibiting hormone-sensitive lipase (118). Simultaneously, insulin promotes expression and activation of the enzyme lipoprotein lipase (119-121). This enzyme, located on the extracellular membrane of vascular endothelial cells, acts to hydrolyse lipoproteins in the circulation generating fatty acids (122). This therefore allows for the increased uptake of such newly liberated fatty acids by adipocytes. Furthermore, insulin also increases the synthesis of a number of enzymes involved in lipid synthesis, through activation of transcription factors such as ubiquitous cellular transcription factor (USF) and sterol regulatory element binding protein 1c (SREBP1c) (123). This in turn facilitates increased synthesis of triglycerides from the influx of free fatty acids.

Insulin receptors are also present in the liver and therefore insulin exerts a number of direct effects on liver metabolism. Firstly, like in adipose tissue, insulin drives an increase in lipid synthesis. Indeed, specific knockdown of the hepatic insulin receptor prevents hepatic lipid accumulation, even in response to challenges with high fat diet (124). This effect is again partly due to increased expression of enzymes that promote lipid synthesis, mediated by insulin induced increases in SREBP-1c, via mTORC1, (125, 126). Additionally, FOXO-1 is also implicated in driving hepatic lipid synthesis. FOXO-1

is a transcription factor that when active reduces lipogenesis, potentially via suppression of SREBP-1c (127). However phosphorylation of FOXO1 by AKT inhibits this function, thus driving hepatic lipid synthesis (128).

Furthermore, liver glucose metabolism is also regulated by insulin. Since the human liver is responsible for up to 80% of glucose production and stores up to 35% of ingested glucose following a meal such regulation is vital (129). Firstly, insulin can directly reduce liver gluconeogenesis, via the inhibition of gluconeogenic gene transcription (130). Additionally, similarly to in muscle, direct activation of insulin signalling in the liver inhibits hepatic glycogenolysis and instead drives increased glycogenesis via the activation of glycogen synthase (131). Additionally, tissue cross talk provides important indirect regulation of liver glucose metabolism. Following increased insulin stimulated glucose uptake by skeletal muscle, glucose can be rapidly converted to lactate and secreted, particularly in times when muscle glycogen stores are already considerable (132, 133). This primarily acts to maintain a glucose diffusion gradient in muscle, facilitating continued glucose uptake. However this also has an important indirect effect on the liver, as the secreted lactate is taken up by hepatocytes and in turn converted to glycogen (132).

Similarly, indirect regulation of hepatic lipid metabolism has also been reported. As described above, insulin reduces lipolysis in adipose tissue and consequently levels of circulating free fatty acids decline. Importantly, FFA have been shown to increase glucose production in the liver of healthy individuals, therefore this process is blunted following insulin stimulation due to the decline in circulating FFAs, further promoting net glycogen synthesis (134, 135).

1.4 Skeletal muscle insulin resistance and the development of type II diabetes

T2D is a metabolic disorder in which blood glucose concentrations are unable to be managed effectively. This is due to a combination of factors, including the increased insulin resistance of target tissues and also a decline in insulin secretion caused by pancreatic β-cell dysfunction (136). In insulin resistant individuals, the quantity and functionality of insulin receptors are similar to that of non-insulin resistant individuals (137). This therefore indicates insulin resistance is mediated by a disruption in insulin signalling in target tissues, such as skeletal muscle and adipose tissue, thus preventing glucose uptake from the blood (137-139). Unfortunately, there is no cure for T2D and treatments are limited. Furthermore, the inability of patients to maintain plasma glucose concentrations in a healthy range is associated with a number of chronic pathologies, including microvascular diseases and macrovascular diseases such as stroke and coronary artery disease (140, 141).

One of the major treatment strategies for T2D patients is to increase insulin sensitivity, either through lifestyle modifications such as weight loss, or via the administration of insulin-sensitising drug therapies including Biguanides such as Metformin (142, 143) and Thiazolidinediones (144). Alternatively, some patients are prescribed Sulphoylureas, which stimulate insulin secretion (145, 146). However, these medications are associated with significant side-effects when taken chronically and can become ineffective as disease progresses (147-152). Therefore, there is great unmet clinical need to develop more effective and more targeting therapeutics for T2D patients.

In attempting to identify new therapies, skeletal muscle has emerged as an important area of drug discovery research. Skeletal muscle metabolic function is considered central to maintaining insulin sensitivity (153, 154), being responsible for up to 80% of insulin-mediated glucose uptake in healthy individuals (155).

It is well known that T2D patients display significantly impaired skeletal muscle glucose uptake in response to insulin, however the direct cause of such impaired glucose uptake is currently not well defined and is likely multifactorial. Leading hypotheses include the ectopic accumulation of intramuscular lipids and exposure to chronic low grade inflammation associated with ageing and increased adiposity.

In obese individuals, adipose tissue is known to become more “inflammatory”, with an increase in the infiltration of immune cells including T-cell subsets (156) and inflammatory M1 macrophages (157), which drive the production of proinflammatory cytokines, referred to in this context as adipokines. Importantly, secretome analysis of human adipocyte culture medium has identified over 200 adipokines (158) and recent studies have implicated that adipokines play a central role in the development of a number of obesity associated diseases. Therefore, understanding the functional and mechanistic role of adipokines on skeletal muscle insulin signalling may identify novel targets for therapeutic intervention of insulin resistance and T2D.

Although obesity is the primary risk factor for T2D, a number of other factors are also associated with its development. Firstly, a greater proportion of men present with T2D in comparison to women with the same BMI (159). This is likely attributable to gender specific fat distribution. Although women typically have greater adipose tissue mass, they display increased gluteal-femoral adipose accumulation, which has been demonstrated to protect against the development of T2D and metabolic disease (160, 161). In contrast, men typically present with greater central, and visceral adiposity associated with increased inflammation (162).

Genetically, it appears that the risk of developing type II diabetes is significantly (2-fold) increased in individuals of an Asian or Pima Indian ethnicity, particularly when exposed to a Westernised diet (163). T2D also appears to run in families, with an individual being 6 times more likely to develop T2D if their parents have the disease, in comparison to someone born to non-diabetic parents (163).

Finally, environmental factors such as alcohol consumption and smoking, as well as sleep deprivation have also been reported to significantly increase the risk of developing T2D (164-166).

1.5 Intramuscular lipids and the development of skeletal muscle insulin resistance

1.5.1 Intramyocellular lipids

In addition to intracellular glycogen stores and metabolic substrates obtained via the circulation, intramyocellular lipid (IMCL) droplets provide an important substrate for the generation of energy via oxidative phosphorylation, particularly during moderate to intense exercise, where IMCL can provide up to 25% of energy (167, 168). Lipid droplets are intracellular structures comprising of a core of organic neutral lipids, encapsulated by phospholipids, thus organic lipids are separated from the aqueous cytoplasm (169). Additionally, phospholipids are often decorated with additional proteins specific to cell type and function. Such proteins include perilipins, a family of structural proteins involved in both lipid synthesis such as acyl-CoA synthetase, and lipid breakdown such as lipases (169).

Lipid droplet size, lipid content and intracellular location also differ between cell types. In the skeletal muscle of lean individuals, intramyocellular lipid droplets primarily consist of esterified lipids including triacylglycerol (TAG), cholesterol and diacylglycerol (DAG) and contribute approximately 1% to total myocyte volume (170). Additionally, intramyocellular lipid droplets associate with mitochondria and primarily localise between myofibrils and to a lesser extent near the sarcolemma (171). In comparison to lipid droplets found in white adipocytes, intramyocellular lipid droplets are considerably smaller in diameter (100 μm and 0.3 -1.5 μm respectively), but are found in much

greater quantities (172, 173). This increases the ability for enzymatic interaction with lipid droplets, therefore facilitating more rapid fat oxidation when required.

1.5.2 The generation of intramyocellular lipid droplets

The starting material for the generation of lipid structures present within lipid droplets are FFAs. Within skeletal muscle, FFAs derived from either the circulation or intracellular lipolysis are initially linked to acyl-CoA by CoA synthetases, in turn forming FA-CoAs. From this point, FA-CoAs have two fates, they can be either oxidised or stored predominately via the formation of the neutral lipid TAG. The synthesis of TAG initially involves monoacylglycerol molecules first being re-acylated via addition of FA-CoAs to monoacylglycerol via acyltransferase to form diacylglycerol. In turn, diacylglycerol can be further acylated via DAG-O-acyltransferase to form TAG (174).

Other notable lipids present within skeletal muscle lipid droplets are sphingolipids. Synthesised from serine and palmitate, these lipids, such as ceramide, have a number of important bioactive roles. These include the regulation of both cellular processes and intercellular signalling pathways and are implemented as central drivers of skeletal muscle insulin resistance as discussed below (175). How such intracellular lipids get packaged and form the lipid droplet structure is a topic of debate, with complete mechanisms not yet fully elucidated. A leading theory is that phospholipids bud from the ER membrane in a process driven by the lipid coat proteins, encapsulating the lipid core (169).

1.5.3 Intramyocellular lipids and the development of insulin resistance.

There is substantial evidence that demonstrates the concentration of IMCL increases with obesity in humans. Specifically, infusion of non-essential fatty acids produces increases in IMCL stores in as little as 2 hours in humans, while consumption of a high fat diet (55–60% of energy intake), for just 3 consecutive days, has a similar effect (176). Conversely IMCL content decreases following diet induced weight loss (177).

There is also evidence demonstrating increased IMLC correlates with the development of insulin resistance (178, 179), while weight loss and in turn a reduction of IMLC is associated with improvements in insulin sensitivity (180). However it should be noted that this is only relevant to untrained individuals, since exercise trained subjects often exhibit an elevated IMLC, while also having increased insulin sensitivity. This suggests that total TAG content is not necessarily the principal driver of insulin resistance. Indeed, in some cases obese insulin sensitive and insulin resistant cohorts have been shown to display similar IMLC (181, 182). As a result, it is hypothesised that the accumulation of lipotoxic intermediates, primarily DAG and ceramide play a more important role in this process (183).

1.5.4 DAG and the development of skeletal muscle insulin resistance

Concentrations of intracellular DAG are increased with obesity and demonstrate a negative association with the development of insulin sensitivity in humans (184). Additionally, a reduction in the enzyme diacylglycerol kinase δ (DGK δ), which functions to convert DAG to phosphatidic acid is reported in individuals with T2D (185). This suggests such individuals not only have increased DAG accumulation through diet but also have a disruption in DAG metabolism; in turn further increasing DAG induced insulin resistance (185).

DAG increases the activity of a number of protein kinase C (PKC) isoforms, of which PKCθ and PKCε subtypes appear to have significant roles in the development of insulin resistance by inhibiting IRS-1 and thus downstream insulin signalling (186).

PKCθ achieves such IRS-1 inhibition by two different mechanisms. Firstly, Li et al. demonstrated that PKCθ directly phosphorylates IRS-1 at its serine residue 1101 in C2C12 myotubes (187, 188). Additionally, Werner et al. demonstrated that PKCθ also evokes insulin resistance via promoting indirect phosphorylation of IRS-1^{ser302} and IRS-1^{ser307} via JNK *in vitro*. The authors also demonstrated that such residues are phosphorylated in murine models of insulin resistance, namely following HFD, ob/ob mice and hyper-insulineamic mice (189). Similarly, PKCε phosphorylates $IRS1^{Ser\ 636}$ and $IRS1^{Ser639}$ in the skeletal muscle of *Psammomys obesus* gerbils, whilst preventing such phosphorylation protects against diet induced insulin resistance in these animals (190). Improvements in insulin sensitivity are also observed following PKCε knockout in diabetic mice (191). Furthermore, Ikeda et al. reported that PKCε directly inhibits the activation of the insulin receptor through a direct structural association, in addition to inducing IR downregulation, further limiting IRS-1 activation (192).

1.5.5 Ceramide and the development of skeletal muscle insulin resistance

A clear positive correlation exists between intramyocellular ceramide content and obesity (193) (194). There is also significant evidence indicating the accumulation of ceramide is associated with the development of insulin resistance in humans (195).

Treatment of both L6 and C2C12 myotubes with either palmitate or low-density lipoprotein (LDL) containing ceramide increases intramyocellular ceramide content and myotube insulin resistance (194) (196). In support of this, Chavez et al. demonstrated that overexpression of ceramidases in C2C12 myotubes results in an increased ability to reduce ceramide content, which prevented the

development of myotube insulin resistance following treatment with fatty acids (197). Preventing ceramide accumulation in C2C12 myotubes by increasing the expression of glucosylceramidase has recently been demonstrated to have a similar effect (198). Conversely, both inhibition and knockdown of this enzyme has the opposite effect, facilitating the development of insulin resistance in this myotube model (198).

Similarly to DAG, ceramides also activate PKC, specifically PKCζ. In turn, PKCζ has been demonstrated to phosphorylate Thr^{34} and Ser^{34} residues of AKT in L6 myotubes (199, 200). This prevents the recruitment of AKT to the plasma membrane, a crucial step for its activation. In support of this, Mahfouz et al. recently demonstrated that palmitate treated primary human myotubes and primary human myotubes cultured from diabetic subjects display increased ceramide content and insulin resistance mediated by PKC (201). Ceramide also directly activates the protein phosphatase-2A, which in turn targets and dephosphorylates active AKT, further blunting the downstream effects of this crucial protein in the insulin signalling pathway (202, 203). Although these mechanisms are well defined in animal models and rodent cell lines, it is important to note that evidence in primary human myotubes is currently lacking. Validation of these mechanisms in human muscle tissues is important in order to identify and validate candidate "druggable" targets for the treatment of insulin resistance

1.6 The impact of obesity on adipose tissue structure and function

1.6.1 Adipose tissue structure

As described in section 1.3.6, adipose tissue is critical for energy balance in humans. Post-prandially and during caloric surplus, white adipocytes (the predominant cell population within adipose tissue) primarily act to uptake and store FFAs and glucose. Conversely, fasting and limited nutrient availability upregulates lipolysis, generating energy as required. As discussed above, adipose tissue exhibits distinct sex differences in humans, with women exhibiting around 10% more adipose tissue at the same BMI as men (204). Typically, such increased fat mass in females is accumulated around the abdominal and gluteal regions (162).

Adipose tissue can be further classified as subcutaneous white adipose tissue (SWAT), visceral adipose tissue (VAT) and brown adipose tissue (BAT). SWAT is located directly beneath the skin and is the largest adipose depot by total mass, typically contributing up to 80% of total adipose tissue (205). VAT is located centrally, around the viscera, where it provides physical protection of the internal organs in addition to its metabolic role. In comparison to SWAT, VAT has a reduced capacity to expand in response to chronic caloric surplus due to fewer, small insulin responsive adipocytes which more readily uptake FFAs (206). However, visceral adipose tissue is more inflammatory and increased VAT mass with obesity has been extensively linked with a host of diseases including T2D, cardiovascular disease, cancer, atherosclerosis, as well as non-alcoholic fatty liver disease (207-209). In contrast, BAT is formed of 'brown adipocytes'. These cells express mitochondrial uncoupling protein 1 (UCP1) and have a far greater mitochondrial content in comparison to white adipocytes (210). Consequently, brown adipocytes are able to uncouple mitochondrial respiration, generating considerable amounts of heat energy. This process is thought to be driven primarily by exposure of brown adipocytes to cold conditions (211, 212). In humans, BAT is typically found in greater amounts during childhood before declining with age and as a result was thought to have a negligible function

in adults. However, recent evidence indicates that BAT is present in paravertebral, supraclavicular and periadrenal regions in much larger amounts than previously believed, contributing up to 2% of total body mass or 5% of total adipose tissue (213).

Interestingly, in contrast to SWAT and VAT, BAT displays an inverse correlation with both increasing BMI and total fat mass and recent evidence suggests it may play a considerable role in whole body energy homeostasis (214-216). Pioneering work by Stanford et al. demonstrated that transplantation of murine brown adipose tissue depots into the central region of recipient mice increased energy expenditure, induced weight loss and importantly prevented high fat diet induced insulin resistance (217). Additionally, BAT is also capable of considerable triglyceride clearance in mice, mediated by increased BAT endothelial permeability and activation of lipoprotein lipase in response to cold (218).

It now appears that there is also a subset of white adipocytes, typically expressing CD137 and transmembrane protein 26 (Tmem26), that are able to undergo a functional shift or "browning" resulting in the gain of functional properties associated with brown adipocytes. As a result, such adipocytes are often referred to as being 'brite' or 'beige' adipocytes (219). Current evidence suggests that adipose tissue browning can be initiated by either sustained exposure to cold conditions, the sympathetic nervous system and also exercise (220). Such stimuli activate PGC-1α, which in turn upregulates UCP1 and drives mitochondrial biogenesis, thus promoting the brown adipocyte phenotype (220). In light of such data, the potential to induce white adipose tissue browning has gathered interest in recent years as a potential therapeutic mechanism to substantially increase energy expenditure and improve symptoms of metabolic disease. Murine studies have demonstrated that caloric restriction may promote adipocyte browning (221). However, this does not seem to translate to humans since 8 weeks of caloric restriction in a relatively large cohort of 289 individuals induced significant weight loss, but had no effect on the expression of brown adipocyte markers (222). Although, the β3-adrenoceptor agonist mirabegron did elevate metabolic rate and

elicit direct glucose uptake via activation of BAT in a trial of 12 healthy humans (223). Further research, particularly in obese and diseased cohorts, is needed to confirm potential benefits of BAT and adipose tissue browning on metabolic diseases.

Finally, in addition to adipocytes and their precursors (pre-adipocytes), adipose tissue also has a substantial immune cell population. Critically, secretion of monocyte chemoattractant 1 (MCP-1) and to a lesser extent cytokines such as TNFα, IL-6 and IFN-γ by adipocytes recruits monocytes from the circulation (224). The local adipose tissue microenvironment then drives infiltrating monocyte differentiation into the more proinflammatory M1 macrophage subset. Obesity induced dysregulation of immune cell infiltration and consequent adipose tissue inflammation has profound effects on total body metabolic health as discussed below.

1.6.2 The impact of obesity on adipose tissue function

Excess circulating lipids are buffered by white adipocytes, leading to an increase in white adipocyte size (hypertrophy). In lean individuals this is necessary to maintain energy balance and importantly prevents damage to other organs through lipid toxicity. However, exposure to a chronic caloric surplus over months and years leads to progressive and sustained adipocyte hypertrophy and ultimately adipocyte dysfunction.

One of the major implications of adipocyte hypertrophy is the generation of a hypoxic microenvironment. In comparison to other tissues, adipose tissue has a limited vasculature network (225). Therefore, when adipocytes surpass approximately 100 μM in diameter the diffusion of O_2 to adipocytes becomes inefficient, at a time when demand is high due to increased adipose tissue mass (226). Subsequently, this leads to a significant disruption of multiple adipocyte functions.

Hypoxia is thought to drive increased adipocyte lipolysis and reduced lipid clearance from the circulation, resulting in a net release of FFA from hypertrophic adipocytes into the circulation (227) (228). Additionally, hypoxia is associated with increased adipocyte cell death and therefore the direct release of FFAs from dying cells may also contribute to increased accumulation of lipids in the circulation (229). Increased concentrations of circulating FFAs results in aberrant accumulation of lipids in internal organs such as the liver and skeletal muscle, with this process associated with the development of a number of obesity related pathologies, such as insulin resistance as described above.

Additionally, hypoxia increases adipocyte expression of hypoxia-inducible factor 1a (HIF-1a) a transcription factor which induces NF-κB signalling and in turn leads to increased proinflammatory cytokine secretion (230, 231). Due to this increased inflammatory burden with obesity, adipose tissue becomes inflamed, leading to increased accumulation of proinflammatory immune cells including M1 macrophages and T-cell subsets (231). This further increases adipose tissue inflammation and is thought to be an underlying mechanism for many chronic obesity associated conditions.

1.7 The role of established adipokines in obesity associated inflammation and skeletal muscle insulin sensitivity.

As introduced in sections 1.4 and 1.6.2, it is now widely accepted that adipose tissue also functions as an important endocrine organ, secreting a number of adipokines which play important roles in mediating tissue crosstalk and physiological processes. Importantly, secretome analysis of human adipocyte culture medium has identified over 200 adipokines (158) and there is substantial evidence that such adipokines contribute to the development of chronic low grade inflammation, associated with ageing and obesity (236). For example, serum TNFα concentrations display a significant positive correlation with both BMI and a waist to hip ratio (237). Leptin, adiponectin, resistin and visfatin are amongst the most well studied adipokines and have all been implicated in the development of metabolic diseases, including T2D. Studies conducted on these adipokines which relate to their functional role in skeletal muscle insulin signalling are discussed below and summarised in Table 1.2 in relation to animal and human data.

1.7.1 Leptin

The role of leptin as an inflammatory adipokine in metabolic disorders is well studied. Systemic levels of leptin positively correlate with both BMI and waist circumference, and are associated with the development of insulin resistance (238, 239). Several studies have reported that leptin impacts on skeletal muscle insulin signalling. Stimulation of the rat L6 skeletal muscle cell line with recombinant leptin reduced phosphorylation of IRS-1 and impaired glucose uptake, suggesting that leptin promotes insulin resistance (240). However, in contrast, leptin stimulation of murine C2C12 myotubes was found to increase glucose uptake, whilst overexpression of leptin in a 'skinny' mouse model increased insulin sensitivity (241, 242). These contrasting data highlight the need to conduct functional studies on leptin in human myotubes. To this end, Yau et al. reported that leptin increased

AKT phosphorylation in commercially available human myotubes (243). However, to date the functional role of leptin on human skeletal muscle insulin signalling is still understudied.

1.7.2 Adiponectin

Adiponectin, a 30 KDa protein with structural similarities to collagen types XIII and X, has been identified to be predominantly secreted by adipocytes into the blood, where plasma levels in healthy individuals reach approximately 10 μg/ml (238). This concentration is approximately 3-fold greater than the majority of other hormones, indicating an important role for adiponectin in human physiology. Adiponectin is considered to be a beneficial adipokine in relation to metabolism; plasma concentrations inversely correlate with weight, central obesity, risk of T2D and insulin resistance in humans (244, 245). Furthermore, maintenance of a low calorie intake increases both adipocyte expression of adiponectin and circulatory concentrations (246).

Three different molecular weight isoforms of adiponectin are found in the circulation, of which the high molecular-weight isoform is believed to be the most functional in terms of glucose homeostasis. Functional studies suggest that adiponectin promotes insulin sensitivity in skeletal muscle. In C2C12 myocytes, adiponectin increases fatty acid oxidation via sequential activation of AMPK, p38 MAPK and PPARα (247, 248) and promotes glucose uptake (248). Similarly, in L6 myotubes adiponectin induces GLUT4 translocation and glucose uptake (249). *In vivo*, adiponectin knockout mice demonstrate an obese, insulin resistant phenotype, whereas systemic administration of adiponectin, or its delivery as a transgene direct to skeletal muscle, improves insulin sensitivity (250-253). Adiponectin has also been shown to induce fat oxidation via AMPK activation in human myotubes, and further, this mechanism was found to be impaired in myotubes from obese T2D patients (254). Critically, this suggests that the function of adiponectin as a promoter of insulin sensitivity translates

to humans. Furthermore, it suggests that impairment of adiponectin function in skeletal muscle of obese T2D patients may contribute to the development of insulin resistance.

1.7.3 Resistin

First identified in murine adipocytes as a secreted protein capable of inducing insulin resistance (255), resistin is a proinflammatory adipokine that induces the secretion of TNFα and IL-6 from various cell types including PBMCs and pancreatic acinar cells (256, 257). The correlation between plasma resistin with both obesity and insulin resistance in humans supports a role for resistin in the development of insulin resistance (258, 259). *In vitro*, studies have demonstrated a reduction in AKT phosphorylation and glucose uptake in C2C12 and L6 myotubes stimulated with recombinant resistin (260-262). However, at present, few studies have investigated the functional role of resistin in the development of insulin resistance in human skeletal muscle cells.

1.7.4 Visfatin

Visfatin exists in both an intracellular (iVisfatin) and extracellular (eVisfatin) form (263, 264). eVisfatin is primarily produced and secreted from visceral adipose tissue, where it is more highly expressed in obese individuals(265). Similarly, higher systemic levels of eVisfatin are associated with obesity, ageing and the development of T2D (266-268).

Regarding the role of visfatin in mediating insulin sensitivity, overexpression of visfatin in male wistar rats increased whole body insulin sensitivity (269), and in adipose tissue and liver, promoted insulin-mediated IRS-1 phosphorylation (269). Data on the function of visfatin in skeletal muscle insulin sensitivity is limited to studies in rodents. Visfatin increases glucose transport in rat skeletal muscle fibres (270). Furthermore, in C2C12 myotubes, visfatin activates AMPK/p38 MAPK, induces GLUT4

expression and translocation, and promotes glucose uptake (270). Based on these data, similar insulin sensitizing effects may occur in human skeletal muscle.

1.8 The role of novel adipokines in skeletal muscle inflammation and insulin sensitivity.

In addition to the well-known adipokines, proteomic studies of adipose tissue have identified several less characterised adipokines that may also play important roles in mediating skeletal muscle insulin sensitivity. At present the functional effects of the majority of these novel adipokines on human skeletal muscle insulin sensitivity is poorly understood. Some of the more prominent novel adipokines are discussed below and also summarised in Table 1.3.

1.8.1 Vaspin

First reported as a 47 KDa protein in the visceral adipose tissue of genetically obese OLETF rats (271), administration of vaspin to obese mice increased insulin sensitivity and glucose tolerance (272). Additionally, subcutaneous adipose tissue expression of leptin, resistin and TNFα was suppressed, whilst GLUT4 and adiponectin expression was increased following vaspin administration (272). Similar increases in insulin sensitivity have since been reported in db/db and C57BL6 mice following recombinant vaspin delivery (273). Central administration of vaspin to obese mice resulted in a sustained suppression of appetite that resulted in reduced bodyweight and plasma glucose concentrations (274). Furthermore, transgenic mice overexpressing vaspin displayed improved glucose tolerance, reduced systemic IL-6 concentrations and were protected from obesity when fed a high fat diet (275).

In humans, vaspin expression has been reported in several tissues including subcutaneous adipose tissue, skin, stomach and skeletal muscle (274, 276, 277). Serum concentrations of vaspin in non-diabetic and diabetic patients positively correlate with BMI, bodyweight and impaired glucose tolerance (278-281). Given the functional effects of vaspin demonstrated in rodent models, its increased expression with BMI in humans may reflect a compensatory mechanism.

The effect of vaspin on insulin signalling and metabolism in human skeletal muscle is currently undetermined. Similarly, the mechanism of action and receptor for vaspin has also not been elucidated. Recently, it was reported that in HepG2 cells vaspin binds glucose-regulated protein (GRP78), a 7KDa voltage-dependent anion channel. Further, stimulation of H-4-II-E-C3 cells with recombinant vaspin activated AKT and AMPK signalling pathways, which was prevented by GRP78 inhibition (275). Vaspin may therefore mediate its effects on insulin signalling via binding to GRP78. However, at present the expression of GRP78 has not been profiled in human adipose or skeletal muscle tissue, nor the functional studies conducted in human skeletal cells to validate GRP78 as the vaspin receptor.

1.8.2 Fibroblast growth factor 21

Fibroblast growth factor 21 (FGF-21) is established as a key mediator of fat oxidation and energy homeostasis (282-284). Numerous studies report that serum concentrations of FGF-21 are elevated in obese individuals and positively correlate with insulin resistance, BMI, % fat mass and circulatory concentrations of leptin and LDL (285-288). Although predominantly produced by the liver, FGF-21 is also expressed in adipose tissue, where it is more highly expressed in both obese and diabetic mouse models.

In vivo, administration of FGF-21 to mice fed a high fat diet decreased intramuscular triglyceride content, increased insulin sensitivity and glucose uptake, and elevated secretion of adiponectin from

adipocytes (289). Continuous cerebral administration of FGF-21 for 2 weeks increased whole body insulin sensitivity in rats with dietary-induced obesity (290), whilst daily intravenous or subcutaneous delivery of FGF-21 for 6 weeks improved glucose handling in diabetic rhesus monkeys (291). Following such positive effects on insulin sensitivity and glucose tolerance, two FGF-21 mimetics (LY2405319 and PF-05231023) have progressed to phase 1 clinical trials (NCT01869959, NCT01923389) (292-296), and antibodies targeting FGFR1c/b-Klotho have been developed (297, 298). With regards to a direct functional role of FGF-21 in skeletal muscle, incubation of isolated mouse EDL muscle with FGF-21 increased insulin-stimulated glucose uptake, and in human myotubes FGF-21 increased both basal and insulin-stimulated glucose uptake (299). Furthermore, FGF-21 has also been shown to prevent palmitate-induced insulin resistance in primary human myotubes by inhibiting stress kinases and NF-κB (300). Finally, FGF-21 is has also been demonstrated to be a myokine. In turn, such skeletal muscle derived FGF-21 can reportedly drive adipocyte browning, by upregulating adipocyte UCP-1 expression. Thus increased FGF-21 may also indirectly reduce adipose tissue mass via this mechanism (301).

1.8.3 Chemerin

Chemerin, was initially described as a novel chemoattractant for macrophages and dendritic cells via activation of several GPCRs including CMKLR1/ChemR23, GPR1, and CCRL2 (302, 303). More recent data suggests chemerin plays an important role in the differentiation of human adipocytes, and in the development of insulin resistance (304, 305). Circulatory concentrations of chemerin are associated with obesity, diabetes and metabolic syndrome (306-308). Furthermore, adipose tissue from obese subjects exhibits greater secretion of chemerin (309).

At present, *in vivo* studies have drawn differing conclusions regarding the role of chemerin in the development of insulin resistance and glucose tolerance. Becker et al. reported that overexpression

of chemerin increased insulin resistance in LDL-receptor deficient mice fed a high fat diet, as evidenced by reduced insulin-mediated AKT phosphorylation (310). Importantly this effect was only observed in skeletal muscle, and not liver or pancreas (310). Additionally, glucose handling and serum insulin concentrations were reduced by chemerin administration to both obese and diabetic mice (311). However, no such effect was observed following chemerin administration to control mice. Takahashi et al. also report a negative effect of chemerin on skeletal muscle insulin sensitivity, with chemerin knockout mice displaying increased skeletal muscle insulin stimulated AKT phosphorylation and glucose uptake. However, despite this effect chemerin -/- mice demonstrated whole body glucose intolerance, due to a disruption of hepatic glucose production and reduced insulin secretion from pancreatic ß-cells (312).

In vitro studies provide support for chemerin as a driver of insulin resistance. Pre-treatment of C2C12 myotubes with chemerin reduced insulin-stimulated glucose uptake, while increasing the secretion of proinflammatory cytokines including IL-6 and TNF-α (313). Additionally, treatment of primary human myotubes with recombinant chemerin reduced insulin-stimulated glucose uptake (314). Further cross-talk studies with primary human myocytes and myotubes, particularly from obese and diabetic cohorts may help to clarify the function of chemerin in human metabolic disease states.

1.8.4 Preadipocyte factor 1

Preadipocyte factor 1 (Pref-1) is a transmembrane protein processed to generate a circulating form, which is also known as Foetal Antigen 1 (FA1) (315). Studies have described an association of increased Pref-1/FA1 serum concentrations with obesity and T2D (316, 317). Pref-1 is also reported to negatively regulate adipogenesis, with Pref-1 deficient mice displaying significant obesity and stunted growth (318, 319). Overexpression of Pref-1 in mice promotes a lipodystrophic phenotype

and insulin resistance via decreased skeletal muscle glucose uptake and impaired skeletal muscle insulin signalling (320).

In humans, Pref-1 stimulation of myotubes from lean, obese, and T2D patients did not affect insulin sensitivity. However Pref-1 did induce the production of the proinflammatory cytokines IL-6 and CCL2 (321), and thus chronic exposure of muscle to pathological levels of Pref-1 may impair insulin sensitivity indirectly. Clearly, further studies utilising human myotubes are warranted to fully determine the functional role of Pref-1 in skeletal muscle insulin sensitivity.

1.8.5 Follistatin-like 1

Follistatin-like 1 (FSTL1) is a glycoprotein with homology to osteonectin and its expression is associated with systemic inflammatory diseases including rheumatoid arthritis, lupus and ulcerative colitis. Several *in vitro* studies have established FSTL1 as a proinflammatory cytokine. For example, over-expression of FSTL1 in the fibroblast-like COS7 cell line or in human U937 monocytes induced the secretion of proinflammatory cytokines IL-6, TNF-α and IL-1β (322).

With regards to adipose biology, FSTL1 is highly expressed in 3T3-L1 pre-adipocytes and its downregulation is implicated in their differentiation to adipocytes (323, 324). Furthermore, stimulation of 3T3-L1 adipocytes with recombinant FSTL1 inhibited insulin signalling (323). *In vivo*, increased adipose tissue expression of FSTL1 is reported in the leptin-deficient ob/ob mouse, and in humans serum levels of FSTL1 positively correlate with BMI (323). Despite being expressed and secreted by human myotubes (325) no studies to date have reported the functional effects of FSTL1 on skeletal muscle insulin signalling, using either rodent or human cells.

1.8.6 SPARC

SPARC (osteonectin) was first discovered as a glycoprotein secreted from bone. However, it is now known that SPARC is also expressed and secreted from adipose tissue. SPARC adipose tissue expression is increased in dietary-induced obesity in rats (326). In humans, SPARC is secreted from adipose tissue and appears to be an important driver of adipocyte differentiation and hyperplasia (327), while its expression in adipose tissue correlates with fat mass (328). Furthermore, serum levels of SPARC are associated with insulin resistance, dyslipidaemia and inflammation in patients with gestational diabetes mellitus (329). Mechanistically, overexpression of SPARC in 3T3-L1 adipocytes downregulated GLUT4 expression and inhibited insulin-stimulated glucose uptake (326). Given these data, it seems likely that SPARC could impair skeletal muscle insulin signalling. At present, these studies have not yet been conducted and so its functional role in skeletal muscle is not established.

1.8.7 CTRP3

CTRP3 is a member of a family of proteins which includes adiponectin. Similar to adiponectin, CTRP3 has been identified as an anti-inflammatory adipokine. In humans, CTRP3 levels in the serum are lower in obese subjects compared to normal-weight individuals (330, 331), and negatively correlate with markers of insulin resistance (331). *In vitro*, CTRP3 inhibits LPS-induced expression of proinflammatory cytokines in human macrophages (332), whilst RNAi-mediated knockdown in preadipocytes increased the expression of chemokines and reduced adiponectin expression (333). Its functional role in skeletal muscle insulin signalling has not been characterised.

1.8.8 Omentin-1

Originally identified as a lectin-binding protein (334), Omentin-1 (intelectin-1) is highly expressed in visceral adipose tissue (335). In humans, systemic concentrations and adipose tissue expression of

Omentin-1 are lower in obese individuals (335) and negatively correlate with BMI and insulin resistance (335). Furthermore, lower serum levels of omentin-1 are observed in newly diagnosed T2D patients and its secretion from human adipose tissue is decreased by both insulin and glucose (336, 337).

In vitro, studies support a role for Omentin-1 as an anti-inflammatory adipokine, which suppresses the activity of TNF-α in vascular inflammation via inhibiting p38 and JNK pathways. A role for Omentin-1 in promoting insulin sensitivity is supported by studies in human adipocytes where recombinant Omentin-1 induced AKT phosphorylation and enhanced insulin-stimulated glucose uptake (338). Thus far, studies to determine its functional role in skeletal muscle using either rodent models or human tissue have not been reported.

1.8.9 Lipocalins

Lipocalins are a functionally diverse group of proteins with a highly conserved tertiary structure that have been implicated in inflammation and immune responses. Importantly, a number of lipocalins, most notably lipocalin-2 (LCN2) and RBP4 have been associated with adipose tissue expression and obesity. Recently, a new member of the lipocalin family was identified, termed lipocalin-14 (LCN14), which in mice was found to be predominantly expressed in WAT and was downregulated in dietary-induced obese mice (339). Furthermore, adenovirus over-expression of LCN14 in obese mice improved insulin sensitivity (339). Again, the functional role of lipocalins in mediating human skeletal muscle insulin sensitivity has not been reported.

Adipokine	Association with obesity and/or T2D in humans	Adipokine effect on insulin signalling in animal models		Adipokine effect on insulin signalling in human skeletal muscle
		In Vivo	*In Vitro*	
Leptin	Increased (238, 239, 340).	Overexpression of leptin in a skinny mouse model increased insulin sensitivity (242). Administration of leptin (12-15 days) reversed insulin resistance in obese Wistar rats (341). Leptin reversed high fat diet induced skeletal muscle insulin resistance in rats, indirectly via reducing intramuscular triglycerides not though direct modulation of insulin signalling (342).	Recombinant leptin reduces IRS-1 phosphorylation and glucose uptake in L6 myotubes (240). Recombinant leptin increased glucose uptake in C2C12 myotubes (241). Acute (10 mins-1 h) stimulation of L6 Myotubes directly increased glucose uptake via a PI3K-dependent pathway. Leptin pre-treatment (10min) of L6 myotubes inhibits insulin stimulated glucose uptake (343). 24 h Pre-treatment of L6 myotubes had no effect on glucose uptake but did inhibit adiponectin stimulated glucose uptake (344).	Increased phosphorylation of AKT in commercially available primary human myotubes (243).
Adiponectin	Decreased (244, 245).	Adiponectin knockout mice demonstrate an obese and insulin resistant phenotype (250, 252). Systemic administration and	Promotes glucose uptake in both C2C12 and L6 Myotubes (248, 249). Recombinant adiponectin increased	Induces fat oxidation through activation of AMPK in myotubes from lean subjects. Mechanism impaired in myotubes from T2D patients (254).

		Overexpression of adiponectin drives increased insulin sensitivity in insulin resistant mice [38, 40].	glucose uptake via AMPK mediated reorganisation of the actin cytoskeleton and GLUT4 translocation via an independent mechanism [132].	
Resistin	Increased (258, 259).	Administration of resistin (6 days) to wild type mice induces a state of insulin resistance (345). Targeted reduction of resistin in insulin resistant mice via antisense oligodeoxynucleotide restored hepatic but not skeletal muscle insulin sensitivity (346).	Recombinant resistin impaired insulin signalling and glucose uptake in both C2C12 and L6 myotubes (261, 262).	Unknown
Visfatin	Increased (347-349).	Visfatin overexpression in rats increased whole body insulin sensitivity and adipose tissue and liver IRS-1 phosphorylation in response to insulin (269).	Stimulated glucose uptake and increased GLUT4 membrane translocation and mRNA and protein expression in C2C12 myotubes via AMPK p38 MAPK signalling (270). Increased glucose uptake in rat EDL muscle (350).	Unknown

Table 1. 2 Evidence for the role of known adipokines in mediating skeletal muscle insulin sensitivity.

Adipokine	Association with obesity and/or T2D in humans	Adipokine effect on insulin signalling in animal models		Adipokine effect on insulin signalling in human skeletal muscle
		In Vivo	*In Vitro*	
FGF-21	Increased (299).	Increased insulin sensitivity and glucose uptake in mice, via FGF-21 mediated increases in adiponectin production and secretion from adipocytes (289). Continuous cerebral administration for 2 weeks increased whole body insulin sensitivity in rats with dietary induced obesity (290). Daily administration for 6 weeks improved glucose handling in diabetic rhesus monkeys (291).	6h incubation of mouse EDL muscle with FGF-21 resulted in a 54% increase in insulin stimulated glucose uptake (299).	Directly increased glucose uptake in primary human myotubes(299). Prevents palmitate-induced insulin resistance in primary human myotubes by inhibiting stress kinases and NF-κB (300).
Chemerin	Increased (308, 351).	Overexpression increased insulin resistance in LDL receptor deficient mice by reducing AKT phosphorylation in response to insulin in skeletal muscle, but not liver or pancreas (310). Knockout mice display increased skeletal muscle insulin resistance while transgenic mice exhibit increased skeletal muscle insulin resistance (312).	24h pre-treatment reduces insulin stimulated glucose uptake in C2C12 myotubes in a dose dependent manor (313).	24h chemerin Increased insulin resistance and reduced insulin stimulated glucose uptake in primary human myotubes, mediated by increased ERK signalling (309).

		Acute chemerin treatment exacerbated glucose intolerance and lowered serum insulin levels in obese and diabetic mice. No effect observed in normoglycemic mice (311).		
CTRP3	Decreased (330, 352, 353).	Administration of recombinant CTRP3 directly lowers glucose levels in normal and insulin-resistant ob/ob mice (354). Overexpression of CTRP3 improved insulin sensitivity in HFD fed mice (355).	Administration of recombinant CTRP3 to L6 myotubes had no effect on glucose uptake (354). Increased glucose uptake and GLUT 4 mRNA expression in insulin resistant adipocytes (356).	Unknown
RBP4	Increased (357, 358).	Overexpression or direct administration of RBP4 increased insulin resistance in mice. RBP4 knockout improves insulin sensitivity in mice (358). Reducing circulating RBP4 in obese mice models improved glucose tolerance and increased insulin stimulated glucose uptake in skeletal muscle up to 60% (359).	unknown	Unknown
Vaspin	Increased (278, 280, 281).	Vaspin treatment increased insulin sensitivity and glucose tolerance in obese and diabetic mice (272, 273). Transgenic mice overexpressing vaspin displayed improved glucose tolerance	Unknown	Unknown

		and were protected from obesity when challenged with a high fat diet (275).		
Pref-1	Increased (316).	Overexpression in mice drives insulin resistance via decreased adipose tissue and skeletal muscle glucose uptake and impaired skeletal muscle insulin signalling (320).	Unknown	4 Day exposure to primary human myotubes from lean, obese and T2D subjects had no effect on glucose uptake (321).
Follistatin-like 1	Increased (360).	Unknown	Blunts insulin signalling-adipocytes (323).	Unknown
Omentin-1	Decreased (361, 362).	Unknown	Omentin-1 induced AKT phosphorylation and enhanced insulin-stimulated glucose uptake in human adipocytes (338).	Unknown Unknown
Lipocallin-14	Unknown	Over expression in diet induced obese mice reduced glucose and insulin levels while improving glucose tolerance (339).	Unknown	

Table 1. 3 Evidence for the role of novel adipokines in mediating insulin sensitivity

1.9 The impact of exercise on insulin sensitivity

Both aerobic fitness and the physical activity levels demonstrate positive correlations with insulin sensitivity, while numerous studies have reported a significant improvement of insulin sensitivity following exercise intervention (363-366). Furthermore, it appears such beneficial effects occur both acutely in the hours after exercise and persist for several days post exercise (367). However, exercise is quite a generalised term and therefore deciphering the effects of different types of exercise, including; aerobic, resistance and high intensity interval training (HIIT) on insulin sensitivity in different cohorts has gained significant attention. A detailed discussion of such research is not possible here, so only key impacts of different exercise modalities on insulin sensitivity are discussed below. A more comprehensive summary of recent studies can be found in the recent review article by Bird et al. (366).

There is significant evidence demonstrating that performing a minimum of 30 minutes of moderate intensity aerobic exercise, 3 times per week for at least 8 weeks, elicits a significant improvement in insulin sensitivity in a broad range of cohorts. This includes both young and old males and females, T2D patients, obese adolescents and even young sedentary individuals (368, 369). Increasing the volume of moderate intensity exercise elicits increased improvements in insulin sensitivity, but with diminishing returns. For example, moderate exercise equating to 600 calories per day produced only slight improvements in insulin sensitivity in comparison to 300 calories per day protocols (370).

Furthermore, improvements in insulin sensitivity have also been reported in response to performing high intensity exercise, particularly HIIT exercise (367, 371, 372). Such HIIT may also evoke greater improvements in insulin sensitivity when compared to moderate aerobic exercise, despite lower total energy expenditure and significantly reduced exercise time (372, 373). Indeed, recent data indicates that even a single bout of maximal exercise of 2-3 minutes is enough to improve insulin sensitivity of

overweight/obese males for many hours post exercise, with a 38% increase in fat oxidation still present 1 day post-exercise (374).

Additionally, resistance exercise such as weightlifting also demonstrates improvements in insulin sensitivity in diabetic and obese cohorts (375, 376). Interestingly, it appears that resistance exercise mediated improvements may occur independently to aerobic exercise, with a combination of aerobic exercise and resistance exercise being more effective than aerobic exercise alone (377, 378). One possible explanation for this is that the increased muscular demands of resistance exercise necessitates increased recruitment and activation of type II muscle fibres, in comparison to aerobic exercise that is more predominantly associated with type I fibre activation. Therefore, it may be of benefit for patients with insulin resistance/T2D to follow a diverse exercise programme consisting of both resistance and aerobic exercise.

A final consideration when investigating the effect of exercise on insulin sensitivity is that of the nutritional state of the individual temporal to exercise. It appears performing exercise in the fasted state may evoke greater improvements in insulin sensitivity post exercise, with this effect potentially attributable to an increase in exercise induced myocellular GLUT4 protein content (379). Additionally, Taylor et al. presented evidence that, in healthy individuals, consuming carbohydrates to replenish glycogen stores after performing 90 min of exercise (70% VO_2 max) resulted in blunted insulin sensitivity the following morning when compared to individuals who did not consume carbohydrates post exercise. Therefore, performing fasted exercise and limiting carbohydrate intake immediately following exercise is potentially the most effective strategy to maximise beneficial effects of exercise on insulin sensitivity in obese/diabetic cohorts (380).

Mechanistically, both aerobic exercise and resistance exercise training directly increase the content of GLUT4 protein in skeletal muscle and thus facilitate increased insulin stimulated glucose uptake (381-383). With time, increased vascularisation of the skeletal muscle in adaptation to regular

exercise also likely contributes to improvements in insulin sensitivity, by increasing insulin and glucose delivery (384-386). Finally, exercise may also improve pancreatic ß-cell function and thus improve insulin secretion, as recently observed in T2D and obese populations (387, 388).

In summary, exercise is a potentially effective treatment option for many individuals with poor insulin sensitivity. Therefore, lifestyle changes to increase physical activity that incorporate both aerobic and resistance exercise would likely be beneficial in such individuals. The fact that lower intensity exercise can be beneficial is of particular interest, as initially, performing high intensity exercise is often challenging for many individuals who are obese or display T2D, especially as these conditions are also often associated with numerous co-morbidities, such as cardiovascular disease, which limit exercise capacity.

1.10 Thesis Hypothesis and Aims

1.10.1 Hypothesis

It is evident that adipose tissue has a considerable effect on skeletal muscle function in the obese state, driving skeletal muscle dysfunction associated with the development of insulin resistance and T2D, as summarised in Figure 1.3. However, the functional role of many adipokines in mediating such insulin sensitivity is unknown. We propose that novel adipokines, currently unstudied in human skeletal muscle, mediate changes in skeletal muscle insulin sensitivity and inflammation associated with the obese state. We also hypothesise that, like adipokines, adipose tissue derived extracellular vesicles are novel mediators of adipose tissue and skeletal muscle crosstalk and are implicated in the development of obesity associated skeletal muscle dysfunction.

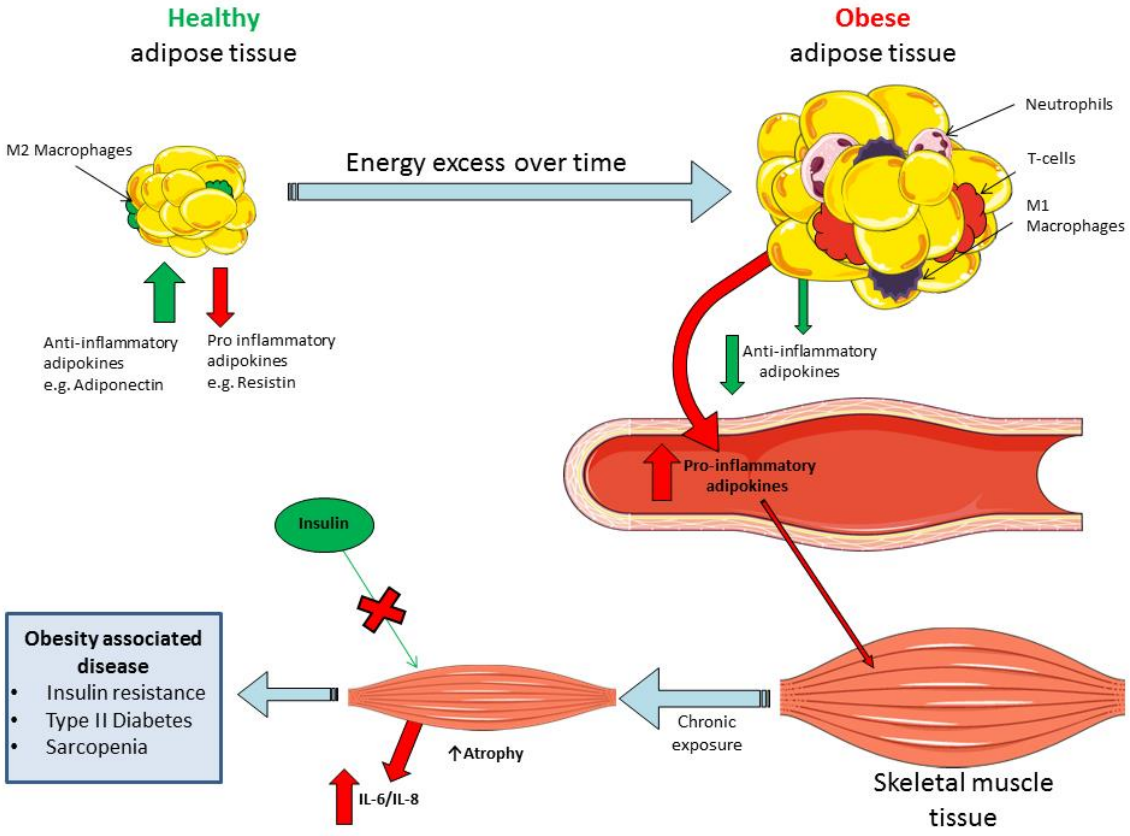

Figure 1. 3. Proposed mechanism for skeletal muscle dysfunction associated increased adipokine secretion in the obese state

1.10.2 Aims

1. Determine the impact of obesity on the functional properties of primary human myotubes in order to validate primary human myotubes as an *in vitro* model for studies investigating the impact of candidate adipokine in mediating the obese phenotype (Chapter 3).

2. Characterise the effect of obesity on the expression and secretion of the novel adipokine vaspin in human skeletal muscle and adipose tissues and determine the functional effect of vaspin on primary human myotube insulin sensitivity (Chapter 4).

3. Validate extracellular vesicles as novel mediators of adipose tissue and skeletal muscle crosstalk. Perform the first characterisation of extracellular vesicles derived from lean and obese human adipose tissue and investigate the effect of human adipose tissue derived extracellular vesicles on primary human myotube inflammation and insulin sensitivity (Chapter 5).

CHAPTER 2: Materials and Methods

2.1 Ethical approval and subject recruitment

Informed consent was obtained from all patients prior to sample collection and full ethical approval for the study was obtained from the UK Research Ethics Committee (NRES 13/NE/0222). Sample collection, processing, storage and subsequent experimental procedures were carried out in compliance with Human Tissue Authority guidelines under the Human Tissue Act (2004).

2.2 Subject data and sample collection

Gluteus maximus skeletal muscle, subcutaneous adipose tissue (SAT) and blood samples were obtained intraoperatively from individuals undergoing elective hip-replacement surgery at either the Royal Orthopaedic Hospital (Birmingham, UK) or at Russell's Hall Hospital (Dudley, UK). Diabetic patients and those taking anti-inflammatory medication within two weeks prior to surgery were excluded from the study.

2.3 Blood sample processing

5 ml of blood was collected at the time of surgery in a red-top vacutainer and allowed to clot at room temperature (RT) for 20–30 min. Next, samples were centrifuged at 1620 X g for 10 min. The upper serum layer was collected and aliquoted into 1 ml cryovials. Samples were snap frozen immediately in liquid nitrogen and stored at -80 °C until thawed on ice for analysis. Freeze-thaw cycles were avoided.

2.4 Primary human myoblast isolation and culture

Skeletal muscle samples (~200 mg) obtained as described in section 2.2 were sliced with a scalpel, placed in 5 ml of 0.05% trypsin-EDTA (Gibco®, Invitrogen, Paisley, UK) solution and rotated in an incubator (37 °C, 5% CO_2) for 15 min. Trypsin was inactivated by the addition 5 ml of myoblast growth media [Ham's F10 nutrient mix (Sigma-Aldrich, Dorset), supplemented with 20% HyClone™ research grade foetal bovine serum (GE healthcare, Buckinghamshire, UK) and 1% penicillin and streptomycin (Sigma-Aldrich, Dorset, UK)]. This solution was centrifuged for 5 min at 360 X g and the resulting pellet re-suspended in 12 ml of myoblast growth medium and incubated in an uncoated T75 cell culture flask for 20 min. Finally, the solution was transferred to a T75 cell culture flask pre-coated with 0.2% gelatin (Sigma-Aldrich, Dorset, UK) in PBS. Myoblast growth medium was replaced every 48 h.

When cultures approached approximately 80% confluency, myoblasts were passaged 1:2-1:5, depending on the growth rate of each individual cell culture, or seeded into multi-well plates as required for experimentation. Specifically, cells were washed with PBS, followed by incubation with 5 ml of 0.05% trypsin EDTA for 5 min (37 °C, 5% CO_2) to detach the cells. Cells were then immediately transferred to a universal tube containing an equal volume of myoblast growth media to quench the trypsin. Next, myoblasts were pelleted by centrifugation (360 X g, 5 min), re-suspended in myoblast growth media and then transferred into either a T-75 flask, 96, 48, 24, 12 or 6 well plate (pre-coated coated with 0.2% gelatin). The volume of myoblast growth media used in each vessel is reported in Table 2.1. For experiments that required a specific number of myoblasts, the cell pellet was first re-suspended in 1 ml of growth media. Next, a 10 µl aliquot was removed and mixed with 10 µl of trypan blue and cell count performed using a Countess II (life technologies, Paisley, UK).

Culture flask	Volume per flask/well
T-75 flask	12 ml
6-well plate	2 ml
12-well plate	1 ml
24-well plate	500 µl
48-well plate	250 µl
96-well plate	150 µl

Table 2. 1 Volume of culture medium used during the culture of primary human myoblasts/ myotubes.

2.5 Cryopreservation of primary human myoblasts

If myoblasts were not required for subculture or experimentation, myoblast pellets were re-suspended in 1 ml of freezing media (90% myoblast growth media + 10% dimethylsulfoxide (Sigma-Aldrich, Dorset, UK) before being aliquoted into 1 ml cryovials and transferred to a freezing container (Mr Frosty, Thermo Fisher Scientific, MA, USA). Cells were then immediately placed into a -80 °C freezer before being transferred to liquid nitrogen the following day for long term storage at approximately -150 °C.

2.6 Differentiation of primary human myoblasts

Differentiation of myoblasts into multinucleated myotubes was induced by replacing myoblast growth media from >90% confluent myoblasts with differentiation media [Ham's F10 nutrient mix, supplemented with 6% horse serum (Sigma-Aldrich, Dorset, UK) and 1% penicillin and streptomycin]. The volume of differentiation media used was equal to growth media (Table 2.1) and was also replaced every second day. All experiments were conducted on the 8th day of differentiation.

Myoblast cultures generated desmin positive, multinucleated myotubes, which have previously been confirmed to be negative for the fibroblast marker TE7 (389).

2.7 Generation of adipose/skeletal muscle tissue conditioned medium

SAT or skeletal muscle derived from lean and obese subjects was incubated (37 °C, 5% CO_2) in serum free Ham's F10 nutrient mix (Sigma-Aldrich, Dorset, UK), containing 1% penicillin and streptomycin, for up to 24 h at a ratio of 1 g: 10 ml. Larger samples were divided into segments of ~ 1 g to ensure that the surface area of tissue exposed to medium remained approximately constant. For time course analysis, 50 µl aliquots were taken hourly for 6 h. Following incubation, supernatants were removed and stored at -80 °C.

Additionally, SAT samples were also incubated (37 °C, 5% CO2) in myotube differentiation media at a ratio of 1 g: 10 ml, to facilitate chronic incubation of primary human myotubes with adipose conditioned media (ACM). Following incubation, supernatants were removed and stored at -80°C.

2.8 Preparation of adipose conditioned media samples for extracellular vesicle isolation

Following collection of serum free ACM as described in section 2.7, samples were immediately centrifuged at 2000 X g, 4 °C, for 20 min using a benchtop micro-centrifuge (S418R, Eppendorf, Stevenage, UK). Supernatants, containing EVs were then transferred to a sterile Eppendorf tube and spun again at 12,000 X g, 4 °C, for 2 min. Finally, supernatants containing EVs were collected, transferred to bijoux tubes and stored at -80 °C.

2.9 Isolation of extracellular vesicles from ACM

ACM samples prepared as described in section 2.8 were thawed on ice on the day of experimentation. Samples were transferred to ultracentrifuge tubes. Samples were centrifuged at 100,000 X g, 4 °C, for 1 h using an ultracentrifuge (WX Ultra80, Thermo Fisher Scientific, MA, USA) in order to pellet EVs.

2.10 Stimulation of primary human myoblast and myotubes with recombinant proteins

Primary human myoblasts and myotubes were stimulated with a variety of recombinant proteins as detailed in Table 2.2. Lyophilised recombinant proteins were diluted in double distilled H_2O (ddH_2O) or PBS as specified by the manufacturer, to produce a concentrated stock solution in accordance with the manufacturer's protocol. Stock solutions were then aliquoted and frozen at -20 °C, allowing the same batch of recombinant protein to be used across experiments. For experimentation, stock solutions were diluted in myoblast growth medium or myotube differentiation medium as required and incubated with cells.

Recombinant protein	Manufacturer	Source	Sequence	Catalogue #
Insulin	Sigma	Yeast (Proprietary host)	N/A	I2643
Vaspin	Bio Vision	E. Coli	Full length (aa 1-415)	4915
IL-1ß	Sigma	E. Coli	Unknown (153 aa residues	I9401

Table 2. 2 Recombinant proteins used to stimulate primary human myoblasts and myotubes

2.11 Isolation of total protein from primary human myoblasts and myotubes

Myotubes grown in 6-well plates were lysed with 250 µl of ice-cold RIPA buffer (Thermo Fisher Scientific, MA, USA), containing phosphatase inhibitor cocktail 3 (1:100) (Sigma-Aldrich, Dorset, UK) and protease inhibitor cocktail (1:100) (Sigma, Dorset, UK). After addition of RIPA buffer, plates were placed on ice for 20 min before each well was scraped using a cell scraper and contents transferred to a 1.5 ml Eppendorf tube. Total protein was quantified by performing a BCA assay (Thermo Fisher Scientific, MA, USA) in a clear 96-well plate as described by the manufacture's protocol. Samples and standards were assayed in duplicate and optical density was measured at 550 nm using a Biotek EL808 spectrophotometer (Biotek, Swindon, UK). Subsequently a standard curve was generated in Microsoft Excel and used to determine the protein concentration of samples (µg/µl).

2.12 Isolation of total protein from skeletal muscle tissue

Snap-frozen skeletal muscle tissue samples (~100 mg) were ground into a fine powder using a pestle and mortar under liquid nitrogen. Powdered tissue was immediately transferred to a 1.5ml Eppendorf tube containing 500 µl of ice-cold RIPA buffer as described in 2.11. After addition of RIPA buffer, samples were placed on ice for 20 min and total protein content quantified by performing a BCA assay (Life technologies, Paisley, UK) as described in section 2.11.

2.13 SDS polyacrylamide gel electrophoresis and immunoblotting

Protein samples from cell and tissue lysates were diluted to a desired concentration in loading buffer consisting of 2-mercaptoethanol (Sigma-Aldrich, Dorset, UK), 4x Laemmli Sample (Bio-Rad, Hertfordshire, UK) and ddH_2O as required.

Samples were loaded into a 5% SDS-polyacrylamide stacking gel and separated by performing 10-12% SDS-page depending on the protein of interest. Gels were cast in Novex 1.0 mm Cassettes (Life technologies, Paisley, UK) as described in Table 2.3. Cassettes were placed into an Invitrogen Novex mini-cell (Thermo Fisher Scientific, MA, USA), filled with 1 X running buffer prepared from ultrapure 10 X tris/glycine/SDS (Geneflow, Staffordshire, UK) and ddH_20. Gels were then run at 150 Volts and 50 milliamps using a Novex x-cell surelock (Thermo Fisher Scientific MA, USA), powered by a Omnipac CS-300 V power supply (Cleaver Scientific, Rugby, UK).

Separated proteins were transferred to a methanol activated PVDF membrane (Bio-Rad, Hertfordshire, UK) using a Trans Turboblot™ transfer system (Bio-Rad, Hertfordshire, UK). Following transfer, membranes were rinsed in ddH_20 and washed in 1 X tris buffered saline with 0.1% Tween®20 (Sigma-Aldrich, Dorset, UK) (TBS-T) for 15 min, on a shaker at RT. Next, membranes were blocked with TBS-T containing 5% bovine serum albumin (BSA) for 1 h, on a shaker at RT. Membranes containing protein samples from serum and conditioned media were blocked with TBS-T containing 5% milk, 2% BSA and 0.5% H_2O_2 for 1 h, on a shaker at RT. Membranes were then immuno-probed overnight at 4 °C on a shaker, with primary antibodies as described in Table 2.4. The following day membranes were subject to 3 x 15 min washes with 1X TBS-T and incubated with the appropriate secondary antibody (Table 2.5) in TBS-T, for 2 h, on a shaker at RT. Antibody was then removed and membranes washed 3 x 15 min with 1 X TBS-T on a shaker at RT.

Finally, Amersham ECL Western Blotting Detection Reagent (GE Healthcare, Buckinghamshire, UK) was added to cover membranes. Proteins were then visualised using a ChemiDoc™ MP System (Bio-Rad, Hertfordshire, UK). In order to normalise protein load, membranes were stripped by performing 2 X 10 min washes on a shaker at RT with Restore™ Western Blot Stripping Buffer (Life technologies, Paisley, UK). Membranes were then blocked as described above before being re-probed with the appropriate primary antibody (Table 2.4) overnight at 4 °C on a shaker. Proteins were probed with secondary antibody (Table 2.5) and visualised as described above. Protein expression was quantified using image J software.

	Protogel	**ddH_2O**	**1.5M Tris HCL pH 8.8**	**0.5M Tris HCL pH 6.5**	**10% APS**	**20% SDS**	**Temed**
10% Separating gel	10.0 ml	12.5 ml	7.5 ml	N/A	150 µl	150 µl	30 µl
12% Separating gel	12.0 ml	10.5 ml	7.5 ml	N/A	150 µl	150 µl	30 µl
5% Stacking gel	2.6 ml	12.2 ml	N/A	5.0 ml	100 µl	100 µl	20 µl

Table 2. 3 Constituents of SDS-polyacrylamide gels used for SDS page.

Protein target	Manufacturer	Catalogue #	Clone	Dilution	Species
Phospho AKT ^{308}	Cell signalling technology	CST 9275	05/2015	1:1000	Rabbit
Phospho AKT ^{473}	Cell signalling technology	CST 9271	193H12	1:1000	Rabbit
Total AKT	Cell signalling technology	CST 9272	C67E7	1:1000	Rabbit
Phospho AMPK	Cell signalling technology	CST 2535S	40H9	1:1000	Rabbit
Total AMPK	Cell signalling technology	CST 2532	N/A polyclonal	1:1000	Rabbit
ß actin	Sigma	AC40	N/A polyclonal	1:5000	Mouse
GLUT4	Abcam	ab65267	mAbcam65267	1:1000	Mouse
PI3K p85	Cell signalling technology	CST 42285	19H8	1:1000	Rabbit
Total PI3K	Cell signalling technology	CST 4257	N/A polyclonal	1:1000	Rabbit
Phospho P38 MAPK	Cell signalling technology	CST 9211	N/A polyclonal	1:1000	Rabbit
P38 MAPK	Cell signalling technology	CST 9212	D13E1	1:1000	Rabbit
Puromycin	Millipore	MABE343	12D10	1:1000	Rabbit
Vaspin	Abcam	Ab 101391	N/A polyclonal	1:1000	Rabbit

Table 2. 4 Primary antibodies used for immunoblotting

Protein target	Manufacturer	Catalogue #	Dilution
Rabbit IgG	GE Healthcare Life Sciences	NA931	1: 10,000
Mouse IgG	GE Healthcare Life Sciences	NA934	1: 10,000

Table 2. 5 Secondary antibodies used for immunoblotting

2.14 ELISA Enzyme-Linked Immunosorbent Assays (ELISA)

2.14.1 IL6/IL-8 ELISA

Concentrations of IL-6 and IL-8 in myotube supernatants were quantified using the relevant ELISA DuoSet (DY206/ DY208 R&D Systems, Minneapolis, MN, USA) following the manufacturer's protocol. Firstly, capture antibody was diluted in PBS (pH 7.2) as specified by the manufacturer and added to the required wells of an uncoated nunc-ImmunoT ELISA plate (Thermo Fisher Scientific, MA, USA) overnight at RT. The following day, wells were washed 3 times with 300 µl wash buffer (PBS pH 7.2, containing 0.05% Tween® 20) and then blocked with reagent diluent (PBS containing 1% BSA) for 1 h. Plates were then aspirated and washed as described above. Next, protein standards were serially diluted 2-fold in reagent diluent. Standards and samples were then added to the plate in duplicate and incubated for 2 h at RT. Following incubation, plates were again washed as above, before the addition of capture antibody (diluted in reagent diluent to manufactures specification) for 2 h at RT. Streptavidin-HRP (diluted in reagent diluent) was then added to wells for 20 min at RT, in the dark. Following a final wash step as above, substrate solution was added to wells for up to 20 min. Finally, reactions were stopped by the addition of stop solution (2N H_2SO_4) and optical density immediately measured at 450 nm using a BioTek EL808 microtiter plate reader (BioTek, Swindon, UK). Optical imperfections in the plate were limited by correcting with absorbance measured at 570 nm. The average absorbance for each standard was used to generate a standard curve using GraphPad Prism v5 statistical package. Concentrations of unknown samples were then calculated using this standard curve. Samples with an absorbance below the lowest standard were considered to be 0 ng/ µl.

2.14.2 Vaspin ELISA

Serum vaspin concentrations were measured using a commercially available human vaspin ELISA kit (AdipoGen Life Sciences, San Diego, CA, USA), following the manufacturer's instructions. Firstly, vaspin standards were serially diluted 2-fold with ELISA buffer provided. Standards were then added to the ELISA plate along with serum samples (diluted 1:4 in ELISA buffer) in duplicate. The plate was then covered and incubated for 1 h at 37 °C. Afterwards, wells were aspirated and washed 3 times with 1 X wash buffer supplied. Then, detection antibody was diluted 1:2000 with ELISA buffer and added to wells for 1 h at 37 °C. Next, wells were aspirated and washed 3 times as described above before the addition of TMB substrate for 20 min, in the dark, at RT. Thorough mixing was ensured by tapping the plate gently. Finally, stop solution was added to wells and optical density was measured at 450 nm immediately using a BioTek EL808 microtiter plate reader (BioTek, Swindon, UK). Vaspin concentrations were determined from a standard curve as described in 2.14.1

2.14.3 Human glycated haemoglobin A1c (HbA1c)

Human serum HbA1c was quantified using a commercially available ELISA kit (Cusabio Biotek Hertfordshire, UK) following the manufacturer's protocol. Firstly, standards were diluted in sample diluent to produce a 4-fold dilution series. Additionally, serum samples were diluted 1:5 in sample diluent. 50 µl of standards and samples were added to ELISA wells in duplicate. Next, 50 µl of Biotin-conjugate was added to all wells except a blank and the plate incubated for 40 min at RT. Wells were then aspirated and washed 3 times by the addition of 200 µl of wash buffer provided. Then, 100 µl of HRP-avidin was added to all wells except the blank and incubated for 40 min at 37 °C. Following incubation, wells were washed 5 times as above before the addition of 90 µl TMB for 20 min at 37 °C in the dark. Finally, 50 µl of stop solution was added and optical density measured as described in 2.14.1.

2.15 Isolation of total RNA

Snap-frozen skeletal muscle and subcutaneous adipose tissue samples (~100 mg) were first ground into a fine powder using a pestle and mortar under liquid nitrogen. Powdered tissue was immediately transferred to a 1.5 ml RNAse free Lo-bind Eppendorf tube (Eppendorf, Stevenage, UK) containing 1 ml of Trizol® reagent (Life technologies, Paisley, UK) and homogenised using a Qiagen Tissue Ruptor (Qiagen, Manchester, UK). Primary human myotubes were lysed by the addition of 1 ml of TRIzol® reagent directly to the tissue culture plate. Wells were scraped using a filter tip and TRIzol® solution transferred to a 1.5ml RNAse free Lo-bind Eppendorf tube. RNA was then extracted as described in the manufacturer's protocol. Specifically, 200 µl of chloroform (CO549, Sigma-Aldrich, Dorset, UK) was added to TRIzol® samples and the chloroform/Trizol mixture shaken by hand for 15 s. Samples were then incubated at RT for 3 min before centrifugation (12,000 x g , 15 min, 4 °C). Next, the upper clear layer was transferred to a fresh Eppendorf tube and 500 µl of isopropanol (19516, Sigma-Aldrich, Dorset, UK) and 2 µg of glycoblue (AM9156, Thermo Fisher Scientific MA, USA) was added to samples, before incubation overnight at -20 °C. The following day, samples were centrifuged (12,000 X g, 4 °C, 15 min), supernatants were removed and RNA pellets re-suspended in 1 ml of 70% ethanol diluted in ddH_2O. RNA was again pelleted by centrifugation (7500 X g, 5 min, 4°C) and the supernatant removed. Finally, RNA was vacuum dried and re-suspended in 30 µl of RNAse free water (Thermo Fisher Scientific, MA, USA) before heating at 55°C for 10 min. RNA was quantified using a Nanodrop 2000 (Life technologies, Paisley, UK).

2.16 Quantitative Real-Time PCR

One-step quantitative real-rime polymerase chain (qRT-PCR) was performed using either SYBR green or TaqMan chemistry in a 384 well PCR plate. The constituents per reaction are detailed in Table 2.6 for SYBR chemistry and 2.7 for Taqman chemistry. The sequence of primers and probes used are reported in appendix 1. All reactions were performed using a Bio-rad sfx cycler (Bio-Rad Hertfordshire, UK) as described in Table 2.8. Samples were assayed in triplicate and a non-template control was included for each gene of interest to identify the formation of primer-dimers. CT values were determined as the point where the curve crossed the defined threshold in the exponential phase of RNA amplification. The efficiency of all primers was validated to be >95% and melt curves were included for all reactions to confirm the amplification of a single product. The quantity of target gene RNA, relative to the quantity of housekeeping gene RNA was calculated by $2^{-\Delta Ct \text{ of target gene (treated - control)}} / 2^{-\Delta Ct \text{ housekeeping gene(treated -control)}}$.

Additionally, the expression of 48 genes (appendix 2) related to the insulin signalling pathway were measured in human skeletal muscle tissue from lean, overweight and obese individuals using custom designed micro fluidics Taqman array cards (Thermo Fisher Scientific, MA, USA) as specified by the manufacture's protocol. Briefly, RNA was extracted as described in section 2.15 and reverse transcribed to generate cDNA using TaqMan® MicroRNA Reverse Transcription Kit (Thermo Fisher Scientific, MA, USA). For each set of 48 genes, a 100 µl mastermix was then prepared from 50 µl of TaqMan® Fast Advanced Master Mix (2X) and 50 µl cDNA (10 ng/µl) in nuclease-free Water. Next, mastermix was transferred to wells by loading 100 µl of mastermix into the plate reservoirs. qRT-PCR was performed as described in table 2.8 (without reverse transcription) using a Quant Studio 12K Flex Real-Time PCR System (Thermo Fisher Scientific, MA, USA). Each sample was run in duplicate for all 48 genes. Data were analysed as above.

Reagent	Volume/ reaction (µl)
2X Precision one-step plus qRT-PCR (with SYBRgreen) mastermix (primer design, Eastleigh, UK)	2.5
Primers	0.2
RNAse free H_2O (primer design, Eastleigh, UK)	1.3
RNA (5ng/µl)	1.0

Table 2. 6 Constituents per reaction used to perform qRT-PCR with SYBR green chemistry

Reagent	Volume/ reaction (µl)
2X iTaq Universal Probes reaction mix (Bio-Rad, Hertfordshire, UK)	2.5
iScript advanced reverse transcriptase (Bio-Rad, Hertfordshire, UK)	0.125
Probe/primer mix	0.2
RNAse free H_2O	1.175
RNA (5ng/µl)	1.0

Table 2. 7 Constituents per reaction used to perform qRT-PCR with Taqman chemistry

Protocol step	Temperature (°C)	Time	Number of cycles
1. Reverse transcription	55	10 min	1
2. Activation of polymerase	95	8 min	1
3. Denaturation	95	10 s	40
4. Annealing and extension	60	60 s	40
5. Melt curve	95	continuous	1
6. Cooling	37	30s	1

Table 2. 8 qRT-PCR Protocol

2.17 Transfection of primary human myoblasts and Myotubes

siRNA complexes (Table 2.9) were thawed on ice and TransIT-X2 reagent (Mirus Bio, WA, USA) was warmed to room temperature and vortexed gently. Transfection mixtures were then prepared in an RNAse free Eppendorf tube with volumes stated in table 2.10 and incubated at RT for 30 min. Fully differentiated primary human myotubes, or 2.5 X 10^4 primary human myoblasts seeded in a 96-well plate 24 h prior to transfection were incubated with the transfection mixture for 24 h. Following transfection, RNA was extracted as described in section 2.15 or functional studies performed.

Target	**Manufacturer**	**siRNA**
Non-targeting control (NTC 1)	Dharmacon	Non-targeting ON-TARGETplus™ Control siRNA #1
Non-targeting control (NTC 2)	Dharmacon	Non-targeting ON-TARGETplus™ Control siRNA #2
HSPA5 (GRP78) (siRNA #1)	Dharmacon	ON-TARGETplus J-00819-09-0002 #1
HSPA5 (GRP78) (siRNA #2)	Dharmacon	ON-TARGETplus J-00819-06-0002 #2

Table 2. 9 siRNAs used during myoblast and myotube transfection

Culture vessel	**96-well plate**	**48-well plate**	**24-well plate**	**12-well plate**	**6-well plate**
Myoblast growth medium/Myotube differentiation medium	92 µl	263 µl	500 µl	1.0 ml	2.5 ml
Optimem medium	9µl	26µl	50µl	100µl	250 µl
siRNA (20 nM stock)	0.125 µl	0.35µl	0.7 µl	1.4 µl	2.8µl
TransIT-X2 reagent	0.3 µl	0.78 µl	1.5 µl	3 µl	7.5µl

Table 2. 10 Constituents per reaction for transfection using TransIT-X2 Dynamic Delivery System

2.18 Oil Red O staining of primary human myotubes

Primary human myotubes grown in a 24-well plate were washed in PBS and fixed by the addition of 250 µl 2% paraformaldehyde (PFA) (10160052, Thermo Fisher Scientific, MA, USA) diluted in PBS, for 30 min at RT. PFA was removed and cells washed a further 3 times in PBS. Next, Oil red O (0625, Sigma-Aldrich, Dorset, UK) was diluted (0.5% (w/v) in 60% triethyl-phosphate (538726, Sigma-Aldrich, Dorset, UK) (diluted in ddH_20). This stock was diluted 3:2 in ddH_20 and filtered using a 0.22 µm filter. Working Oil red O stain was applied to myotubes for 1 h at RT. Oil red O stain was then removed and the cells washed 3 times with PBS. Cells were then imaged by bright field microscopy using a Leica DMI6000 microscope, with images taken from multiple locations per well. Lipid particle size was then quantified using image J software. To do this, images were first converted to 8-bit grayscale (2.1 A-B), next, the threshold of each image was adjusted to highlight pixels containing lipid stained areas (2.1 C), and exclude background and large artefacts. Image J software was then used to calculate the average particle size of those selected particles (2.1 D).

Following imaging, 250 µl of 100% isopropanol was added to liberate total oil red stain. 100 µl of Oil red containing isopropanol was then added in duplicate to a clear flat bottom 96-well plate. Absorbance was measured at 480 nm using a Synergy 2 Multi-Detection Microplate Reader (BioTek, Swindon, UK) and normalised to total protein content by performing a BCA assay as described in 2.11.

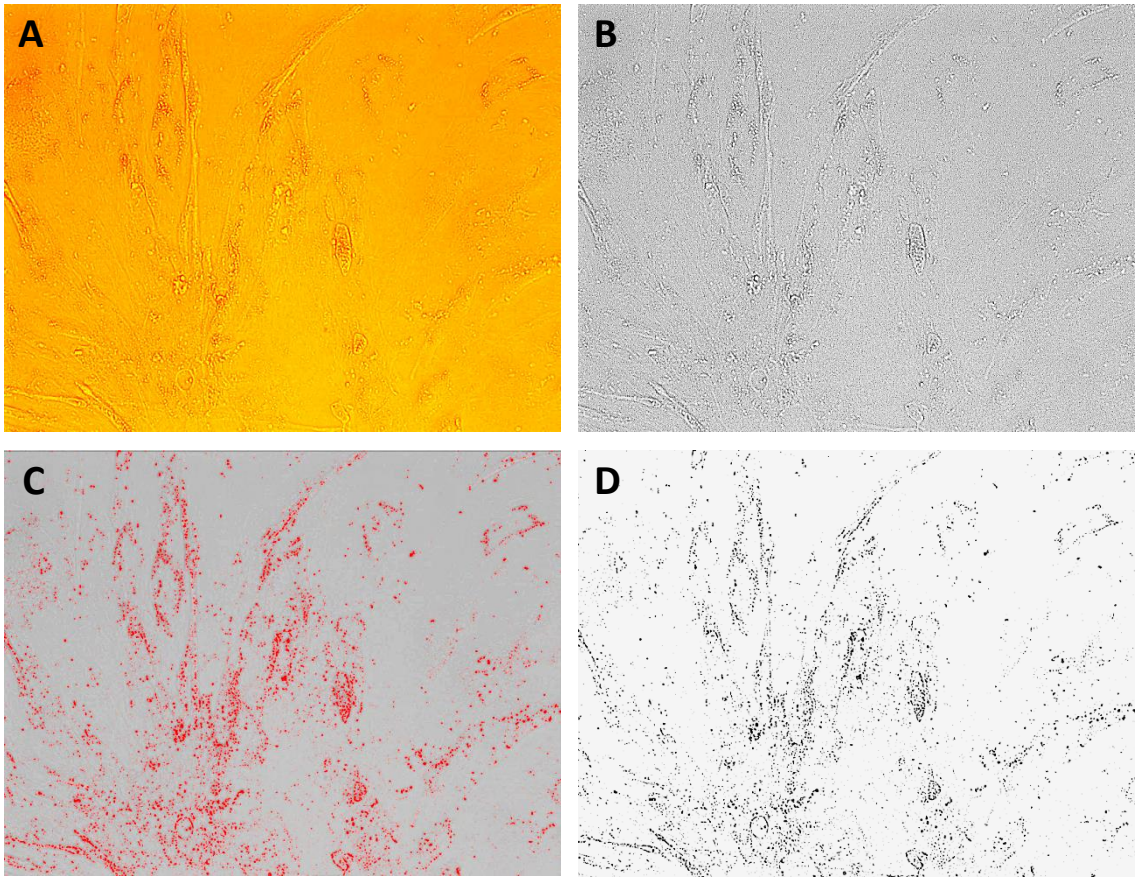

Figure 2. 1. Conversion of a bright field microscopy image to allow quantification of oil red O positive area using image J.

2.19 Immunofluorescent staining of primary human myotubes

Primary human myotubes were cultured in a 24-well plate and fixed in PFA as described in section 2.19. Next cells were washed 3 X with PBS (500 µl) before being permeabilised by the addition of 100% methanol for 10 min. Cells were then blocked for 30 min with 5% (v/v) goat serum diluted in PBS. Cells were then incubated with primary antibody (Table 2.11) overnight at 4 °C. The following day, primary antibody was removed and cells washed 3 times with PBS. Wells were then probed with an anti-mouse secondary antibody (Table 2.10) for 1 h in the dark. Wells were washed and nuclei stained by the addition of 200 µl DAPI (diluted 1:5000 in PBS) for 5 min in the dark. Finally, cells were washed as above, before the application of mountant and a cover slip. Cells were imaged immediately using a Leica DMI6000 microscope.

Protein target	Manufacturer	Catalogue #	Dilution
Desmin	Thermo Fisher	MA5-13259	1: 200
GLUT4	Abcam	ab65267	1: 200
Mouse IgG	Thermo Fisher	R37120	1:1000

Table 2. 11 Antibodies used for immunofluorescent staining of primary human myotubes

2.20 MesoScale immunoassays

Myotubes were cultured in 96-well plates and stimulated with 10 nM human insulin or 25-100 ng/ml of recombinant human vaspin. Cells were lysed in 90 µl MSD lysis buffer (MesoScale Discovery, Gaithersburg, Massachusetts) containing Phosphatase Inhibitor Cocktail 3 (1:100 dilution, Sigma-Aldrich, Dorset, UK) and Protease Inhibitor Cocktail (1:100 dilution, Sigma-Aldrich, Dorset, UK). Insulin receptor, IGF1 receptor and AKT (Thr^{308}) phosphorylation, as a percentage of total protein, was determined using Mesoscale Discovery phospho and total protein assays (MesoScale Discovery, MA, USA), performed according to the manufacturer's instructions and detected on the SECTOR Imager 6000 (MesoScale Discovery, MA, USA).

2.21 Measurement of primary human myotube glucose uptake

Glucose uptake in primary human myotubes was quantified using either a radiometric or a fluorometric assay. For the radiometric assay, obese myotubes (differentiated for 8 days) were cultured in 6-well plates and either left unstimulated or were pre-incubated for 24 h with vaspin (100 ng/ml). The next day myotubes were washed twice in warm PBS and incubated in serum-free media (Ham's F10) for 2 h. Myotubes were washed a further two times before incubation with 2 ml reaction buffer (138 mM NaCl, 1.85 mM CaCl2, 1.3 mM MgSO4, 4.8 mM KCl, 50 mM HEPES, pH 7.4, 0.2% (W/V) BSA) for 45 min at 37 °C. Myotubes were then incubated with or without insulin (100 nM) for 30 min on a plate warmer at 37 °C before the addition of 250 µL of 27.8 kBq [3H]-2-DOG and 10 µM 2-DOG at timed intervals to each well for 15 min. The buffer was aspirated with a vacuum pump and myotubes were washed three times with ice cold PBS containing 10 mM glucose. Myotubes were then lysed in 500 µL 0.5 M NaOH and 0.1% SDS then transferred to scintillation vials and 5 ml liquid scintillation fluid was added. Samples were vortexed and assayed for [3H]-2-DOG uptake expressed as disintegrations/min/well using a β-counter.

For the fluorometric assay, lean and obese myotubes cultured in 96-well plates were washed three times in PBS before incubation with glucose-free DMEM media (Gibco) for 3 h. Myotubes were washed a further three times before incubation with 100 µM 2-NBDG glucose (Sigma-Aldrich, Dorset, UK), diluted in glucose-free media with or without 100 nM insulin, for 30 min. Myotubes were subject to a further three washes with PBS before final addition of 100 µL PBS/well. Fluorescence was measured by excitation at 485 nm and emission at 528 nm using a Synergy 2 Multi-Detection Microplate Reader (BioTek, Swindon, UK). Untreated myotubes were included to correct for myotube auto-fluorescence. Five biological replicates were performed per condition for each primary human culture.

2.22 Quantification of membrane-localised GLUT4 expression

Primary human myoblasts (Passage 1-3, 10^5 cells/condition) from obese subjects were treated with either vaspin (100 ng/ml, 15 min) or insulin (100 nM, 15 min). Post-treatment, cells were washed with PBS (250 x g, 5 min, 4 °C) and stained for 20 minutes on ice with a mouse anti-human GLUT4 monoclonal antibody (mAbcam65267, Abcam. 0.05 µg/10^5 cells, diluted in 2% BSA PBS). A second wash with PBS (250 x g, 5 min, 4 °C) was then performed, before cells were stained with 5 µg/ml Alexa Flour 488 goat anti-mouse IgG (Invitrogen, Thermofisher Scientific) for 20 min on ice. Following a single wash in PBS (250 x g, 5 min, 4 °C), cells were fixed for 20 minutes at RT with 50 µl of fixation medium (Medium A, Life Technologies). Following a single wash in PBS (250 x g, 5 mins, 4 °C), cells were re-suspended in 200 µl PBS and transferred to polypropylene FACS tubes in preparation for flow cytometric analysis. A minimum of 1,500 myoblasts were gated based on their forward/side scatter properties and analysed for GLUT4 expression, which was recorded as mean fluorescence intensity. Flow cytometry was performed on an AccuriC6TM bench top cytometer and analysis conducted using BD Accuri C6 software (BD Biosciences, Berkshire, UK).

2.23 Detection and quantification of adipose tissue derived extracellular vesicles

Extracellular vesicles (EVs) were captured using a tetraspanin chip set with CD9, CD63, CD81 and Mouse IgG antibodies (Nanoview Biosciences, Boston, MA, USA). All assays were performed in accordance with the manufacturer's protocol. Firstly, chip files on the USB drive provided were loaded onto the ExoView computer and chips pre-scanned using nScan2 V 2.76 acquisition software. Next, the void between wells of a 24-well tissue culture plate were filled with 0.22 μM filtered ddH_20 for humidification. Chips were then removed from storage (4 °C) using tweezers and placed in the centre of a well with the chip ID facing up. Care was taken to avoid touching the face of the chip in order to prevent damage to antibody coated regions. Then, ACM samples, spun as described in 2.8 were diluted 1:7 in incubation solution. 35 μL of diluted sample was then loaded onto the centre of the chip. The plate lid was then reapplied, before incubation for 16 h at RT in the dark.

Following incubation, chips were washed by the addition of 1 ml of incubation solution, followed by shaking at 500 rpm for 3 min at RT. Afterwards, 750 μl of the incubation solution was removed from the well and replaced with 750 μl of fresh incubation solution, followed by shaking at 500 rpm for 3 min at RT. This process was repeated 3 times with 750 μl of incubation solution being removed after the final wash. Blocking solution was then prepared by diluting 2 ml of blocking solution (provided) 1:1 with incubation solution. 5 μl of CD9 Alexa-647, CD63 Alexa 488 and CD81 Alexa-555 fluorescent antibodies (provided) were then added to 3 ml of blocking solution. 250 μl of the antibody cocktail was then added to the well and incubated for 1 h at RT. 500 μl of incubation solution was then added to the well, followed by the immediate removal of 750 μl. 750 μl of fresh incubation buffer was then added to wells and plates washed at 500 rpm on a shaker for 3 min at RT. This process was repeated for a total of 3 washes. A final wash was then carried out by removing 750 μl of incubation buffer followed by the addition of 750 μl of rinse solution at 500 rpm on a shaker for 3 min at RT.

Finally, chips were removed using tweezers and placed into a 6 cm dish containing rinse solution. Chips were washed further with rinse solution by manually moving chips in a horizontal motion using tweezers. Chips were then slowly removed at a 45° angle, and placed on an absorbent paper towel to ensure chips were dry. Chips were then analysed using ExoView R100 (Nanoview Biosciences, Boston, MA, USA) with nScan2 V 2.76 acquisition software. Data was exported using nano-viewer V2.82 software, with particle size thresholds set to 50 to 200 nm.

2.24 Treatment of primary human myotubes with adipose tissue derived extracellular vesicles

EVs were isolated from ACM as described in section 2.9. Following ultracentrifugation, the EV pellet was re-suspended in an equal volume of myotube differentiation media. Primary human myotubes were then washed with PBS and incubated with EVs for 48 h followed by either functional experiments or extraction of RNA as described in section 2.15.

2.25 Electrical pulse stimulation (EPS) of primary human myotubes

Primary human myotubes derived from lean and obese individuals were cultured in a 6-well plate and subject to electrical pulse stimulation (EPS) at 11.5 V, 1 Hz and 2 ms for 24 h using a C-Pace EP (IonOptix, MA, USA). Differentiation media was replaced immediately prior to the start of EPS. Following EPS, protein or RNA was extracted as described in section 2.11 and 2.15 respectively. Three biological replicates for each condition were performed for primary human myotube culture.

2.26 Non-Radioactive Surface Sensing of Translation (SUnSET) Protein Synthesis

Protein synthesis in response to EPS was measured via the SUnSET method, as described by Crossland et al. (390). Puromycin (Sigma-Aldrich, Dorset, UK) was added directly to myotubes 30 min prior to end of EPS to a concentration of 1 μM. Protein was then extracted as described in section 2.11 and immunoblotting for puromycin performed as described in section 2.13.

2.27 Tissue Collection from Rodent models of Obesity and T2D

Brown adipose tissue (BAT), subcutaneous white adipose tissue (SWAT) and epididymal white adipose tissue (EWAT) from various rat models of obesity and T2D (Table 2.11) were purchased from Charles River (Massachusetts, USA) and stored at -80°C until RNA was extracted as described in section 2.15. BAT, SWAT and EWAT from various mouse models of obesity and T2D (Table 2.12) were purchased from the Jackson Laboratory (Maine, USA) and stored at -80°C until RNA was extracted as described in section 2.15.

Strain	Animal Characteristics	Strain Code
CD®	Control Sprague Dawley rats, maintained on CRL 5L79 rodent chow.	1
Zucker (Zuk) FA/FA Rat	Obesity, Insulin Resistance, Hyperinsulinemia, Hypertriglyceridemia, Hypercholesterolemia, Metabolic Syndrome. Commonly used as an obese metabolic syndrome model.	185
ZDF FA/FA ZDF (Zucker Diabetic Fatty) Rat	Obesity, Insulin Resistance, Hyperinsulinemia, Type 2 Diabetes, Hyperglycemia, Hypertriglyceridemia, Hypercholesterolemia.	370
Obese Prone (OP)-CD Standard Diet (OP-CD)Rat	Developed from a line of CD rats by selecting future breeders with accelerated weight gain. The OP-CD become obese when fed high-fat diets. Polygenic obesity develops despite having a fully functioning leptin receptor.	463
Obese Resistant-CD Standard Diet (OR-CD) Rat	Developed from a line of CD rats. This model does not become obese when fed high-fat diets.	462
OR-CD (60% high fat diet) 10 weeks- age matched to SD	Fed D12492i rodent diet with 60 % Kcal fat, starting at 6 weeks of age and remained on HFD diet for 6 weeks (total 12 weeks of age).	462
OP-CD (60% high fat diet) 10 weeks- age matched to SD	Fed D12492i rodent diet with 60 Kcal% fat starting at 6 weeks of age and remained on HFD diet for 6 weeks (total 12 weeks of age).	463

Table 2. 12 Details of mouse models from which adipose tissue samples were used.

Strain	Animal Characteristics	Strain Code
C57Bl6 J (SD)	Control animals, fed LabDiet® 5K52 formulation (6% fat).	000664
C57Bl6 J (HFD)	C57BL/6J mice fed D12492 (60 kcal% fat) diet. Mice are obese and display mild hyperglycaemia, dyslipidaemia, and impaired glucose tolerance.	380050
B6.Cg-Lep ob/J (ob ob)	Mice exhibit obesity, hyperphagia, transient hyperglycemia, glucose intolerance, and elevated plasma insulin. Mice were maintained on LabDiet® 5K20 formulation (10% fat).	000632
B6.BKS (D)-Lep db/J (db db)	Mice exhibit obesity, polyphagia and hyperinsulinemia throughout an 18- to 20-month life span. Mice were maintained on LabDiet® 5K52 formulation (6% fat)	000697

Table 2. 13 Details of rat models from which adipose tissue samples were used.

2.28 Data handling and statistical analysis

Data analysis was carried out using GraphPad Prism v5 statistical package. Normality of data was established by performing Shapiro–Wilk analysis. For normally distributed data, statistical significance was determined by performing paired and unpaired t-tests as appropriate or ANOVA with Dunnett's post-hoc tests for experiments with multiple groups, as detailed in the figure legends. Statistical significance of non-parametric data was assessed by performing a Wilcoxon-signed rank test for paired data or Man-Whitney U test for data with 2 independent groups. Correlations were assessed by determining the Pearson correlation coefficient for parametric data. Parametric data with more than 2 variables was assessed by performing 2-way ANOVA. Data is presented as mean ± standard error of the mean (S.E.M). A P value of <0.05 was considered statistically significant.

CHAPTER 3: The impact of obesity on primary human myotube function

3.1 Introduction

Obesity is a significant risk factor for the development of skeletal muscle insulin resistance and is also associated with chronic inflammation and skeletal muscle atrophy (Sarcopenic obesity) (391). However, performing *in vivo* mechanistic studies to investigate the impact of increased adiposity on human skeletal muscle metabolic function is challenging, due to the presence of inter-organ crosstalk and limitations in both experimental conditions and subject numbers. As a result, immortalised murine (C2C12) and Rat (L6) myoblast cell lines have commonly been used in skeletal muscle research since the late 1960s (392, 393). These cell lines provide a valuable tool, as they can be rapidly expanded to facilitate numerous investigations, devoid of external stimuli. However, despite being of skeletal muscle origin, the translation of findings from such studies to human skeletal muscle has not been studied in depth and so should be interpreted with caution.

It is also possible to culture primary human myotubes from satellite cells obtained via enzymatic digestion of human skeletal muscle tissue. Although obtaining human skeletal muscle tissue is an invasive procedure and culture growth rates are considerably slower than rodent cell lines, primary human myotubes are advantageous as they facilitate studies of skeletal muscle metabolic function that are physiologically relevant to humans. Indeed, a number of studies have reported that primary human myotubes from individuals with T2D retain the phenotype of their donor. Firstly, Nikoulina et al. demonstrated an impaired interaction of IRS1 with PI3K following insulin stimulation of primary human myotubes derived from individuals with T2D (394), a finding since corroborated by Bouzakri et al. (395). Further downstream in the insulin signalling cascade, Cozzone et al. reported blunted insulin induced phosphorylation of both AKT^{Ser473} and AKT^{Thr308} residues in primary human myotubes cultured from diabetic individuals (396).

Functionally, it appears that, as *in vivo,* such blunted activation of the insulin signalling pathway in T2D myotubes results in a reduction of both insulin stimulated glycogen synthesis and glucose uptake (397, 398).

However, studies investigating the impact of obesity on primary human myotube function are limited, particularly in cells derived from elderly donors, the population most associated with skeletal muscle dysfunction. Therefore, in this chapter we aimed to investigate the impact of obesity on elderly primary human myotube function and determine if primary human myotubes provide a physiologically relevant model of obese elderly muscle for further mechanistic studies.

3.1.1 Chapter aims

This chapter aims to:

- Measure the mRNA expression of genes associated with insulin signalling and glucose metabolism in human skeletal muscle tissue from lean and obese individuals to identify candidate genes that are differentially expressed with increased adiposity.

- Determine if differential gene expression in human skeletal muscle tissue is retained in primary human myotubes cultured from lean and obese individuals.

- Determine the impact of obesity on primary human myotube function, including myotube insulin sensitivity and inflammation.

- Utilising an *in vitro* model of exercise, determine the impact of obesity on the hypertrophic response of primary human myotubes.

3.2 Results

3.2.1 Insulin signalling associated gene expression in skeletal muscle tissue from individuals with differing adiposity

We first investigated the expression of 48 genes related to the insulin signalling pathway in skeletal muscle tissue derived from lean, overweight and obese individuals, in order to identify candidate genes that are differentially expressed with increasing adiposity and may impact skeletal muscle insulin sensitivity.

Overall, there was little difference in the gene expression profile between lean and obese individuals in all groups of genes (Figure 3.1 A-E). However, the expression of fructose bisphosphatase 1 (FBP1) was approximately 2-fold greater in skeletal muscle tissue obtained from obese individuals (2.8 ± 0.4) in comparison to both lean (1.4 ± 0.4) and overweight (1.5 ± 0.1) individuals (P = 0.011). Additionally, FBP1 expression displayed a significant positive correlation with BMI (P = 0.0058 r^2 0.35), bodyweight (P = 0.028 r^2 = 0.24) and % body fat (P = 0.0008, r^2 = 0.48) (Figure 3.2 A-C). FBP1 expression also displayed a positive trend with waist to hip ratio; however this was not statistically significant (Figure 3.2 D). Additionally, the mean expression of TBC1D4, (coding for AS160), was lower in skeletal muscle tissue derived from obese individuals (0.51 ± 0.05) in comparison to overweight individuals (0.9 ± 0.1, P = <0.05). Despite such differential expression, there was no correlation between TBC1D4 expression and patient characteristics.

Furthermore, mean PPARD expression was less on average in obese individuals in comparison to both lean and overweight individuals, although this difference did not reach statistical significance (P = 0.072) and again did not correlate with patient characteristics. Conversely both CEBPA and CEBPB expression was observed to be elevated in both overweight and obese skeletal muscle tissue in comparison to lean skeletal muscle tissue (Figure 3.1 D). Although such differences were not statistically significant, there was a significant positive correlation between CEBPA expression and %

body fat (P = 0.030, r^2 = 0.20). Similarly a positive trend in CEBPB mRNA expression and % body fat (P = 0.052, r^2 = 0.16) was also observed.

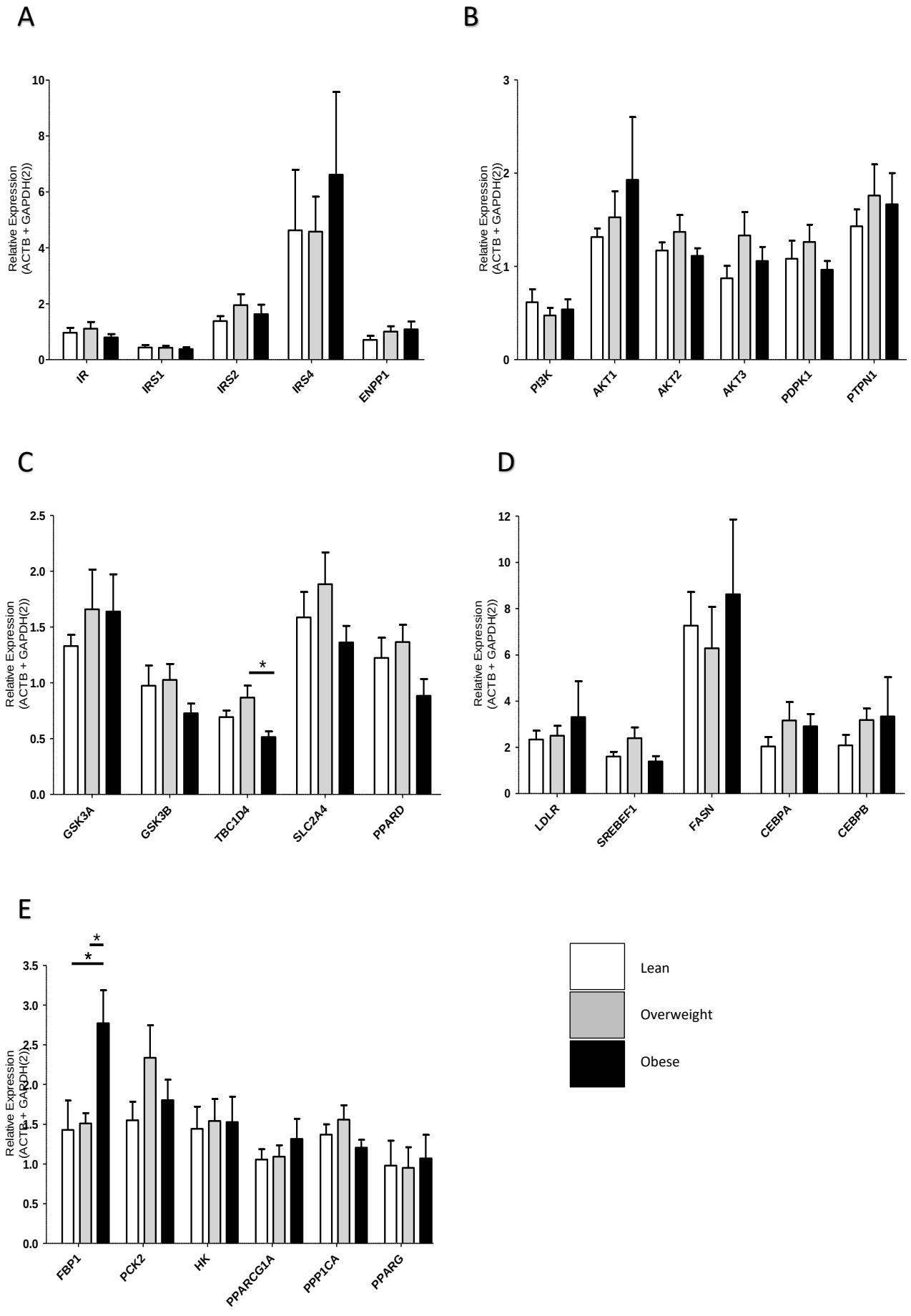
A
B
C
D
E
Relative Expression (ACTB + GAPDH(2))
IR
IRS1
IRS2
IRS4
ENPP1
PI3K
AKT1
AKT2
AKT3
PDPK1
PTPN1
GSK3A
GSK3B
TBC1D4
SLC2A4
PPARD
LDLR
SREBEF1
FASN
CEBPA
CEBPB
FBP1
PCK2
HK
PPARCG1A
PPP1CA
PPARG
*
Lean
Overweight
Obese

Figure 3. 1. mRNA expression of insulin signalling pathway associated genes in human skeletal muscle tissue of individuals with varying BMI.

A. mRNA expression of early insulin signalling pathway genes, n = 8 Lean (L), n = 9 overweight (Ow) and n = 7 obese (Ob) for all genes, except IRS2 (n = 8 L, n = 9 Ow, n = 6 Ob) and IRS4 (n = 7 L, n = 6 Ow, n = 4 Ob). **B.** mRNA expression of PI3K-AKT signalling pathway genes, n = 8 L, n = 9 Ow and n = 7 Ob for all genes, except PI3K (n = 8 L, n = 9 Ow, n = 6 Ob). **C.** mRNA expression of insulin signalling downstream effector genes, n = 8 L, n = 9 Ow and n = 7 Ob for all genes. **D.** mRNA expression of genes associated with lipid metabolisms, n = 8 L, n = 9 Ow and n = 7 Ob for all genes, except CEBPB (n = 8 L, n = 9 Ow, n = 6 Ob) and IRS4 (n = 7 L, n = 6 Ow, n = 4 Ob). **E.** mRNA expression of genes associated with glucose metabolism. n = 8 L, n = 9 Ow and n = 7 Ob for all genes, except FEBP1 (n = 6 L, n = 8 Ow, n = 6 Ob. Expression of mRNA was normalised to the mean of GAPDH and β actin housekeeping genes. Data are presented as mean ± S.E.M. *denotes a significant ($P < 0.05$) difference between groups as determined by post hoc t-tests with Bonferroni adjustment, following One-way ANOVA.

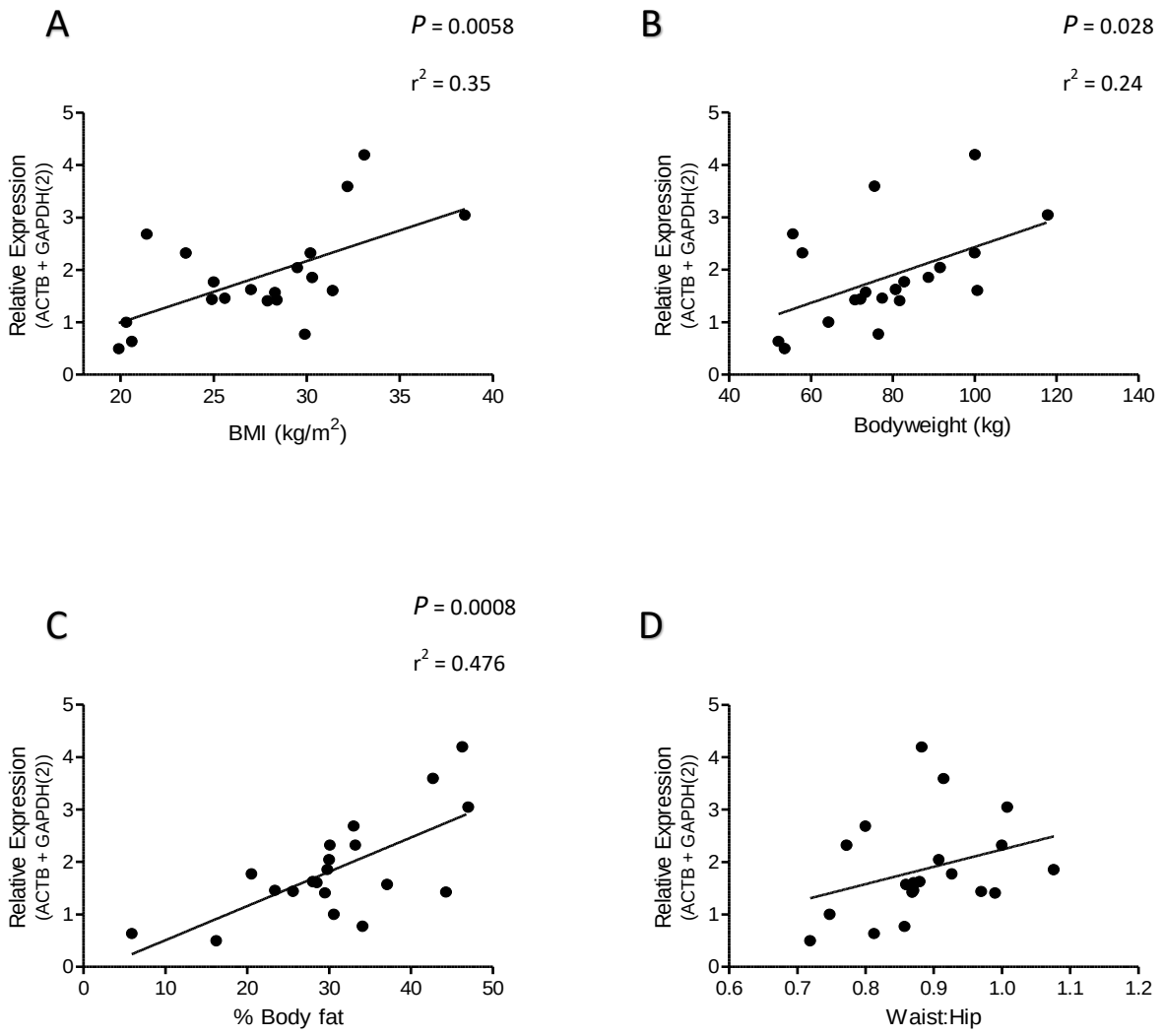

Figure 3. 2. Correlation of FBP1 mRNA expression in skeletal muscle tissue with subject characteristics.

A. Correlation of FBP1 expression in skeletal muscle tissue with BMI. **B.** Correlation of FBP1 expression in skeletal muscle tissue with bodyweight. **C.** Correlation of FBP1 expression in skeletal muscle tissue with % body fat as measured by bioimpedance. **D.** Correlation of FBP1 expression in skeletal muscle tissue with waist:hip. n = 20 for all correlations. Expression of mRNA was quantified by qRT-PCR, and normalised to the mean of GAPDH and β actin housekeeping genes.

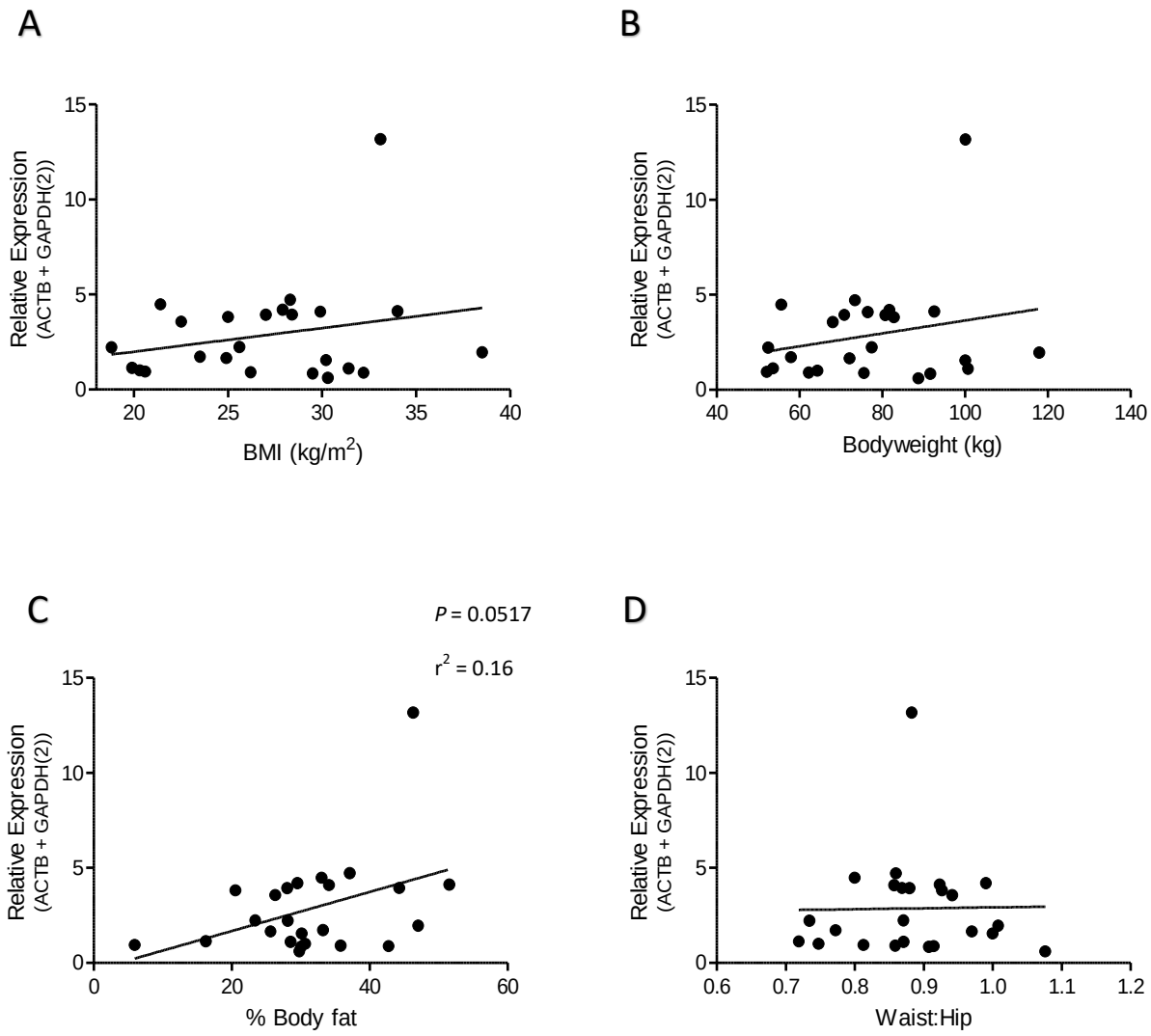

Figure 3. 3. Correlation of CEBPA mRNA expression in skeletal muscle tissue with subject characteristics.

A. Correlation of CEBPA expression in skeletal muscle tissue with BMI. **B.** Correlation of CEBPA expression in skeletal muscle tissue with bodyweight. **C.** Correlation of CEBPA expression in skeletal muscle tissue with % body fat as measured by bioimpedance. **D.** Correlation of CEBPA expression in skeletal muscle tissue with waist:hip. n = 24 for all correlations. Expression of mRNA was quantified by qRT-PCR, and and normalised to the mean of GAPDH and β actin housekeeping genes.

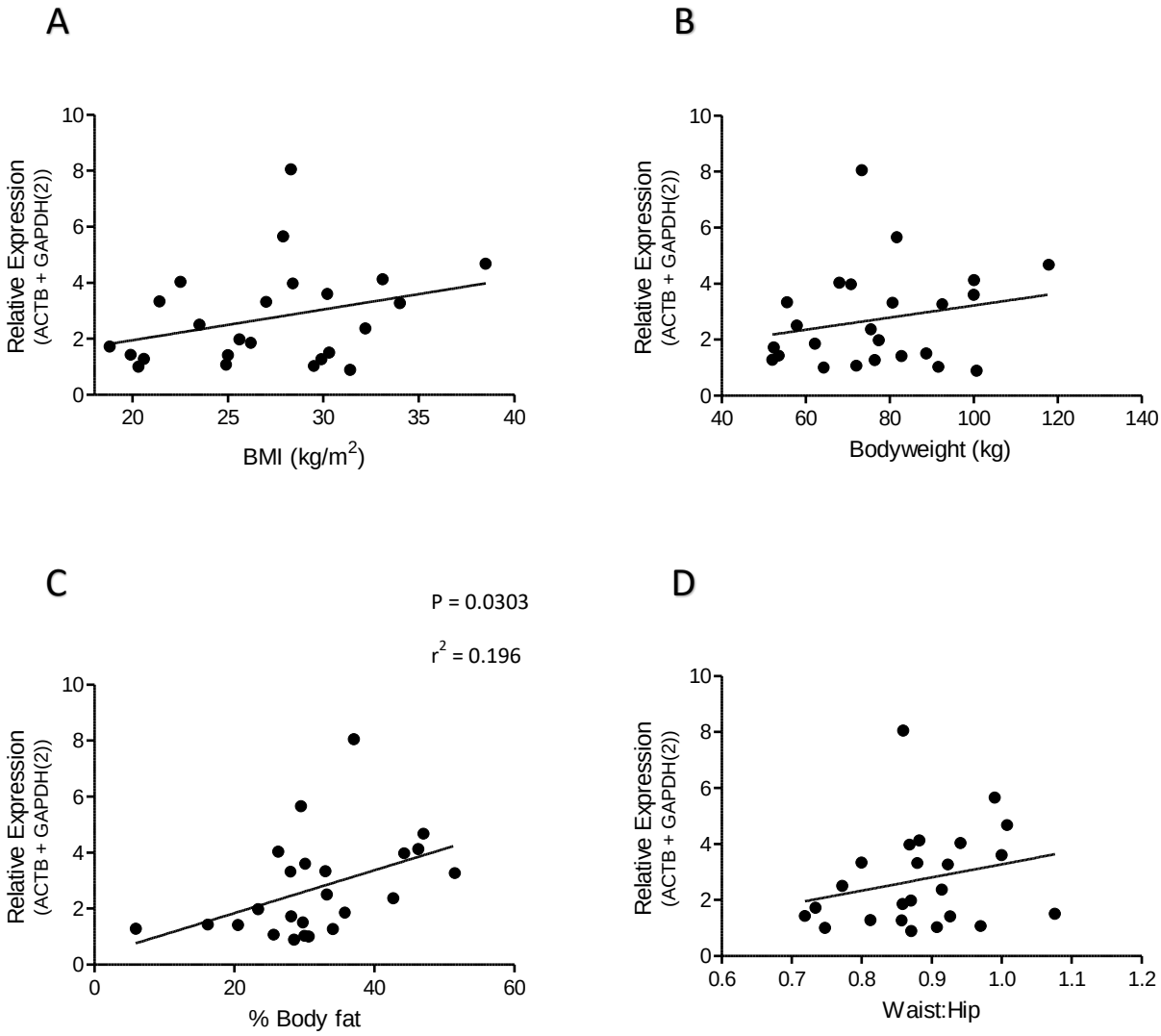

Figure 3. 4. Correlation of CEBPB mRNA expression in skeletal muscle tissue with subject characteristics.

A. Correlation of CEBPB expression in skeletal muscle tissue with BMI. **B.** Correlation of CEBPB expression in skeletal muscle tissue with bodyweight. **C.** Correlation of CEBPB expression in skeletal muscle tissue with % body fat as measured by bioimpedance. **D.** Correlation of CEBPB expression in skeletal muscle tissue with waist: hip. n = 24 for all correlations. Expression of mRNA was quantified by qRT-PCR, and normalised to the mean of GAPDH and β actin housekeeping genes.

3.2.2 Validation of differential gene expression in skeletal muscle tissue by qRT-PCR

Next, in order to validate the differential gene expression of FBP1 and TBC1D4 observed in the skeletal muscle tissue of obese individuals, we measured FBP1 and TBC1D4 mRNA expression in human skeletal muscle tissue samples derived from lean and obese individuals by performing individual qRT PCR. As in 3.2.1, mean FBP1 expression was greater in skeletal muscle tissue of obese individuals in comparison to lean individuals, but this was not statistically significant (Figure 3.5 A), while TBC1D4 expression was again significantly less in skeletal muscle tissue derived from obese tissue (Figure 3.5 B).

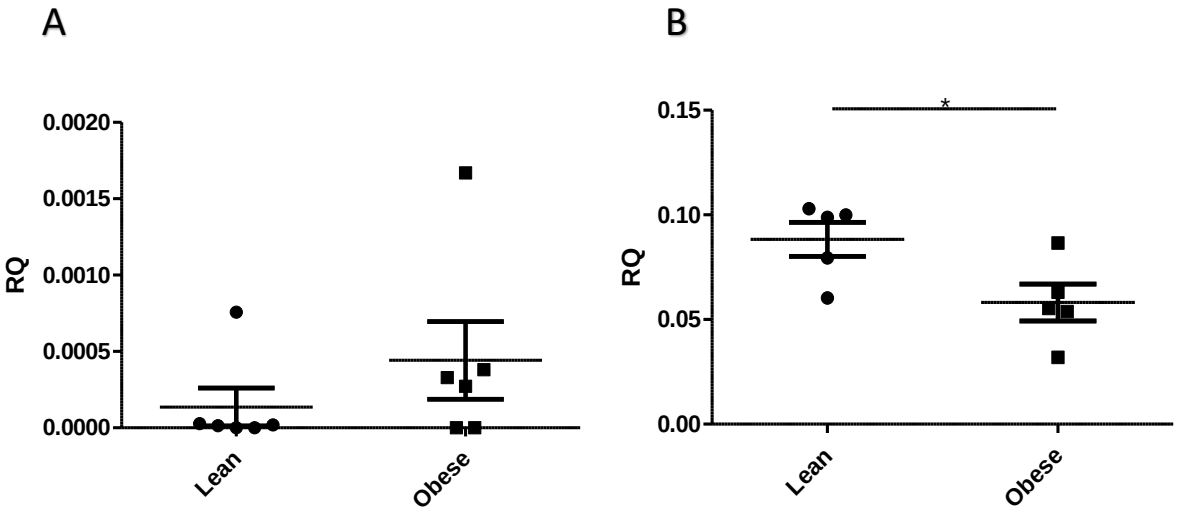

Figure 3. 5. Validation of differential gene expression in skeletal muscle tissue by qRT-PCR.

A. FBP1 expression in skeletal muscle tissue from lean (n = 6) and obese (n = 6) subjects. **B.** TBC1D4 expression in skeletal muscle tissue from lean (n = 5) and obese (n = 5) subjects. Data presented as mean ± S.E.M. Expression of mRNA was quantified by qRT-PCR, and normalised using GAPDH, expressed as relative quantification (RQ). * signifies $P < 0.05$ as determined via unpaired T-tests.

3.2.3 Validation of differential gene expression in primary human myotubes by qRT-PCR

Having identified differentially expressed gene targets in the skeletal muscle tissue of obese individuals, we then aimed to identify if such differential expression is retained in primary human myotubes cultured from lean and obese individuals. All experiments were performed on myotubes differentiated for 8 days.

Firstly, the successful culture of primary human myotubes from skeletal muscle tissue was confirmed via immunofluorescent staining of primary human myotubes for the muscle specific marker, desmin. Cells cultured from human skeletal muscle tissue consistently displayed multinucleated, desmin positive myotube structures (Figure 3.6 A). Similar to skeletal muscle tissue, the expression of FBP1 was greater on average in primary human myotubes from obese individuals (0.002 ± 0.001) in comparison to lean individuals (0.0002 ± 0.0001), however this was not statistically significant (Figure 3.6 C, $P = 0.11$). Additionally, TBC1D4 mRNA expression was ~50% less on average in obese primary human myotubes (0.04 ± 0.01) in comparison to lean myotubes (0.1 ± 0.06), however again this did not reach statistical significance (Figure 3.6 D).

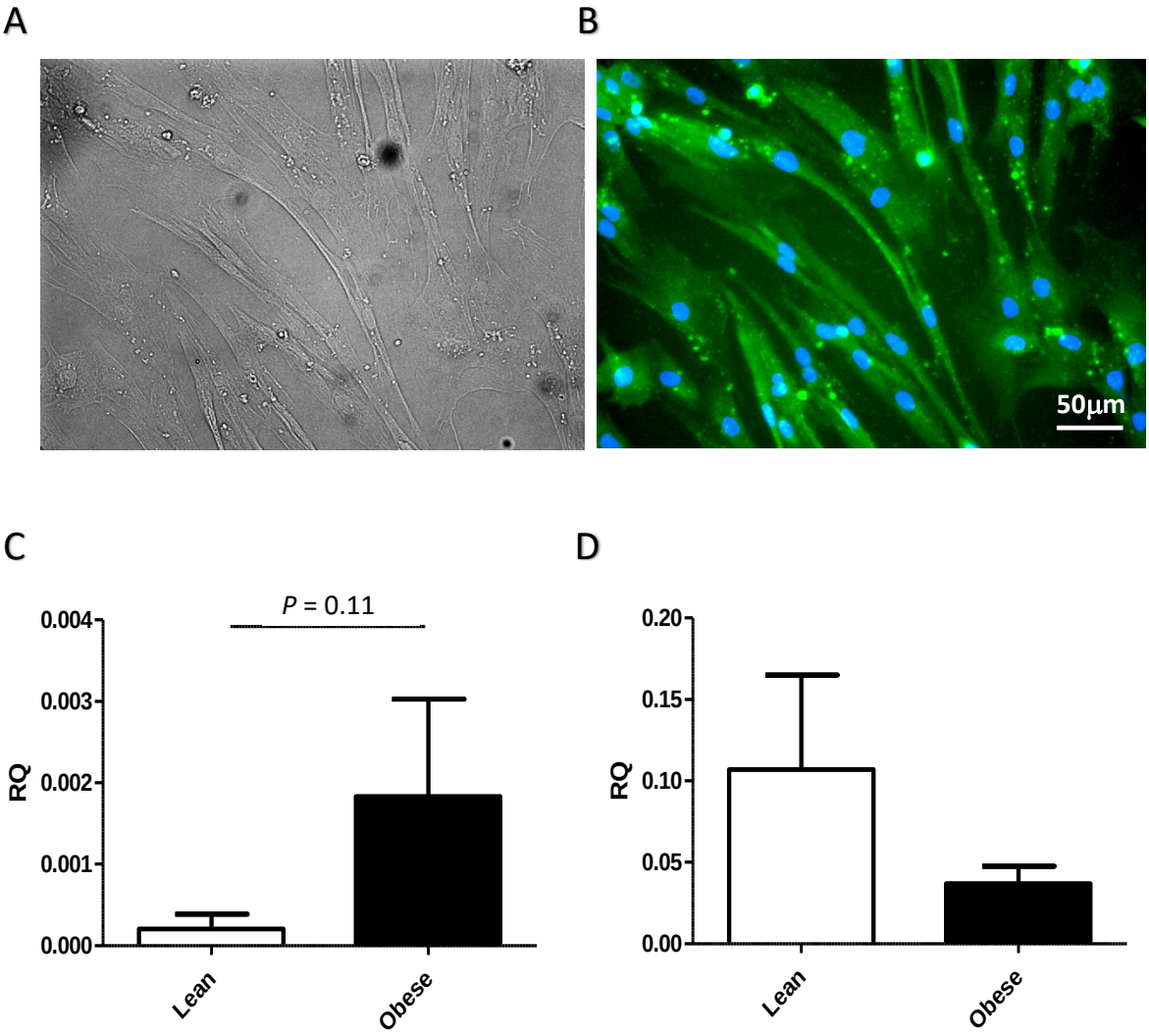

Figure 3. 6. Differential gene expression in primary human myotubes from lean and obese donors.

A. Brightfield imaging of primary human myotubes. **B.** Immunofluorescent staining of primary human myotubes for desmin (green) and DAPI (blue). **C.** FBP1 mRNA expression in primary human myotubes from lean (n = 5) and obese (n = 5). **D.** TBC1D4 mRNA expression in primary human myotubes from lean (n = 5) and obese (n = 5) donors. Expression of mRNA was quantified by qRT-PCR, and normalised using GAPDH, expressed as relative quantification (RQ). Data presented as mean ± S.E.M. Statistical significance was determined via unpaired T-tests.

3.2.4 Obesity impairs insulin sensitivity in primary human myotubes

Following the observation that primary human myotubes may retain donor characteristics of mRNA expression, we next investigated if primary human myotubes derived from obese individuals (differentiated for 8-days) exhibit functional differences in insulin sensitivity.

Primary human myotubes derived from lean individuals displayed relatively little basal phosphorylation of AKT^{Ser473}. Following acute insulin stimulation (100 nM, 0-30 mins) AKT phosphorylation increased rapidly in a time dependant manner, up to 3-fold (Figure 3.7 A). In contrast, myotubes derived from obese individuals appeared to exhibit increased phosphorylation of AKT at baseline and displayed a blunted response to insulin, increasing only 1.2-fold following 30 min of insulin stimulation (Figure 3.7 B). Additionally, insulin induced phosphorylation of AKT^{Thr308} was also measured by mesoscale analysis (Figure 3.7 D). Phosphorylation of AKT^{Thr308} increased approximately 1.5-fold in response to 3 - 30 nM insulin in lean myotubes. However, again, myotubes derived from obese individuals demonstrated a reduced response, increasing only approximately 1.2-fold in response to 30 nM insulin.

Following the observation of blunted insulin induced activation of the insulin signalling pathway in obese myotubes, we then investigated the potential downstream impact on glucose uptake. Primary human myotubes cultured from lean subjects increased glucose uptake approximately 2-fold in response to insulin (100 nM, 30 min) (Figure 3.8). In contrast, myotubes cultured from obese subjects displayed blunted glucose uptake to the same stimuli (Figure 3.8).

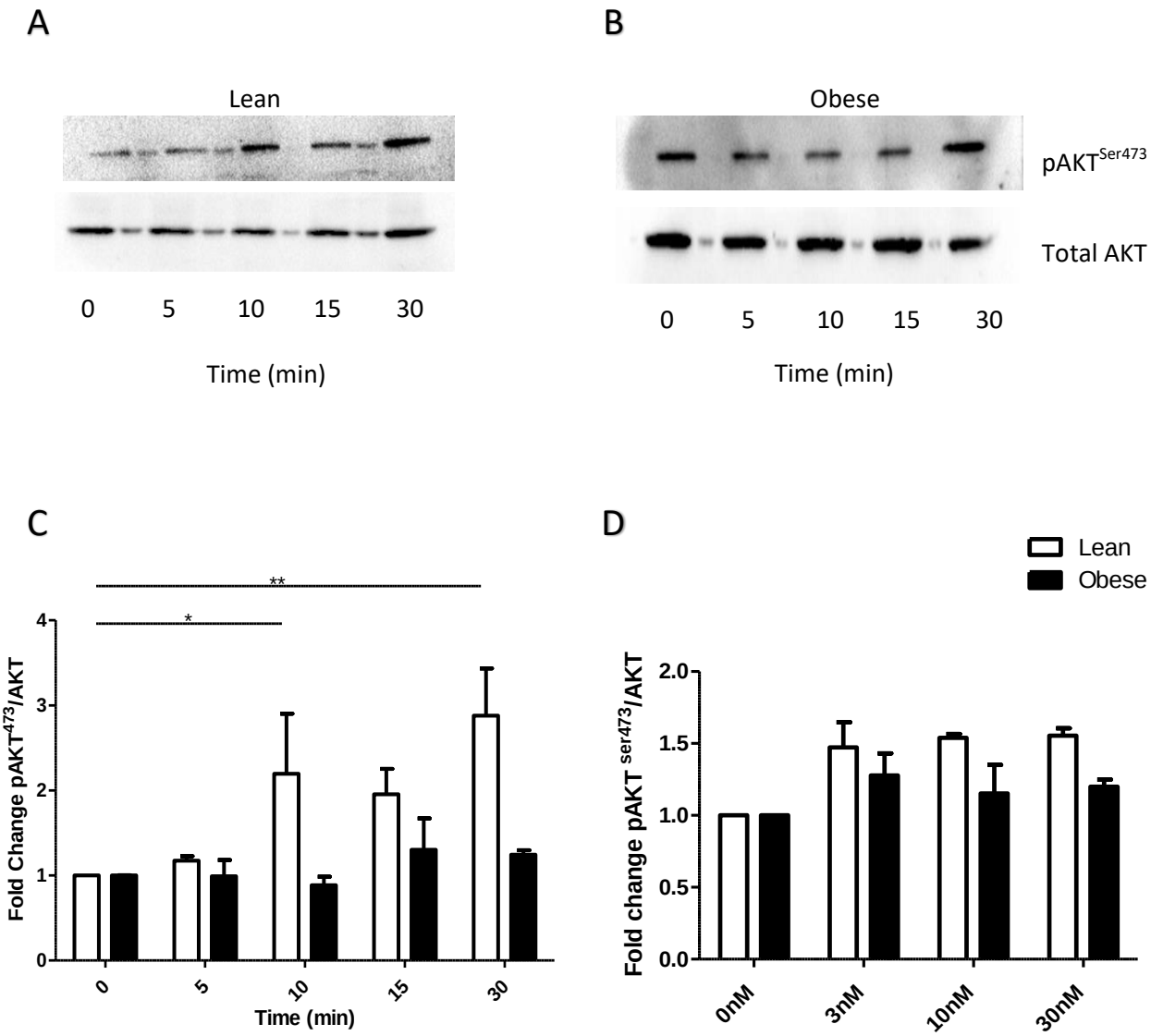

Figure 3. 7. The insulin signalling response is blunted in primary human myotubes derived from obese individuals.

A. Phosphorylation of AKT^{Ser473} in primary human myotubes derived from lean individuals following 100 nM insulin stimulation (n = 3 primary donors, 15 μg protein loaded per lane). **B.** Phosphorylation of AKT^{Ser473} in primary human myotubes derived from lean individuals following 100 nM insulin stimulation (n = 3 primary donors, 15 μg protein loaded per lane). **C.** Densitometric analysis of Phospho AKT^{Ser473} western blots normalised to total AKT. **D.** Phosphorylation of AKT^{Thr308} in lean (n = 2) and obese (n = 2) primary human myotubes in response to 30 min insulin, measured by mesoscale analysis. Data are represented as mean ± S.E.M. * signifies $P < 0.05$, ** signifies $P < 0.01$, indicating a significant increase in AKT phosphorylation following insulin stimulation, as determined by Bonferroni post- hoc tests following 2-Way ANOVA.

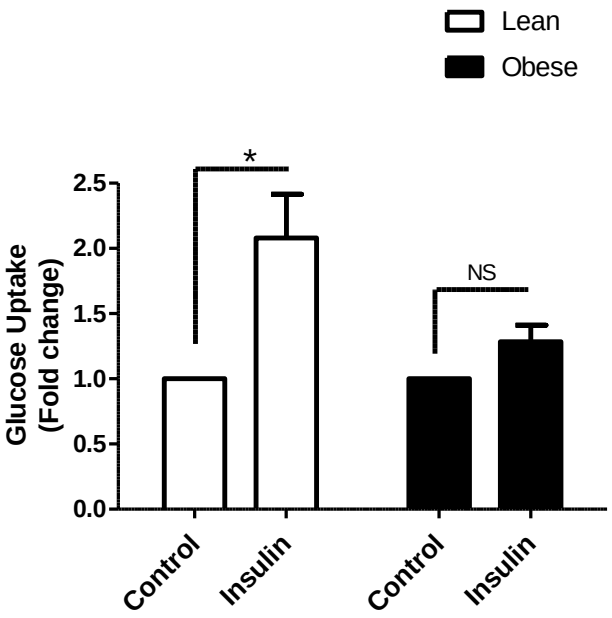

Figure 3. 8. Insulin stimulated glucose uptake is blunted in primary human myotubes cultured from obese individuals.

Effect of insulin (100 nM, 30 min) on 2-NBDG glucose uptake in primary human myotubes derived from lean (n = 4 females) and obese (n = 3 females) subjects. Data presented as mean ± S.E.M. *P < 0.05, indicates a significant effect of insulin stimulation as determined by Bonferroni post-hoc tests following 2-Way ANOVA.

3.2.5 Obesity increases proinflammatory cytokine release from primary human myotubes

Obesity is often associated with a chronic increased inflammatory burden that may also contribute to the development of skeletal muscle insulin resistance. Therefore, we investigated whether primary human myotubes from obese individuals are inherently more inflammatory. Myotubes cultured from obese individuals secreted a significantly greater amount of IL-6 (144 ± 82 pg/ml) under basal conditions in comparison to lean individuals (Figure 3.9 A, $P = 0.027$), with IL-6 being undetectable in the supernatants from 3 of 4 lean individuals. Additionally, basal IL-6 secretion displayed a significant positive correlation with BMI (Figure 3.9 B, $r^2 = 0.89$, $P = 0.0072$). Stimulation of primary human myotubes with IL-1 (1 ng/ml, 4 h) evoked a significant increase in IL-6 secretion of a similar amount in both lean and obese individuals (Figure 3.9 A). On average, basal secretion of IL-8 was also greater in obese myotubes compared to lean myotubes. However, the amount of secreted IL-8 detected was highly variable across patient samples and as such this observation did not reach statistical significance (Figure 3.9 C).

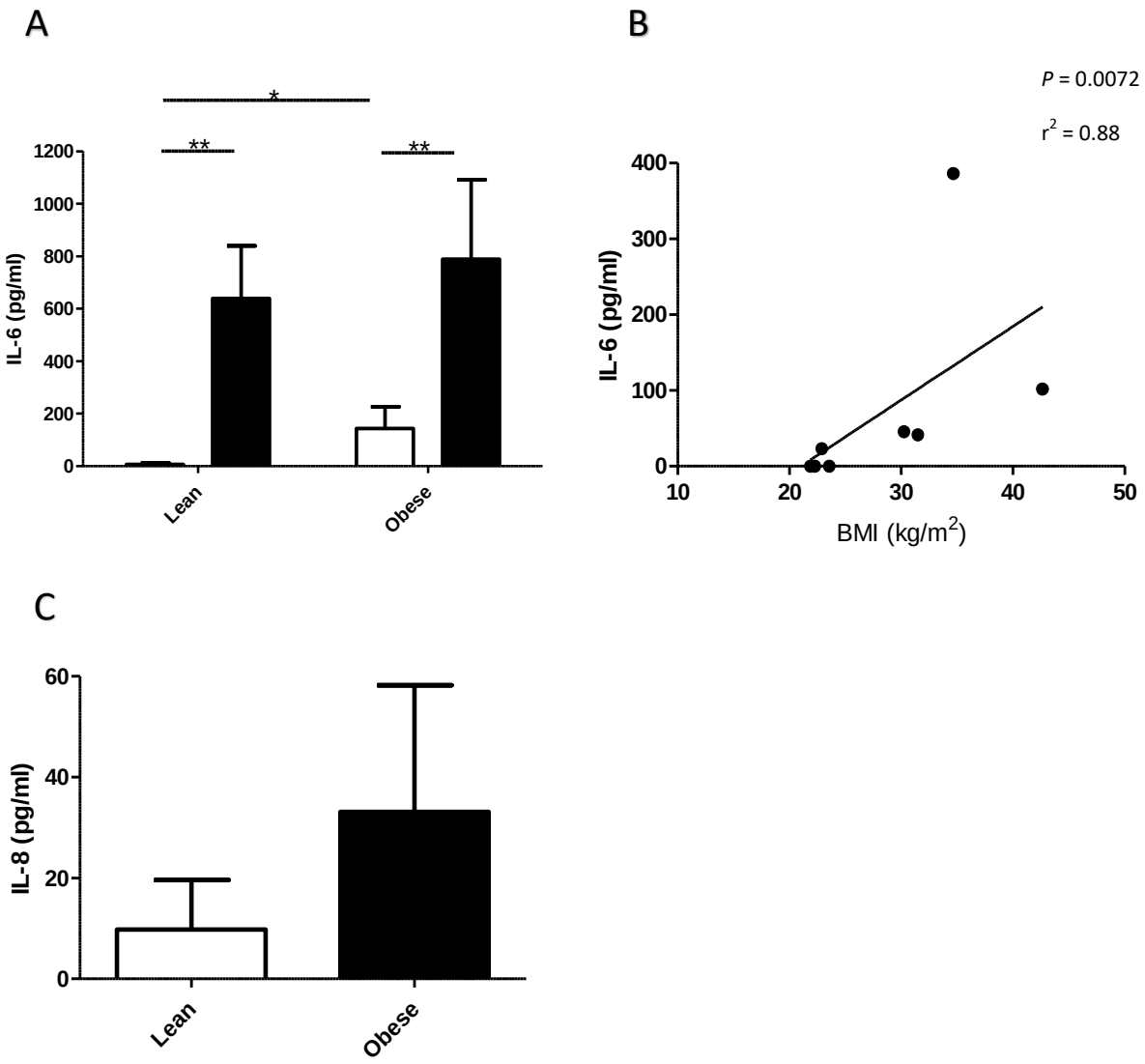

Figure 3. 9. Pro-inflammatory cytokine secretion from primary human myotubes derived from lean and obese individuals.

A. Concentration of IL-6 in the supernatant of primary human myotubes from lean (n = 4) and obese (n = 4) individuals under basal conditions (24 h) (clear bars) and following IL-1 stimulation (1 ng/ ml, 4 h,) (filled bars). **B.** Correlation of basal IL-6 secretion (24 h) from primary human myotubes with BMI. **C** Concentration of IL-8 in the supernatant of primary human myotubes cultured from lean (n = 4) and obese (n = 4) individuals under basal conditions (24 h). All myotubes were differentiated for 8 days. Data are represented as mean ± S.E.M. *signifies a significant ($P < 0.05$) difference in IL-6 secretion between unstimulated lean and obese myotubes as determined by Bonferroni post-hoc tests following 2-Way ANOVA. ** signifies a significant $P < 0.01$ effect of IL-1 stimulation on Il-6 secretion as determined by Bonferroni post- hoc tests following 2-Way ANOVA.

3.2.6 Obesity does not affect intramyocellular lipid content in primary human myotubes

In order to investigate the effect of obesity on intramyocellular lipid content, primary human myotubes were stained with Oil Red O. No significant difference in either the average particle size, or total intracellular lipid content (normalised to total protein content) was observed between primary human myotubes cultured from lean and obese individuals (Figure 3.10).

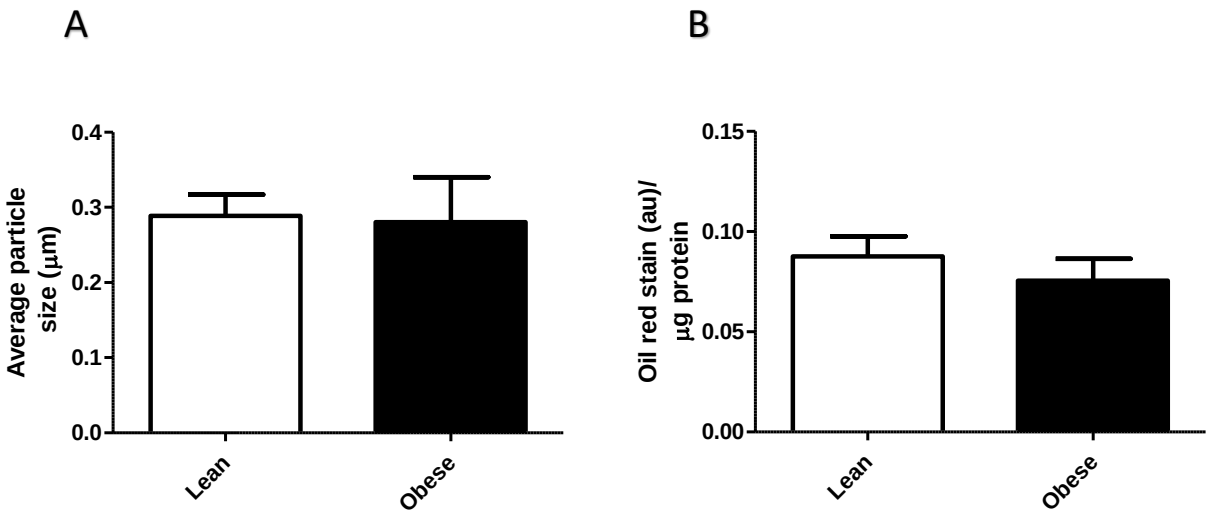

Figure 3. 10. Oil Red O Staining of primary human myotubes cultured from lean and obese individuals.

A. Size of Oil Red O positive lipid droplet particles in lean (n = 3) and obese (n = 3) primary human myotubes. **B**. Absorbance of liberated Oil Red O stain in lean (n = 3) and obese (n = 3) primary human myotubes, normalised to total protein content. Data are represented as mean ± S.E.M.

3.2.7 Atrophic gene expression is upregulated in the skeletal muscle of obese individuals

In addition to insulin resistance, obesity is associated with the development of sarcopenic obesity, characterised a reduction of skeletal muscle mass and quality. Thus, we measured mRNA expression of atrophic genes in skeletal muscle tissue from lean and obese individuals.

The expression of both the cysteine protease calpain 2 and myostatin was approximately 2-fold greater in the skeletal muscle tissue of obese individuals (P = 0.017 and P = 0.0026 respectively). Additionally, the expression of calpain 1 in obese individuals (1.6 ± 0.2) was greater on average than in lean individuals (1.1 ± 0.2) (P = 0.096). In contrast, no significant difference in MAFbx of MuRF1 expression was observed between lean and obese individuals (Figure 3.11 A).

Following the identification of differential expression of atrophic genes in human skeletal muscle tissue, we next measured such gene expression in primary human myotubes cultured from lean and obese individuals, in order to determine if differential expression of atrophic genes is maintained in primary human cultures. The expression of FOXO3, MAFbx and myostatin was significantly ($P < 0.05$) upregulated in the primary human myotubes cultured from obese individuals (Figure 3.11 B). However, there was no difference in MuRF1, calpain 1 or calpain 2 expression.

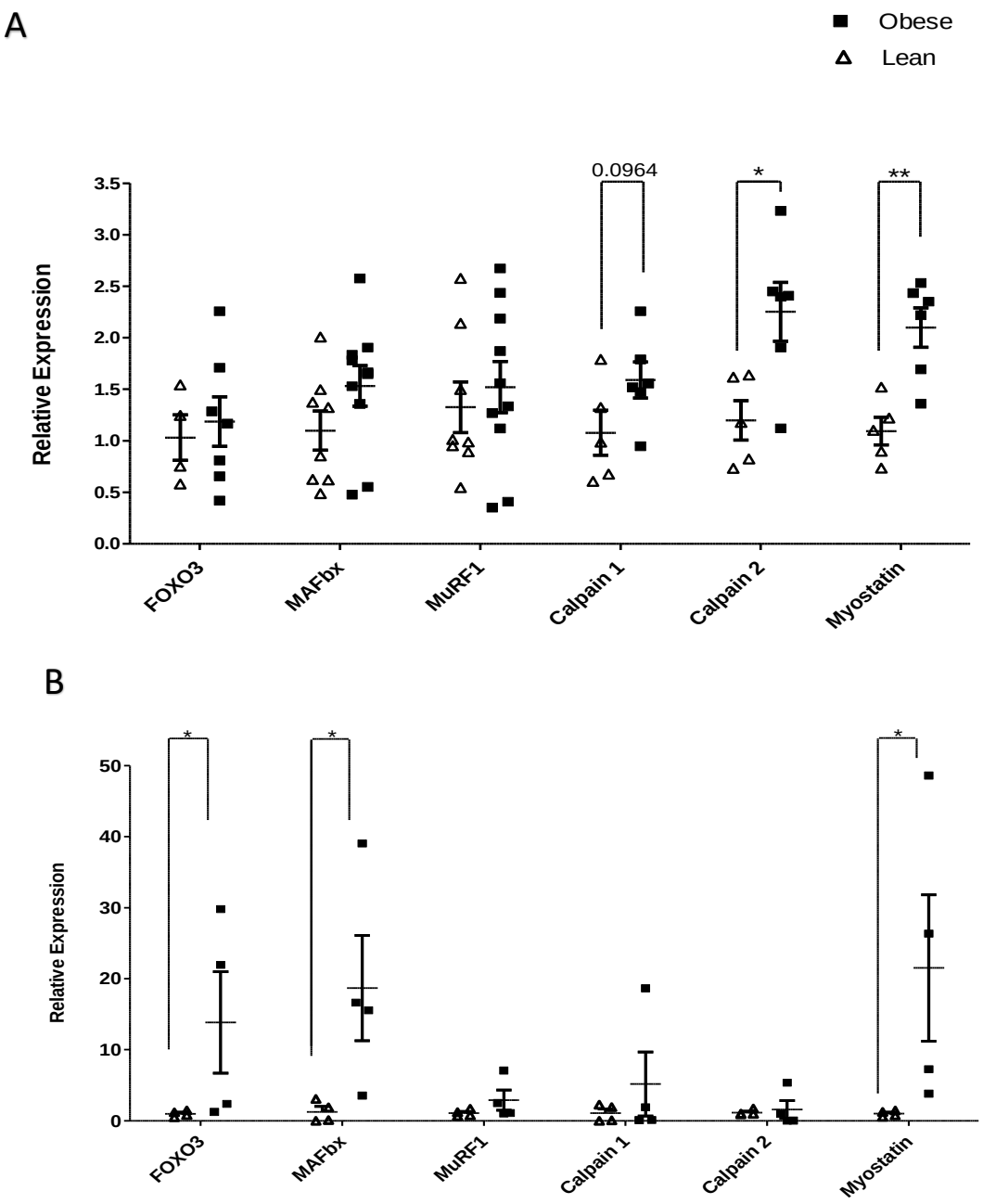

Figure 3. 11. Atrophic gene expression in human skeletal muscle tissue and primary human myotubes from lean and obese individuals.

A. mRNA expression of MAFbx, MuRF1 (n = 8 lean, n = 10 obese) FOXO3, calpain 1, calpain 2 and myostatin (n = 5 lean, n = 6 obese) in skeletal muscle tissue. **B** Atrophic gene expression in primary human myotubes (n = 4 lean and n = 4 obese). Data are represented as mean ± S.E.M. Expression of mRNA was quantified by qRT-PCR, and normalised using GAPDH. Data are represented as mean ± S.E.M. * signifies $P < 0.05$, ** signifies $P < 0.01$ as determined by unpaired T-tests.

3.2.8 The Contraction induced hypertrophic response of myostatin suppression is intrinsically impaired in obese primary human myotubes

Finally, we aimed to determine whether myotubes cultured from lean and obese individuals display a differential hypertrophic response to exercise. To achieve this, primary human myotubes were subject to electrical pulse stimulation (EPS) to replicate a hypertrophic exercise response *in vitro*.

First, to validate that EPS induced hypertrophy, protein synthesis was measured via the SUnSET method. Treatment of primary human myotubes with puromycin (30 min) increased puromycin positive protein expression indicating puromycin incorporation, as detected by immunoblotting (Figure 3.12). Additionally, puromycin positive protein was detected following EPS, even in the absence of puromycin. Following 24 h of EPS, more puromycin was detected in comparison to unstimulated myotubes via immunoblotting, indicating greater puromycin incorporation and therefore increased protein synthesis (Figure 3.12 A).

EPS evoked a significant (2-fold) decrease in the expression of myostatin mRNA in primary human myotubes from lean individuals (Figure 3.12 B). In contrast, no decrease in myostatin mRNA was observed in myotubes derived from obese individuals in response to the same stimuli.

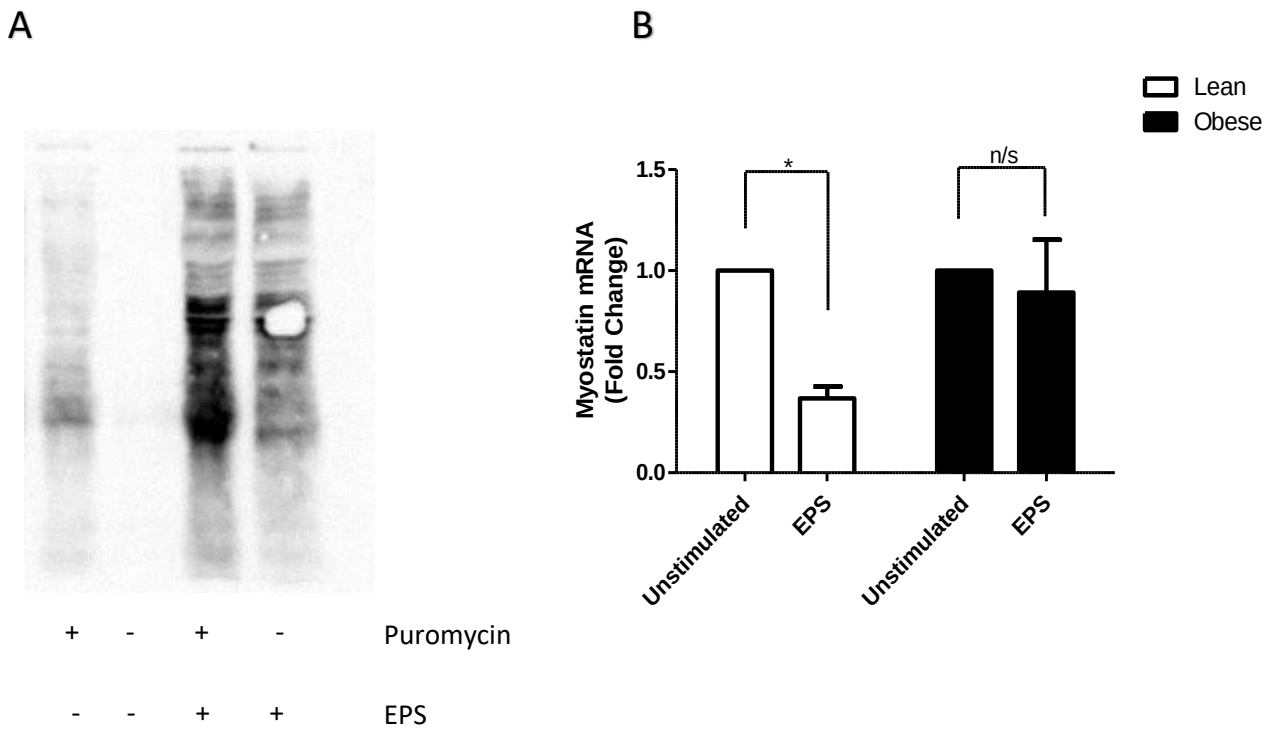

Figure 3. 12. The hypertrophic response to EPS in primary human myotubes.

A. Representative western blot of puromycin protein content in primary human myotubes with and with without EPS (24 h) and with and without puromycin (final 30 min of EPS stimulation) (15 µg protein loaded per lane). **B.** Myostatin mRNA expression in lean and obese primary human myotubes following 24 h EPS. Expression of mRNA was quantified by qRT-PCR, and normalised using GAPDH. Data are presented as mean ±S.E.M. * signifies a significant ($P < 0.05$) effect of EPS on myostatin expression as determined by post hoc T-tests with Bonferroni adjustment following 2-way ANOVA.

3.3 Discussion

3.3.1 The impact of obesity and primary human myotube insulin sensitivity and glucose uptake

Profiling of genes associated with insulin signalling and glucose metabolism in human skeletal muscle tissue from lean, overweight and obese subjects identified a significant upregulation of FBP1 and a significant downregulation of TBC1D4 mRNA expression in obese individuals, in comparison to lean and overweight individuals. Additionally, differential expression of FPB1 and TBC1D4 was also observed between primary human myotubes cultured from lean and obese individuals, although such changes were not statistically significant.

The gene FBP1 encodes for the protein fructose-1, 6-bisphosphatase (FBPase), a rate-limiting enzyme within the gluconeogenesis pathway, which acts to catalyse the irreversible hydrolysis of fructose 1, 6-bisphosphate, in turn generating fructose-6-phosphate and inorganic phosphate. In line with the findings of this investigation, increased hepatic FBPase protein expression and activation has been reported in rodent models of obesity and insulin resistance (399, 400). Additionally, gluconeogenesis is upregulated in humans with T2D and contributes to the hyperglycaemia typically seen in this patient population (401). It is likely that such increased gluconeogenesis is due to increased FBPase protein expression and or activity (402, 403) although direct evidence of this in human tissue has not been reported to date.

Experimentally, Zhang et al. demonstrated that FBP1 expression also increased in pancreatic β-cells following high glucose and lipid challenge and over-expression of FBP1 significantly impaired insulin secretion in these cells (404). In contrast, siRNA-mediated downregulation of FBP1 in pancreatic β-cells induced insulin secretion, while pharmacological inhibition of FBPase in a ZDF rat model of T2D, significantly reduced gluconeogenesis and blood glucose concentrations within 2 weeks (404, 405).

Interestingly, glucose stimulated insulin secretion in this model was also increased following FBP1 inhibition, indicating improved pancreatic function (405).

In light of such data, FBP1 has gained interest as a therapeutic target for the treatment of T2D, with the aim of limiting hyperglycaemia by reducing glucose production at the source, as opposed to increasing insulin production and insulin sensitivity of target tissues. To this end, a number of FBP1 inhibitors have progressed to clinical trials (406). Additionally, metformin, one of the most commonly used treatments for T2D, was recently demonstrated to achieve its anti-hyperglycaemic effect in part through FBP1 inhibition (407). It is important to note that the studies discussed above have almost exclusively been performed with a focus on liver metabolism and function, due to the liver being the primary site of gluconeogenesis in humans. As increased FBP1 expression was observed in skeletal muscle in this thesis, further investigation into the impact of increased FBP1 on skeletal muscle metabolism and its contribution to hyperglycaemia associated with obesity and T2D is needed.

As discussed in depth in section 1.3.4, TBC1D4 codes for the protein AS160, a GEF that facilitates the conversion of a Rab protein associated with GLUT4 translocation from its GTP to GDP bound state. RabGDP is functionally inactive and as a result GLUT4 translocation to the cell membrane is inhibited, resulting in decreased glucose uptake. Therefore, a decrease in TBC1D4 expression would be expected to result in less conversion of RabGTP to RabGDP, facilitating greater GLUT4 translocation to the sarcolemma. This was unexpected, as obesity is associated with decreased glucose uptake and insulin resistance (408). A possible explanation for this observation is that a reduction in TBC1D4 occurs as a compensatory mechanism to overcome reduced insulin stimulated AKT activation in the obese state. However, TBC1D4 knockdown models do in fact display impaired insulin resistance due to a dysregulation of GLUT4 trafficking, causing elevated membrane GLUT4 at baseline (409). Therefore such an effect may also be present in primary human myotubes.

Moreover, no significant differences in the mRNA expression of genes encoding for early insulin signalling pathway proteins, such as IR, IRS, PI3K, or AKT were observed between skeletal muscle tissue from lean, overweight and obese individuals. However, this was not surprising as a number of studies, including comparisons between diabetic and non-diabetic twins, have reported little change in the expression of such genes or their gene products (410, 411). Thus, skeletal muscle insulin resistance is more likely attributable to a disruption of protein kinase activation rather than a reduction in the insulin signalling capability of muscle.

Therefore, we next investigated the functional impact of increased adiposity on primary human myotube insulin signalling and glucose uptake. As expected, acute insulin stimulation evoked an increase in both AKT activation and glucose uptake in lean myotubes. Critically, myotubes derived from obese individuals displayed a considerably blunted response to insulin stimulation, with no significant increase in either AKT phosphorylation or glucose uptake observed. A similar blunting of AKT phosphorylation has previously been reported in primary human myotubes derived from diabetic individuals, with AKT2 and AKT3 isoforms showing the greatest impairment (396). Additionally, a reduction in glucose uptake and glycogen synthesis has also been reported in primary human myotubes from diabetic individuals (397). In contrast, a similar investigation by Gaster et al. found no discernible difference in insulin stimulated glucose uptake in primary human myotubes derived from lean or obese individuals (412). However, this may have been due to the average age of subjects being considerably lower (49 years) in comparison to this thesis, suggesting metabolic differences in myotubes are more apparent in the elderly.

3.3.2 Obesity increases proinflammatory cytokine release from primary human myotubes

Obesity is associated with a state of chronic low grade inflammation, attributable to an increased mass of inflamed adipose tissue, secreting a plethora of proinflammatory cytokines. In turn, such increased inflammation is associated with the development of skeletal muscle insulin resistance (413). However, few studies have investigated the direct impact of obesity on skeletal muscle inflammation. To this end, we measured proinflammatory cytokine release from primary human myotubes cultured from lean and obese donors.

Under basal conditions, primary human myotubes cultured from obese individuals secreted a significantly greater amount of IL-6, in comparison to lean individuals. A similar increase in IL-6 release from T2D myotubes has recently been observed by Ciaraldi et al. (414). In contrast, Jiang et al. reported that IL-6 secretion did not differ between primary human myotubes from T2D individuals in comparison to healthy individuals (415). However, this lack of differential IL-6 secretion may be attributable to both the control and T2D subjects being overweight, and of a similar BMI. Therefore, IL-6 secretion may still have been elevated in comparison to a lean control group. Transient IL-6 secretion from skeletal muscle occurs in response to exercise, and in turn may improve skeletal muscle insulin sensitivity (416). Such a sensitising effect of IL-6 has since been demonstrated in primary human myotubes (415, 417-419). However, chronic elevation of IL-6 is associated with the development of skeletal muscle insulin resistance, potentially mediated by impairment of IRS1/2 activation (420). Thus, increased skeletal muscle derived IL-6 in obese individuals, may act in an autocrine and paracrine fashion to drive the development of skeletal muscle insulin resistance.

Furthermore, we also demonstrated, for the first time, the IL-1β-mediated secretion of IL-6 from primary human myotubes. Although there was no significant difference in the amount of IL-1β induced IL-6 secretion between donor groups, this finding may carry a greater impact *in vivo*. This is because muscle interstitial IL-1β concentrations are likely to be greater in the obese state and thus

more likely to evoke muscle IL-6 release, further contributing to a localised proinflammatory microenvironment conducive to the development of insulin resistance (421).

Myotubes cultured from obese individuals also secreted a greater amount of IL-8 on average in comparison to lean myotubes, although this did not reach statistical significance. Similarly, Ciaraldi et al. also demonstrated that primary human myotubes cultured from individuals with T2D secreted a significantly greater amount IL-8, in addition to other myokines such as IL-15, MCP1 and TNFα in comparison to non-diabetic individuals (414). IL-8 is a potent neutrophil attractant; however the impact of obesity on neutrophil infiltration of skeletal muscle has not been reported. Indeed, studies investigating obesity induced immune cell infiltration of skeletal muscle and the consequent impact on its function are scarce, especially in comparison to similar studies in adipose tissue. However, there is evidence of M1 macrophage and T cell (CD4+ and CD8+) infiltration in both HFD fed mice and in obese insulin resistant humans (422-424). Additionally, such immune cell infiltration has been associated with muscle insulin resistance (422, 424). Thus, further studies investigating skeletal muscle and immune cell crosstalk in obesity and its impact on insulin sensitivity are warranted.

The increase in proinflammatory cytokine secretion observed from obese myotubes in this thesis could be due, in part, to increased activation of NFKB signalling. NFKB is a well-known positive regulator of proinflammatory cytokine expression and has previously been shown to be activated to a greater extent in both obese muscle and myotubes cultured from obese individuals (425, 426). Additionally, CEBPA and CEBPB are members of the CCAAT/enhancer binding factor family of proteins and also function as positive regulators of proinflammatory cytokine transcription (427).

Although not significantly different, a positive correlation of both CEBPA and CEBPB (P = 0.057) expression with percentage body fat was observed in skeletal muscle tissue in this thesis. Therefore, such an upregulation in CEBPA/B may also contribute to the increased proinflammatory cytokine secretion observed in obese myotubes. However currently, no studies have investigated CEBP family

mediated regulation of inflammation in skeletal muscle or primary human myotubes, thus further studies would be needed to confirm this.

3.3.3 Obesity does not impact primary human myotube lipid content.

Obese and T2D individuals classically present with ectopic accumulation of intramuscular adipose tissue and increased intramuscular lipid content (176, 396). Such increased intramyocellular lipid content has since been implicated in the development of skeletal muscle insulin resistance, as discussed in section 1.5 of this thesis. However, we observed no significant difference in lipid content or lipid droplet size between myotubes cultured from lean and obese individuals, as determined by oil red O staining. In line with this finding, Bajbeyi et al. also saw no significant difference in myotube lipid content in lean and obese individuals with T2D (184). This suggests such altered lipid accumulation observed *in vivo* is not retained in myotubes in culture, perhaps indicating that lipid accumulation is more dependent on available nutrient supply. However, it should be noted that although lipid staining in this thesis appeared to be located within myotubes, further immunohistochemical staining would have been useful to confirm that the cells used in this experiment were indeed multinucleated myotubes and that oil red O positive areas were not due to the presence of another contaminating population, e.g adipocytes.

3.3.4 Primary human myotubes from obese individuals maintain upregulated expression of atrophic genes

Chronic low grade inflammation present in elderly obese individuals is also associated with increased skeletal muscle atrophy and such atrophy may also be associated with the development of T2D (428). Here we show for the first time that the mRNA expression of genes associated with atrophic signalling are upregulated in both the skeletal muscle tissue and myotubes from elderly obese individuals, in comparison to elderly lean individuals.

Myostatin was upregulated in both the skeletal muscle and primary human myotubes of obese individuals in comparison to lean individuals. In support of this finding, increased myostatin protein secretion has previously been reported in myotubes cultured from obese middle aged women, while HFD feeding drives myostatin expression in mice (429, 430). Additionally, myostatin expression decreases in the skeletal muscle tissue of obese humans following weight loss and both aerobic and resistance exercise intervention (431-433). It is well defined that myostatin plays a central role in the TGF-β signalling pathway, functioning as a negative regulator of skeletal muscle mass, as demonstrated by the extreme increases in musculature in myostatin knockout animal models (434). Thus, the results of this thesis and the current literature suggest myostatin expression is closely linked to adiposity and may therefore play a critical role in the loss of muscle mass and quality in obese individuals.

Interestingly, recent data has demonstrated that CEBPs are upregulated in mouse skeletal muscle during space flight (modelling disuse) and it appears that such increased expression of CEBPs drives activation of the myostatin promotor in C2C12 myotubes (435). Additionally, CEBPB expression has been demonstrated to be an important negative regulator of myogenesis, with CEBPB knockout mice having increased muscle mass (436). The fact that a positive correlation of CEBPA/B with adiposity

was observed in skeletal muscle in this thesis provides further support of these findings and may also explain the increased myostatin expression observed in obese individuals (436).

Additionally, recently published data has also directly implicated myostatin in the development of insulin resistance. Firstly, Wilkes et al. provide evidence that short term administration of myostatin induces insulin resistance in mice, independent of changes in both adipose tissue and skeletal muscle mass (437). Further, administration of a myostatin neutralising peptibody upregulated GLUT4 expression and augmented insulin signalling in the muscle of mice, whilst also protecting against HFD induced insulin resistance (438). Evidence in humans is less abundant, however exercise induced reductions in myostatin expression in muscle also correlate with improved insulin sensitivity, again independent of changes in adipose tissue or skeletal muscle mass (433). Thus, further research to elucidate the mechanism of both myostatin upregulation with obesity and consequently the induction of insulin resistance may identify novel therapeutic targets for the treatment of T2D in addition to atrophy.

However, some discrepancies between tissue and myotube gene expression were observed in this thesis. Firstly, although both calpain 1 and 2 mRNA expression was upregulated in obese muscle, no significant difference in the mRNA expression of either gene was observed between lean and obese myotubes. In contrast, the expression of FOXO3 and its downstream target MAFbx were both significantly greater in obese myotubes in comparison to lean myotubes, but were not different in skeletal muscle tissue. Such inconsistencies between skeletal muscle tissue and isolated myotube gene expression likely reflects several factors. Firstly, unlike skeletal muscle tissue *in vivo*, primary human myotubes did not receive external stimuli such as contraction. Additionally, muscle tissue is made up of other cells types including those of the vasculature, connective tissue and neurons, not just myofibres, therefore potential influences of cellular crosstalk are lost *in vitro.* Finally, it is

possible that due to the absence of such external influences, de-differentiation of primary human myotubes may have occurred, impacting gene expression.

3.3.5 The contraction induced hypertrophic response of myostatin suppression is intrinsically impaired in obese myotubes.

Similarly to exercise *in vivo*, 24 h EPS decreased myostatin expression in primary human myotubes cultured from lean individuals. In agreement with this finding Tarum et al. reported a similar reduction of myostatin mRNA in primary human myotubes subject to 4 h of EPS (439). This EPS protocol was also associated with increased myotube thickness and activation of hypertrophic signalling pathways (439). Such an increase in hypertrophy following EPS is in line with the increased protein synthesis observed in this thesis and further supports EPS as a useful model of *in vitro* muscle contraction/exercise. In comparison, obese myotubes displayed a considerably blunted response to EPS, with no decrease in myostatin expression observed in response to the same EPS protocol. A similar blunted response to EPS-induced insulin sensitisation has also recently been demonstrated in obese myotubes by Park et al. while additionally, Feng et al. reported that EPS failed to increase lipid oxidation in obese myotubes (440, 441). Thus, collectively, these data and the results of this thesis provide further evidence to support the retention of donor characteristics in primary human myotubes.

It should be noted that although EPS increased Puromycin expression in this thesis, indicating increased protein synthesis, puromycin positive protein was also detected in myotubes treated with EPS, in the absence of recombinant promyocin. A possible explanation for this may be that EPS increased protein synthesis to a level that resulted in non-specific binding of the puromycin antibody, giving the false indication of the presence of puromycin. This could perhaps indicate that EPS caused a supraphysiological increase in protein synthesis in primary human myotubes and therefore future

studies aiming to investigate how EPS protocols relate to *in vivo* exercise would be useful. Additionally, myotube thickness or size in response to EPS was not measured in this thesis, therefore future studies to confirm the effect of EPS on these parameters, in both lean and obese individuals, would also be valuable.

3.3.6 Limitations

The above studies have some limitations. The sample size used for the RT2 profiler gene card study was small and thus patient variability is likely to have masked potential gene expression changes between donor groups. Furthermore, although differential expression of target genes was identified, both protein expression and the functional impact of such differential expression were not determined in myotubes. Therefore, future studies investigating the function of these candidate genes would be beneficial.

Additionally, although this thesis and other studies have demonstrated that primary human myotubes provide a valuable *in vitro* model of human skeletal muscle, it is not without limitation. For example, primary human myotubes are devoid of external stimuli unless stimulated by EPS. Although this is valuable for experimental studies, it means that the myotube model does not take into consideration the effects of cellular crosstalk and circulating factors. In particular, myotubes have no neural innervation and therefore lack both fluctuations in calcium currents and physical contraction which may limit myotube functionality. An example of this is GLUT4 translocation and glucose uptake. Myotubes display a reduced expression of GLUT4 and increased expression of GLUT1 compared to tissue (442). Consequently, the approximate 2-fold increase in insulin induced glucose uptake in primary human myotubes observed in this thesis and similar studies is approximately 5-fold less than that of the *in vivo* response (397, 443, 444).

Furthermore, prolonged culture of primary human myotubes may also impact their function. For example, although useful for increasing the growth rate of myogenic cultures, supraphysiological glucose concentrations, often found in cell culture media, can induce myotube insulin resistance (445). Therefore, although low glucose media was utilised for this thesis (1.1 g/L) and cultures were limited to passage 4, a direct impact of culture conditions may have contributed to the differential insulin responses observed between subjects. Additionally, although primary human myotubes are multinucleated structures that express contraction machinery, the inherent nature of cell culture leads to a random organisation of myotubes on a 2-dimensional plane, rather than the organised 3-dimensional parallel structures observed in striated muscle. In an attempt to overcome this, recent investigations have explored the use of 3-D culture systems to help guide myotube alignment (446). The ultimate goal for future studies of *in vitro* skeletal muscle would be to use such techniques in combination with either co-culture systems or electrical stimulation. In relation to studies utilising EPS, a recent publication by Evers-van Gogh et al. demonstrated that physiological changes in myotube function induced by EPS could also be induced via the application of EPS stimulated culture media to myotubes (447). Therefore, studies into the effect of EPS on primary human myotubes should currently be interpreted with caution.

Additionally, although our group has previously demonstrated that the myoblast culture method used in this thesis generates multinucleated structures that express muscle specific genes (448), this thesis did not measure markers of myotube differentiation or nuclear fusion index for each experiment. Therefore, although all myoblasts were differentiated for 8 days, myoblasts were limited to passage 4 and all experiments were repeated with patient replicates, it is possible that some of the results presented in this thesis may be attributable to differing levels of myotube differentiation, rather than adiposity.

3.3.7 Conclusions

Ageing and obesity are associated with increased inflammation, a blunted anabolic hypertrophic response and skeletal muscle insulin insensitivity. Myotubes from elderly obese individuals appear to maintain these facets, displaying increased insulin resistance, expression of atrophic markers and proinflammatory cytokine secretion. Therefore, the next chapters of this thesis will investigate the role of adipose tissue and skeletal muscle crosstalk in mediating these changes in elderly skeletal muscle insulin sensitivity.

CHAPTER 4: The novel adipokine vaspin is upregulated in obesity and promotes insulin sensitivity of elderly human muscle

4.1 Introduction

Adipokines have emerged as central mediators of tissue cross talk, playing important roles in the regulation of metabolism, energy homeostasis and inflammatory responses. Critically, in obese individuals, adipose tissue is known to become more “inflammatory”, leading to an increased production of proinflammatory adipokines and a reduction in beneficial, anti-inflammatory adipokines (449). At present, the effect of adipokines on human skeletal muscle insulin sensitivity and glucose handling is poorly understood (413). This is largely due to the fact that the majority of studies in this field have been performed using non-human skeletal muscle cell lines or animal models. Understanding the functional and mechanistic role of adipokines on skeletal muscle insulin signalling may provide new insights into how obesity affects insulin resistance and could identify novel targets for therapeutic intervention.

A novel adipokine that may play an important role in regulating skeletal muscle insulin sensitivity with obesity is vaspin. First reported as a 47 KDa protein in the visceral adipose tissue of genetically obese OLETF rats, administration of vaspin to obese mice has been shown to increase insulin sensitivity and glucose tolerance (450). Additionally, in SAT; leptin, resistin and TNFα mRNA was suppressed, while the expression of GLUT4 and adiponectin gene transcripts increased following vaspin administration (450). Similar increases in insulin sensitivity have since been reported in db/db and C57BL6 mice following vaspin delivery (451). Central administration of vaspin to obese mice resulted in a sustained suppression of appetite that consequently resulted in a reduction in both bodyweight and plasma glucose concentrations (274). Furthermore, transgenic mice overexpressing vaspin displayed improved glucose tolerance and were protected from obesity when challenged with a high fat diet (275). The results of this study also suggest vaspin may have an anti-inflammatory role, as a reduction in serum IL-6 was observed following vaspin treatment (275).

Currently, vaspin has been poorly characterised in human tissue and its potential crosstalk with human skeletal muscle has not been explored. This chapter aimed to investigate the impact of obesity on vaspin expression in human adipose tissue and skeletal muscle and in turn the impact of vaspin on human skeletal muscle insulin sensitivity, by utilising a primary human myotube model.

4.1.1 Chapter aims

This chapter aims to:

- Determine the expression of vaspin in human subcutaneous adipose tissue, skeletal muscle and primary human myotubes.

- Confirm vaspin secretion from human adipose tissue in order to validate vaspin as a novel adipokine capable of performing tissue crosstalk.

- Determine the role of vaspin in mediating insulin sensitivity in primary human myotubes by performing functional studies utilising recombinant vaspin protein.

- Validate GRP78 as a potential receptor for vaspin in human skeletal muscle tissue and primary human myotubes.

Some of the results within this chapter have been published by Nicholson et al. in the Journal of Endocrinology.

Nicholson T, Church C, Tsintzas K, Jones R, Breen L, Davis ET, et al. Vaspin promotes insulin sensitivity of elderly muscle and is upregulated in obesity. J Endocrinol. 2019; 241:1.

4.2 Results

4.2.1 Vaspin is differentially expressed in rodent models of obesity and insulin resistance

To validate vaspin as a candidate adipokine central to metabolic homeostasis, we first investigated its mRNA expression, and that of its putative receptor GRP78, in epididymal white adipose tissue (EWAT), SWAT and BAT depots in Zucker (Zuc FA/FA) and Zucker diabetic (ZDF FA/FA) fatty rat models. We also examined the mRNA expression of leptin in order to confirm the effect of the obese phenotype on the adipose tissue expression of adipokines.

Leptin mRNA expression was significantly greater in both the SWAT and EWAT of Zuc FA/FA and Zuc ZDF FA/FA rats, in comparison to control animals (Fig. 4.1). Similarly, SWAT and EWAT vaspin mRNA expression was also significantly greater in Zuc FA/FA rats compared to control animals (Fig. 4.1). SWAT and EWAT vaspin expression was also greater on average in Zuc ZDF FA/FA rats, however this did not reach statistical significance. Conversely, no difference in GRP78 expression was observed in the SWAT or EWAT of Zuc FA/FA or Zuc ZDF FA/FA animals in comparison to control animals (Figure 4.1). Additionally, no difference in BAT leptin, vaspin or GRP78 expression was observed between groups (Figure 4.1).

Furthermore, we also investigated leptin, vaspin and GRP78 expression in the SWAT and EWAT of obese resistant (OR) and obese prone (OP) rats fed either a control diet (CD) or a high fat diet (60% of total kcal) for a period of 6 weeks. HFD increased leptin expression in the EWAT and SWAT of both OP and OR rats (Fig. 4.2 A and D). Of note, there was no significant difference between the effect of the HFD on leptin expression between OP and OR rats (Fig. 4.2 A and D). Following HFD, EWAT vaspin expression decreased (P = 0.057) in OP rats, but remained unchanged in OR rats (Fig. 4.2 B). EWAT vaspin expression following HFD was also significantly greater in OR rats compared to OP rats (Fig. 4.2 B). In SWAT, no significant difference in vaspin mRNA expression was observed in either OP or OR fed a control diet (Fig. 4.2 D). Additionally, HFD did not affect the expression of vaspin in either OR or

OP rats (Fig. 4.2 E). Furthermore, GRP78 mRNA expression in both EWAT and SWAT was significantly greater following HFD in both OP and OR rats (Fig. 4.2 C and F) However, there was no significant difference in the expression of GRP78 between OP and OR rats (Fig. 4.2 C and F).

Moreover, we also investigated the effect of HFD, obesity and the diabetic phenotype on the expression of vaspin and GRP78 mRNA expression in the SWAT, EWAT and BAT of mice. In EWAT, db/db mice displayed significantly greater vaspin mRNA (59 ± 19) expression in comparison to control mice (2 ± 0.5) (Fig. 4.3 A). Vaspin mRNA expression was also ~ 5-fold and 50-fold greater on average in HFD fed and ob/ob mice respectively, however these observations did not reach statistical significance (Fig. 4.3 A). Additionally, vaspin mRNA expression was also significantly upregulated in the BAT of ob/ob mice, (Fig. 4.3 E). BAT vaspin mRNA expression was also greater on average in HFD fed and db/db mice, in comparison to control mice, but again such differential expression did not reach statistical significance. No significant difference in SWAT vaspin mRNA expression was observed in murine models of obesity and diabetes (Fig. 4.3 C). SWAT and EWAT GRP78 expression was not different between groups (Fig. 4.3 B, D). However, BAT GRP78 expression was upregulated in all groups in comparison to control animals (Fig. 4.3 F).

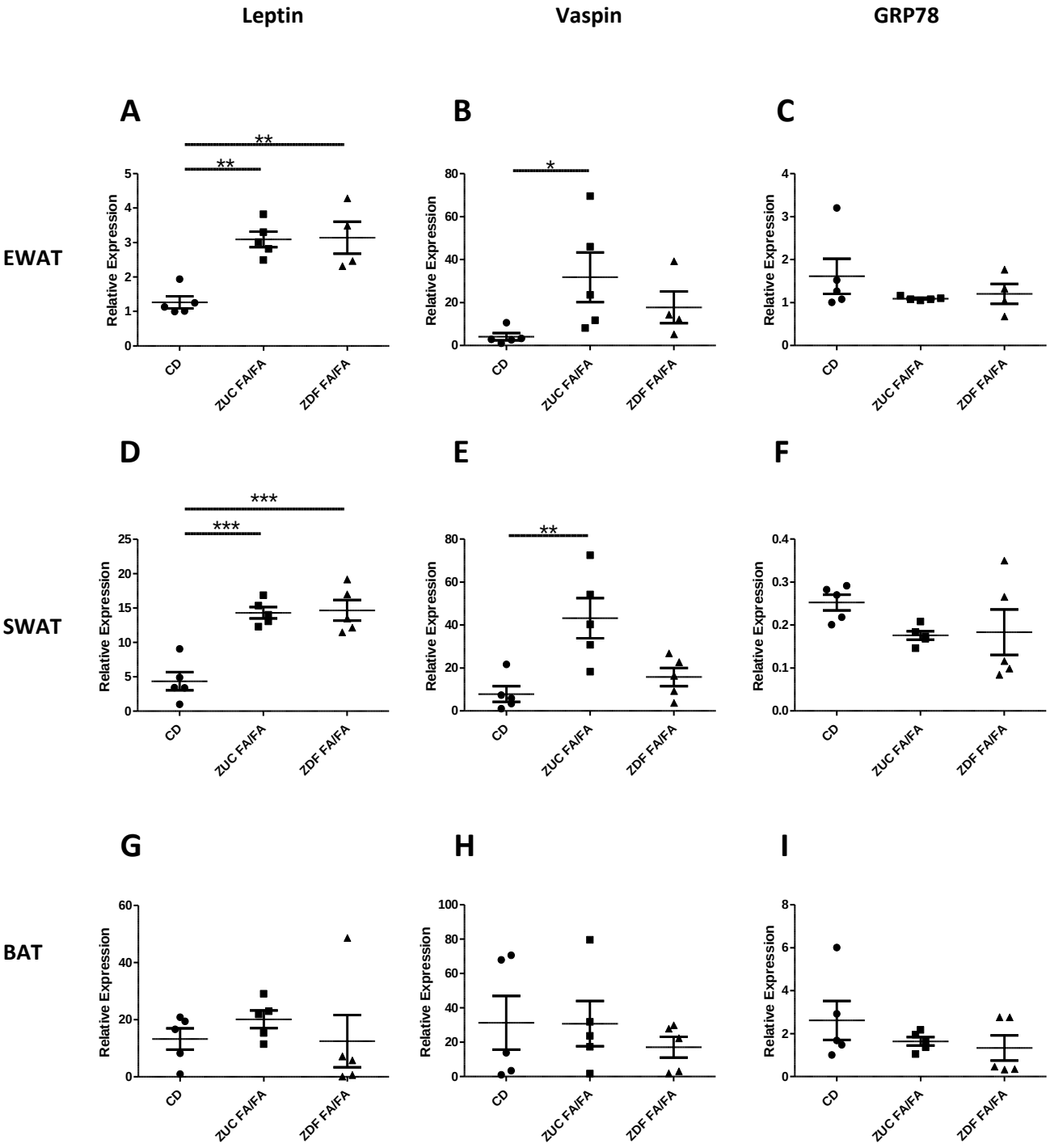

Figure 4. 1. Vaspin mRNA is upregulated in rat models of obesity and insulin resistance.

A-C. Leptin, vaspin and GRP78 mRNA expression in EWAT of control diet (CD), Zuc FA/FA and Zuc ZDF FA/FA rats. **D-F.** Leptin, vaspin and GRP78 mRNA expression in SWAT of control diet, Zuc FA/FA and Zuc ZDF FA/FA rats. **G-I.** Leptin, vaspin and GRP78 mRNA expression in BAT of control diet, Zuc FA/FA and Zuc ZDF FA/FA rats. n = 5 animals per group, except ZDF FA FA EWAT where n = 4. Data are represented as mean ± S.E.M. * signifies P < 0.05, ** signifies *P* <0.01, ***signifies P ≤ 0.001, significant difference from control animals as determined by one-way ANOVA followed by Dunnett's post hoc tests.

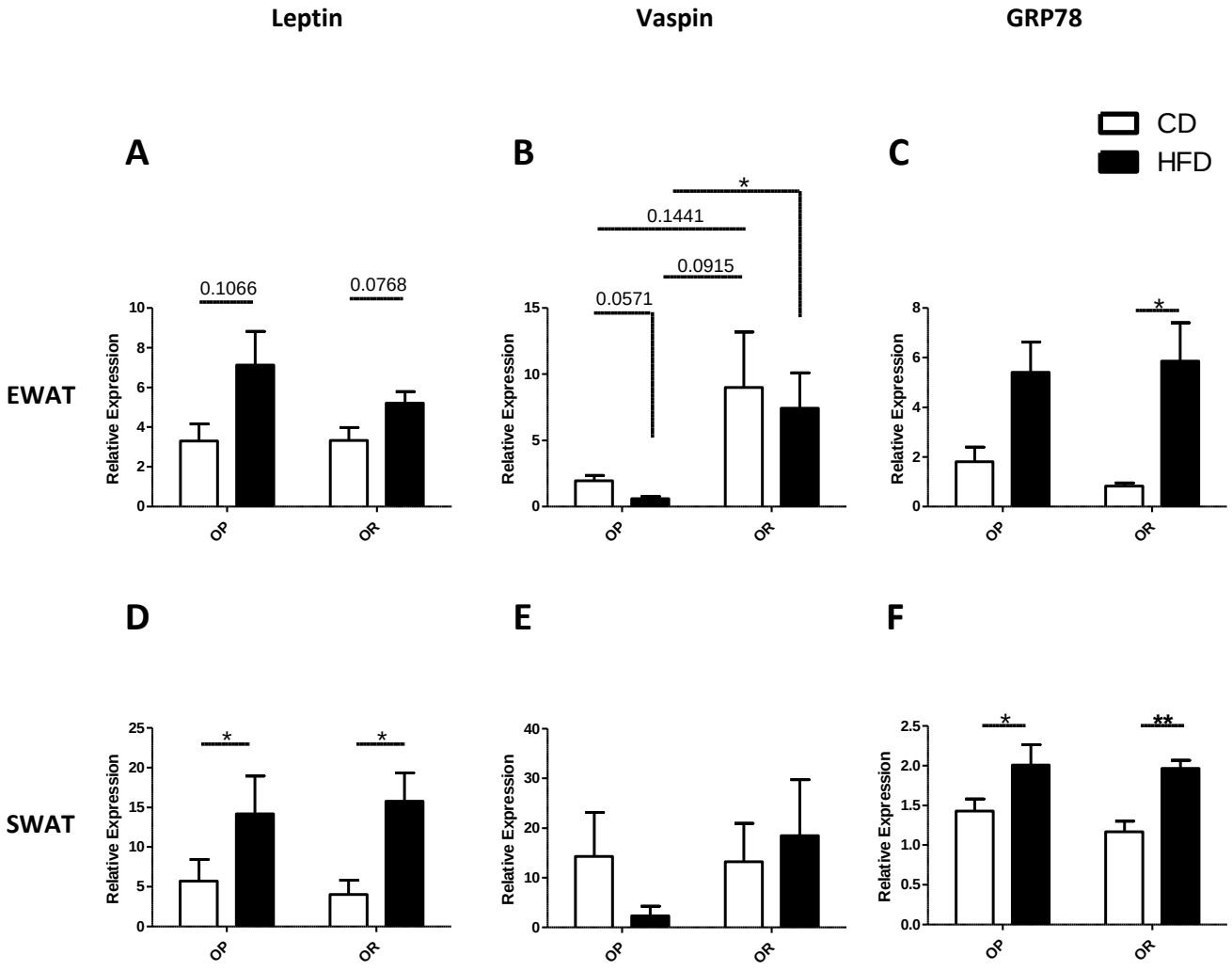

Figure 4. 2. Vaspin is differentially expressed in obese prone and obese resistant rat models.

A-C. Leptin, vaspin and GRP78 mRNA expression in the EWAT of obese prone (OP) and obese resistant (OR) rats with and without HFD. **D-F.** Leptin, vaspin and GRP78 mRNA expression in SWAT of obese prone (OP) and obese resistant (OR) rats with and without HFD. n = 4 animals per group, except OP HFD where n = 5. Data are represented as mean ± S.E.M. *signifies P < 0.05, **signifies *P* <0.01 as determined by Post-hoc T-tests following 2-way ANOVA.

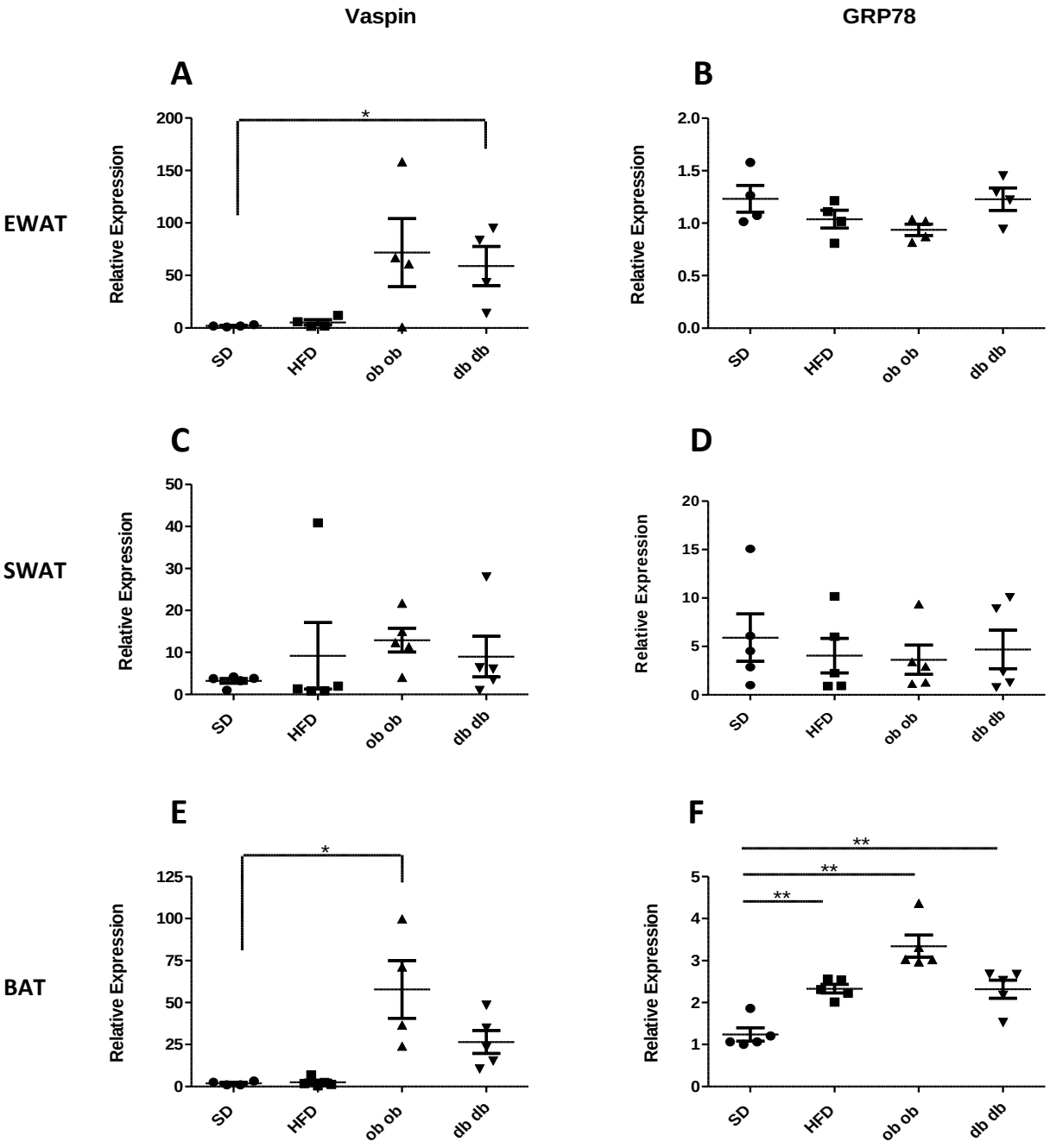

Figure 4. 3. Vaspin is differentially expressed in mouse models of obesity and insulin resistance. **A-B.** Vaspin and GRP78 mRNA expression in EWAT of SD, HFD, ob ob and db db mice. **C-D.** vaspin and GRP78 expression in SWAT of SD, HFD, ob ob and db db mice. **E-F.** vaspin and GRP78 mRNA expression in BAT of SD, HFD, ob ob and db db mice. n = 5 animals per group. Data are represented as mean ± S.E.M. * $P < 0.05$, ** $P < 0.01$ significantly different from SD mice as determined by ANOVA followed by Dunnett's post hoc tests.

4.2.2 The expression of vaspin and its putative receptor GRP78 are increased in the skeletal muscle and SAT of obese humans

Following the observation that vaspin mRNA expression was increased in rodent models of obesity and diabetes, we next examined the expression of vaspin and its putative plasma membrane receptor GRP78 (HSPA5) in both SAT and skeletal muscle tissue of humans with varying BMI. Characteristics of subjects included in this thesis are presented in Table 4.1 and Figure 4.4. Vaspin mRNA expression was significantly greater in both SAT (2.5-fold, $P < 0.01$) and skeletal muscle (1.5-fold, $P < 0.05$) of obese subjects in comparison to lean subjects (Fig. 4.5 A-B) and demonstrated a significant positive correlation with BMI (Fig. 4.5 E-F). Similarly, expression of GRP78 was significantly greater in both SAT (1.5-fold, $P < 0.05$) and skeletal muscle (1.8-fold, $P < 0.05$) of obese subjects in comparison to lean subjects (Fig. 4.5 C-D) and was positively correlated with BMI in both tissue types (Fig. 4.5 G and 4.5 H).

We next investigated whether such increased vaspin and GRP78 expression was maintained in primary human myotube cultures from lean and obese individuals (Figure 4.6). The mean expression of both vaspin and GRP78 mRNA was again greater in primary human myotubes from obese individuals in comparison to lean individuals, although such differences did not reach statistical significance.

	Lean	Obese	*P* value
n	21	17	N/A
Male/female (*n*)	9/12	10/7	N/A
Age	70.6 ± 1.6	65.8 ± 2.1	0.0718
BMI	22.8 ± 0.3	34.5 ± 0.9	<0.0001
Body fat %	23.6 ± 3.0	38.6 ± 2.1	0.0006
Weight (kg)	61.5 ± 2.7	99.2 ± 3.3	<0.0001
Waist circumference (cm)	81.6 ± 2.9	111.0 ± 2.2	<0.0001
Hip circumference (cm)	95.9 ± 1.9	115.0 ± 2.2	<0.0001
Waist: hip	0.85 ± 0.02	0.95 ± 0.02	0.004
% HbA1c	5.4 ± 0.1	5.7 ± 0.07	0.11

Table 4. 1 Human subject characteristics

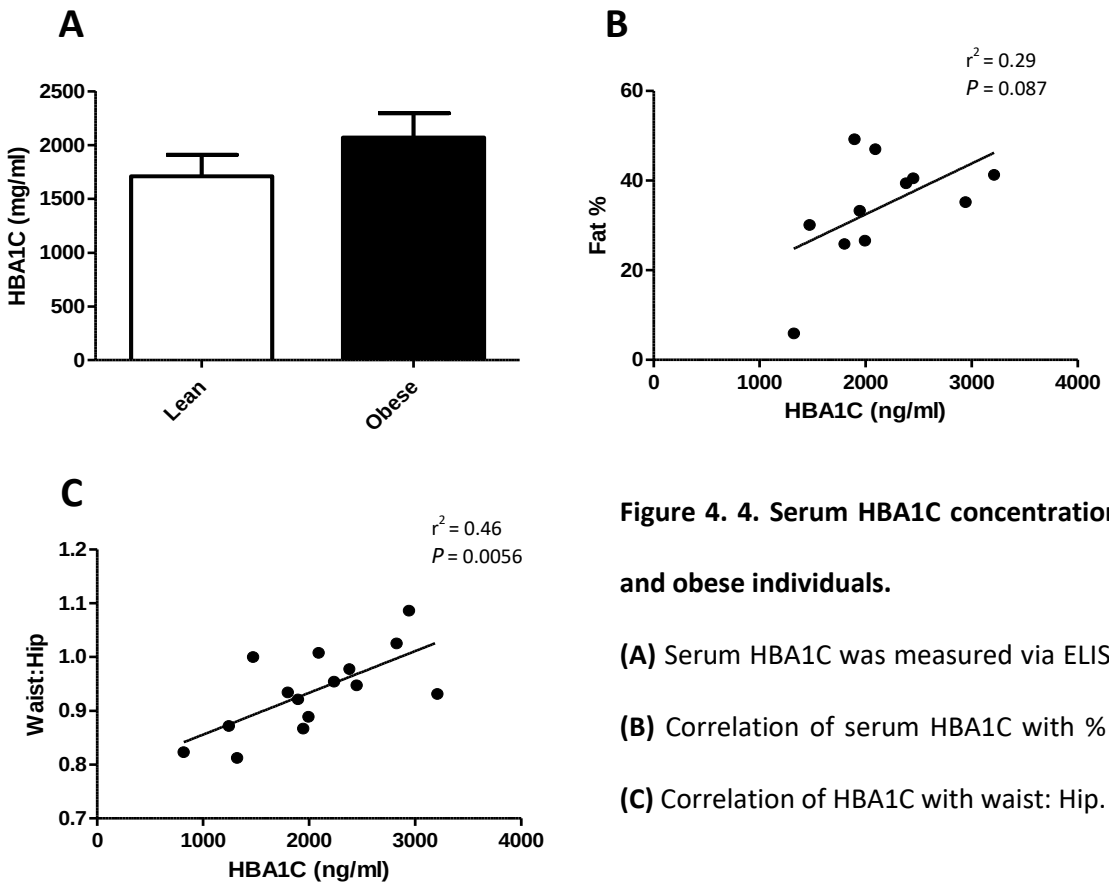

Figure 4. 4. Serum HBA1C concentrations in lean and obese individuals.

(A) Serum HBA1C was measured via ELISA. n = 27.

(B) Correlation of serum HBA1C with % body fat.

(C) Correlation of HBA1C with waist: Hip.

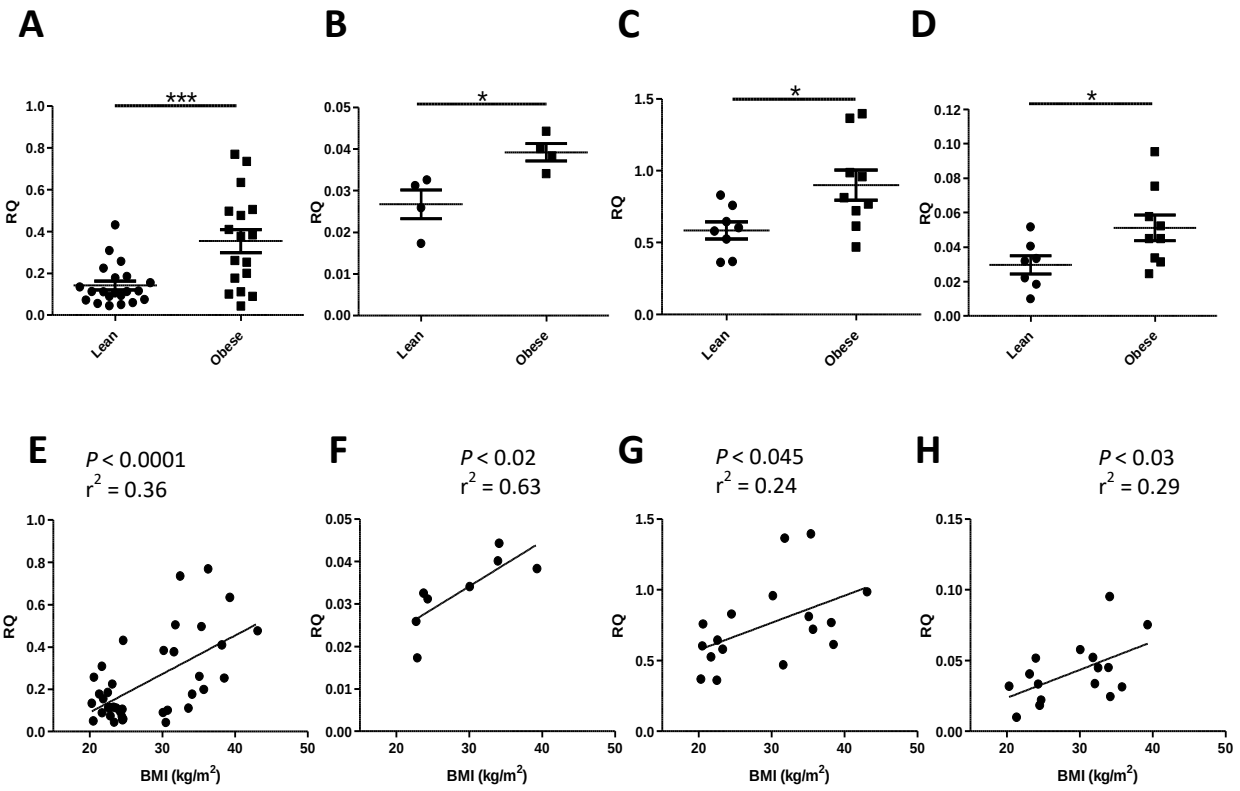

Figure 4. 5. Vaspin and GRP78 mRNA expression are upregulated in subcutaneous adipose tissue and skeletal muscle in obese elderly individuals.

A. The mRNA expression of vaspin in SAT of lean (n = 21) and obese (n = 17) elderly individuals. **B.** The mRNA expression of vaspin in skeletal muscle tissue of lean (n = 4) and obese (n = 4) elderly individuals. **C.** The mRNA expression of GRP78 in SAT of lean (n = 8) and obese (n = 9) elderly individuals. **D.** The mRNA expression of GRP78 in skeletal muscle of lean (n = 7) and obese (n = 9) elderly individuals. **E.** Correlation of vaspin mRNA expression in SAT with BMI. **F.** Correlation of vaspin mRNA expression in skeletal muscle tissue with BMI. **G.** Correlation of GRP78 mRNA expression in SAT with BMI. **H.** Correlation of GRP78 mRNA expression in skeletal muscle tissue with BMI. Expression of mRNA was quantified by qRT-PCR, and normalised using GAPDH. Data are represented as mean ± S.E.M. * signifies $P < 0.05$, *** signifies $P \leq 0.001$, as determined by unpaired t-tests.

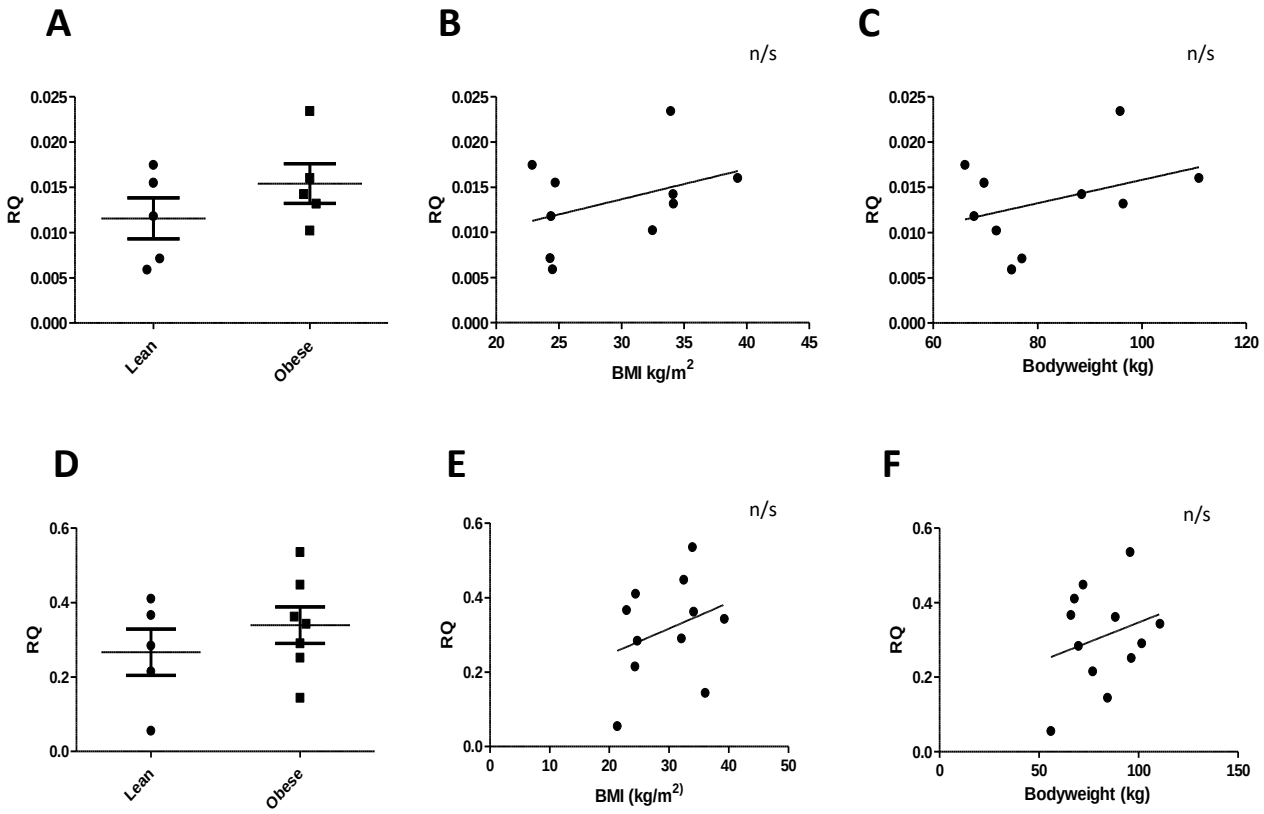

Figure 4. 6. Vaspin and GRP78 in primary human myotubes from lean and obese individuals. **A.** Vaspin mRNA expression in lean (n = 5) and obese (n = 5) primary human myotubes. **B.** correlation of myotube vaspin mRNA expression with BMI. **C.** correlation of myotube vaspin mRNA expression with bodyweight. **D.** GRP78 mRNA expression in lean (n = 5) and obese (n = 7) primary human myotubes. **E.** correlation of myotube vaspin mRNA expression with BMI. **F.** correlation of myotube vaspin mRNA expression with bodyweight. (n/s signifies no significance).

In order to identify possible drivers of the increased vaspin mRNA expression observed in skeletal muscle tissue with obesity, lean primary human myotubes were cultured for 24 h in conditions aiming to replicate an obese microenvironment. Vaspin mRNA expression was increased on average following stimulation with all treatment conditions, with the largest increase in vaspin mRNA occurring in response to glucose, insulin and palmitate combined. However these data did not reach statistical significance.

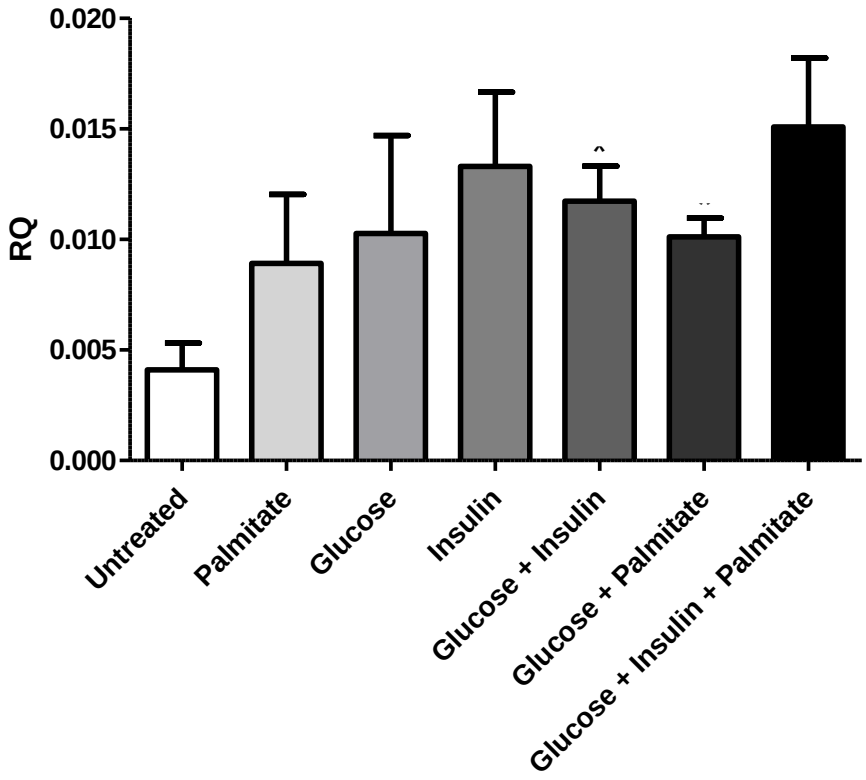

Figure 4. 7. Lean myotube Vaspin mRNA expression in response to an obese microenvironment. Lean primary human myotubes (n = 4 biological replicates) were stimulated with palmitate (0.3 M), glucose (10 mM), insulin alone (100 nM), or in various combinations for 24 h. Vaspin mRNA expression was determined by qRT-PCR and normalised to GAPDH. Data are reported as mean ± S.E.M. Data was analysed fow statistical significance via one way ANOVA.

4.2.3 Vaspin is rapidly secreted from human adipose tissue and muscle tissue and is detectable systemically in both lean and obese individuals

To investigate the potential for vaspin to signal between human SAT and skeletal muscle we first examined, by immunoblotting, the *ex vivo* secretion of vaspin from SAT and skeletal muscle into serum free Ham's F10 media over a 24 h time course as described in section 2.7. Vaspin was detected in serum-free culture media that had been conditioned with either SAT or skeletal muscle for 1 h, indicating that vaspin is rapidly secreted from both tissue types. The amount of vaspin detected in both SAT and skeletal muscle-conditioned media increased up to 6 h and was maintained for the duration of 24 h (Fig. 4.8 A and B). Further, a significantly greater level of vaspin was detected in SAT conditioned media of obese individuals (n = 16) in comparison to lean (n = 17) at 24 h (Fig. 4.9 A).

We then examined by ELISA whether vaspin could be detected systemically in human sera, and whether there was a difference in the systemic concentration of vaspin between lean (n = 16) and obese (n = 15) individuals. Vaspin was detected in the serum of both lean and obese individuals, but there was no significant difference between levels found in obese individuals in comparison to lean individuals in either males or females (Fig. 2.9 B). However, serum vaspin was on average higher in obese females compared to lean females. Furthermore, although there was no significant correlation between serum vaspin and BMI in males (Fig. 2.9 C), in females we found a significant positive correlation ($r^2 = 0.28$, $P < 0.05$) with BMI (Fig. 2.9 D).

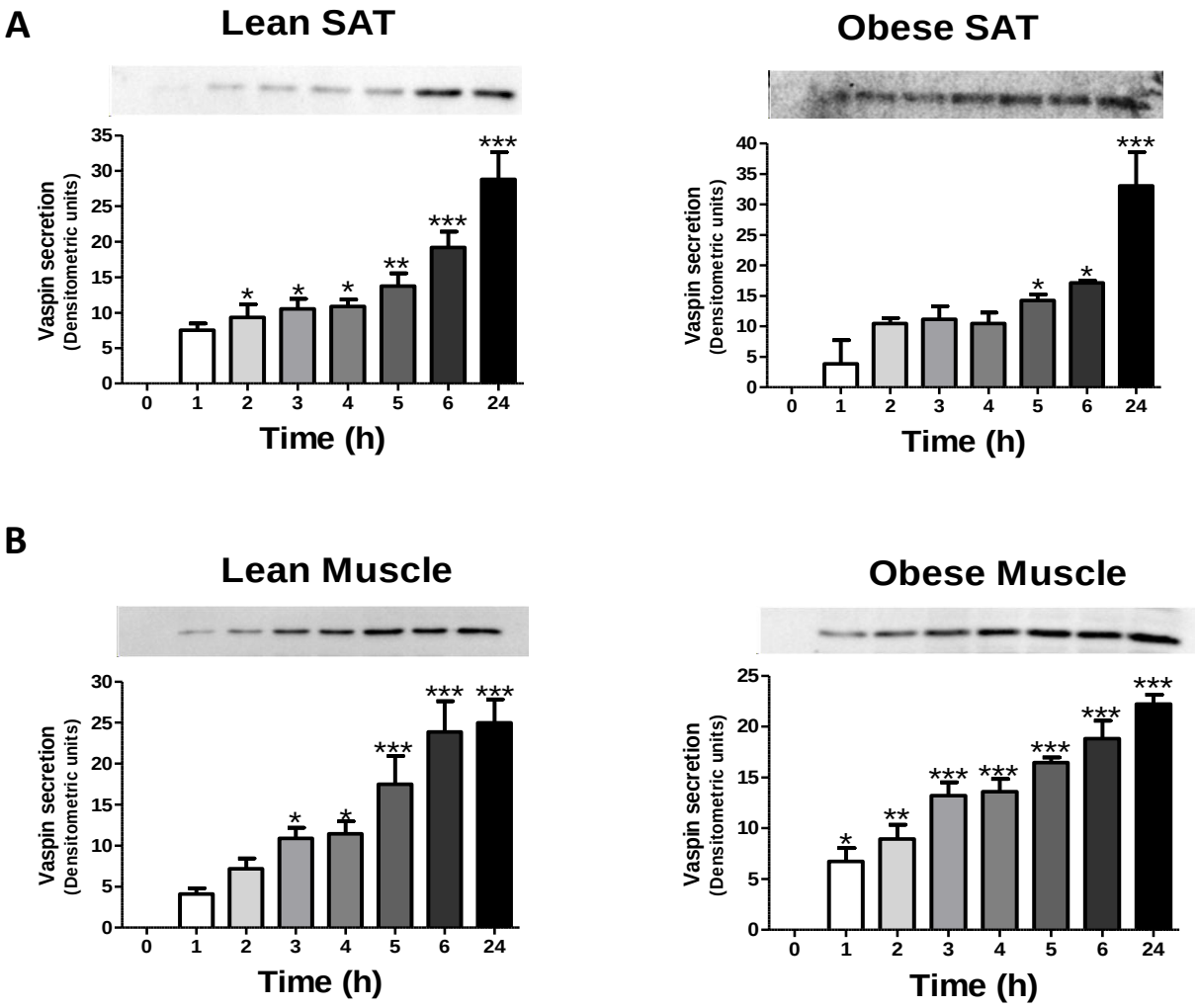

Figure 4. 8. Vaspin is rapidly secreted from human subcutaneous adipose tissue.

Detection of vaspin protein in **A.** SAT conditioned media and **B.** skeletal muscle-conditioned media in lean (n = 3 patient replicates) and obese (n = 3 patient replicates) subjects over a 24 h time course, as measured by immunoblotting. 10 µL adipose or skeletal muscle-conditioned media was loaded per sample lane. Bars represent mean densitometric units ± S.E.M. of immunoblots from lean (n = 3) and obese (n=3) subjects. *P < 0.05, **P < 0.01, ***P < 0.001, significantly different from time = 0 media control sample as determined by one-way ANOVA with Dunnett's post-hoc tests.

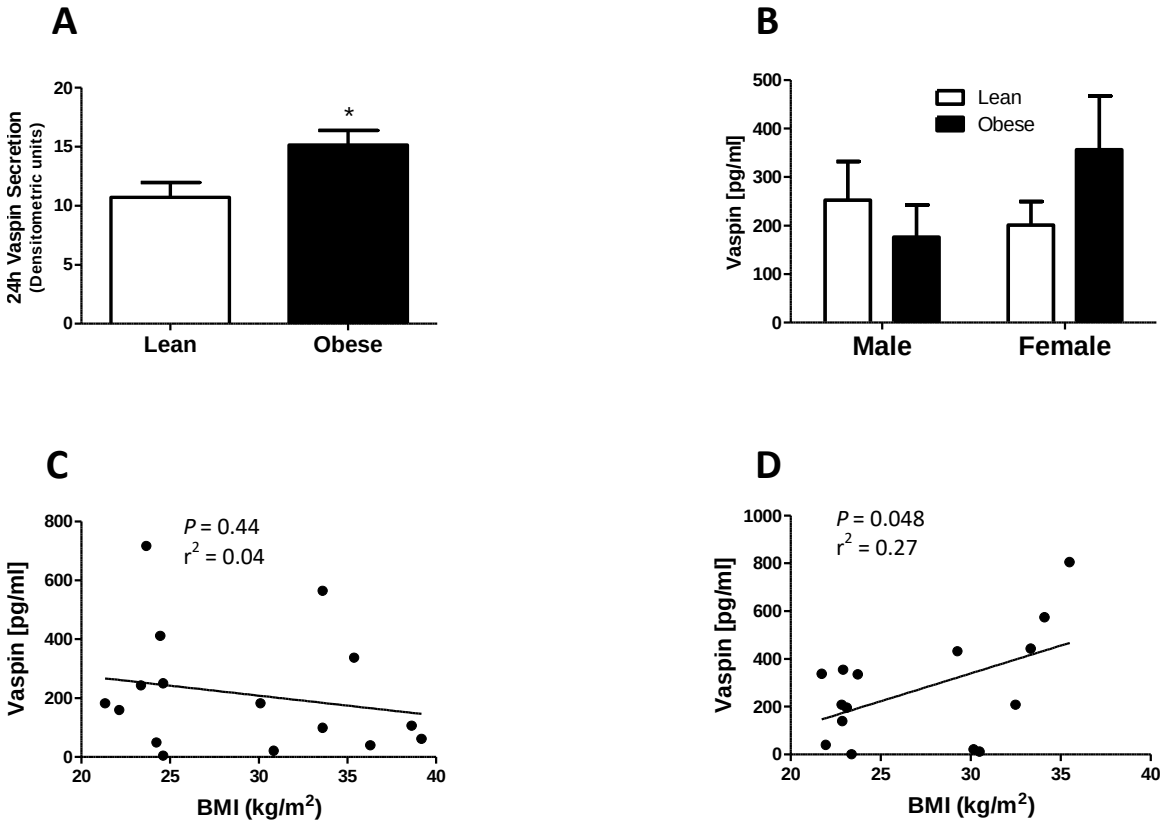

Figure 4. 9. Vaspin is systemically elevated in obese individuals.

A. Densitometric analysis of vaspin protein expression in adipose conditioned media at 24 h from lean (n = 17) and obese (n = 16) subjects as measured by immunoblotting. 10 µL of adipose conditioned media was loaded per sample lane. $P < 0.05$ as determined by unpaired t-test. **B.** Detection of vaspin protein in the serum of male (n = 8 lean; n = 8 obese) and female (n = 8 lean; n = 7 obese) subjects by ELISA, data was analysed for statistical significance by performing 2-way ANOVA. **C.** Pearson correlation of serum vaspin with BMI in males. **D.** Pearson correlation of serum vaspin with BMI in females.

4.2.4 The effect of vaspin on insulin signalling pathways in primary human myotubes

We next examined the effect of stimulating primary human myotubes with recombinant human vaspin on insulin signalling pathways. First, lean primary myotubes were acutely stimulated with recombinant vaspin (100 ng/mL) for 5, 10 or 15 min and AKT activity (phosphorylation) quantified using MesoScale immunoassays (MesoScale Discovery). Myotubes stimulated with vaspin for either 10 or 15 min showed a significant 3-fold increase in phospho AKT$^{(Thr308)}$/total AKT expression (which along with activation of the other AKT phosphorylation site (serine^{473}) was validated by immunoblotting (n = 4 patient replicates) (Fig. 4.10).

To investigate the mechanism of the vaspin-mediated induction in basal AKT activity we examined whether acute or chronic stimulation of human myotubes with vaspin led to activation of either the IR or the IGF receptor. As expected, 15 min of insulin stimulation alone induced a significant increase in the phosphorylation of both the IR and the IGF receptor (Fig. 4.11 A and B). However, stimulation of myotubes with vaspin for either 15 min or chronic stimulation for 24 h induced no phosphorylation of either the IR or the IGF receptor (Fig. 4.11 A and B) indicating that vaspin did not directly affect activation of upstream insulin signalling. Given these findings, we then examined whether vaspin affected the activity of downstream insulin signalling by determining the activity status of PI3K by immunoblotting. Acute stimulation of primary human myotubes (n = 4 patients) with vaspin (100 ng/mL) induced a transient increase in phosphorylation of PI3K between 10 and 15 min as determined by immunoblotting (Fig. 4.11 C and D).

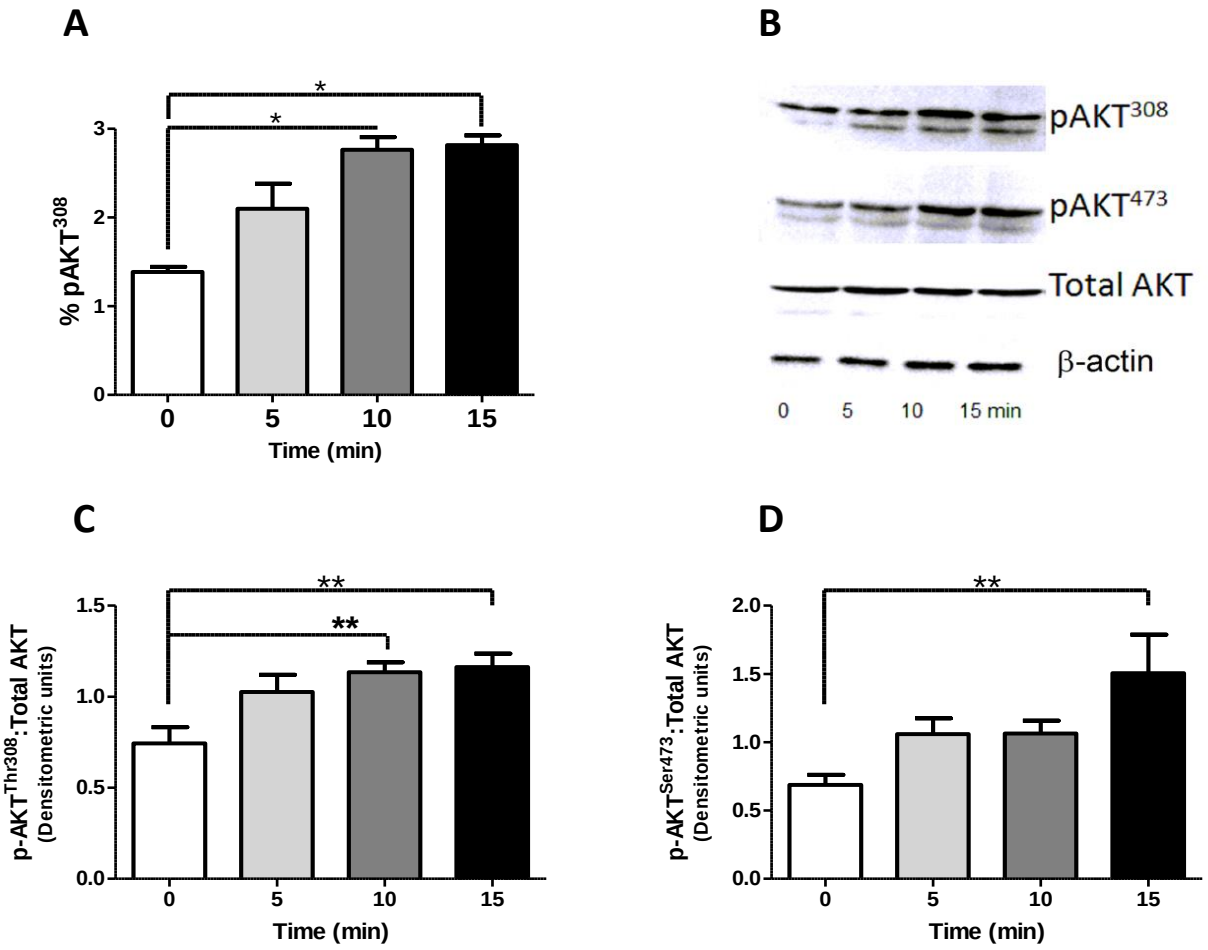

Figure 4. 10. Vaspin activates AKT in primary human myotubes.

A. The effect of acute stimulation (0, 5, 10, 15 min) of primary human myotubes with recombinant human vaspin (100 ng/mL) on AKT^{Thr308} phosphorylation measured by mesoscale analysis (n = 4 biological replicates, 2 male and 2 female). **B.** Representative immunoblots of AKT^{Ser473} and AKT^{Thr308} phosphorylation in untreated and vaspin (100 ng/mL)-stimulated myotubes after 0, 5, 10 and 15 min stimulation (n = 4 primary donors: 2 male, 2 female, 15 µg of total protein was loaded per sample). **C.** Densitometric analysis of $AKTT^{hr308}$ western blots normalised to Total AKT protein (n = 4). **D.** Densitometric analysis of AKT^{Ser473} western blots relative to Total AKT protein (n = 4). Data are represented as mean ± S.E.M. * $P < 0.05$, *** $P < 0.001$ significantly different from untreated control as determined by Dunnett's post-hoc tests following 1 way ANOVA).

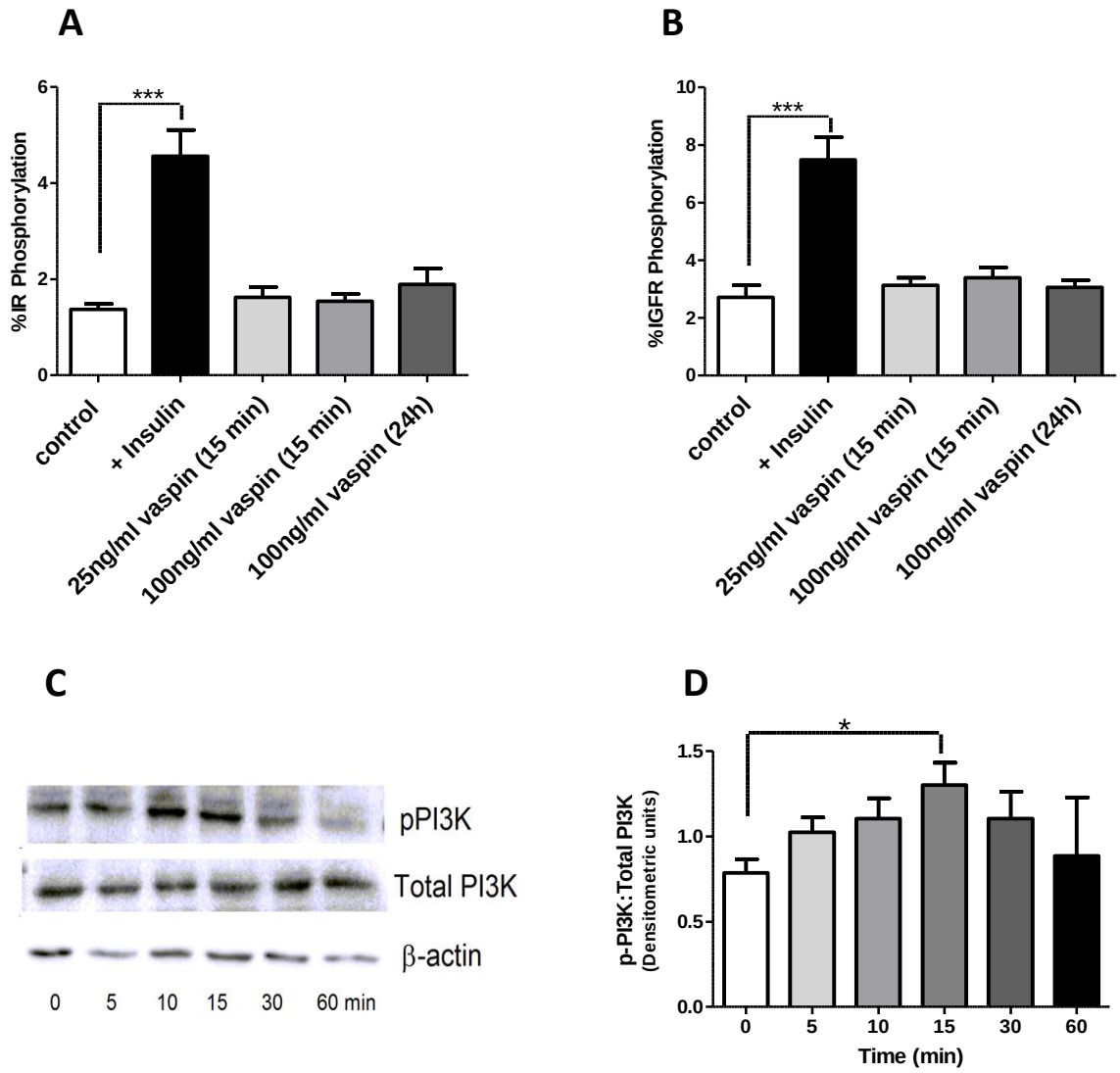

Figure 4. 11. Vaspin activates PI3K in primary human myotubes.

A. Effect of insulin (0–30 nM, 30 min) and acute (15 min) or chronic (24 h) vaspin stimulation (100 ng/mL) on the phosphorylation of insulin receptor and **B.** IGF receptor as measured by mesoscale analysis (n = 16 biological replicates from 8 primary donors: 4 male, 4 female). **C.** Time course of acute vaspin stimulation (100 ng/mL) on the activation of PI3K assessed by immunoblotting (n = 4 primary donors: 1 male, 3 female, 15 µg total protein was loaded per sample). **D.** Densitometric analysis of Phospho-PI3K P85 western blots normalised to total PI3K. Data are represented as mean ± S.E.M. * signifies $P < 0.05$, ** signifies $P < 0.01$, *** signifies $P < 0.001$ significantly different to control as determined by Dunnett's post-hoc tests, following 1-way ANOVA.

4.2.5 Vaspin induces the expression and translocation of GLUT4 protein and promotes glucose uptake in obese elderly primary human myotubes

Following these data, and with the observation that vaspin induced activation of downstream insulin signalling components, we then investigated the functional metabolic role of vaspin by examining whether vaspin affected GLUT4 expression and glucose uptake in primary human myoblasts and myotubes from obese subjects.

First, we examined whether there was a difference in skeletal muscle GLUT4 mRNA expression between old obese (n = 8), old lean (n = 8) and young (n = 7) subjects. Compared to young subjects, GLUT4 expression was 69% lower in the skeletal muscles from old obese subjects ($P < 0.05$; Fig. 4.12 A). In line with the relatively low expression of GLUT4 in old obese muscle, myotubes derived from old obese subjects also displayed a blunted glucose uptake response to insulin (100 nM, 30 min), in comparison to myotubes cultured from old lean subjects, as reported above (Figure 3.8). Stimulation of old obese myotubes with vaspin (100 ng/mL) for 24 h induced a significant ($P < 0.05$) ~5-fold increase in the expression of GLUT4 mRNA (Fig. 4.12 B), which translated into a significant ($P < 0.05$) increase in GLUT4 protein (Fig. 4.12 C). Furthermore, stimulation of primary human myoblasts with either insulin (100 nM) or vaspin (100 ng/mL) for 15 min caused a significant ($P < 0.05$) increase in GLUT4 protein surface expression, compared to non-stimulated myoblasts, indicative of an increase in GLUT4 protein translocation (Figure 4.12 D). Such increased vaspin mediated GLUT4 translocation appeared to be confirmed in primary human myotubes via immunohistochemical staining of GLUT4 (Figure 4.13).

We then investigated whether these vaspin-mediated effects on both the expression and translocation of GLUT4 were sufficient to impact on glucose uptake in previously insulin-insensitive old obese myotubes. Primary human myotubes from old obese subjects that had not been pre-treated with vaspin showed no increase in glucose uptake in response to 30 min of insulin stimulation (100 nM), compared to unstimulated controls (Fig. 4.12 E). However, 30 min insulin stimulation significantly increased glucose uptake in vaspin pre-treated myotubes, compared to control myotubes (Fig. 4.12 E). Finally, since p38 and AMPK activation have been implicated in promoting GLUT4 expression we examined the effect of vaspin stimulation on their activation status. Acute stimulation of primary human myotubes (0 – 15 min) with 100 ng/mL vaspin induced a significant activation of both p38 (n = 4 biological replicates) and AMPK (n = 4 biological replicates), as measured by immunoblotting (Fig. 4.14 A and B).

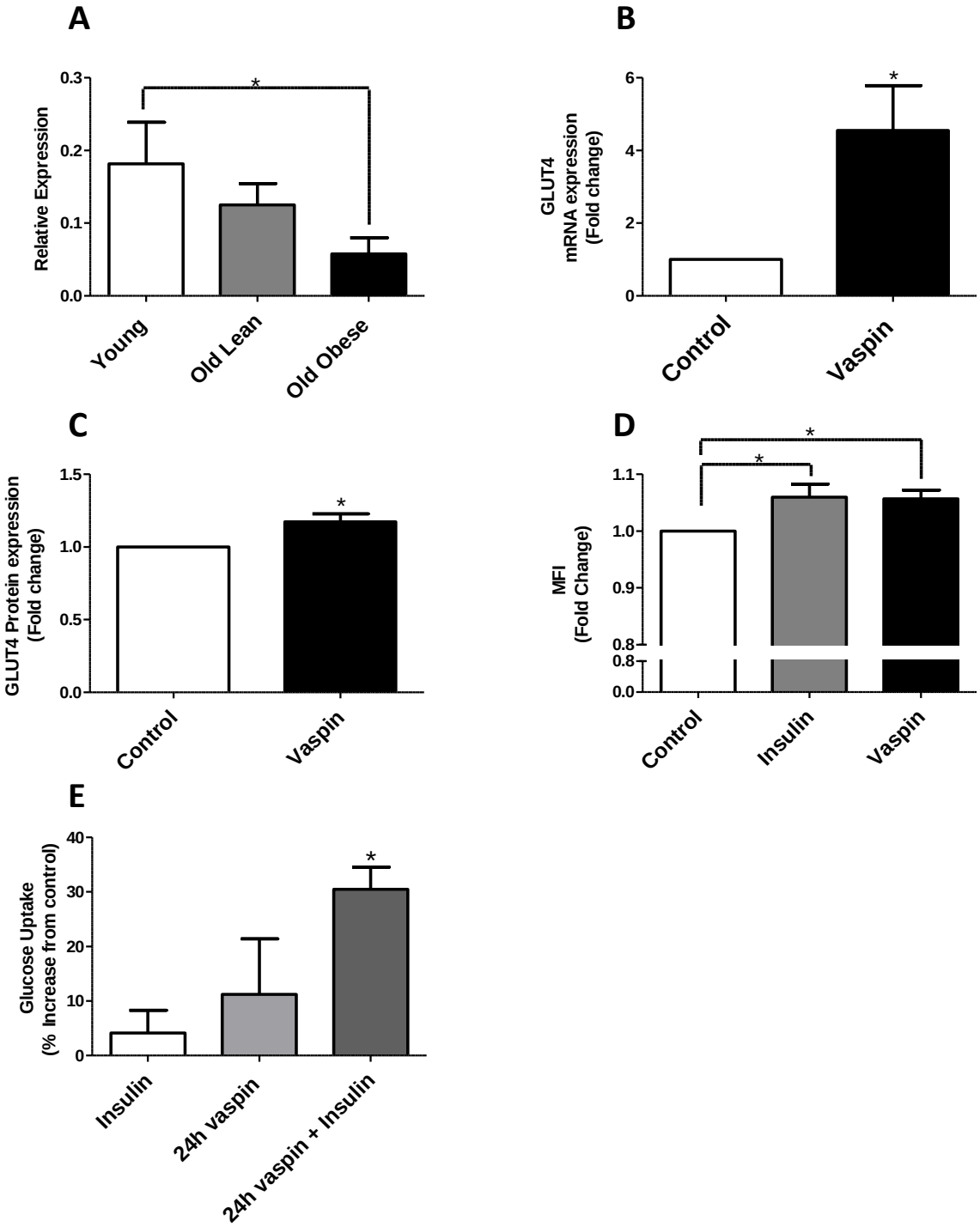
A
Relative Expression
0.3
0.2
0.1
0.0
*
Young
Old Lean
Old Obese
B
GLUT4
mRNA expression
(Fold change)
6
4
2
0
*
Control
Vaspin
C
GLUT4 Protein expression
(Fold change)
1.5
1.0
0.5
0.0
*
Control
Vaspin
D
MFI
(Fold Change)
1.1
1.0
0.9
0.8
0.8
0.0
*
*
Control
Insulin
Vaspin
E
Glucose Uptake
(% Increase from control)
40
30
20
10
0
*
Insulin
24h vaspin
24h vaspin + Insulin

Figure 4. 12. Vaspin induces GLUT4 expression and sensitises insulin-mediated glucose uptake in primary human myotubes.

A. GLUT4 mRNA expression relative to GAPDH in skeletal muscle tissue derived from lean young (n = 7), lean old (n = 8) and obese old (n = 8) subjects. *P < 0.05, significantly different between young and old obese as determined by one-way ANOVA with Dunnett's post-hoc tests. **B.** GLUT4 mRNA expression in primary human myotubes from obese subjects stimulated for 24 h with recombinant vaspin (100 ng/mL) or left untreated (n = 5 primary donors: 2 male, 3 female). Expression was determined by qRT-PCR and normalised to GAPDH. *P < 0.05, significantly different from unstimulated control, as determined by t-test. **C.** GLUT4 protein expression as measured by immunoblotting in primary human myotubes from obese subjects stimulated for 24 h with vaspin (100 ng/mL) or left untreated (n = 6 primary donors: 2 male, 4 female). * signifies P < 0.05, significantly different from unstimulated control, as determined by t-test. **D.** Primary human myoblast membrane localised GLUT4 expression in response to insulin (100 nM 15 min), or vaspin (100 ng/mL 15 min), (n = 5 obese primary donors: 2 male, 3 female). Relative surface expression of GLUT4 was quantified by measuring the mean fluorescence intensity (MFI) of GLUT4 staining in a minimum of 1500 cells/condition by flow cytometry. *P < 0.05, significantly different from unstimulated control as determined by one-way ANOVA with Dunnett's post-hoc tests. **E.** Effect of 24 h exposure of primary obese myotubes (n = 3, female donor) to recombinant vaspin (100 ng/mL) on basal and insulin-stimulated radiolabelled glucose uptake ([3H]-2-DOG). *P < 0.05, significantly different from unstimulated control as determined by one-way ANOVA with Dunnett's post-hoc tests. Data are represented as mean ± S.E.M.

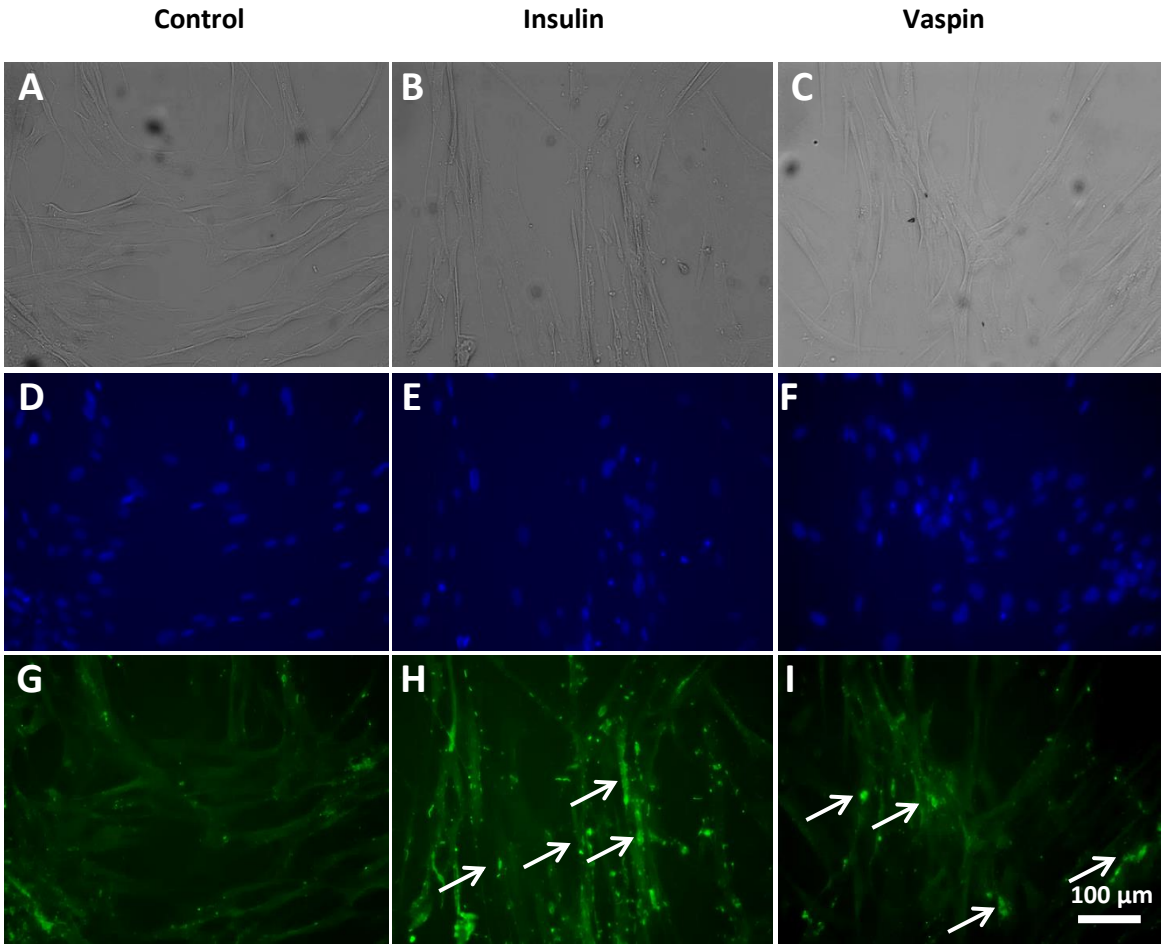

Figure 4. 13. Vaspin increases GLUT4 translocation in primary human myotubes.

A- C. Bright field imaging of control, insulin stimulated (100 nM, 15 min) and Vaspin stimulated (100 ng/ ml, 15 min) primary human myotubes. **D – F.** DAPI Stained nuclei of control, insulin stimulated (100 nM, 15 min) and Vaspin stimulated (100 ng/ ml, 15 min) primary human myotubes. **G- I.** GLUT4 expression in control, insulin stimulated (100 nM, 15 min) and Vaspin stimulated (100 ng/ ml, 15 min) primary human myotubes. Arrows indicate examples of increased fluorescence at the myotube sarcolemma (n = 3 patient replicates).

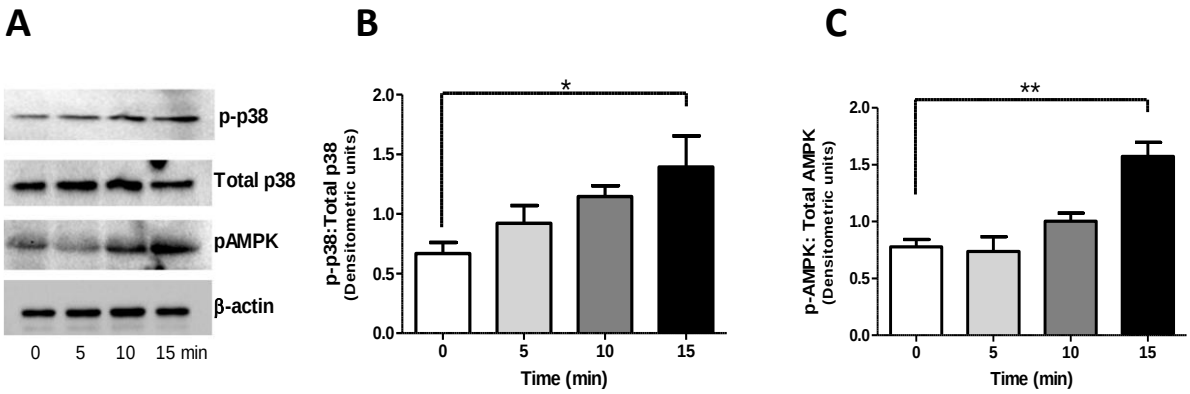

Figure 4. 14. Acute vaspin stimulation increases activation of P38 and AMPK.

A. Representative immunoblots for phospho and total p38 (n = 4 primary donors) and phospho AMPK and total AMPK (n = 4 primary donors: 1 male, 3 female) in untreated and vaspin (100 ng/ml) stimulated myotubes after 0, 5, 10 and 15 min stimulation. 10 µg of total protein was loaded per sample. **B.** Densitometrtic quantification of phospho-p38 immunoblots relative to total p38 protein. Bars represent mean densitometric units ± S.E.M. (n = 4). *P < 0.05, significantly different from unstimulated control as determined by one-way ANOVA. **C.** Densitometric quantification of phospho-AMPK immunoblots relative to total AMPK. Bars represent mean densitometric units ± S.E.M. (n = 3). **P < 0.01, significantly different from unstimulated control as determined by Dunnett's post hoc tests following one-way ANOVA.

4.2.6 Validation of GRP78 as a vaspin receptor in primary human myotubes

Finally, we aimed to validate GRP78 as a potential vaspin receptor in skeletal muscle by performing siRNA mediated loss of function studies in primary human myotubes. Delivery of siRNA targeting GRP78 to both primary human myoblasts and primary human myotubes using TranIT-X2 resulted in significant knockdown of GRP78 mRNA expression of approximately 85% and 50% respectively in comparison to control cells, as determined via qRT-PCR (Figure 4.15 A and B).

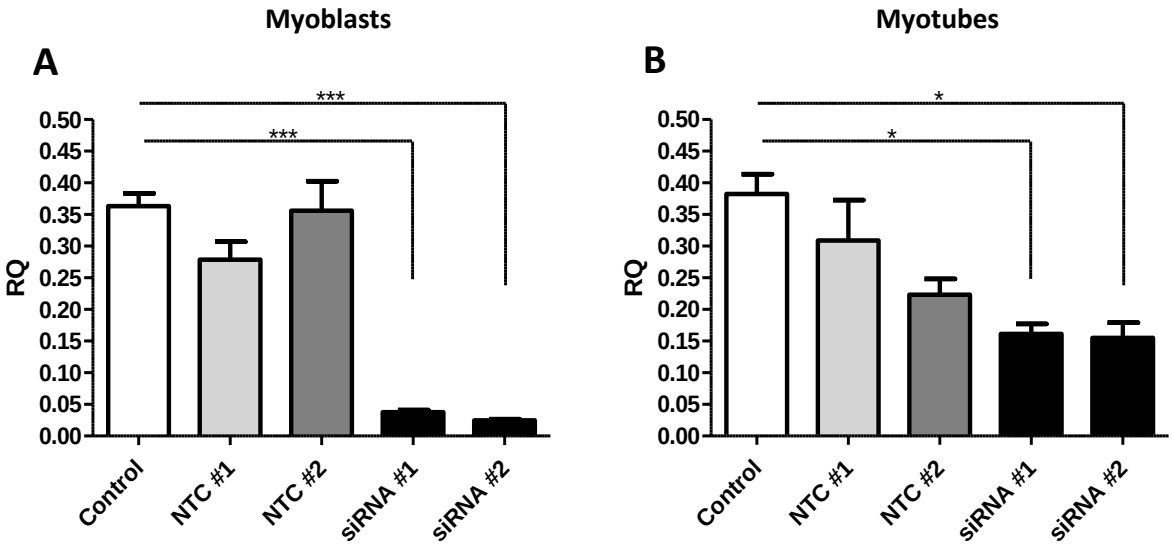

Figure 4. 15. siRNA mediated knockdown of GRP78 in primary human myoblasts and myotubes.

A. GRP78 mRNA expression in primary human myoblasts 24 h post treatment with either TransIT-X2 lipid only (control), non-targeting control siRNAs #1/#2 or siRNA #1/#2 targeting GRP78 (n = 3 biological replicates). **B.** GRP78 mRNA expression in primary human myotubes 24 h post treatment with either TransIT-X2 lipid only (control) non-targeting siRNA #1/#2 or siRNAs targeting GRP78 (#1 and #2). (n = 3 biological replicates). GRP78 mRNA expression was determined by qRT-PCR and normalised to GAPDH. Data are presented as mean ± S.E.M. $*P < 0.05$, $***P < 0.001$ significantly different from control as determined by one-way ANOVA with Dunnett's post-hoc tests.

Next, as we reported that vaspin increases GLUT4 mRNA expression in section 4.2.5 of this thesis, we investigated the effect of 24 h vaspin stimulation on myoblast GLUT4 mRNA expression, following GRP78 knockdown. Post transfection with GRP78 siRNAs for 24 h, myoblasts were treated with vaspin (100ng/ml) for a further 24h. At 48 h post transfection, GRP78 mRNA expression was not significantly different in comparison to control cells (Figure 4.16 A). Additionally, no significant increase in GLUT4 mRNA expression was observed following vaspin stimulation in control cells (Figure 4.16 B). The expression of GLUT4 mRNA was similar across all other conditions (Figure 4.16 B).

We also investigated whether GRP78 knockdown could prevent vaspin stimulated activation of AKT in primary human myotubes. 24 h post GRP78 knockdown, primary human myotubes were treated with vaspin (100 ng/ml, 15 min). In control cells, vaspin evoked a significant increase in the activation of $AKT^{(Ser473)}$. Such an increase in AKT phosphorylation did not occur in myotubes with GRP78 knockdown (Figure 4.16 C-D). However, significant activation of AKT was observed at baseline in myotubes treated with siRNA #2 (Figure 4.16 D).

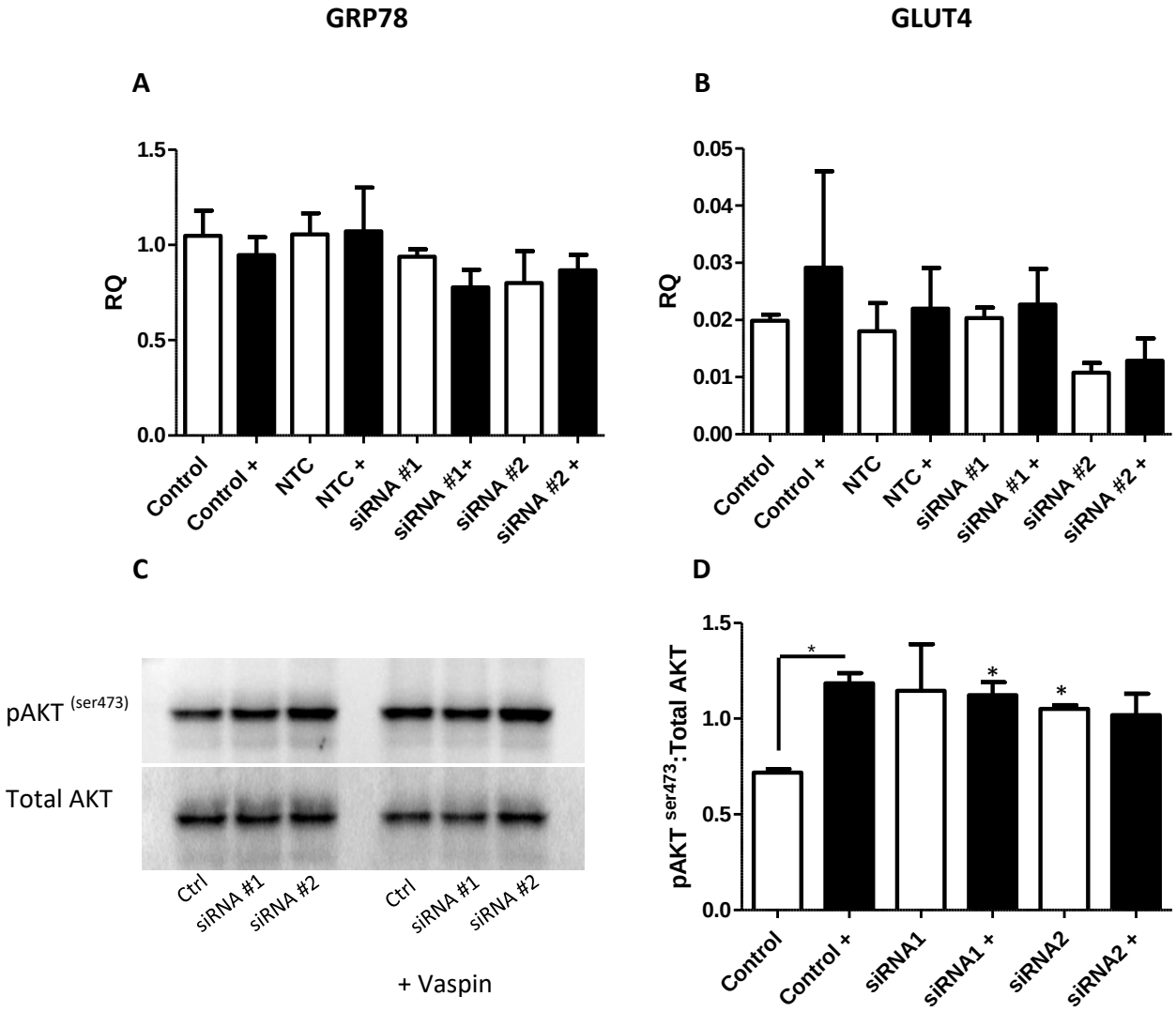

Figure 4. 16. The effect of GRP78 knockdown on the functional effects of vaspin

A. GRP78 mRNA expression in lean primary human myoblasts 48h h post treatment with either TransIT-X2 lipid only (control), siRNA #1/#2 or NTC1 in the absence or presence (+) of recombinant human vaspin (100 ng/ml, final 24 h of transfection) (n = 3 biological replicates). **B.** GLUT4 mRNA expression in primary human myoblasts 48h post treatment with either TransIT-X2 lipid only (control), siRNA #1/#2 or NTC1 in the absence or presence (+) of recombinant human vaspin (100 ng/ml, final 24 h of transfection) (n = 3 biological replicates). **C.** Phospho and total AKT expression in lean primary human myotubes in the absence or presence of recombinant human vaspin (100 ng/ml, 15 min) following 24 h treatment with either TransIT-X2 lipid only (control) or siRNA #1/#2, measured by immunoblotting (n = 2 biological replicates). **D.** Densitometric quantification of phospho-AKT immunoblots relative to total AKT protein. Bars represent mean Densitometric units ± S.E.M. *P < 0.05, significantly different from control as determined by Dunnett's post hoc tests following 2-way ANOVA.

4.3 Discussion

With the current dearth of human data on the adipokine vaspin, this thesis is the first to characterise the expression of vaspin in both skeletal muscle and adipose tissue in elderly individuals of varying BMI and to report the functional effect of vaspin on human skeletal muscle insulin signalling pathways and glucose uptake.

4.3.1 Adipose tissue vaspin mRNA expression is increased in obese and diabetic rodent models

Firstly, before progressing to work in human tissue and primary cells, we investigated the effect of obese and diabetic phenotypes on the expression of vaspin in adipose tissue depots of rodent models, to confirm vaspin as a candidate adipokine associated with obesity. To validate the use of such models, we first examined the expression of leptin, an adipokine known to increase with adiposity. As expected, SWAT and EWAT leptin mRNA expression was upregulated in Zucker FA/FA, ZDF FA/FA, HFD obese prone and HFD obese resistant rats, compared to control animals, indicating these animal models displayed a characteristic response associated with obesity.

In support of previously published data reporting increased vaspin mRNA expression in obese rats (450), both SWAT and EWAT Vaspin mRNA expression was significantly upregulated in Zucker FA/FA animals in comparison to control animals (450), (452). Interestingly, vaspin expression was also higher at baseline in obese resistant animals compared to obese prone animals (P = 0.14) and was significantly greater in the EWAT of obese resistant animals fed a HFD, in comparison to obese prone animals fed a HFD. Indeed, vaspin mRNA expression in obese prone animals was observed to decrease with HFD (P = 0.057). Furthermore, we also demonstrate, for the first time, that vaspin mRNA expression was significantly greater in the EWAT and BAT of db/db and ob/ob mice respectively. Additionally, a number of considerable increases (up to 50-fold) were also observed in ob/ob, db/db and control mice fed a HFD, although such differential expression did not reach

statistical significance, likely due to the small sample size in this investigation. Collectively, these data suggest that increased vaspin mRNA expression in both EWAT and SWAT is positively associated with increased adiposity. Additionally, unlike most adipokines, it appears such increased vaspin expression may be beneficial, protecting against obesity. However, in contrast to EWAT and SWAT, the expression of leptin and vaspin were not differentially expressed in the BAT of obese or diabetic rat models. This may reflect BATs more prominent role in regulating energy expenditure rather than regulating adipokine production and secretion (as discussed in section 1.6 of this thesis).

4.3.2 Characterisation of vaspin expression and secretion in humans

In humans, vaspin mRNA has previously been reported to be detectable in only around 15% of SAT samples, with no expression reported in SAT of lean subjects (453). In the present study, we detected vaspin mRNA in both SAT and skeletal muscle from both lean and obese individuals. However, vaspin was more highly expressed in the SAT and skeletal muscles from obese individuals and in both tissue types its expression positively correlated with BMI. We also found that vaspin expression was maintained in primary human myotubes and vaspin protein was rapidly secreted from both human SAT and skeletal muscle tissue, with the quantity secreted from obese tissues being greater than from lean tissues. Together these data support the findings in rodents from this thesis and previous studies that describe an increase in vaspin tissue expression with obesity (450). It is important to note that our finding that vaspin expression in adipose and muscle tissue was increased with obesity was in patients without T2D.

Gene array data in the GEO database does not reveal any significant difference in vaspin adipose tissue expression between patients with or without insulin resistance or in those with T2D compared to individuals with normal glucose tolerance (454). Furthermore, a recent report found that circulatory levels of vaspin in morbidly obese individuals declined following weight loss induced by

laparoscopic sleeve gastrectomy (455). In addition, newly published data has also demonstrated a strong positive correlation of serum vaspin with other markers of obesity, including serum TAG and cholesterol (456). These findings, together with our data here, support the notion that vaspin expression in humans is dependent on BMI irrespective of diabetic status.

Contrary to previous reports (281), we found no significant difference in serum levels of vaspin in obese individuals compared to lean. This was despite the greater expression and secretion of vaspin from obese SAT of these individuals. This might suggest that elevated secretion of vaspin from SAT in obese individuals is more likely to have localised effects, rather than systemic effects on distal tissues. However, it should be noted that serum concentrations of vaspin were variable and so a significant difference in circulating vaspin concentrations in lean and obese individuals may have been identified with larger cohorts. A number of previous publications have examined systemic levels of vaspin in males and females of varying BMI, with contrasting results. In individuals aged 17–79 it was found that serum vaspin was significantly higher in obese male subjects compared to lean male subjects, but was not significantly different between obese and lean females (281). However, the study by Esteghamati et al. found that serum vaspin levels positively correlated with BMI in both males and females (457). In addition, higher levels of serum vaspin were reported in females compared to males in individuals with normal glucose tolerance, but no gender difference was seen in individuals with T2D (281). However, Seeger et al. examined serum vaspin levels in diabetic and non-diabetic patients in both controls and in patients on chronic haemodialysis with BMI between 26 and 30 and found that vaspin was higher in females and furthermore that gender was an independent predictor of circulating vaspin concentrations (458). Together these observations could reflect sex dimorphism in SAT distribution and quantity (459, 460). It is known for example that females predominantly accumulate more SAT than males (461), and thus vaspin may play a greater role in mediating glucose homeostasis in females than in males. Indeed, some studies have

previously reported that the prevalence of metabolic syndrome is higher in females than in males (462), with central adiposity being a greater risk factor for metabolic diseases in females (463, 464).

Contrary to the above studies, we found no significant difference between serum vaspin concentration between males and females in either lean or obese individuals. Furthermore, unlike the findings of Esteghamati et al. we did not find a significant correlation between BMI and vaspin levels in males (457). However, we did observe that serum vaspin in females significantly correlated with BMI. These disparities may be a reflection of the relatively smaller sample size used in our study, but also likely reflects differences between subject cohorts. For example, the male subjects studied by Youn et al. had a mean age of 39 years, whilst both the male and female subjects studied by Esteghamati et al. had a mean age of 49 years, considerably lower than the mean age of subjects in this thesis (male 71 years, 66 years female) (281, 457).

What drives such increased vaspin expression with increasing adiposity is currently unknown. To address this, we attempted to replicate an obese microenvironment by culturing primary human myotubes with high glucose, insulin and palmitate, either individually or in combination. Vaspin mRNA expression increased on average with all treatment conditions; however such effects did not reach statistical significance. The greatest increase in vaspin mRNA (2-fold) occurred in response to simultaneous glucose, insulin and palmitate, which may suggests that a combination of factors drives increased vaspin mRNA expression in obese individuals, however further study with larger sample sizes are needed to confirm such an effect. Recent data by Aibara et al. has demonstrated a similar increase in murine hepatic vaspin mRNA in response to refeeding with a high fructose diet. Conversely, fasting and specific destruction of pancreatic β-cells reduced hepatic vaspin mRNA in mice (465). The authors suggest that vaspin mRNA may be positively regulated by CEBPA/B, which is interesting, as in chapter 1 of this thesis we report increased CEBPA/B expression in human skeletal muscle with increasing adiposity (466). Further studies would be beneficial to determine the

mechanism in which such circulating factors may drive vaspin mRNA expression in humans and whether CEBPA/B is involved in this process. Furthermore, we only investigated the effect of glucose, insulin and palmitate on myotube expression for 24 h, therefore it would also be interesting to explore the role of other obesity associated factors such as adipokines and more chronic stimulations in the regulation of primary human myotube vaspin mRNA expression. Further studies are also necessary to identify the stimuli and mechanisms responsible for increasing vaspin expression and secretion from SAT, either *ex vivo*, or by utilising primary adipocyte cultures.

4.3.3 Vaspin increases insulin sensitivity in obese primary human myotubes

Functionally, vaspin-mediated activation of PI3K/AKT has been reported previously in several other cell types, including pancreatic cells (467), 3T3-L1 preadipocytes (468) and endothelial progenitor cells (469). Furthermore, it was recently reported that vaspin promotes the PI3K/AKT signalling pathway leading to increased GLUT4 protein expression in rats fed a high-fat diet (470) and can improve glucose tolerance in mice (471). Therefore, our demonstration that vaspin induces activation of PI3K-AKT signalling and increases insulin sensitivity in obese human myotubes is significant. These vaspin-induced effects appear to occur independently of upstream insulin signalling, since vaspin had no direct effect on either the insulin receptor or IGF-1 receptor phosphorylation status. Activation of PI3K/AKT signalling is known to promote GLUT4 translocation and glucose uptake in skeletal muscle cells (472), and here we report that vaspin promotes GLUT4 expression and translocation and facilitates glucose uptake in human obese myotubes. Notably, 15 min stimulation of primary human myoblasts derived from obese subjects with vaspin was able to significantly increase GLUT4 surface translocation to a similar magnitude to that observed with insulin stimulation. This finding may be of clinical significance given that GLUT4 translocation is impaired in T2D patients with insulin insensitivity (473). Indeed, since our data shows that vaspin

induces insulin signalling independent of activating the insulin receptor, this could provide a novel route to therapeutically improve glucose maintenance in insulin-resistant individuals.

Despite being able to promote GLUT4 translocation we found that insulin stimulation of obese myotubes did not result in glucose uptake. Previous studies in rats have demonstrated that GLUT4 expression declines with age (474) and obesity (475). Here we report for the first time in humans that muscle tissue derived from elderly obese individuals displayed a significantly lower expression of GLUT4 mRNA in comparison to young lean individuals. The retention of this phenotype in primary human myotubes from elderly obese subjects may therefore explain the blunted insulin response observed at baseline.

Importantly, prolonged (24 h) pre-treatment of obese myotubes with vaspin sensitised them to insulin-mediated glucose uptake. This sensitisation is likely due to vaspin increasing the bioavailable intracellular pool of GLUT4. Previous studies in 3T3-L1 adipocytes and mice have reported that vaspin induces GLUT4 mRNA expression (450, 468). Here, we report for the first time that vaspin significantly induces GLUT4 mRNA and GLUT4 protein expression in human skeletal muscle. Importantly, we also demonstrate that vaspin is able to activate both AMPK and p38 signalling in primary human myotubes. AMPK activation has previously been reported to upregulate GLUT4 expression in primary human myotubes (476), while p38 is known to regulate transcription factors that control the expression of GLUT4 (477, 478). Activation of these signalling pathways may therefore be a potential mechanism to explain the vaspin-induced upregulation in GLUT4 mRNA and protein expression observed.

However, it should be noted that primary human myotubes in culture elicit relatively low insulin-stimulated glucose uptake, compared to skeletal muscle tissue (479-481). This could be due to low basal expression of GLUT4, which has been attributed to denervation (482-484) and the subsequent absence of contraction. Therefore, in our model system, treatment of myotubes with vaspin may

only be increasing the pool of bioavailable GLUT4 towards physiological levels. Whether vaspin administration in obese elderly humans *in vivo* would have the same effect remains to be seen.

4.3.4 Validation of GRP78 as a possible vaspin receptor in primary human myotubes.

A cell surface receptor for vaspin has yet to be fully elucidated. One possible mechanism is that vaspin signals through GRP78, a protein that has an important intracellular regulatory role during cellular ER stress (484, 485). However, recent evidence shows GRP78 also functions as a cell surface receptor, with membrane localised GRP78 binding vaspin and in turn promoting AKT and AMPK signalling in H-4-II-E-C3 cells (471).

Here, we show GRP78 expression is present in SWAT, EWAT and BAT depots of both mouse and rat animal models. Additionally a significant increase in GRP78 expression was observed in HFD fed obese prone and obese resistant models. A similar increase in GRP78 protein has previously been reported in the abdominal adipose tissue of rats fed a HFD (486). Furthermore we also demonstrate that GRP78 is expressed in both human SAT and skeletal muscle in older individuals. Expression of GRP78 was found to be significantly greater in both SAT and skeletal muscle of obese subjects and displayed a positive correlation with BMI in each case. This is concurrent with the results of Khadir et al. who also found increased GRP78 expression in SAT of obese humans (487). Chronic ER stress can be induced by obesity (488) and is associated with inflammatory adipose tissue (489), this may explain the increased GRP78 expression in muscle and adipose tissue of obese individuals in our present study. Additionally, ER stress has been shown to promote re-localisation of GRP78 to the cell membrane, thus increasing ligand-binding capacity (490).

In an attempt to determine if the effects of vaspin on primary human myotube function reported in this thesis were mediated by GRP78 signalling, we performed siRNA mediated loss of function studies utilising primary human myoblasts and myotubes. Successful knockdown of GRP78 was achieved in

both primary human myoblasts and myotubes 24 h post transfection. Next, following knockdown, primary human myoblasts were treated with recombinant human vaspin for a further 24 h in order to investigate whether GRP78 knockdown would prevent vaspin mediated increases in GLUT4 mRNA. In control cells, GLUT4 expression following vaspin stimulation was variable, with no significant increase in GLUT4 mRNA observed. This was unexpected, as in section 4.2.6 of this thesis we observed a strong induction of vaspin mRNA expression in primary human myotubes. This suggests the TransIT-X2 reagent may have interfered with this vaspin mediated effect, preventing GLUT4 mRNA upregulation. Additionally, it appeared GRP78 knockdown was either unsuccessful in this attempt or was transient, returning towards basal levels by the 48 h time point. Consequently, we are unable to conclude the role of GRP78 on vaspin mediated GLUT4 expression. We also investigated whether GRP78 knockdown could blunt vaspin induced activation of AKT, as described in section 4.2.4 of this thesis. As expected, acute vaspin stimulation significantly increased the activation of $AKT^{(ser473)}$ in primary human myotubes, as measured by immunoblotting. In contrast, no such vaspin mediated effect was observed in primary human myotubes treated with either siRNA #1 or siRNA #2. However, basal AKT activation was also greater in myotubes treated with both siRNA #1/#2. Therefore an off-target effect of siRNA treatment may have caused an induction of AKT that meant further activation by vaspin was not possible. Thus we cannot conclude whether the blunted AKT activation was indeed due to GRP78 knockdown. As a result, future studies are still required to elucidate the potential role of GRP78 in vaspin signalling. Utilising lentiviral knockout or CRISPRi gene editing would be useful to remove the potential effect of lipid interaction and off target effects of siRNAs. Lentiviral knockout or CRISPRi gene editing could also produce more sustained knockdown to overcome the issue of transient GRP78 knockdown encountered in this thesis.

4. 3.5 Limitations

In addition to the limitations of the myotube model and cohort numbers as previously discussed, it is also important to note that these studies were conducted using *ex vivo* adipose tissue rather than isolated adipocyte cells. Although the use of whole adipose tissue is physiologically more relevant, we are unable to determine the cellular source of the adipose-secreted vaspin. Therefore, future studies should aim to identify the predominant source of vaspin from adipose tissue, by performing studies utilising primary human adipocytes and immune cells. Additionally, due to issues with antibody specificity, we only report vaspin expression at the mRNA level in human skeletal muscle tissue, adipose tissue and primary human myotubes. Use of different antibodies would be beneficial to confirm differential vaspin protein expression within such tissues and primary human cultures.

4.3.6 Conclusions

In summary, this thesis chapter shows that vaspin is directly secreted from both human SAT and skeletal muscle and its expression is increased with increasing adiposity in older individuals. Functionally, vaspin induces PI3K/AKT activation, increases both GLUT4 expression and translocation and promotes insulin-stimulated glucose uptake in primary obese older human myotubes. These data support a role for vaspin as a protective adipokine in the development of insulin resistance in elderly obese individuals. Further studies are needed to identify the mechanism of action of vaspin as this may provide a novel therapeutic target to improve insulin sensitivity independent of the insulin receptor.

CHAPTER 5: Adipose tissue derived extracellular vesicles: a novel mechanism of adipose tissue and skeletal muscle crosstalk

5.1 Introduction

It has become increasingly recognised that extracellular vesicles (EVs) are an important mechanism of tissue crosstalk throughout the body. EVs can be further sub-classified as exosomes (50-150 nm in diameter), created intracellularly via the endosomal system, or microvesicles (approximately 100 - 1000 nm in diameter), derived by budding from the plasma membrane (Figure 5.1) (491). EVs carry a variety of internal cargo including mRNAs, non-coding RNAs and proteins (492). Recent evidence has even shown the presence of functionally active enzymes and phosphorylated proteins within EVs (493). Systemic transportation of such cargo between cells appears to be vital for health, while it is also becoming apparent that dysregulated vesicle release is an important driver of many pathological processes in disease (494).

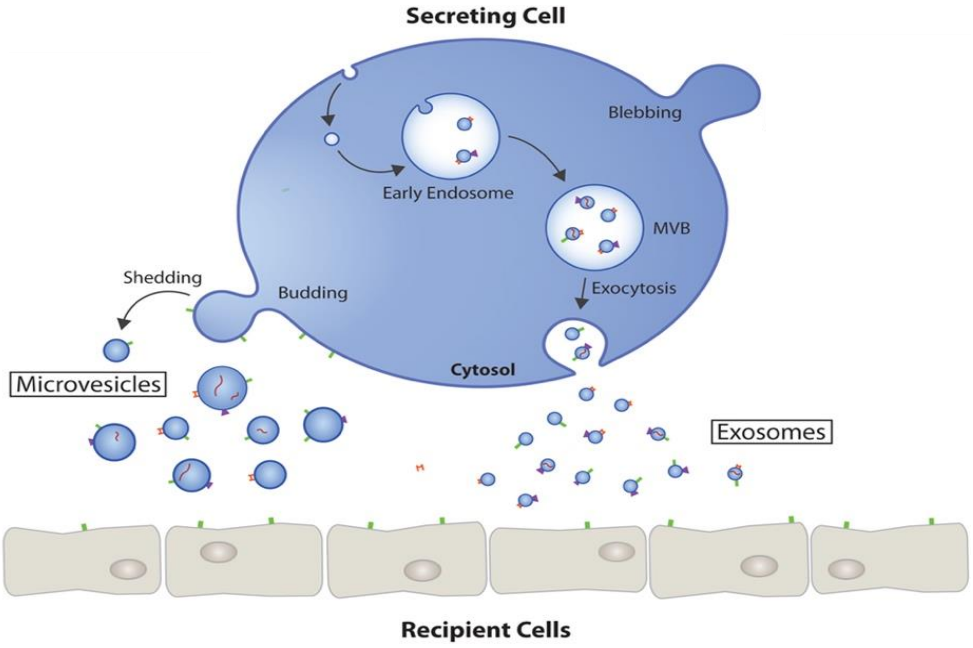

Figure 5. 1. The biogenesis and secretion of exosomes and microvesicles.

Exosomes are formed within the cytosol of the secreting cell, with cargo packaged before their release via exocytosis. In contrast, microvesicles are shed from the plasma membrane through membrane budding and cleavage and thus often express cell surface markers.
Adapted from Gustafson et al. (495).

As discussed in the earlier chapters of this thesis, adipose tissue is known to secrete a plethora of adipokines, which in turn impact the function of other tissues such as skeletal muscle (496). Furthermore, it is now well established that the production of adipokines becomes dysregulated with obesity, likely contributing to the development of many obesity associated pathologies, including skeletal muscle insulin resistance (413). Similarly, recent work by Kranendonk described both the secretion of EVs from human adipose tissue and the presence of adiponectin positive EVs in human plasma (497). Additionally, elegant experiments by Thomou et al. demonstrated that microRNAs carried in adipose tissue derived EVs regulate liver gene expression in mice, providing the first evidence that adipose tissue derived EVs are capable of mediating tissue crosstalk (498).

In light of such data we hypothesise that, as seen with adipokines, obesity drives increased vesicle release from human adipose tissue. Additionally, we propose that such vesicles may mediate obesity associated changes in skeletal muscle function in humans; such as increased inflammation and skeletal muscle insulin resistance.

5.1.1 Chapter aims

This chapter aims to:

- Characterise EVs derived from both lean and obese human adipose tissue.
- Determine the functional role of EVs derived from both lean and obese human adipose tissue in mediating the obese phenotype of human skeletal muscle by performing crosstalk studies with isolated EVs and primary human myotubes.

5.2 Results

5.2.1 Detection of differential populations of EVs derived from lean and obese human adipose tissue

Firstly, Exoview chips specific for the tetraspanins CD9, CD81 and CD63 (markers of EVs), were used to detect the presence of EVs in serum free ACM derived from both lean (n = 5) and obese (n = 5) individuals. EVs were successfully captured on all human tetraspanin antibody spots, for all individuals, while there was very little interaction with the mouse IgG negative control (Figure 5.2). The average total number of EVs captured with each antibody was approximately 2-fold lower in obese individuals (Figure 5.3), however this was only significant (P = 0.031) for vesicles captured on CD81 antibody spots (Figure 5.3). Additionally, in both lean and obese populations, approximately 2-fold less EVs were captured on the CD63 spots compared to CD9 and CD81 spots (Figure 5.3). The sizes of vesicles were similar on all capture antibody spots, for both lean and obese individuals, with the majority of vesicles having a diameter of 50-100 nm, typical of exosomes (Figure 5.4).

Next, EVs captured on CD63 antibody spots were probed with fluorescent antibodies against CD9, CD63 and CD81 to identify if captured vesicles also expressed other tetraspanin markers. In lean individuals, 52 ± 8% of captured vesicles displayed CD63 fluorescence. This was significantly greater than the number of particles positive for CD81 (18 ± 3%), but not particles positive for CD9 (31 ± 8%). In contrast, 71 ± 8% of particles displayed expression of CD63 in obese individuals. Although this was not significantly different to lean individuals, such CD63 expression was significantly greater than both the number of vesicles expressing CD9 (16 ± 5%) and CD81 (13 ± 4%). This difference in vesicle populations between lean and obese subjects is visually represented in Figure 5.5, with Figure 5.5 B demonstrating greater fluorescence heterogeneity in EVs derived from lean individuals in comparison to the more dominant red staining attributable to CD63 apparent in EVs derived from obese individuals (Figure 5.5 C). No significant difference between lean and obese induvial was

observed in the fluorescence data for vesicles captured on either CD9 or CD81 antibody spots (Figure 5.6 A-B).

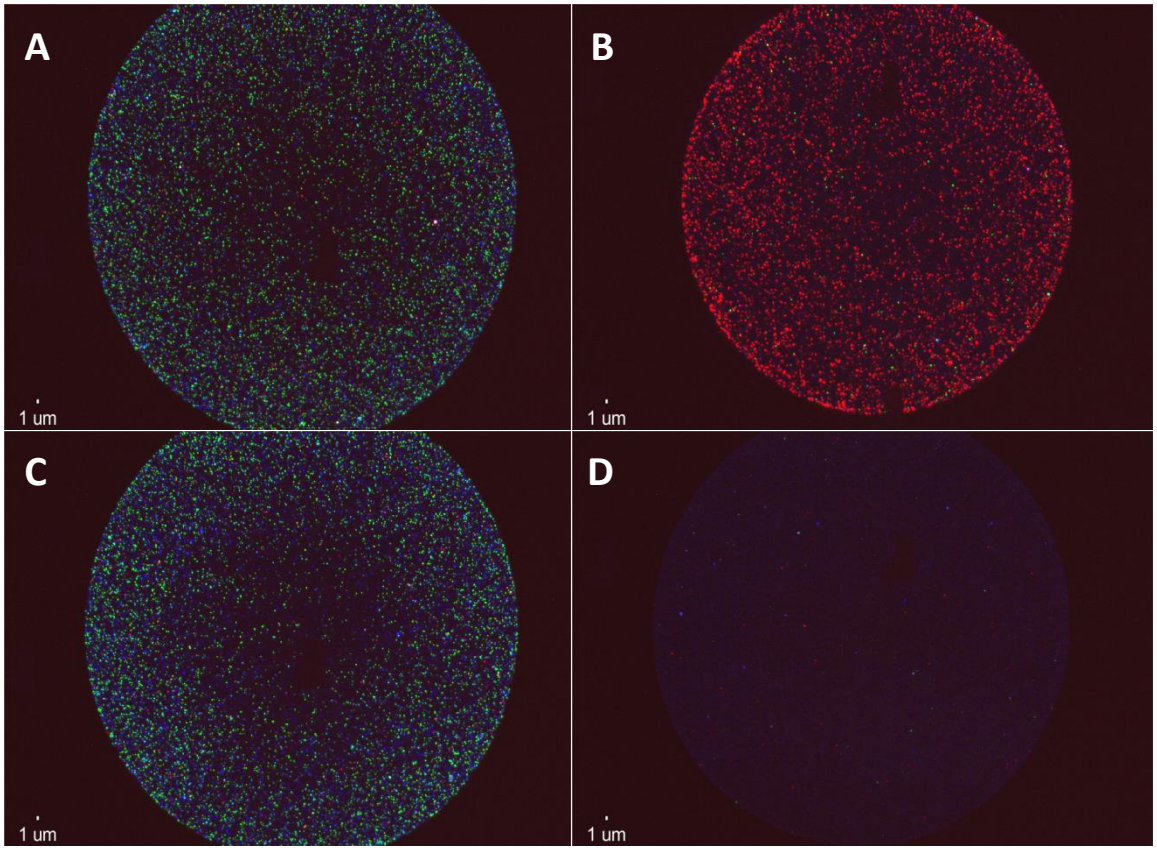

Figure 5. 2. Fluorescently labelled adipose tissue derived EVs in serum free media for EV markers.

Representative images of serum free ACM derived EVs from an obese individual captured on a CD63 capture antibody spot of an exoview tetraspanin chip followed by staining with secondary antibodies against **A.** CD9 (green) **B.** CD63 (red) and **C.** CD81 (blue). **D.** serum free ACM derived EVs captured with a mouse IgG antibody spot of the same tetraspanin chip and probed with CD63 (Red) secondary antibody.

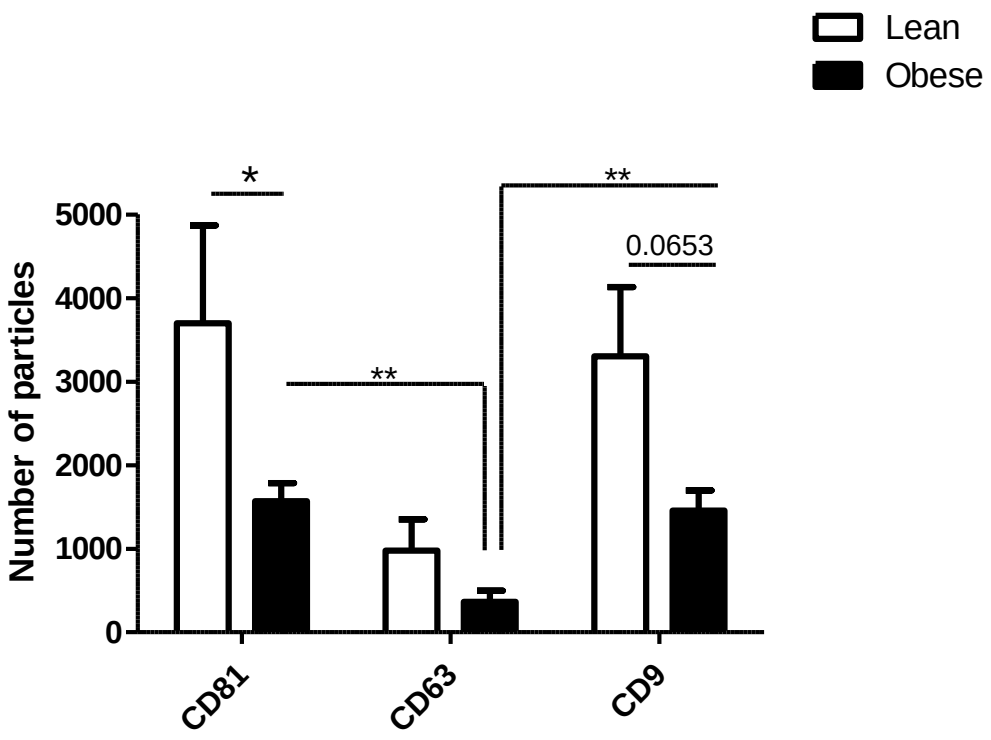

Figure 5. 3. Quantification of EVs in serum free ACM derived from lean and obese individuals.

Total number of EVs captured on the CD81, CD63 and CD9 capture antibody spots in serum free ACM derived from lean and obese individuals, determined by light scatter using Exoview. n = 5 lean and n = 5 obese. Data are expressed as mean ± S.E.M. * (*P* < 0.05), ** (P <0.01) denotes a significantly different number of vesicles as determined by Bonferroni post-hoc tests following 2-way ANOVA.

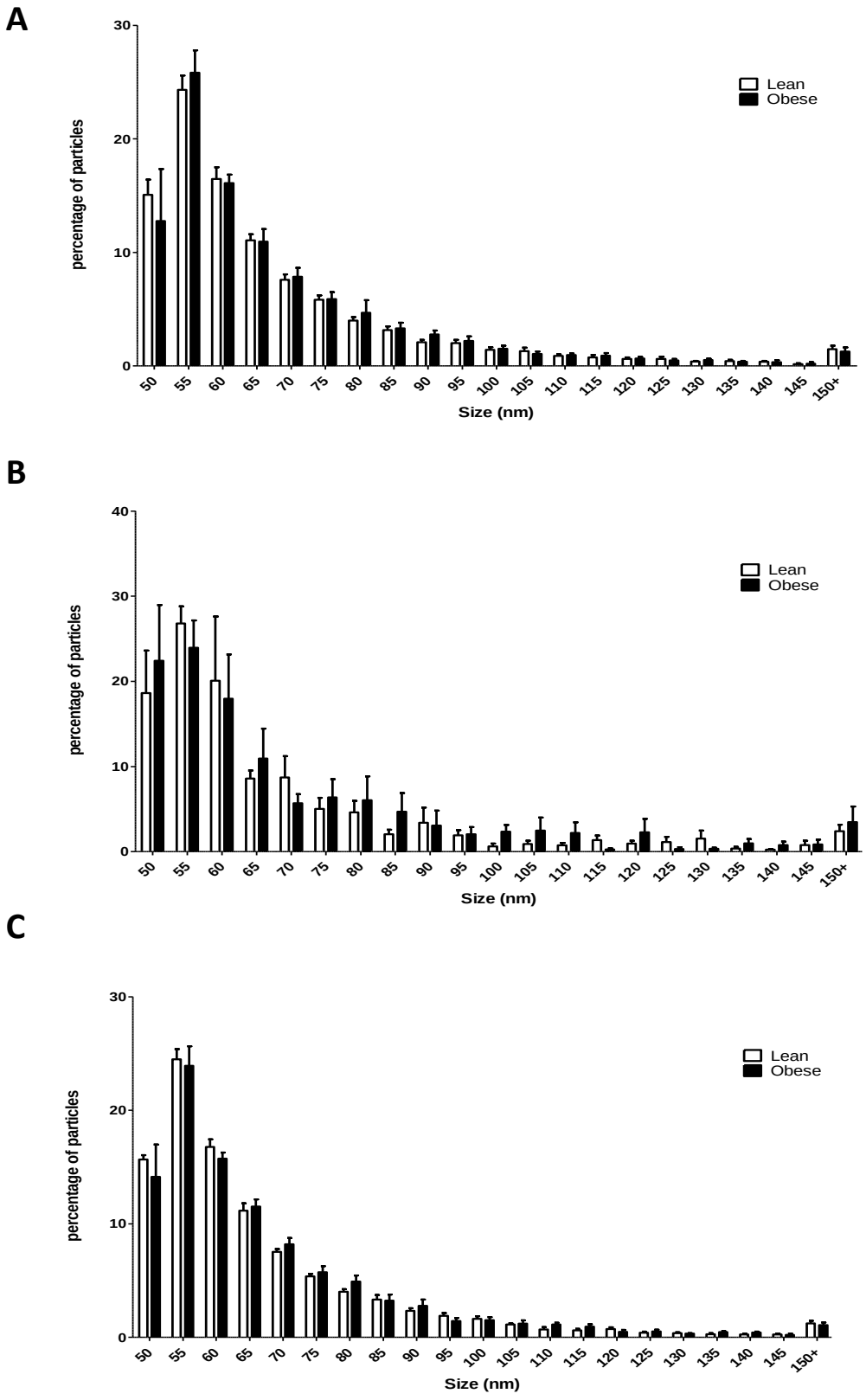

Figure 5. 4. Diameter of EVs in serum free ACM derived from lean and obese individuals.

Average diameter of EVs captured on the CD81 **A.** CD63 **B.** and CD9 **C.** antibody spots of exoview tetraspanin chips in serum free ACM derived from lean and obese individuals. n = 5 lean and n = 5 obese. Data are expressed as mean ± S.E.M.

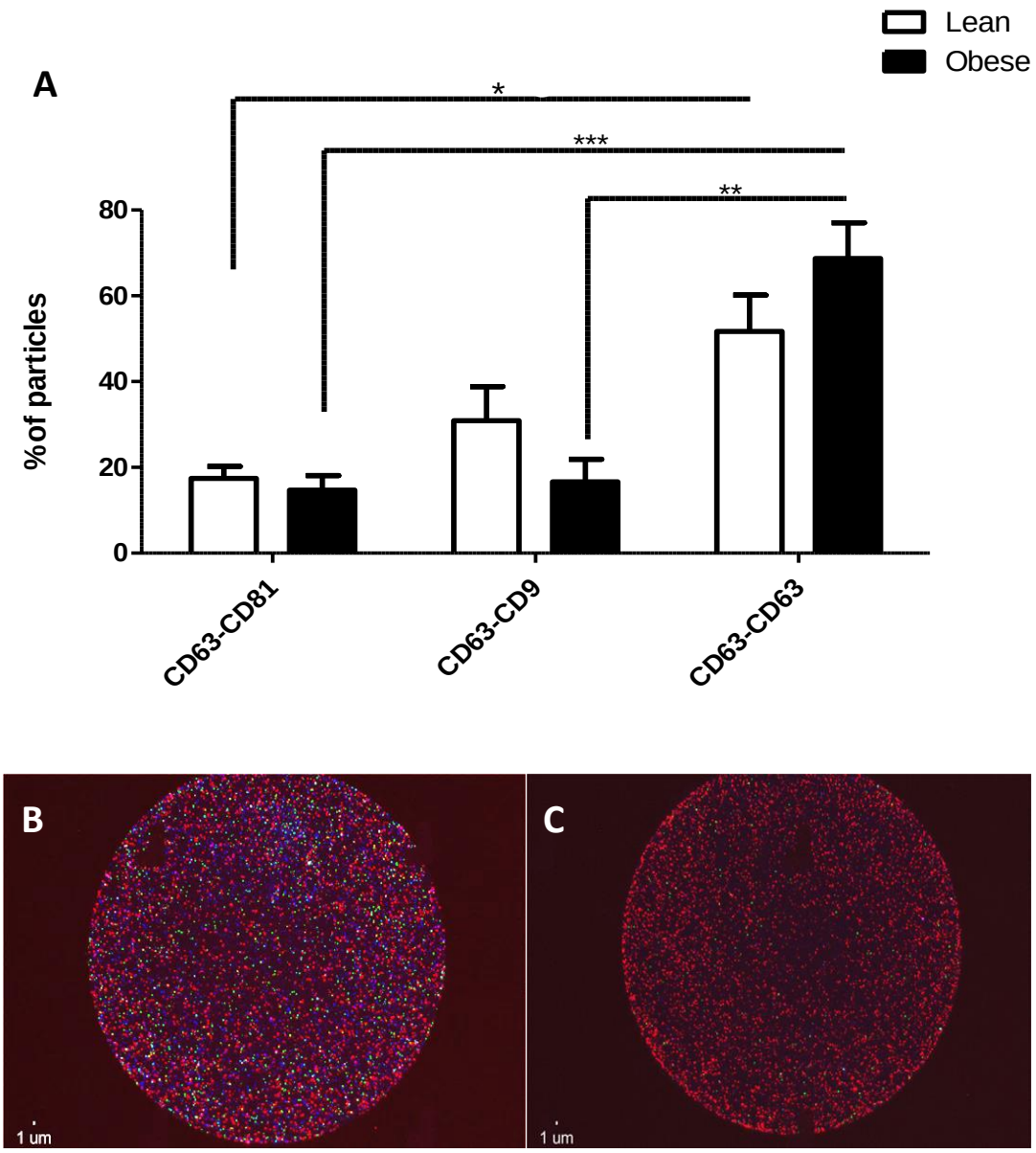

Figure 5. 5. Differential populations of EVs derived from lean and obese individuals.

A. Detection of CD81, CD9 and CD63 expressing vesicles derived from lean (n = 5) and obese (n = 5) adipose tissue captured on a CD63 capture antibody spot. Data are expressed as mean ± S.E.M. *** indicates $P < 0.001$, ** indicates $P < 0.01$, * Indicates $P < 0.05$ as determined by Bonferroni post-hoc tests following 2-way ANOVA. **B** Representative image of EVs derived from a lean individual captured on the CD63 capture antibody**.** Red fluorescence indicates CD63. Green fluorescence indicates CD81, Blue indicates CD9. **C.** Representative image of EVs derived from an obese individual captured on a CD63 capture antibody spot**.** Red fluorescence indicates CD63. Green indicates CD81, Blue indicates CD9. EVs were captured on 3 spots for each antibody, for each

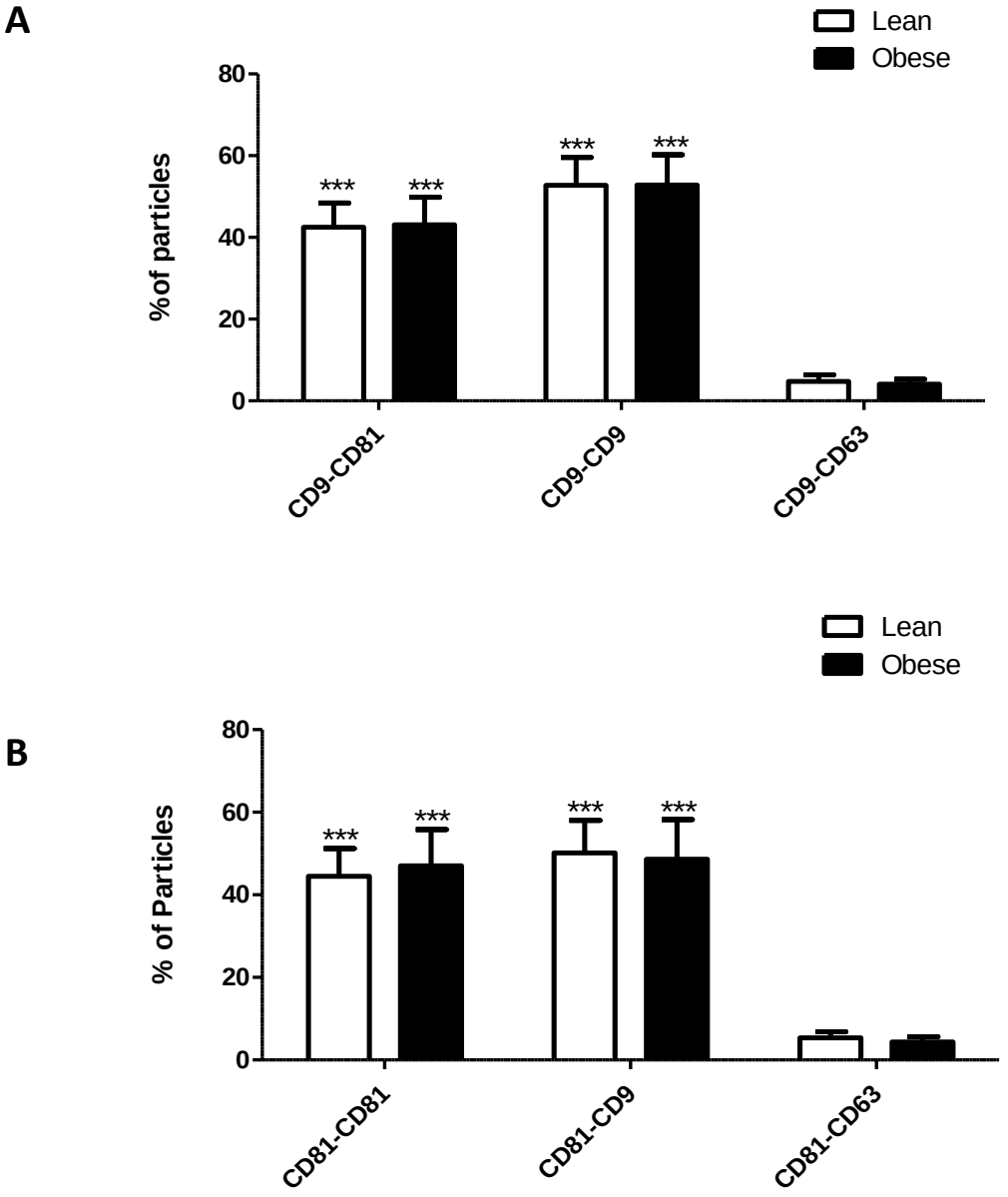

Figure 5. 6. Fluorescent staining of EVs detected on CD9 and CD81 capture antibody spots.

A. Detection of CD81, CD9 and CD63 expressing vesicles derived from lean (n = 5) and obese (n = 5) EVs captured on CD9 capture antibody spots. *** indicates a significant difference from CD9-CD63 as determined by Tukey post-hoc tests following 2 way ANOVA 2 way ANOVA. **B.** Detection of CD81, CD9 and CD63 expressing vesicles derived from lean (n = 5) and obese (n = 5) EVs captured on the CD81 capture antibody spots. EVs were captured on 3 spots for each antibody, for each sample. *** indicates a significant difference from CD81-CD63 vesicles ($P < 0.001$) as determined by Tukey post-hoc tests following 2 way ANOVA.

5.2.2 Adipose tissue derived EVs increase proinflammatory cytokine release from lean primary human myotubes

We next investigated whether EVs isolated from either lean or obese individuals impact on primary human myotube function. Previous studies and data presented in chapter 3 of this thesis indicated that obese skeletal muscle is more inflammatory, secreting increased amounts of proinflammatory cytokines such as IL-6. We therefore hypothesised that adipose tissue derived EVs may be implicated in mediating this effect. To investigate this, primary human myotubes from a lean individual were treated with EVs derived from the adipose tissue of both lean and obese individuals for 24-48 h and the impact on proinflammatory cytokine secretion measured by ELISA.

Primary human myotubes treated for 24 h with EVs derived from lean adipose tissue secreted a significantly greater amount of IL-6 (1328 + 17 pg/ml) in comparison to untreated controls (415 ± 67 pg/ml) (Figure 5.7 A). Similarly, myotubes treated with EVs derived from obese adipose tissue also secreted approximately 2-fold more IL-6 on average (1565 + 645 pg/ml). However, vesicles derived from 1 of the 3 obese individuals did not elicit an IL-6 response (334 pg/ml) and so this effect did not reach statistical significance. Similar to IL-6, myotubes treated with both lean and obese EVs for 24 h also secreted approximately 2-fold more IL-8 on average, although this did not reach statistical significance (Figure 5.7 B).

We next investigated whether pre-treatment with EVs would prime myotubes to become more inflammatory and thus secrete greater amounts of IL-6 in response to challenge with an inflammatory stimulus. To this end, lean primary human myotubes were treated with either lean or obese EVs for 48h. Media containing EVs was then removed and myotubes were then treated with IL-1β (1 ng/ml IL-1β, 3 h). Il-1β stimulation evoked a significant increase in IL-6 secretion from untreated lean primary human myotubes, as reported in chapter 3 of this thesis. Similarly, IL-1β also evoked a significant increase in IL-6 secretion from myotubes pre-treated with both lean and obese EVs.

Although such a response was approximately 1.5-fold greater in myotubes pre-treated with obese EVs (1283 ± 102 pg/ml) this was not statistically significant from untreated myotubes (863 ± 162 pg/ml). Similarly, no significant difference in IL-1β mediated IL-6 secretion was observed in myotubes pre-treated with lean EVs. Finally, ELISA was also performed in order to determine if such EV-mediated increased IL-6 and IL-8 secretion in myotubes was due to the presence of these cytokines in isolated vesicles. Significantly greater concentrations of IL-6 and IL-8 were detected in media containing obese vesicles. However, the concentration of both IL-6 and IL-8 in EVs was negligible (5-20 pg/ml), in comparison to the concentrations detected in EV-stimulated primary human myotubes.

To identify a possible mechanism for such EV induced secretion of proinflammatory cytokines, we next investigated the impact of adipose tissue derived EVs on the activation of NF-κB signalling, a known regulatory pathway of inflammatory cytokine secretion (425, 499). Firstly, it was necessary to determine whether the complete secretome of adipose tissue caused activation of NF-κB in primary human myotubes. To this end, lean primary human myotubes were treated with obese ACM for 48 h in the presence or absence of the IKKβ inhibitor 5-(p-Fluorophenyl)-2-ureidothiophene-3-carboxamide (TPCA-1). ACM caused a significant ($P < 0.05$) increase in NF-κB activation, as evidenced by increased phosphorylation of $P65^{Ser536}$, which was prevented by the co-stimulation with TCPA1 (Figure 5.8 A-B). Similarly, treatment of myotubes with EVs isolated from both lean (n = 3) and obese (n = 3) ACM also induced activation of $P65^{Ser536}$ (Figure 5.8 C), although densitometric analysis did not reach statistical significance ($P = 0.104$) (Figure 5.8 D).

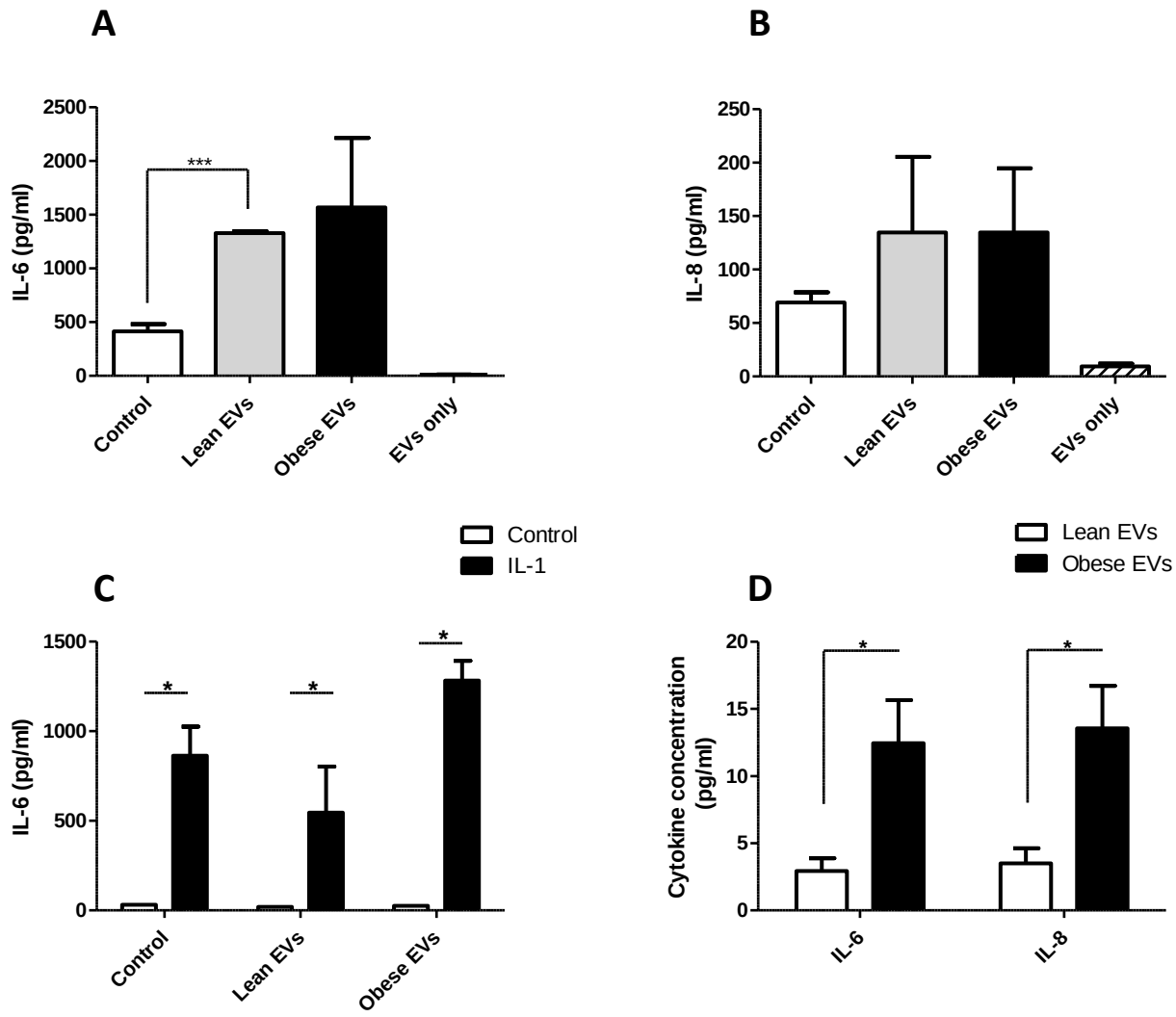

Figure 5. 7. Adipose tissue derived EVs drive pro-inflammatory cytokine release from lean primary human myotubes

A. IL-6 Secretion from lean primary human myotubes in response to 24 h stimulation with lean (n = 3) and obese (n = 3) EVs. *** Indicates a significant ($p<0.01$) difference from control as determined by Dunnet's post-hoc tests following 1-way ANOVA. **B.** IL-6 Secretion from lean primary human myotubes in response to 24 h stimulation with lean (n = 3) and obese (n = 3) EVs. **C.** IL-6 secretion in response to 3 h IL-1 stimulation (1 ng/ ml), in lean primary human myotubes pre-treated with either lean (n = 3) or obese (n = 3) EVs for 48 h, * indicates a significant ($P < 0.05$) increase in IL-6 secretion in response to IL-1 treatment, as determined by Bonferroni post-hoc tests following 2-way ANOVA. **D.** IL-6 and IL-8 concentration in culture media treated with either lean or obese vesicles only for 24 h. * indicates a significant ($P < 0.05$) difference in cytokine concentration as determined by unpaired T-tests. Data are presented as mean ± S.E.M.

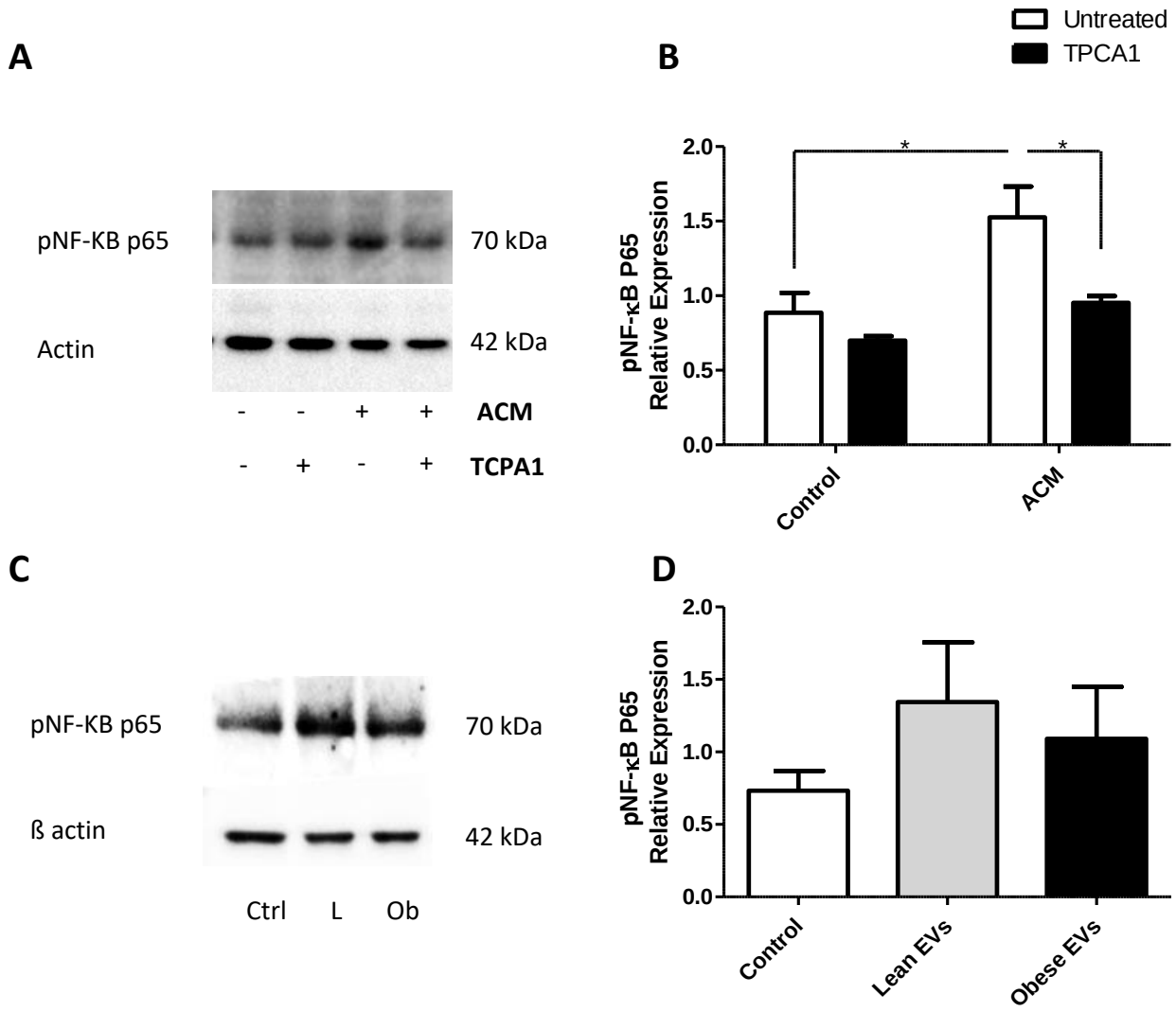

Figure 5. 8. Adipose tissue derived EVs activate NF-KB signalling in lean primary human myotubes

A. Activation of NF-KB P65 $^{(Ser536)}$ in primary human myotubes following 48 h stimulation with adipose conditioned media (n = 3) in the absence or presence of TCPA1 (40 nM), as determined by western blotting (10 µg protein loaded per sample). **B** Densitometric analysis of NF-KB P65 blots normalised to β-actin. **C.** Activation of NF-KB P65 in lean primary human myotubes following 48h stimulation with EVs derived from either lean (L) (n = 3) or obese (Ob) (n = 3) individuals as determined by western blotting (10 µg protein loaded per sample). **D** Densitometric analysis of EV stimulated phosphorylation of NF-KB P65 blots normalised to normalised to β-actin. Data are presented as mean ± S.E.M.* Signifies significant difference from control as determined by 2 way ANOVA followed by Dunnett's post-hoc tests.

5.2.3 EVs derived from lean and obese adipose tissue affect the expression of candidate genes in primary human myotubes

We next investigated whether EVs drive changes in lean primary human myotube gene expression associated with increased adiposity, as identified in chapters 3 and 4 of this thesis by stimulating lean primary human myotubes with EVs from lean and obese adipose tissue for 24h. Treatment of lean primary human myotubes with EVs from both lean and obese individuals evoked an approximate 2-fold increase in vaspin mRNA expression (P = 0.079) as determined by qRT-PCR. Additionally EVs derived from obese individuals elicited a 3-fold increase in the expression calpain 1 ($P < 0.05$). Interestingly, no such effect on calpain 1 expression was observed in myotubes treated with lean EVs. No significant difference was observed in the expression of FBP-1, IL-6 or other genes associated with the regulation of skeletal muscle mass, including calpain 2, myostatin, MAFbx or MuRF1.

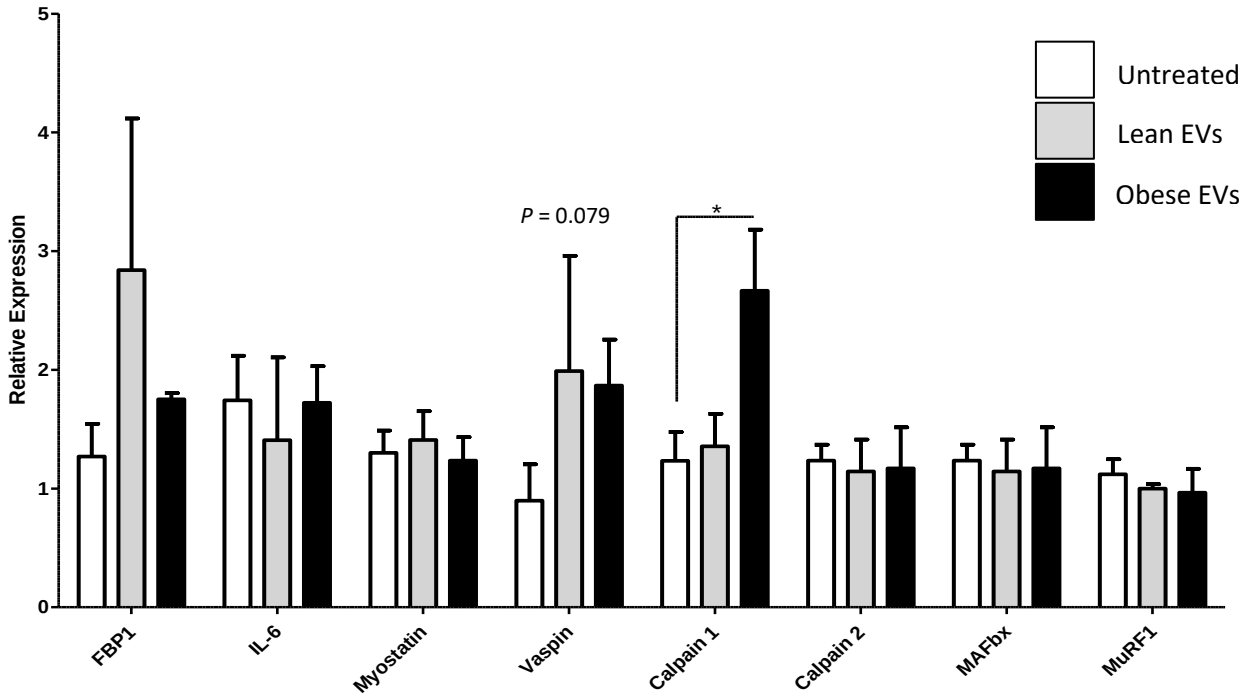

Figure 5. 9. EVs derived from lean and obese adipose tissue upregulate candidate gene expression in primary human myotubes

Gene expression was determined via qRT-PCR and normalised to GAPDH (n = 3 lean, n = 4 obese EVs). Data are represented as mean ± S.E.M. * indicates significantly different expression from untreated myotubes as determined via 1-way ANOVA, followed by Dunnett's post-hoc tests.

5.2.4 Effect of EVs derived from lean and obese adipose tissue on primary human myotube insulin signalling

Finally, ACM from obese individuals and adipokines upregulated with obesity have been reported to drive primary human myotube insulin resistance associated with obesity and T2D. Therefore we also investigated whether adipose tissue derived EVs could induce a similar blunting of insulin signalling in lean primary human myotubes. Insulin increased phosphorylation of AKT approximately 1.2-fold in untreated myotubes (Fig. 5.10 A). Insulin induced activation of AKT was reduced on average in primary human myotubes pre-treated with both lean and obese EVs, however none of these insulin induced effects were statistically significant based on densitometric analysis (Fig. 5.10 B).

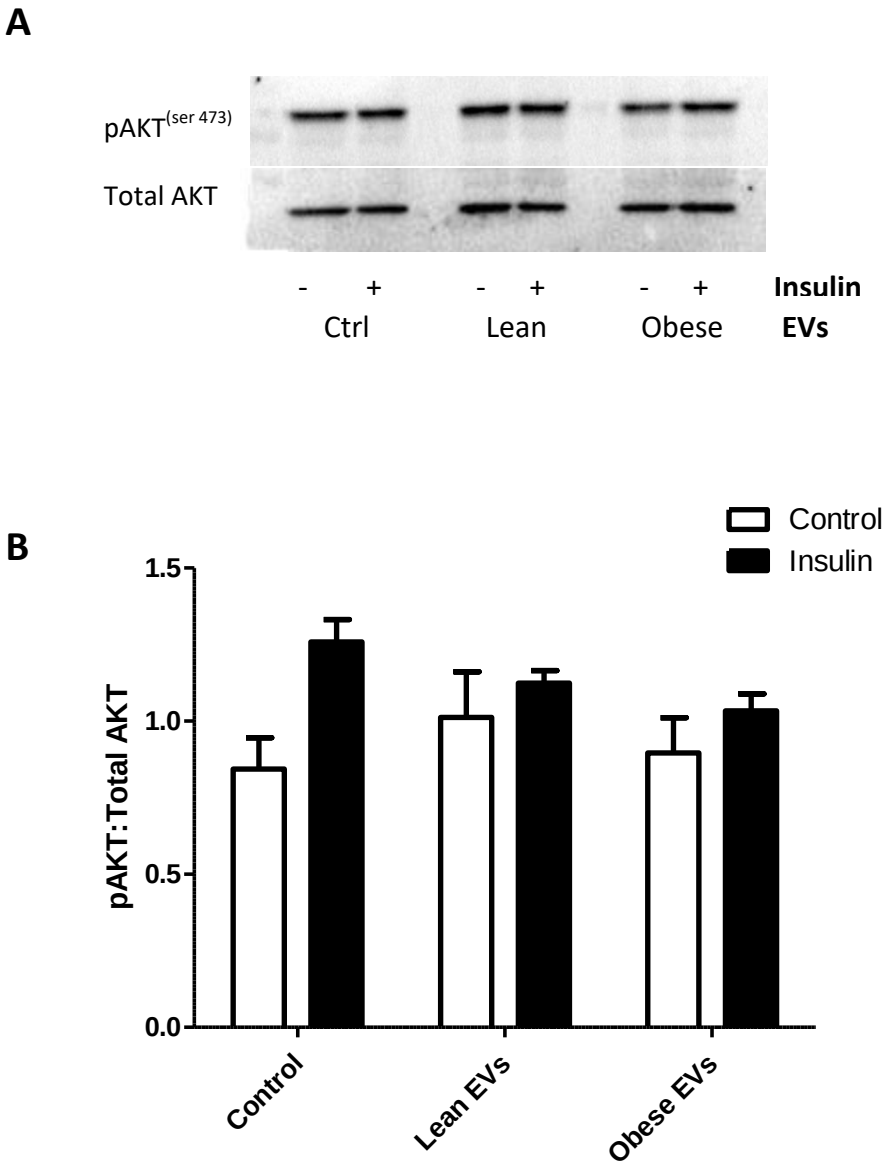

Figure 5. 10. Effect of pre-treating lean primary human myotubes with adipose tissue derived EVs on the insulin induced activation of AKT

Lean primary human myotubes were pre-treated with EVs derived from the adipose tissue of lean (n = 3) or obese (n = 3) individuals for 48 h. Primary human myotubes were then stimulated with insulin (100 nM, 30 min) or left untreated. **A.** Activation of AKT^{ser473} in primary human myotubes as determined by western blotting (10 µg protein loaded per sample). **B.** Densitometric analysis of western blots. Data are represented as mean ± S.E.M.

5.3 Discussion

Extracellular vesicles are becoming increasingly regarded as an important mechanism of intercellular communication and are implicated in the development of many pathologies. This is the first study to identify and characterise human adipose tissue derived EVs from both lean and obese individuals and report the novel EV mediated crosstalk between human adipose tissue and primary human myotubes.

5.3.1 Human adipose tissue derived EVs are differentially secreted between lean and obese individuals

Adipose tissue derived EVs from both lean and obese individuals were detected on CD9, CD63 and CD81 capture antibodies using Exoview in combination with tetraspanin chips. Interestingly, there was approximately 2-fold less EVs in the ACM derived from obese individuals in comparisons to lean individuals, on all capture antibody spots. This was surprising, as previous studies have reported an increased concentration of EVs in both the plasma and serum of obese individuals (500-503). Additionally, circulating EVs have also been demonstrated to display a positive correlation with insulin resistance (497, 503), while plasma vesicles positive for the adipocyte marker perilipin decreased following diet induced weight loss in humans (500).

Such a discrepancy between the findings of this thesis and the current literature may be due to the method of vesicle detection. Previous studies described above used either nanoparticle tracking analysis (NTA) or flow cytometry to quantify vesicles, with each method having considerable limitations in this respect. Firstly, NTA utilises laser light scatter microscopy and Brownian motion in order to detect particles (504). Although this has the advantage of facilitating the detection of all vesicle populations present in a sample, this non-specific nature also results in detection of non-vesicular particles, such as protein aggregates. Therefore, studies utilising NTA may have

overestimated the vesicle populations in both lean and obese individuals, with potential differences between sample populations being attributable to non-vesicular particles. Additionally, NTA also only reliably detects particles with a diameter of 70 nm and above (505). Therefore, as the majority of vesicles detected in this thesis were approximately 50-100 nm, a considerable amount of particles are likely not represented in studies utilising NTA. Similarly, vesicles are often below the lower size limit for detection and characterisation by flow cytometry (506). Subsequently, utilisation of flow cytometry to measure EVs may also give an untrue reflection of the vesicle populations present. However, it should be noted that this thesis did only capture vesicles expressing the tetraspanins CD9, CD63 and CD81, markers typically associated with exosomes (507). Thus, although such exosome populations may indeed decrease in the obese state, other populations of exosomes and microvesicles, not detected in this thesis, could increase with obesity leading to a net increase in total vesicle number as previously reported. For clarification, it would be useful to analyse the same samples using both nanoview and NTA/flow cytometry.

Additionally, this thesis has only investigated SWAT derived EVs. VAT is widely accepted to be more inflammatory in terms of cytokine and adipokine release. Therefore increased vesicle release from VAT depots, in addition to other tissues, may also explain the previously reported elevated circulating vesicles in obesity. Furthermore, SAT is often more inflammatory in obese individuals, displaying a significantly increased population of immune cells (508). Importantly, recent data has reported that adipose tissue derived EVs are taken up by monocytes, in turn driving their differentiation to macrophages (497). Therefore, it may be hypothesised that there was also increased clearance of adipocyte derived vesicles in obese adipose tissue, due to increased monocyte content. Subsequently, it may be useful to measure vesicle release at earlier time points, in order to limit this effect. Critically, in addition to differences in vesicle number, it appears there may also be different vesicle populations released from lean and obese SAT. Vesicles from obese SAT captured on the CD63 capture antibody spot displayed a significantly greater expression of CD63 in comparison to

both CD9 and CD81. This was not observed in vesicles from lean SAT and thus suggests a loss of CD9 and CD81 expression may occur with obesity. Although the functional impact of this population shift was beyond the scope of this thesis, it is becoming increasingly recognised that, in addition to simply being markers associated with exosome biogenesis, the expression of tetraspanins may mediate the functional effects of EVs. Firstly, tetraspanins have been shown to play an important role in the uptake of vesicles, often through their interaction with other proteins such as integrins at the membrane of target cells (509). Indeed, overexpression of Tspan8, on vesicles derived from the BSp73ASML cell line, directs vesicles to the pancreas and lungs of rats *in vivo* (510). Therefore, differential expression of tetraspanins on EVs derived from obese SAT may direct vesicles to different target cells. Additionally, tetraspanin expression may also affect vesicle production or release. For example, CD9 knockout mice demonstrate significantly reduced vesicle release from dendritic cells (511). As EVs derived from obese SAT also appeared to have reduced CD9 expression, this may offer another explanation for the reduced total vesicle number in the ACM of obese individuals. Importantly, tetraspanin expression may also impact vesicle function. Brzozowski et al. recently reported that CD9 knockdown in the RWPE1 human prostate cell line significantly affected the proteome of EVs released from these cells (512). Thus vesicles derived from obese adipose tissue may harbour different protein or RNA cargo.

5.3.2 Adipose tissue derived EVS mediate crosstalk with primary human myotubes

We next sought to determine if human SAT derived EVs, from either lean or obese individuals affect skeletal muscle function. Following the identification of increased proinflammatory cytokine release from obese primary human myotubes in chapter 3 of this thesis, we first investigated whether SAT derived EVs are involved in mediating this effect.

24 h incubation of EVs derived from lean SAT evoked a significant increase in IL-6 secretion from lean primary human myotubes. Similarly, vesicles from 2 of 3 obese individuals also evoked an increase in IL-6 secretion from primary human myotubes and to a greater extent than observed with lean EVs. However, a limited response with EVs derived from a third obese individual meant that this effect did not reach statistical significance. Similarly, the secretion of IL-8 from lean primary human myotubes also increased, on average, in response to both lean and obese EVs, although this also did not reach statistical significance, again likely due to the small sample size. Critically, increases in IL-6 and IL-8 secretion were not simply derived from EVs, as IL-6 and IL-8 measured in media containing vesicles alone was negligible. In support of these findings, pioneering work by Deng et al. demonstrated that injecting EVs derived from the VAT of donor mice, into recipient mice, caused a similar increase in the release of the proinflammatory cytokines; IL-6 and TNF from bone marrow derived macrophages (513). These findings and the results of the present investigation suggest that chronic exposure of skeletal muscle to SAT derived EVs may contribute to the development of the inflammatory skeletal muscle phenotype described in chapter 3 of this thesis.

To identify a mechanism for such increased cytokine release, we investigated whether EVs activate the NF-κB signalling pathway, a major regulator of proinflammatory cytokine transcription (499). Whole ACM evoked a robust activation of NF-κB signalling after 48 h. NF-κB activation was also observed following 48 h stimulation with EVs, although this did not reach statistical significance. This suggests that EVs are responsible, at least in part, for mediating the proinflammatory effect of

adipose tissue on primary human myotubes. It should be noted that the measurement of NF-κB activation was performed after 48 h treatment with EVs rather than 24 h, to coincide with the investigation of 48 h pre-treatment of myotubes with EVs before IL-1β stimulation. Therefore it is possible that NF-κB activation had already peaked and began to decline by 48 h. Additional time course experiments would be valuable to confirm this.

Despite increased NF-κB activation and IL-6 secretion, no effect of EVs on IL-6 mRNA expression was observed in this thesis. Nevertheless, this investigation only measured IL-6 mRNA expression following 24 h stimulation with EVs. Previous studies have observed transient increases in IL-6 mRNA that peak at around 4-6 h in response to proinflammatory stimuli; therefore again it is possible that IL-6 mRNA expression peaked within this 4-6 h window and then returned to baseline by 24 h (514, 515). Alternatively, EVs may promote the translation and/or secretion of IL-6 without affecting mRNA expression. Further time course experiments would also be needed to clarify the effect of EVs on primary human myotube gene expression.

This thesis also investigated the impact of EVs on the expression of other genes found to be differentially expressed with increased adiposity in chapters 3 and 4 of this thesis, in order to determine if EVs may also play a role in mediating such effects. Interestingly, vaspin mRNA was found to be increased in primary human myotubes cultured from lean individuals in response to 24 h treatment with EVs (P = 0.079). Thus EVs from SAT may be partly responsible for driving the increased expression of vaspin in the obese state as reported in chapter 4 of this thesis. Obese EVs also increased calpain 1 expression in lean primary human myotubes. Consequently SAT EVs may also play a role in driving increased muscle catabolism with obesity (391). In contrast, other genes associated with skeletal muscle atrophy such as MAFbx, MuRF1 and myostatin (also identified to be upregulated with obesity; chapter 3) were unaffected by either lean or obese SAT EV stimulation.

However, again, this was only at a 24 h time point and thus changes in mRNA expression could have occurred with different stimulation duration.

Finally, as ACM and individual adipokines have previously been reported to drive insulin resistance in primary human myotubes (413, 516), we also investigated whether SAT EVs derived from lean and obese individuals blunt insulin signalling in lean primary human myotubes. No significant difference in insulin induced activation of AKT^{Ser473} was observed in primary human myotubes pre-treated with either lean or obese EVs for 48 h. However, this was based on the response of primary human myotubes cultured from one individual. Additionally, this particular individual did not display a strong insulin response in untreated conditions and so replication of this experiment is necessary. A similar study by Kranendonk et al. also found no effect of human adipose derived EVs on AKT phosphorylation in C2C12 myotubes; however insulin induced activation of AKT was blunted in liver cells following 24 h pre-treatment with EVs (517). Interestingly, considerable inter-donor variation was also observed in this study, with vesicles from some individuals even causing increased insulin sensitivity. In contrast, Deng et al. report that 24 h pre-treatment of EVs derived from murine visceral adipose tissue did in fact impair glucose uptake in C2C12 myotubes, however no mechanistic studies were performed in this investigation (513). Further studies are needed to conclusively determine the impact of adipose tissue derived EVs on human skeletal muscle insulin sensitivity and glucose metabolism.

5.3.3 Limitations and future directions

Initial experiments in this thesis chapter were performed using EVs isolated from SAT cultured in myotube differentiation medium, with the aim of performing future crosstalk studies between SAT derived EVs and primary human myotubes. However, due to a significant interaction between horse serum derived EVs and the human CD9 antibody spots on exoview chips, SAT was cultured in serum free media for 24 h. This is likely to have caused stress to adipocytes and immune cells present within adipose tissue and so may have stimulated aberrant vesicle release. Therefore, although comparisons between lean and obese samples in this thesis remain valid, due to exposure to the same conditions, future studies utilising culture media with EV depleted serum to better maintain cellular viability would provide more representative data of *in vivo* EV secretion from SAT.

Another limitation of this study was that for the functional studies it was not possible to quantify and normalise the number of vesicles before their application to primary human myotubes. Subsequently myotubes will likely have been treated with a different total numbers of EVs from each donor. This could partly explain the varied responses of primary human myotubes observed when performing functional studies. Furthermore, although EVs were released under basal condition in this study, further investigation is needed to identify stimuli that evoke adipose tissue EV release. In turn, this might identify novel therapeutic targets with the aim of modulating EV release to improve skeletal muscle function in obesity.

Moreover, further functional studies, such as primary human myotube glucose uptake and glucose metabolism are required to further establish the functional impact of adipose tissue derived EVs on primary human myotubes. Furthermore, the biggest un-answered question in this thesis chapter remains to be, what is the cargo of adipose tissue derived EVs and is such cargo affected by increasing adiposity? To address this at a protein level, we are currently performing proteomic analysis on the contents of SAT EVs derived from both lean and obese individuals. Such proteomic

screening may help identify differential protein cargo associated with increased adiposity an in turn enable more targeted functional studies to be performed in recipient cells such as primary human myotubes.

Additionally, EVs have also been frequently reported to be associated with carrying micoRNAs (518). Such micro RNAs and potentially other non-coding RNAs, including lncRNAs and circRNAs could be another potential mechanism of adipose tissue derived EV crosstalk, by regulating mRNA and protein content in target cells. Hence performing RNA sequencing of such vesicle content would be valuable.

5.3.4 Conclusions

This chapter reports the first data demonstrating differential populations of EVs derived from lean and obese SAT. We also provide evidence that SAT derived EVs are novel mediators of adipose tissue and skeletal muscle crosstalk, capable of driving inflammation and regulating mRNA expression in primary human myotubes. In conclusion, EVs likely have a significant impact on skeletal muscle function in obese individuals. Developing a further understanding of EV functions and mechanism of action could identify new therapeutic targets for the treatment of obesity associated skeletal muscle dysfunction, such as insulin resistance.

CHAPTER 6: General discussion

6.1 Discussion of main findings and future directions

One of the major risk factors for the development of insulin resistance and T2D is obesity. Current evidence indicates that the increased secretion of proinflammatory adipokines from adipose tissue leads to the development of a chronic proinflammatory state (519). In turn, chronic exposure to such inflammation over months and years is linked to the development of skeletal muscle dysfunction, including insulin resistance (413) (Figure 6.1). However, there is a dearth of knowledge surrounding the mechanism of action of many candidate adipokines in human tissues, including skeletal muscle, with much of the current knowledge in this field derived from studies utilising non-human cell lines and rodent models (399). Additionally, EVs are also capable of mediating tissue crosstalk in humans (493). However again, adipose tissue derived EVs have not been characterised from lean and obese individuals and their functional impact on human skeletal muscle is unknown. To address these gaps in current knowledge, this thesis utilised *ex vivo* human adipose tissue and primary human myotubes derived from elderly human muscle as an *in vitro* model in order to perform novel crosstalk studies examining the impact of adiposity on human skeletal muscle inflammation and insulin sensitivity associated with the ageing obese phenotype.

The first chapter of this thesis established that primary human myotubes provide a viable *in vitro* model of elderly skeletal muscle, with characteristics associated with the obese phenotype, such as the increased expression of atrophic markers, insulin resistance and inflammation retained in myotubes from obese donors. There is currently limited evidence to explain such retention of donor muscle phenotype *in vitro*. It could be hypothesised that chronic exposure of myocytes to either chronic low grade inflammation, or other circulating factors associated with the obese state such as lipids, causes epigenetic changes in skeletal muscle. Such epigenetic changes may in turn regulate gene expression in skeletal muscle satellite cells. Critically, as such satellite cells are isolated and differentiated to myotubes, an inherently altered genome may explain their altered functionality.

Indeed, HFD, ageing and resistance exercise have been implicated in potentiating epigenetic changes in human muscle tissue (520-522). Additionally, a recent investigation by Davegårdh et al. reported the first evidence that obesity impacts the epigenome of primary human myotubes. They observed a 300% increase in the DNA methylation response to myoblast differentiation, in myotubes cultured from obese individuals in comparison to lean individuals (523). Since, Davegårdh et al. have also reported a difference in methylation status of myotubes cultured from men and women, further supporting a role for differential epigenetic modifications in determining primary human myotube phenotype (524). Future studies could investigate the impact of obesity and candidate adipokines on the primary human myotubes epigenome, with the aim of identifying causes for differential gene expression in response to such conditions. This may identify novel therapeutic targets to improve skeletal muscle insulin sensitivity.

Collectively, the findings from chapter 3 of this thesis highlight the need to consider donor characteristics in the design of future studies of musculoskeletal research, in order to ensure that data is representative of the desired cohort. For example, the findings of a study investigating the mechanisms related to sarcopenia utilising primary human myotubes derived from donors in their twenties, may not be replicated in myotubes derived from elderly sarcopenic individuals.

The main limitation with the work presented in this chapter was that the analysis of differential gene expression between lean, overweight and obese skeletal muscle was limited to 48 genes. Therefore, many genetic changes associated with obesity were likely over looked. Future studies would benefit from the utilisation of RNA sequencing to perform a thorough comparison of genetic changes that occur in skeletal muscle tissue with increasing adiposity. Generated data could in turn be analysed with algorithmic software such as Ingenuity Pathway Analysis, in order to identify specific intracellular signalling pathways affected by obesity, thus purposefully directing future research.

Next, this thesis focused on the novel adipokine vaspin. Vaspin was chosen as a candidate adipokine as it had previously been demonstrated to have a number of beneficial effects on rodent insulin sensitivity, but had been unstudied in a human setting. We describe increased expression and secretion of vaspin from the adipose tissue and skeletal muscle of obese humans. We also provide evidence that vaspin is able to activate the PI3K/AKT signalling pathway in primary human myotubes, increase the expression of GLUT4 and in turn sensitise previously insulin resistant obese primary human myotubes to insulin (Figure 6.1). Significantly, these effects appeared to occur independently of insulin receptor activation. Currently, the receptor and mechanism of such vaspin mediated effects in skeletal muscle has not been defined. It appears that vaspin can physically bind to the cell membrane receptor GRP78 (471). We report the expression of GRP78 in human adipose tissue and skeletal muscle and the upregulation of GRP78 in these tissues with obesity. We also provide evidence of GRP78 expression in primary human myotubes. Although we were able to achieve successful knockdown of GRP78 in primary human myotubes, we were not able to conclude whether GRP78 is a functional receptor for vaspin in human muscle. Therefore future studies aiming to continue such work would be valuable in attempting to identify a vaspin receptor which could in turn be targeted, with the aim of improving skeletal muscle insulin sensitivity, independently of the insulin receptor.

Moreover, this chapter mainly focused on the impact of obesity on insulin sensitivity, yet obesity is also associated with a reduction in skeletal muscle mass and quality. Indeed, many adipokines associated with the obese state, such as resistin, have been implicated in driving such skeletal muscle atrophy (448). In contrast, adipokines such as IL-15 may promote increases in skeletal muscle mass (389). As reported in chapter 4, vaspin was able to acutely activate AKT signalling. Importantly, one of the downstream targets of AKT is mTOR, a major regulator of the signalling pathway associated with increasing skeletal muscle hypertrophy (102). Additionally, we have also observed increased proliferation of primary human myoblasts in the presence of vaspin (appendix 3). Therefore, studies

investigating the role of vaspin in mediating changes in skeletal muscle mass would be interesting. It would also be interesting to consider the effect of skeletal muscle contraction on vaspin release and in turn investigate not just potential autocrine effects of vaspin on muscle, but also its effect on other tissues such as adipose and the liver. Elucidating such functional effects will be crucial for the potential development of vaspin based therapeutics. For example, although targeting a vaspin receptor may improve insulin sensitisation, systemic modulation of the vaspin receptor may be harmful.

Ultimately, the findings of this chapter highlight that previously understudied adipokines can have important paracrine physiological effects. Critically, as discussed in the introduction of this thesis (Table 1.2), the impact of many adipokines on human skeletal muscle insulin sensitivity and indeed skeletal muscle function as a whole is very limited. Therefore, it is imperative that there is a continued effort to identify the function and mechanism of action of candidate adipokines in both health and disease. In turn, this may lead to the identification of novel therapeutic targets, either through the development of adipokine mimetics or small molecules to modulate receptor activation, not just in skeletal muscle, but throughout the human body.

Finally, as extracellular vesicles are now acknowledged as an important mechanism of cellular crosstalk in humans, we undertook studies to investigate the possibility that, like adipokines, extracellular vesicles derived from human adipose tissue influence the function of human skeletal muscle. We report, for the first time, the differential secretion of adipose tissue derived EVs positive for the classical exosome markers CD9, CD63 and CD81, between lean and obese individuals. Functionally, we demonstrate the novel EV induced release of inflammatory cytokines and regulation of gene expression in lean primary human myotubes. We therefore propose that adipose tissue derived EVs are novel facilitators of adipose tissue and skeletal muscle crosstalk.

To continue this work, efforts need to be made to further characterise the phenotypic markers of vesicles secreted from adipose tissue and more importantly, their cargo. Highlighting particular cargo of interest such as microRNAs, long non coding RNAs or even functionally active proteins will be important in understanding the crosstalk between skeletal muscle and adipose tissue. Ultimately studies able to sort vesicles into different population prior to characterisation of cargo, or the performance of functional studies would be powerful. However, such studies are currently limited to a certain extent by current technologies, as the small size of EVs still presents a considerable hurdle.

Adipose tissue derived EVs may also impact other functions of skeletal muscle. For example, we identified activation of NFκB as a possible mechanism for increased EV mediated secretion of proinflammatory cytokines from primary human myotubes. There is also increasing evidence to suggest that activation of NFκB is also associated with inhibiting myogenesis (448). Therefore, coupled with the fact that EVs increased the expression of calpain 1 (a skeletal muscle protease), adipose tissue derived EVs could contribute to the development of sarcopenia. Additionally, adipose tissue derived EVs have also been demonstrated to affect the function of both the liver and immune cells (497, 517). Thus, similar to adipokines, adipose tissue derived EVs likely have a number of important effects throughout the body. Subsequently, dysregulation of such EV secretion with obesity may be associated with the development of many obesity associated diseases.

Moreover, as EVs can be detected in fluids such as urine, blood and saliva, in depth profiling of obesity-associated EVs may identify novel biomarkers capable of predicting obesity associated disease. The unique potential for EVs in this regard has recently been demonstrated in cancer biology. For example Melo et al. showed that the presence of EVs expressing markers associated with pancreatic cancer can be detected before any evidence of tumour development (525). Similarly, many cancer specific micro-RNAs have also been detected within serum EVs (526). Efforts to characterise obesity-associated EVs has the potential for the rapid identification of “at risk”

individuals who could then be subject to further diagnostic tests, or stratified to interventions designed to prevent disease development. Such opportunities further highlight the translational potential in profiling adipose tissue derived EV cargo. Conversely, the collection of EVs from adipose tissue may offer a unique vehicle for the delivery of novel therapeutic agents, such as RNAs and small molecules. To this end, adipose tissue derived EVs could be isolated from the patient and 'loaded' with such cargo before being re-administered to the patient. Doing so offers the potential to utilise specific surface markers on adipose tissue derived EVs to perform targeted delivery of therapeutics to tissues as required, which currently presents a significant challenge.

6.2 Lifestyle interventions for the treatment and prevention of T2D

It is evident that there is still a demand for the development of novel therapeutics to treat the increasing number of individuals presenting with T2D. However, it is equally important that significant efforts are made to raise public awareness of the association between weight gain and the development of T2D, as well as the self-measures individuals can take to prevent and manage this disease.

There is increasing evidence that dietary interventions are able to reverse and prevent the development of hyperglycaemia that is typical of T2D pathology, with low carbohydrate diets seeming to yield the best results (527-529). Indeed, some reports even suggest it is possible to stop pharmacological intervention entirely in patients with T2D by using this approach (530-533). Although a simple solution in theory, achieving such results at a population level is difficult, primarily due to relying on patient adherence to often dramatic lifestyle changes. In general, low carbohydrate diets appear to show better adherence than low calorie diets, likely due to the intake of fat and protein facilitating relatively greater total calorie consumption. However studies with long term follow up (> 1 year) are scarce (527). Additionally, the effectiveness of such dietary interventions

appear to be negatively associated with a number of variables, including; the length of time an individual has been diabetic, the number or dosage of medication an individual is taking and increased HbA1c level at the start of intervention (534). Therefore early intervention is also likely needed in order to obtain the best results.

Furthermore, as discussed in chapter 1 of this thesis, both aerobic and resistance exercise are also effective in improving insulin sensitivity in obese and diabetic individuals. Hence, such interventions should also be incorporated into the lifestyle of individuals with, or at risk of the development of T2D. However, this is also easier said than done, since many individuals with T2D are either elderly or present with significant co-morbidities. Therefore, the introduction of regular physical activity in these cohorts is often not feasible. Additionally, adherence also offers a significant challenge for those capable of following exercise intervention. Finally, such lifestyle interventions also come with socio-economic challenges such as the cost of fresh, nutrient dense food and the accessibility and availability of exercise facilities. Therefore, in addition to raising public awareness, ultimately a societal shift is needed in order to prevent the significant and growing issue of obesity and T2D at the population level.

6.3 Final comments

The data presented in this thesis has been generated using biological replicates, performed across multiple patient/subject samples to ensure its validity. Throughout, myotube data has been generated using primary cultures from human muscle biopsy samples, unlike previously published studies that have predominately utilised rodent cell lines. In comparison to the majority of murine studies conducted, human subject replicates are more limited for most functional studies. Due to time restraints involved in recruiting subjects and culturing primary human cells, this was the compromise accepted in order to perform work more physiologically relevant to humans. Consequently, the potential for variability amongst the responses of cultured cells means further research would be needed to corroborate some of the major findings of this work.

Since adipose tissue secretes a number of adipokines that can have both positive and negative effects on insulin sensitivity and metabolism, targeting adipokine signalling has emerged as a potential area to identify and develop novel therapeutics for obesity associated diseases such as T2D. This thesis has demonstrated that vaspin is a novel adipokine associated with obesity, which has insulin sensitising effects on human skeletal muscle (Figure 6.1). Looking to the future it appears that, like adipokines, adipose tissue derived EVs may also impact skeletal muscle function with obesity. Collectively, further understanding how the complete adipose tissue secretory milieu affects skeletal muscle will be valuable for the development of novel treatments for obesity associated skeletal muscle disease.

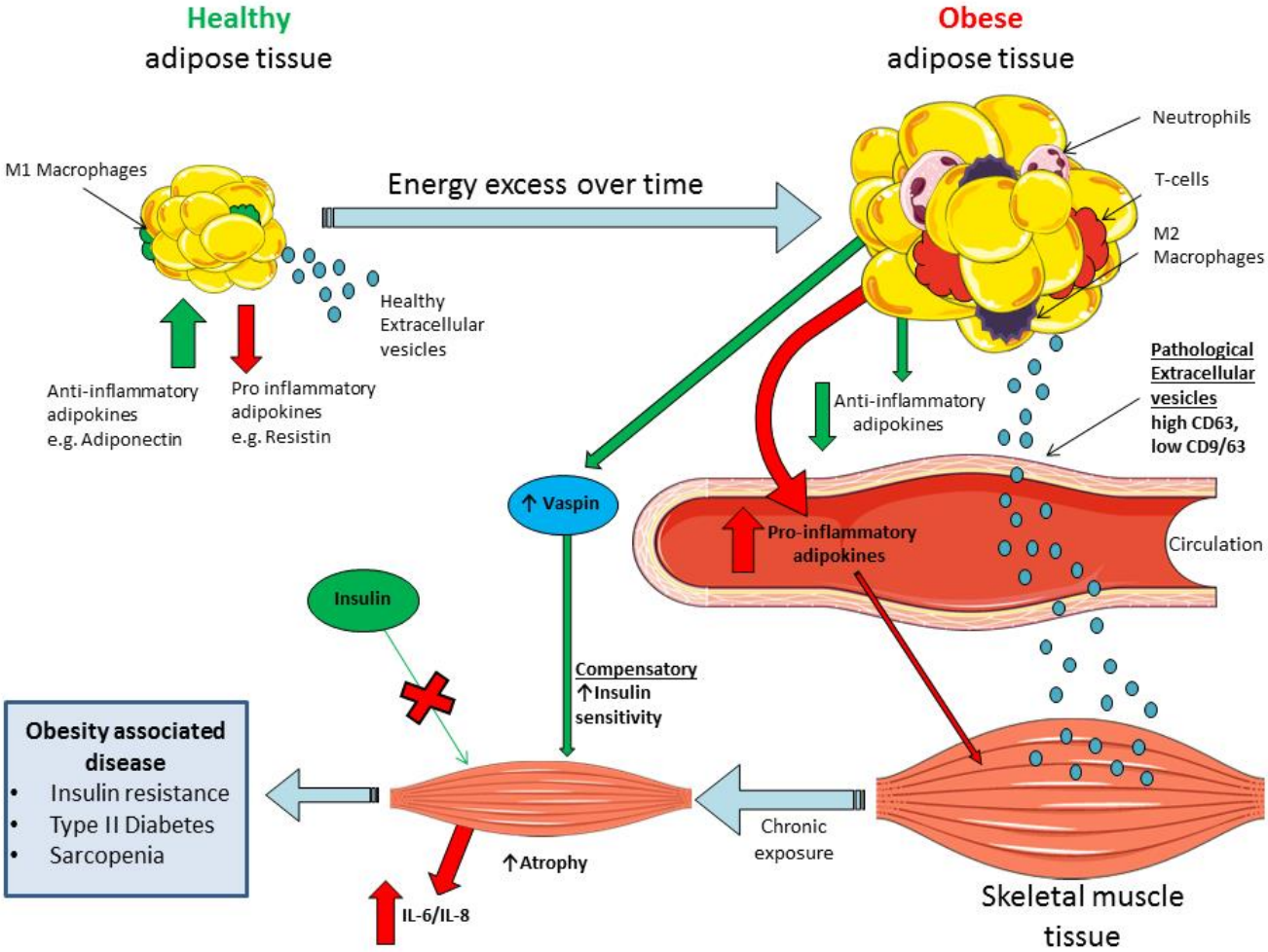

Figure 6. 1. Summary of findings.

Following chronic energy excess, adipose tissue undergoes hypertrophy and becomes inflamed, resulting in increased infiltration of immune cells including T-cells, M2 macrophages and possibly neutrophils. Consequently, obese adipose tissue secretes more proinflammatory cytokines and proportionally less anti-inflammatory adipokines. Additionally, obese adipose tissue secretes a different population of extracellular vesicles exhibiting high CD63 and low CD9 and CD81 surface expression. Together these adipokines and EVs contribute to driving increased skeletal muscle inflammation, atrophy and insulin resistance. Ultimately, this likely contributes to the development of obesity associated diseases such as type II diabetes and sarcopenia. In an attempt to reduce the development of such skeletal muscle insulin resistance, we suggest obese adipose tissue and skeletal muscle secrete vaspin to increase skeletal muscle insulin sensitivity.

CHAPTER 7: References

1. Living longer: how our population is changing and why it matters. Office of National Statistics2018.

2. Future of an ageing population. Government Office for Science: Foresight; July 2016

3. Franceschi C, Garagnani P, Morsiani C, Conte M, Santoro A, Grignolio A, et al. The Continuum of Aging and Age-Related Diseases: Common Mechanisms but Different Rates. Front Med (Lausanne). 2018;5:61.

4. Donato AJ, Henson GD, Hart CR, Layec G, Trinity JD, Bramwell RC, et al. The impact of ageing on adipose structure, function and vasculature in the B6D2F1 mouse: evidence of significant multisystem dysfunction. J Physiol. 2014;592(18):4083-96.

5. Siervo M, Lara J, Celis-Morales C, Vacca M, Oggioni C, Battezzati A, et al. Age-related changes in basal substrate oxidation and visceral adiposity and their association with metabolic syndrome. Eur J Nutr. 2016;55(4):1755-67.

6. Williams PT, Wood PD. The effects of changing exercise levels on weight and age-related weight gain. Int J Obes (Lond). 2006;30(3):543-51.

7. Kuk JL, Saunders TJ, Davidson LE, Ross R. Age-related changes in total and regional fat distribution. Ageing Res Rev. 2009;8(4):339-48.

8. Organisation WH. Obesity and overweight 2018 [Available from: https://www.who.int/news-room/fact-sheets/detail/obesity-and-overweight.

9. Health matters: Obesity and the food environment. Public Health England2017.

10. Gallagher EJ, LeRoith D. Obesity and Diabetes: The Increased Risk of Cancer and Cancer-Related Mortality. Physiological Reviews. 2015;95(3):727-48.

11. Thijssen E, van Caam A, van der Kraan PM. Obesity and osteoarthritis, more than just wear and tear: pivotal roles for inflamed adipose tissue and dyslipidaemia in obesity-induced osteoarthritis. Rheumatology. 2015;54(4):588-600.

12. Hanson C, Rutten EP, Wouters EFM, Rennard S. Influence of diet and obesity on COPD development and outcomes. International Journal of Chronic Obstructive Pulmonary Disease. 2014;9:723-33.

13. Romero-Corral A, Caples SM, Lopez-Jimenez F, Somers VK. Interactions Between Obesity and Obstructive Sleep Apnea: Implications for Treatment. Chest. 2010;137(3):711-9.

14. Holman N, Young B, Gadsby R. Current prevalence of Type 1 and Type 2 diabetes in adults and children in the UK. Diabet Med. 2015;32(9):1119-20.

15. Hex N, Bartlett C, Wright D, Taylor M, Varley D. Estimating the current and future costs of Type 1 and Type 2 diabetes in the UK, including direct health costs and indirect societal and productivity costs. Diabet Med. 2012;29(7):855-62.

16. Michalakis K, Goulis DG, Vazaiou A, Mintziori G, Polymeris A, Abrahamian-Michalakis A. Obesity in the ageing man. Metabolism. 2013;62(10):1341-9.

17. Thiebaud D, Jacot E, DeFronzo RA, Maeder E, Jequier E, Felber JP. The effect of graded doses of insulin on total glucose uptake, glucose oxidation, and glucose storage in man. Diabetes. 1982;31(11):957-63.

18. Frontera WR, Ochala J. Skeletal muscle: a brief review of structure and function. Calcif Tissue Int. 2015;96(3):183-95.

19. Merrell AJ, Kardon G. Development of the diaphragm -- a skeletal muscle essential for mammalian respiration. FEBS J. 2013;280(17):4026-35.

20. Solomonow M, Zhou BH, Harris M, Lu Y, Baratta RV. The ligamento-muscular stabilizing system of the spine. Spine (Phila Pa 1976). 1998;23(23):2552-62.

21. Eyolfson DA, Tikuisis P, Xu X, Weseen G, Giesbrecht GG. Measurement and prediction of peak shivering intensity in humans. Eur J Appl Physiol. 2001;84(1-2):100-6.

22. Pedersen BK, Akerstrom TC, Nielsen AR, Fischer CP. Role of myokines in exercise and metabolism. J Appl Physiol (1985). 2007;103(3):1093-8.

23. Dirks ML, Wall BT, Snijders T, Ottenbros CL, Verdijk LB, van Loon LJ. Neuromuscular electrical stimulation prevents muscle disuse atrophy during leg immobilization in humans. Acta Physiol (Oxf). 2014;210(3):628-41.

24. Jones SW, Hill RJ, Krasney PA, O'Conner B, Peirce N, Greenhaff PL. Disuse atrophy and exercise rehabilitation in humans profoundly affects the expression of genes associated with the regulation of skeletal muscle mass. FASEB J. 2004;18(9):1025-7.

25. Penet MF, Bhujwalla ZM. Cancer cachexia, recent advances, and future directions. Cancer J. 2015;21(2):117-22.

26. Ali NA, O'Brien JM, Jr., Hoffmann SP, Phillips G, Garland A, Finley JC, et al. Acquired weakness, handgrip strength, and mortality in critically ill patients. Am J Respir Crit Care Med. 2008;178(3):261-8.

27. Romero NB, Mezmezian M, Fidzianska A. Main steps of skeletal muscle development in the human: morphological analysis and ultrastructural characteristics of developing human muscle. Handb Clin Neurol. 2013;113:1299-310.

28. Dziedzic D, Bogacka U, Ciszek B. Anatomy of sartorius muscle. Folia Morphol (Warsz). 2014;73(3):359-62.

29. Sanes JR. The basement membrane/basal lamina of skeletal muscle. J Biol Chem. 2003;278(15):12601-4.

30. Gillies AR, Lieber RL. Structure and function of the skeletal muscle extracellular matrix. Muscle Nerve. 2011;44(3):318-31.

31. J. Gordon Betts PD, Eddie Johnson, Jody E. Johnson, Oksana Korol, Dean Kruse, Brandon Poe, James A. Wise Anatomy & Physiology. OpenStax; 2013.

32. Mauro A. Satellite cell of skeletal muscle fibers. J Biophys Biochem Cytol. 1961;9:493-5.

33. Seale P, Sabourin LA, Girgis-Gabardo A, Mansouri A, Gruss P, Rudnicki MA. Pax7 is required for the specification of myogenic satellite cells. Cell. 2000;102(6):777-86.

34. Montarras D, L'Honore A, Buckingham M. Lying low but ready for action: the quiescent muscle satellite cell. FEBS J. 2013;280(17):4036-50.

35. Bischoff R. Interaction between satellite cells and skeletal muscle fibers. Development. 1990;109(4):943-52.

36. Fu X, Wang H, Hu P. Stem cell activation in skeletal muscle regeneration. Cell Mol Life Sci. 2015;72(9):1663-77.

37. Toumi H, F'Guyer S, Best TM. The role of neutrophils in injury and repair following muscle stretch. J Anat. 2006;208(4):459-70.

38. Orimo S, Hiyamuta E, Arahata K, Sugita H. Analysis of inflammatory cells and complement C3 in bupivacaine-induced myonecrosis. Muscle Nerve. 1991;14(6):515-20.

39. Tidball JG, Villalta SA. Regulatory interactions between muscle and the immune system during muscle regeneration. Am J Physiol Regul Integr Comp Physiol. 2010;298(5):R1173-87.

40. Hu P, Geles KG, Paik JH, DePinho RA, Tjian R. Codependent activators direct myoblast-specific MyoD transcription. Dev Cell. 2008;15(4):534-46.

41. Hasty P, Bradley A, Morris JH, Edmondson DG, Venuti JM, Olson EN, et al. Muscle deficiency and neonatal death in mice with a targeted mutation in the myogenin gene. Nature. 1993;364(6437):501-6.

42. Yablonka-Reuveni Z. The skeletal muscle satellite cell: still young and fascinating at 50. J Histochem Cytochem. 2011;59(12):1041-59.

43. Talbot J, Maves L. Skeletal muscle fiber type: using insights from muscle developmental biology to dissect targets for susceptibility and resistance to muscle disease. Wiley Interdiscip Rev Dev Biol. 2016;5(4):518-34.

44. Caiozzo VJ, Baker MJ, Huang K, Chou H, Wu YZ, Baldwin KM. Single-fiber myosin heavy chain polymorphism: how many patterns and what proportions? Am J Physiol Regul Integr Comp Physiol. 2003;285(3):R570-80.

45. Scott W, Stevens J, Binder-Macleod SA. Human skeletal muscle fiber type classifications. Phys Ther. 2001;81(11):1810-6.

46. Wilson JM, Loenneke JP, Jo E, Wilson GJ, Zourdos MC, Kim JS. The effects of endurance, strength, and power training on muscle fiber type shifting. J Strength Cond Res. 2012;26(6):1724-9.

47. Miljkovic N, Lim JY, Miljkovic I, Frontera WR. Aging of skeletal muscle fibers. Ann Rehabil Med. 2015;39(2):155-62.

48. Tanner CJ, Barakat HA, Dohm GL, Pories WJ, MacDonald KG, Cunningham PR, et al. Muscle fiber type is associated with obesity and weight loss. Am J Physiol Endocrinol Metab. 2002;282(6):E1191-6.

49. Oberbach A, Bossenz Y, Lehmann S, Niebauer J, Adams V, Paschke R, et al. Altered fiber distribution and fiber-specific glycolytic and oxidative enzyme activity in skeletal muscle of patients with type 2 diabetes. Diabetes Care. 2006;29(4):895-900.

50. Stuart CA, McCurry MP, Marino A, South MA, Howell ME, Layne AS, et al. Slow-twitch fiber proportion in skeletal muscle correlates with insulin responsiveness. J Clin Endocrinol Metab. 2013;98(5):2027-36.

51. Komatsu M, Takei M, Ishii H, Sato Y. Glucose-stimulated insulin secretion: A newer perspective. Journal of Diabetes Investigation. 2013;4(6):511-6.

52. Tokarz VL, MacDonald PE, Klip A. The cell biology of systemic insulin function. J Cell Biol. 2018;217(7):2273-89.

53. Rorsman P, Renstrom E. Insulin granule dynamics in pancreatic beta cells. Diabetologia. 2003;46(8):1029-45.

54. Lemaire K, Ravier MA, Schraenen A, Creemers JW, Van de Plas R, Granvik M, et al. Insulin crystallization depends on zinc transporter ZnT8 expression, but is not required for normal glucose homeostasis in mice. Proc Natl Acad Sci U S A. 2009;106(35):14872-7.

55. McCulloch LJ, van de Bunt M, Braun M, Frayn KN, Clark A, Gloyn AL. GLUT2 (SLC2A2) is not the principal glucose transporter in human pancreatic beta cells: implications for understanding genetic association signals at this locus. Mol Genet Metab. 2011;104(4):648-53.

56. Rorsman P, Braun M, Zhang Q. Regulation of calcium in pancreatic alpha- and beta-cells in health and disease. Cell Calcium. 2012;51(3-4):300-8.

57. Zarkovic M, Henquin JC. Synchronization and entrainment of cytoplasmic Ca2+ oscillations in cell clusters prepared from single or multiple mouse pancreatic islets. Am J Physiol Endocrinol Metab. 2004;287(2):E340-7.

58. Satin LS, Butler PC, Ha J, Sherman AS. Pulsatile insulin secretion, impaired glucose tolerance and type 2 diabetes. Mol Aspects Med. 2015;42:61-77.

59. Lang DA, Matthews DR, Peto J, Turner RC. Cyclic oscillations of basal plasma glucose and insulin concentrations in human beings. N Engl J Med. 1979;301(19):1023-7.

60. Perez-Armendariz EM. Connexin 36, a key element in pancreatic beta cell function. Neuropharmacology. 2013;75:557-66.

61. Gylfe E, Grapengiesser E, Dansk H, Hellman B. The neurotransmitter ATP triggers Ca2+ responses promoting coordination of pancreatic islet oscillations. Pancreas. 2012;41(2):258-63.

62. Johnston NR, Mitchell RK, Haythorne E, Pessoa MP, Semplici F, Ferrer J, et al. Beta Cell Hubs Dictate Pancreatic Islet Responses to Glucose. Cell Metab. 2016;24(3):389-401.

63. Tang SC, Baeyens L, Shen CN, Peng SJ, Chien HJ, Scheel DW, et al. Human pancreatic neuro-insular network in health and fatty infiltration. Diabetologia. 2018;61(1):168-81.

64. White MF, Livingston JN, Backer JM, Lauris V, Dull TJ, Ullrich A, et al. Mutation of the insulin receptor at tyrosine 960 inhibits signal transmission but does not affect its tyrosine kinase activity. Cell. 1988;54(5):641-9.

65. Shaw LM. The insulin receptor substrate (IRS) proteins: at the intersection of metabolism and cancer. Cell Cycle. 2011;10(11):1750-6.

66. Metz HE, Houghton AM. Insulin receptor substrate regulation of phosphoinositide 3-kinase. Clin Cancer Res. 2011;17(2):206-11.

67. Sarbassov DD, Guertin DA, Ali SM, Sabatini DM. Phosphorylation and regulation of Akt/PKB by the rictor-mTOR complex. Science. 2005;307(5712):1098-101.

68. Alessi DR, Andjelkovic M, Caudwell B, Cron P, Morrice N, Cohen P, et al. Mechanism of activation of protein kinase B by insulin and IGF-1. EMBO J. 1996;15(23):6541-51.

69. Yang G, Murashige DS, Humphrey SJ, James DE. A Positive Feedback Loop between Akt and mTORC2 via SIN1 Phosphorylation. Cell Rep. 2015;12(6):937-43.

70. Matheny RW, Jr., Geddis AV, Abdalla MN, Leandry LA, Ford M, McClung HL, et al. AKT2 is the predominant AKT isoform expressed in human skeletal muscle. Physiol Rep. 2018;6(6):e13652.

71. Cho H, Mu J, Kim JK, Thorvaldsen JL, Chu Q, Crenshaw EB, 3rd, et al. Insulin resistance and a diabetes mellitus-like syndrome in mice lacking the protein kinase Akt2 (PKB beta). Science. 2001;292(5522):1728-31.

72. Harrington LS, Findlay GM, Gray A, Tolkacheva T, Wigfield S, Rebholz H, et al. The TSC1-2 tumor suppressor controls insulin-PI3K signaling via regulation of IRS proteins. J Cell Biol. 2004;166(2):213-23.

73. Shah OJ, Hunter T. Turnover of the active fraction of IRS1 involves raptor-mTOR- and S6K1-dependent serine phosphorylation in cell culture models of tuberous sclerosis. Mol Cell Biol. 2006;26(17):6425-34.

74. Altomare DA, Testa JR. Perturbations of the AKT signaling pathway in human cancer. Oncogene. 2005;24(50):7455-64.

75. Yi KH, Lauring J. Recurrent AKT mutations in human cancers: functional consequences and effects on drug sensitivity. Oncotarget. 2016;7(4):4241-51.

76. Yu H, Littlewood T, Bennett M. Akt isoforms in vascular disease. Vascul Pharmacol. 2015;71:57-64.

77. Huang X, Liu G, Guo J, Su Z. The PI3K/AKT pathway in obesity and type 2 diabetes. Int J Biol Sci. 2018;14(11):1483-96.

78. May O. Diabetes and Insulin Signaling: A New Strategy to Promote Pancreatic b Cell Survival

2008 [cited 2019 March]. Available from: https://www.caymanchem.com/news/diabetes-and-insulin-signaling.

79. Richter EA, Hargreaves M. Exercise, GLUT4, and Skeletal Muscle Glucose Uptake. Physiological Reviews. 2013;93(3):993-1017.

80. Coster AC, Govers R, James DE. Insulin stimulates the entry of GLUT4 into the endosomal recycling pathway by a quantal mechanism. Traffic. 2004;5(10):763-71.

81. Zeigerer A, McBrayer MK, McGraw TE. Insulin stimulation of GLUT4 exocytosis, but not its inhibition of endocytosis, is dependent on RabGAP AS160. Mol Biol Cell. 2004;15(10):4406-15.

82. Zerial M, McBride H. Rab proteins as membrane organizers. Nat Rev Mol Cell Biol. 2001;2(2):107-17.

83. Deneka M, Neeft M, van der Sluijs P. Regulation of membrane transport by rab GTPases. Crit Rev Biochem Mol Biol. 2003;38(2):121-42.

84. Eguez L, Lee A, Chavez JA, Miinea CP, Kane S, Lienhard GE, et al. Full intracellular retention of GLUT4 requires AS160 Rab GTPase activating protein. Cell Metab. 2005;2(4):263-72.

85. Thong FS, Bilan PJ, Klip A. The Rab GTPase-activating protein AS160 integrates Akt, protein kinase C, and AMP-activated protein kinase signals regulating GLUT4 traffic. Diabetes. 2007;56(2):414-23.

86. Sano H, Kane S, Sano E, Miinea CP, Asara JM, Lane WS, et al. Insulin-stimulated phosphorylation of a Rab GTPase-activating protein regulates GLUT4 translocation. J Biol Chem. 2003;278(17):14599-602.

87. Tan SX, Ng Y, Burchfield JG, Ramm G, Lambright DG, Stockli J, et al. The Rab GTPase-activating protein TBC1D4/AS160 contains an atypical phosphotyrosine-binding domain that interacts with plasma membrane phospholipids to facilitate GLUT4 trafficking in adipocytes. Mol Cell Biol. 2012;32(24):4946-59.

88. Consitt LA, Van Meter J, Newton CA, Collier DN, Dar MS, Wojtaszewski JF, et al. Impairments in site-specific AS160 phosphorylation and effects of exercise training. Diabetes. 2013;62(10):3437-47.

89. Karlsson HK, Zierath JR, Kane S, Krook A, Lienhard GE, Wallberg-Henriksson H. Insulin-stimulated phosphorylation of the Akt substrate AS160 is impaired in skeletal muscle of type 2 diabetic subjects. Diabetes. 2005;54(6):1692-7.

90. Hojlund K, Glintborg D, Andersen NR, Birk JB, Treebak JT, Frosig C, et al. Impaired insulin-stimulated phosphorylation of Akt and AS160 in skeletal muscle of women with polycystic ovary syndrome is reversed by pioglitazone treatment. Diabetes. 2008;57(2):357-66.

91. Makinen S, Nguyen YH, Skrobuk P, Koistinen HA. Palmitate and oleate exert differential effects on insulin signalling and glucose uptake in human skeletal muscle cells. Endocr Connect. 2017;6(5):331-9.

92. Richter EA, Hargreaves M. Exercise, GLUT4, and skeletal muscle glucose uptake. Physiol Rev. 2013;93(3):993-1017.

93. Sylow L, Kleinert M, Pehmoller C, Prats C, Chiu TT, Klip A, et al. Akt and Rac1 signaling are jointly required for insulin-stimulated glucose uptake in skeletal muscle and downregulated in insulin resistance. Cell Signal. 2014;26(2):323-31.

94. Bouskila M, Hunter RW, Ibrahim AF, Delattre L, Peggie M, van Diepen JA, et al. Allosteric regulation of glycogen synthase controls glycogen synthesis in muscle. Cell Metab. 2010;12(5):456-66.

95. McManus EJ, Sakamoto K, Armit LJ, Ronaldson L, Shpiro N, Marquez R, et al. Role that phosphorylation of GSK3 plays in insulin and Wnt signalling defined by knockin analysis. EMBO J. 2005;24(8):1571-83.

96. Hasselgren PO, Warner BW, James JH, Takehara H, Fischer JE. Effect of insulin on amino acid uptake and protein turnover in skeletal muscle from septic rats. Evidence for insulin resistance of protein breakdown. Arch Surg. 1987;122(2):228-33.

97. McDowell HE, Eyers PA, Hundal HS. Regulation of System A amino acid transport in L6 rat skeletal muscle cells by insulin, chemical and hyperthermic stress. FEBS Lett. 1998;441(1):15-9.

98. Walker DK, Drummond MJ, Dickinson JM, Borack MS, Jennings K, Volpi E, et al. Insulin increases mRNA abundance of the amino acid transporter SLC7A5/LAT1 via an mTORC1-dependent mechanism in skeletal muscle cells. Physiol Rep. 2014;2(3):e00238.

99. Sandri M, Sandri C, Gilbert A, Skurk C, Calabria E, Picard A, et al. Foxo transcription factors induce the atrophy-related ubiquitin ligase atrogin-1 and cause skeletal muscle atrophy. Cell. 2004;117(3):399-412.

100. Senf SM, Dodd SL, Judge AR. FOXO signaling is required for disuse muscle atrophy and is directly regulated by Hsp70. Am J Physiol Cell Physiol. 2010;298(1):C38-45.

101. Inoki K, Li Y, Zhu T, Wu J, Guan KL. TSC2 is phosphorylated and inhibited by Akt and suppresses mTOR signalling. Nat Cell Biol. 2002;4(9):648-57.

102. Yoon MS. mTOR as a Key Regulator in Maintaining Skeletal Muscle Mass. Front Physiol. 2017;8:788.

103. Aguilar V, Alliouachene S, Sotiropoulos A, Sobering A, Athea Y, Djouadi F, et al. S6 kinase deletion suppresses muscle growth adaptations to nutrient availability by activating AMP kinase. Cell Metab. 2007;5(6):476-87.

104. Marabita M, Baraldo M, Solagna F, Ceelen JJM, Sartori R, Nolte H, et al. S6K1 Is Required for Increasing Skeletal Muscle Force during Hypertrophy. Cell Rep. 2016;17(2):501-13.

105. Shen WH, Boyle DW, Wisniowski P, Bade A, Liechty EA. Insulin and IGF-I stimulate the formation of the eukaryotic initiation factor 4F complex and protein synthesis in C2C12 myotubes independent of availability of external amino acids. J Endocrinol. 2005;185(2):275-89.

106. Kim J, Kundu M, Viollet B, Guan KL. AMPK and mTOR regulate autophagy through direct phosphorylation of Ulk1. Nat Cell Biol. 2011;13(2):132-41.

107. Abdulla H, Smith K, Atherton PJ, Idris I. Role of insulin in the regulation of human skeletal muscle protein synthesis and breakdown: a systematic review and meta-analysis. Diabetologia. 2016;59(1):44-55.

108. Fujita S, Glynn EL, Timmerman KL, Rasmussen BB, Volpi E. Supraphysiological hyperinsulinaemia is necessary to stimulate skeletal muscle protein anabolism in older adults: evidence of a true age-related insulin resistance of muscle protein metabolism. Diabetologia. 2009;52(9):1889-98.

109. Keller K, Engelhardt M. Strength and muscle mass loss with aging process. Age and strength loss. Muscles Ligaments Tendons J. 2013;3(4):346-50.

110. Morton RW, Traylor DA, Weijs PJM, Phillips SM. Defining anabolic resistance: implications for delivery of clinical care nutrition. Curr Opin Crit Care. 2018;24(2):124-30.

111. Morais JA, Jacob KW, Chevalier S. Effects of aging and insulin resistant states on protein anabolic responses in older adults. Exp Gerontol. 2018;108:262-8.

112. Rasmussen BB, Fujita S, Wolfe RR, Mittendorfer B, Roy M, Rowe VL, et al. Insulin resistance of muscle protein metabolism in aging. FASEB J. 2006;20(6):768-9.

113. Kim KS, Park KS, Kim MJ, Kim SK, Cho YW, Park SW. Type 2 diabetes is associated with low muscle mass in older adults. Geriatr Gerontol Int. 2014;14 Suppl 1:115-21.

114. Park SW, Goodpaster BH, Lee JS, Kuller LH, Boudreau R, de Rekeneire N, et al. Excessive loss of skeletal muscle mass in older adults with type 2 diabetes. Diabetes Care. 2009;32(11):1993-7.

115. Teng S, Huang P. The effect of type 2 diabetes mellitus and obesity on muscle progenitor cell function. Stem Cell Res Ther. 2019;10(1):103.

116. Dimitriadis G, Mitrou P, Lambadiari V, Maratou E, Raptis SA. Insulin effects in muscle and adipose tissue. Diabetes Res Clin Pract. 2011;93 Suppl 1:S52-9.

117. Frayn KN, Shadid S, Hamlani R, Humphreys SM, Clark ML, Fielding BA, et al. Regulation of fatty acid movement in human adipose tissue in the postabsorptive-to-postprandial transition. Am J Physiol. 1994;266(3 Pt 1):E308-17.

118. Meijssen S, Cabezas MC, Ballieux CG, Derksen RJ, Bilecen S, Erkelens DW. Insulin mediated inhibition of hormone sensitive lipase activity in vivo in relation to endogenous catecholamines in healthy subjects. J Clin Endocrinol Metab. 2001;86(9):4193-7.

119. Semenkovich CF, Wims M, Noe L, Etienne J, Chan L. Insulin regulation of lipoprotein lipase activity in 3T3-L1 adipocytes is mediated at posttranscriptional and posttranslational levels. J Biol Chem. 1989;264(15):9030-8.

120. Albalat A, Saera-Vila A, Capilla E, Gutierrez J, Perez-Sanchez J, Navarro I. Insulin regulation of lipoprotein lipase (LPL) activity and expression in gilthead sea bream (Sparus aurata). Comp Biochem Physiol B Biochem Mol Biol. 2007;148(2):151-9.

121. Fried SK, Russell CD, Grauso NL, Brolin RE. Lipoprotein lipase regulation by insulin and glucocorticoid in subcutaneous and omental adipose tissues of obese women and men. J Clin Invest. 1993;92(5):2191-8.

122. Wang H, Eckel RH. Lipoprotein lipase: from gene to obesity. Am J Physiol Endocrinol Metab. 2009;297(2):E271-88.

123. Wong RH, Sul HS. Insulin signaling in fatty acid and fat synthesis: a transcriptional perspective. Curr Opin Pharmacol. 2010;10(6):684-91.

124. Biddinger SB, Hernandez-Ono A, Rask-Madsen C, Haas JT, Aleman JO, Suzuki R, et al. Hepatic insulin resistance is sufficient to produce dyslipidemia and susceptibility to atherosclerosis. Cell Metab. 2008;7(2):125-34.

125. Owen JL, Zhang Y, Bae SH, Farooqi MS, Liang G, Hammer RE, et al. Insulin stimulation of SREBP-1c processing in transgenic rat hepatocytes requires p70 S6-kinase. Proc Natl Acad Sci U S A. 2012;109(40):16184-9.

126. Li S, Brown MS, Goldstein JL. Bifurcation of insulin signaling pathway in rat liver: mTORC1 required for stimulation of lipogenesis, but not inhibition of gluconeogenesis. Proc Natl Acad Sci U S A. 2010;107(8):3441-6.

127. Deng X, Zhang W, I OS, Williams JB, Dong Q, Park EA, et al. FoxO1 inhibits sterol regulatory element-binding protein-1c (SREBP-1c) gene expression via transcription factors Sp1 and SREBP-1c. J Biol Chem. 2012;287(24):20132-43.

128. Yecies JL, Zhang HH, Menon S, Liu S, Yecies D, Lipovsky AI, et al. Akt stimulates hepatic SREBP1c and lipogenesis through parallel mTORC1-dependent and independent pathways. Cell Metab. 2011;14(1):21-32.

129. Sharabi K, Tavares CD, Rines AK, Puigserver P. Molecular pathophysiology of hepatic glucose production. Mol Aspects Med. 2015;46:21-33.

130. Hatting M, Tavares CDJ, Sharabi K, Rines AK, Puigserver P. Insulin regulation of gluconeogenesis. Ann N Y Acad Sci. 2018;1411(1):21-35.

131. Rizza RA. Pathogenesis of fasting and postprandial hyperglycemia in type 2 diabetes: implications for therapy. Diabetes. 2010;59(11):2697-707.

132. Jensen J, Rustad PI, Kolnes AJ, Lai YC. The role of skeletal muscle glycogen breakdown for regulation of insulin sensitivity by exercise. Front Physiol. 2011;2:112.

133. Consoli A, Nurjahan N, Gerich JE, Mandarino LJ. Skeletal muscle is a major site of lactate uptake and release during hyperinsulinemia. Metabolism. 1992;41(2):176-9.

134. Clore JN, Glickman PS, Helm ST, Nestler JE, Blackard WG. Evidence for dual control mechanism regulating hepatic glucose output in nondiabetic men. Diabetes. 1991;40(8):1033-40.

135. Boden G, Chen X, Capulong E, Mozzoli M. Effects of free fatty acids on gluconeogenesis and autoregulation of glucose production in type 2 diabetes. Diabetes. 2001;50(4):810-6.

136. Cerf ME. Beta cell dysfunction and insulin resistance. Front Endocrinol (Lausanne). 2013;4:37.

137. Draznin B. Molecular Mechanisms of Insulin Resistance: Serine Phosphorylation of Insulin Receptor Substrate-1 and Increased Expression of p85α. The Two Sides of a Coin. 2006;55(8):2392-7.

138. Abdul-Ghani MA, DeFronzo RA. Pathogenesis of insulin resistance in skeletal muscle. J Biomed Biotechnol. 2010;2010:476279.

139. Draznin B. Molecular Mechanisms of Insulin Resistance: Serine Phosphorylation of Insulin Receptor Substrate-1 and Increased Expression of p85α: The Two Sides of a Coin. Diabetes. 2006;55(8):2392-7.

140. Cade WT. Diabetes-related microvascular and macrovascular diseases in the physical therapy setting. Phys Ther. 2008;88(11):1322-35.

141. Fowler MJ. Microvascular and Macrovascular Complications of Diabetes. Clinical Diabetes. 2008;26(2):77-82.

142. Holman R. Metformin as first choice in oral diabetes treatment: the UKPDS experience. Journ Annu Diabetol Hotel Dieu. 2007:13-20.

143. Maruthur NM, Tseng E, Hutfless S, Wilson LM, Suarez-Cuervo C, Berger Z, et al. Diabetes Medications as Monotherapy or Metformin-Based Combination Therapy for Type 2 Diabetes: A Systematic Review and Meta-analysis. Ann Intern Med. 2016;164(11):740-51.

144. Consoli A, Formoso G. Do thiazolidinediones still have a role in treatment of type 2 diabetes mellitus? Diabetes Obes Metab. 2013;15(11):967-77.

145. Proks P, Reimann F, Green N, Gribble F, Ashcroft F. Sulfonylurea stimulation of insulin secretion. Diabetes. 2002;51 Suppl 3:S368-76.

146. Sola D, Rossi L, Schianca GP, Maffioli P, Bigliocca M, Mella R, et al. Sulfonylureas and their use in clinical practice. Arch Med Sci. 2015;11(4):840-8.

147. de Jager J, Kooy A, Lehert P, Wulffele MG, van der Kolk J, Bets D, et al. Long term treatment with metformin in patients with type 2 diabetes and risk of vitamin B-12 deficiency: randomised placebo controlled trial. BMJ. 2010;340:c2181.

148. Boussageon R, Supper I, Bejan-Angoulvant T, Kellou N, Cucherat M, Boissel JP, et al. Reappraisal of metformin efficacy in the treatment of type 2 diabetes: a meta-analysis of randomised controlled trials. PLoS Med. 2012;9(4):e1001204.

149. Eppenga WL, Lalmohamed A, Geerts AF, Derijks HJ, Wensing M, Egberts A, et al. Risk of lactic acidosis or elevated lactate concentrations in metformin users with renal impairment: a population-based cohort study. Diabetes Care. 2014;37(8):2218-24.

150. Loke YK, Kwok CS, Singh S. Comparative cardiovascular effects of thiazolidinediones: systematic review and meta-analysis of observational studies. BMJ. 2011;342:d1309.

151. Gallagher AM, Smeeth L, Seabroke S, Leufkens HGM, van Staa TP. Risk of Death and Cardiovascular Outcomes with Thiazolidinediones: A Study with the General Practice Research Database and Secondary Care Data. PLoS ONE. 2011;6(12):e28157.

152. Nissen SE, Wolski K. Effect of rosiglitazone on the risk of myocardial infarction and death from cardiovascular causes. N Engl J Med. 2007;356(24):2457-71.

153. Utriainen T, Takala T, Luotolahti M, Ronnemaa T, Laine H, Ruotsalainen U, et al. Insulin resistance characterizes glucose uptake in skeletal muscle but not in the heart in NIDDM. Diabetologia. 1998;41(5):555-9.

154. Pendergrass M, Bertoldo A, Bonadonna R, Nucci G, Mandarino L, Cobelli C, et al. Muscle glucose transport and phosphorylation in type 2 diabetic, obese nondiabetic, and genetically predisposed individuals. American Journal of Physiology - Endocrinology and Metabolism. 2007;292(1):E92-E100.

155. Thiebaud D, Jacot E, Defronzo RA, Maeder E, Jequier E, Felber J-P. The Effect of Graded Doses of Insulin on Total Glucose Uptake, Glucose Oxidation, and Glucose Storage in Man. Diabetes. 1982;31(11):957-63.

156. Zeyda M, Huber J, Prager G, Stulnig TM. Inflammation correlates with markers of T-cell subsets including regulatory T cells in adipose tissue from obese patients. Obesity (Silver Spring). 2011;19(4):743-8.

157. Weisberg SP, McCann D, Desai M, Rosenbaum M, Leibel RL, Ferrante AW, Jr. Obesity is associated with macrophage accumulation in adipose tissue. J Clin Invest. 2003;112(12):1796-808.

158. Lehr S, Hartwig S, Lamers D, Famulla S, Müller S, Hanisch F-G, et al. Identification and Validation of Novel Adipokines Released from Primary Human Adipocytes. Molecular & Cellular Proteomics. 2012;11(1).

159. Kautzky-Willer A, Harreiter J, Pacini G. Sex and Gender Differences in Risk, Pathophysiology and Complications of Type 2 Diabetes Mellitus. Endocr Rev. 2016;37(3):278-316.

160. Yim JE, Heshka S, Albu JB, Heymsfield S, Gallagher D. Femoral-gluteal subcutaneous and intermuscular adipose tissues have independent and opposing relationships with CVD risk. J Appl Physiol (1985). 2008;104(3):700-7.

161. Krotkiewski M, Bjorntorp P, Sjostrom L, Smith U. Impact of obesity on metabolism in men and women. Importance of regional adipose tissue distribution. J Clin Invest. 1983;72(3):1150-62.

162. Karastergiou K, Smith SR, Greenberg AS, Fried SK. Sex differences in human adipose tissues - the biology of pear shape. Biol Sex Differ. 2012;3(1):13.

163. Doria A, Patti ME, Kahn CR. The emerging genetic architecture of type 2 diabetes. Cell Metab. 2008;8(3):186-200.

164. Carlsson S, Hammar N, Grill V, Kaprio J. Alcohol consumption and the incidence of type 2 diabetes: a 20-year follow-up of the Finnish twin cohort study. Diabetes Care. 2003;26(10):2785-90.

165. Maddatu J, Anderson-Baucum E, Evans-Molina C. Smoking and the risk of type 2 diabetes. Transl Res. 2017;184:101-7.

166. Khandelwal D, Dutta D, Chittawar S, Kalra S. Sleep Disorders in Type 2 Diabetes. Indian J Endocrinol Metab. 2017;21(5):758-61.

167. Bosma M. Lipid droplet dynamics in skeletal muscle. Exp Cell Res. 2016;340(2):180-6.

168. Badin PM, Langin D, Moro C. Dynamics of skeletal muscle lipid pools. Trends Endocrinol Metab. 2013;24(12):607-15.

169. Guo Y, Cordes KR, Farese RV, Jr., Walther TC. Lipid droplets at a glance. J Cell Sci. 2009;122(Pt 6):749-52.

170. Goodpaster BH, Theriault R, Watkins SC, Kelley DE. Intramuscular lipid content is increased in obesity and decreased by weight loss. Metabolism. 2000;49(4):467-72.

171. Shaw CS, Jones DA, Wagenmakers AJ. Network distribution of mitochondria and lipid droplets in human muscle fibres. Histochem Cell Biol. 2008;129(1):65-72.

172. Suzuki M, Shinohara Y, Ohsaki Y, Fujimoto T. Lipid droplets: size matters. J Electron Microsc (Tokyo). 2011;60 Suppl 1:S101-16.

173. He J, Goodpaster BH, Kelley DE. Effects of weight loss and physical activity on muscle lipid content and droplet size. Obes Res. 2004;12(5):761-9.

174. Yen CL, Stone SJ, Koliwad S, Harris C, Farese RV, Jr. Thematic review series: glycerolipids. DGAT enzymes and triacylglycerol biosynthesis. J Lipid Res. 2008;49(11):2283-301.

175. Hannun YA, Obeid LM. Principles of bioactive lipid signalling: lessons from sphingolipids. Nat Rev Mol Cell Biol. 2008;9(2):139-50.

176. Bachmann OP, Dahl DB, Brechtel K, Machann J, Haap M, Maier T, et al. Effects of intravenous and dietary lipid challenge on intramyocellular lipid content and the relation with insulin sensitivity in humans. Diabetes. 2001;50(11):2579-84.

177. Toledo FG, Menshikova EV, Azuma K, Radikova Z, Kelley CA, Ritov VB, et al. Mitochondrial capacity in skeletal muscle is not stimulated by weight loss despite increases in insulin action and decreases in intramyocellular lipid content. Diabetes. 2008;57(4):987-94.

178. Sinha R, Dufour S, Petersen KF, LeBon V, Enoksson S, Ma YZ, et al. Assessment of skeletal muscle triglyceride content by (1)H nuclear magnetic resonance spectroscopy in lean and obese adolescents: relationships to insulin sensitivity, total body fat, and central adiposity. Diabetes. 2002;51(4):1022-7.

179. Pan DA, Lillioja S, Kriketos AD, Milner MR, Baur LA, Bogardus C, et al. Skeletal muscle triglyceride levels are inversely related to insulin action. Diabetes. 1997;46(6):983-8.

180. Petersen KF, Dufour S, Morino K, Yoo PS, Cline GW, Shulman GI. Reversal of muscle insulin resistance by weight reduction in young, lean, insulin-resistant offspring of parents with type 2 diabetes. Proc Natl Acad Sci U S A. 2012;109(21):8236-40.

181. van Loon LJ, Koopman R, Manders R, van der Weegen W, van Kranenburg GP, Keizer HA. Intramyocellular lipid content in type 2 diabetes patients compared with overweight sedentary men and highly trained endurance athletes. Am J Physiol Endocrinol Metab. 2004;287(3):E558-65.

182. Schrauwen-Hinderling VB, Kooi ME, Hesselink MK, Jeneson JA, Backes WH, van Echteld CJ, et al. Impaired in vivo mitochondrial function but similar intramyocellular lipid content in patients with type 2 diabetes mellitus and BMI-matched control subjects. Diabetologia. 2007;50(1):113-20.

183. Muoio DM. Intramuscular triacylglycerol and insulin resistance: guilty as charged or wrongly accused? Biochim Biophys Acta. 2010;1801(3):281-8.

184. Bajpeyi S, Myrland CK, Covington JD, Obanda D, Cefalu WT, Smith SR, et al. Lipid in skeletal muscle myotubes is associated to the donors' insulin sensitivity and physical activity phenotypes. Obesity (Silver Spring). 2014;22(2):426-34.

185. Chibalin AV, Leng Y, Vieira E, Krook A, Bjornholm M, Long YC, et al. Downregulation of diacylglycerol kinase delta contributes to hyperglycemia-induced insulin resistance. Cell. 2008;132(3):375-86.

186. Turban S, Hajduch E. Protein kinase C isoforms: mediators of reactive lipid metabolites in the development of insulin resistance. FEBS Lett. 2011;585(2):269-74.

187. Li Y, Soos TJ, Li X, Wu J, Degennaro M, Sun X, et al. Protein kinase C Theta inhibits insulin signaling by phosphorylating IRS1 at Ser(1101). J Biol Chem. 2004;279(44):45304-7.

188. Yu C, Chen Y, Cline GW, Zhang D, Zong H, Wang Y, et al. Mechanism by which fatty acids inhibit insulin activation of insulin receptor substrate-1 (IRS-1)-associated phosphatidylinositol 3-kinase activity in muscle. J Biol Chem. 2002;277(52):50230-6.

189. Werner ED, Lee J, Hansen L, Yuan M, Shoelson SE. Insulin resistance due to phosphorylation of insulin receptor substrate-1 at serine 302. J Biol Chem. 2004;279(34):35298-305.

190. Mack E, Ziv E, Reuveni H, Kalman R, Niv MY, Jorns A, et al. Prevention of insulin resistance and beta-cell loss by abrogating PKCepsilon-induced serine phosphorylation of muscle IRS-1 in Psammomys obesus. Diabetes Metab Res Rev. 2008;24(7):577-84.

191. Schmitz-Peiffer C, Laybutt DR, Burchfield JG, Gurisik E, Narasimhan S, Mitchell CJ, et al. Inhibition of PKCepsilon improves glucose-stimulated insulin secretion and reduces insulin clearance. Cell Metab. 2007;6(4):320-8.

192. Smellie JM. Reflections on 30 years of treating children with urinary tract infections. J Urol. 1991;146(2 (Pt 2)):665-8.

193. Harbold NB, Jr., Gau GT. Echocardiographic diagnosis of right atrial myxoma. Mayo Clin Proc. 1973;48(4):284-6.

194. Boon J, Hoy AJ, Stark R, Brown RD, Meex RC, Henstridge DC, et al. Ceramides contained in LDL are elevated in type 2 diabetes and promote inflammation and skeletal muscle insulin resistance. Diabetes. 2013;62(2):401-10.

195. Coen PM, Dube JJ, Amati F, Stefanovic-Racic M, Ferrell RE, Toledo FG, et al. Insulin resistance is associated with higher intramyocellular triglycerides in type I but not type II myocytes concomitant with higher ceramide content. Diabetes. 2010;59(1):80-8.

196. Park M, Kaddai V, Ching J, Fridianto KT, Sieli RJ, Sugii S, et al. A Role for Ceramides, but Not Sphingomyelins, as Antagonists of Insulin Signaling and Mitochondrial Metabolism in C2C12 Myotubes. J Biol Chem. 2016;291(46):23978-88.

197. Chavez JA, Holland WL, Bar J, Sandhoff K, Summers SA. Acid ceramidase overexpression prevents the inhibitory effects of saturated fatty acids on insulin signaling. J Biol Chem. 2005;280(20):20148-53.

198. Chavez JA, Siddique MM, Wang ST, Ching J, Shayman JA, Summers SA. Ceramides and glucosylceramides are independent antagonists of insulin signaling. J Biol Chem. 2014;289(2):723-34.

199. Powell DJ, Turban S, Gray A, Hajduch E, Hundal HS. Intracellular ceramide synthesis and protein kinase Czeta activation play an essential role in palmitate-induced insulin resistance in rat L6 skeletal muscle cells. Biochem J. 2004;382(Pt 2):619-29.

200. Powell DJ, Hajduch E, Kular G, Hundal HS. Ceramide disables 3-phosphoinositide binding to the pleckstrin homology domain of protein kinase B (PKB)/Akt by a PKCzeta-dependent mechanism. Mol Cell Biol. 2003;23(21):7794-808.

201. Mahfouz R, Khoury R, Blachnio-Zabielska A, Turban S, Loiseau N, Lipina C, et al. Characterising the inhibitory actions of ceramide upon insulin signaling in different skeletal muscle cell models: a mechanistic insight. PLoS One. 2014;9(7):e101865.

202. Holland WL, Summers SA. Sphingolipids, insulin resistance, and metabolic disease: new insights from in vivo manipulation of sphingolipid metabolism. Endocr Rev. 2008;29(4):381-402.

203. Blouin CM, Prado C, Takane KK, Lasnier F, Garcia-Ocana A, Ferre P, et al. Plasma membrane subdomain compartmentalization contributes to distinct mechanisms of ceramide action on insulin signaling. Diabetes. 2010;59(3):600-10.

204. Jackson AS, Stanforth PR, Gagnon J, Rankinen T, Leon AS, Rao DC, et al. The effect of sex, age and race on estimating percentage body fat from body mass index: The Heritage Family Study. Int J Obes Relat Metab Disord. 2002;26(6):789-96.

205. Ibrahim MM. Subcutaneous and visceral adipose tissue: structural and functional differences. Obes Rev. 2010;11(1):11-8.

206. Marin P, Andersson B, Ottosson M, Olbe L, Chowdhury B, Kvist H, et al. The morphology and metabolism of intraabdominal adipose tissue in men. Metabolism. 1992;41(11):1242-8.

207. Berg AH, Scherer PE. Adipose tissue, inflammation, and cardiovascular disease. Circ Res. 2005;96(9):939-49.

208. Doyle SL, Donohoe CL, Lysaght J, Reynolds JV. Visceral obesity, metabolic syndrome, insulin resistance and cancer. Proc Nutr Soc. 2012;71(1):181-9.

209. Chung GE, Kim D, Kwark MS, Kim W, Yim JY, Kim YJ, et al. Visceral adipose tissue area as an independent risk factor for elevated liver enzyme in nonalcoholic fatty liver disease. Medicine (Baltimore). 2015;94(9):e573.

210. Cannon B, Nedergaard J. Brown adipose tissue: function and physiological significance. Physiol Rev. 2004;84(1):277-359.

211. Daikoku T, Shinohara Y, Shima A, Yamazaki N, Terada H. Specific elevation of transcript levels of particular protein subtypes induced in brown adipose tissue by cold exposure. Biochim Biophys Acta. 2000;1457(3):263-72.

212. Hiroshima Y, Yamamoto T, Watanabe M, Baba Y, Shinohara Y. Effects of cold exposure on metabolites in brown adipose tissue of rats. Mol Genet Metab Rep. 2018;15:36-42.

213. Leitner BP, Huang S, Brychta RJ, Duckworth CJ, Baskin AS, McGehee S, et al. Mapping of human brown adipose tissue in lean and obese young men. Proc Natl Acad Sci U S A. 2017;114(32):8649-54.

214. Brendle C, Werner MK, Schmadl M, la Fougere C, Nikolaou K, Stefan N, et al. Correlation of Brown Adipose Tissue with Other Body Fat Compartments and Patient Characteristics: A Retrospective Analysis in a Large Patient Cohort Using PET/CT. Acad Radiol. 2018;25(1):102-10.

215. Cypess AM, Lehman S, Williams G, Tal I, Rodman D, Goldfine AB, et al. Identification and importance of brown adipose tissue in adult humans. N Engl J Med. 2009;360(15):1509-17.

216. Lee P, Swarbrick MM, Ho KK. Brown adipose tissue in adult humans: a metabolic renaissance. Endocr Rev. 2013;34(3):413-38.

217. Stanford KI, Middelbeek RJ, Townsend KL, An D, Nygaard EB, Hitchcox KM, et al. Brown adipose tissue regulates glucose homeostasis and insulin sensitivity. J Clin Invest. 2013;123(1):215-23.

218. Bartelt A, Bruns OT, Reimer R, Hohenberg H, Ittrich H, Peldschus K, et al. Brown adipose tissue activity controls triglyceride clearance. Nat Med. 2011;17(2):200-5.

219. Wu J, Bostrom P, Sparks LM, Ye L, Choi JH, Giang AH, et al. Beige adipocytes are a distinct type of thermogenic fat cell in mouse and human. Cell. 2012;150(2):366-76.

220. Cui XB, Chen SY. White adipose tissue browning and obesity. J Biomed Res. 2016;31(1):1-2.

221. Fabbiano S, Suarez-Zamorano N, Rigo D, Veyrat-Durebex C, Stevanovic Dokic A, Colin DJ, et al. Caloric Restriction Leads to Browning of White Adipose Tissue through Type 2 Immune Signaling. Cell Metab. 2016;24(3):434-46.

222. Barquissau V, Leger B, Beuzelin D, Martins F, Amri EZ, Pisani DF, et al. Caloric Restriction and Diet-Induced Weight Loss Do Not Induce Browning of Human Subcutaneous White Adipose Tissue in Women and Men with Obesity. Cell Rep. 2018;22(4):1079-89.

223. Cypess AM, Weiner LS, Roberts-Toler C, Franquet Elia E, Kessler SH, Kahn PA, et al. Activation of human brown adipose tissue by a beta3-adrenergic receptor agonist. Cell Metab. 2015;21(1):33-8.

224. Bai Y, Sun Q. Macrophage recruitment in obese adipose tissue. Obes Rev. 2015;16(2):127-36.

225. Ye J. Adipose tissue vascularization: its role in chronic inflammation. Curr Diab Rep. 2011;11(3):203-10.

226. Brook CG, Lloyd JK, Wolf OH. Relation between age of onset of obesity and size and number of adipose cells. Br Med J. 1972;2(5804):25-7.

227. Drager LF, Li J, Shin MK, Reinke C, Aggarwal NR, Jun JC, et al. Intermittent hypoxia inhibits clearance of triglyceride-rich lipoproteins and inactivates adipose lipoprotein lipase in a mouse model of sleep apnoea. Eur Heart J. 2012;33(6):783-90.

228. Mahat B, Chasse E, Mauger JF, Imbeault P. Effects of acute hypoxia on human adipose tissue lipoprotein lipase activity and lipolysis. J Transl Med. 2016;14(1):212.

229. Sun K, Kusminski CM, Scherer PE. Adipose tissue remodeling and obesity. J Clin Invest. 2011;121(6):2094-101.

230. Cancello R, Henegar C, Viguerie N, Taleb S, Poitou C, Rouault C, et al. Reduction of macrophage infiltration and chemoattractant gene expression changes in white adipose tissue of morbidly obese subjects after surgery-induced weight loss. Diabetes. 2005;54(8):2277-86.

231. Jiang C, Qu A, Matsubara T, Chanturiya T, Jou W, Gavrilova O, et al. Disruption of hypoxia-inducible factor 1 in adipocytes improves insulin sensitivity and decreases adiposity in high-fat diet-fed mice. Diabetes. 2011;60(10):2484-95.

232. Franceschi C, Bonafe M, Valensin S, Olivieri F, De Luca M, Ottaviani E, et al. Inflamm-aging. An evolutionary perspective on immunosenescence. Ann N Y Acad Sci. 2000;908:244-54.

233. Baylis D, Bartlett DB, Patel HP, Roberts HC. Understanding how we age: insights into inflammaging. Longev Healthspan. 2013;2(1):8.

234. Giunta B, Fernandez F, Nikolic WV, Obregon D, Rrapo E, Town T, et al. Inflammaging as a prodrome to Alzheimer's disease. J Neuroinflammation. 2008;5:51.

235. Engels EA. Inflammation in the development of lung cancer: epidemiological evidence. Expert Rev Anticancer Ther. 2008;8(4):605-15.

236. Makki K, Froguel P, Wolowczuk I. Adipose tissue in obesity-related inflammation and insulin resistance: cells, cytokines, and chemokines. ISRN Inflamm. 2013;2013:139239.

237. Tzanavari T, Giannogonas P, Karalis KP. TNF-alpha and obesity. Curr Dir Autoimmun. 2010;11:145-56.

238. Segal KR, Landt M, Klein S. Relationship Between Insulin Sensitivity and Plasma Leptin Concentration in Lean and Obese Men. Diabetes. 1996;45(7):988-91.

239. Yadav A, jyoti P, Jain SK, Bhattacharjee J. Correlation of Adiponectin and Leptin with Insulin Resistance: A Pilot Study in Healthy North Indian Population. Indian Journal of Clinical Biochemistry. 2011;26(2):193-6.

240. Sweeney G, Keen J, Somwar R, Konrad D, Garg R, Klip A. High leptin levels acutely inhibit insulin-stimulated glucose uptake without affecting glucose transporter 4 translocation in l6 rat skeletal muscle cells. Endocrinology. 2001;142(11):4806-12.

241. Berti L, Gammeltoft S. Leptin stimulates glucose uptake in C2C12 muscle cells by activation of ERK2. Mol Cell Endocrinol. 1999;157(1-2):121-30.

242. Ogawa Y, Masuzaki H, Hosoda K, Aizawa-Abe M, Suga J, Suda M, et al. Increased glucose metabolism and insulin sensitivity in transgenic skinny mice overexpressing leptin. Diabetes. 1999;48(9):1822-9.

243. Yau SW, Henry BA, Russo VC, McConell GK, Clarke IJ, Werther GA, et al. Leptin enhances insulin sensitivity by direct and sympathetic nervous system regulation of muscle IGFBP-2 expression: evidence from nonrodent models. Endocrinology. 2014;155(6):2133-43.

244. Aleidi S, Issa A, Bustanji H, Khalil M, Bustanji Y. Adiponectin serum levels correlate with insulin resistance in type 2 diabetic patients. Saudi Pharmaceutical Journal : SPJ. 2015;23(3):250-6.

245. Nayak BS, Ramsingh D, Gooding S, Legall G, Bissram S, Mohammed A, et al. Plasma adiponectin levels are related to obesity, inflammation, blood lipids and insulin in type 2 diabetic and non-diabetic Trinidadians. Prim Care Diabetes. 2010;4(3):187-92.

246. Lee B, Shao J. Adiponectin and Energy Homeostasis. Reviews in endocrine & metabolic disorders. 2014;15(2):149-56.

247. Yoon MJ, Lee GY, Chung JJ, Ahn YH, Hong SH, Kim JB. Adiponectin increases fatty acid oxidation in skeletal muscle cells by sequential activation of AMP-activated protein kinase, p38 mitogen-activated protein kinase, and peroxisome proliferator-activated receptor alpha. Diabetes. 2006;55(9):2562-70.

248. Yamauchi T, Kamon J, Minokoshi Y, Ito Y, Waki H, Uchida S, et al. Adiponectin stimulates glucose utilization and fatty-acid oxidation by activating AMP-activated protein kinase. Nat Med. 2002;8(11):1288-95.

249. Ceddia RB, Somwar R, Maida A, Fang X, Bikopoulos G, Sweeney G. Globular adiponectin increases GLUT4 translocation and glucose uptake but reduces glycogen synthesis in rat skeletal muscle cells. Diabetologia. 2005;48(1):132-9.

250. Kubota N, Terauchi Y, Yamauchi T, Kubota T, Moroi M, Matsui J, et al. Disruption of adiponectin causes insulin resistance and neointimal formation. J Biol Chem. 2002;277(29):25863-6.

251. Yamauchi T, Kamon J, Waki H, Terauchi Y, Kubota N, Hara K, et al. The fat-derived hormone adiponectin reverses insulin resistance associated with both lipoatrophy and obesity. Nat Med. 2001;7(8):941-6.

252. Yano W, Kubota N, Itoh S, Kubota T, Awazawa M, Moroi M, et al. Molecular mechanism of moderate insulin resistance in adiponectin-knockout mice. Endocr J. 2008;55(3):515-22.

253. Kandasamy AD, Sung MM, Boisvenue JJ, Barr AJ, Dyck JRB. Adiponectin gene therapy ameliorates high-fat, high-sucrose diet-induced metabolic perturbations in mice. Nutrition and Diabetes. 2012;2:e45.

254. Chen MB, McAinch AJ, Macaulay SL, Castelli LA, O'Brien P E, Dixon JB, et al. Impaired activation of AMP-kinase and fatty acid oxidation by globular adiponectin in cultured human skeletal muscle of obese type 2 diabetics. J Clin Endocrinol Metab. 2005;90(6):3665-72.

255. Steppan CM, Bailey ST, Bhat S, Brown EJ, Banerjee RR, Wright CM, et al. The hormone resistin links obesity to diabetes. Nature. 2001;409(6818):307-12.

256. Bokarewa M, Nagaev I, Dahlberg L, Smith U, Tarkowski A. Resistin, an Adipokine with Potent Proinflammatory Properties. The Journal of Immunology. 2005;174(9):5789-95.

257. Jiang CY, Wang W, Tang JX, Yuan ZR. The adipocytokine resistin stimulates the production of proinflammatory cytokines TNF-alpha and IL-6 in pancreatic acinar cells via NF-kappaB activation. Journal of endocrinological investigation. 2013;36(11):986-92.

258. Azuma K, Katsukawa F, Oguchi S, Murata M, Yamazaki H, Shimada A, et al. Correlation between Serum Resistin Level and Adiposity in Obese Individuals. Obesity Research. 2003;11(8):997-1001.

259. Gharibeh MY, Al Tawallbeh GM, Abboud MM, Radaideh A, Alhader AA, Khabour OF. Correlation of plasma resistin with obesity and insulin resistance in type 2 diabetic patients. Diabetes Metab. 2010;36(6 Pt 1):443-9.

260. Fan HQ, Gu N, Liu F, Fei L, Pan XQ, Guo M, et al. Prolonged exposure to resistin inhibits glucose uptake in rat skeletal muscles. Acta Pharmacol Sin. 2007;28(3):410-6.

261. Palanivel R, Maida A, Liu Y, Sweeney G. Regulation of insulin signalling, glucose uptake and metabolism in rat skeletal muscle cells upon prolonged exposure to resistin. Diabetologia. 2006;49(1):183-90.

262. Sheng CH, Du ZW, Song Y, Wu XD, Zhang YC, Wu M, et al. Human resistin inhibits myogenic differentiation and induces insulin resistance in myocytes. Biomed Res Int. 2013;2013:804632.

263. Jia SH, Li Y, Parodo J, Kapus A, Fan L, Rotstein OD, et al. Pre–B cell colony–enhancing factor inhibits neutrophil apoptosis in experimental inflammation and clinical sepsis. Journal of Clinical Investigation. 2004;113(9):1318-27.

264. Samal B, Sun Y, Stearns G, Xie C, Suggs S, McNiece I. Cloning and characterization of the cDNA encoding a novel human pre-B-cell colony-enhancing factor. Molecular and Cellular Biology. 1994;14(2):1431-7.

265. Terra X, Auguet T, Quesada I, Aguilar C, Luna AM, Hernandez M, et al. Increased levels and adipose tissue expression of visfatin in morbidly obese women: the relationship with pro-inflammatory cytokines. Clinical endocrinology. 2012;77(5):691-8.

266. Esteghamati A, Alamdari A, Zandieh A, Elahi S, Khalilzadeh O, Nakhjavani M, et al. Serum visfatin is associated with type 2 diabetes mellitus independent of insulin resistance and obesity. Diabetes research and clinical practice. 2011;91(2):154-8.

267. Catalan V, Gomez-Ambrosi J, Rodriguez A, Ramirez B, Silva C, Rotellar F, et al. Association of increased visfatin/PBEF/NAMPT circulating concentrations and gene expression levels in peripheral blood cells with lipid metabolism and fatty liver in human morbid obesity. Nutrition, metabolism, and cardiovascular diseases : NMCD. 2011;21(4):245-53.

268. Chang YH, Chang DM, Lin KC, Shin SJ, Lee YJ. Visfatin in overweight/obesity, type 2 diabetes mellitus, insulin resistance, metabolic syndrome and cardiovascular diseases: a meta-analysis and systemic review. Diabetes Metab Res Rev. 2011;27(6):515-27.

269. Sun Q, Li L, Li R, Yang M, Liu H, Nowicki MJ, et al. Overexpression of visfatin/PBEF/Nampt alters whole-body insulin sensitivity and lipid profile in rats. Annals of medicine. 2009;41(4):311-20.

270. Lee JO, Kim N, Lee HJ, Lee YW, Kim JK, Kim HI, et al. Visfatin, a novel adipokine, stimulates glucose uptake through the Ca2 +-dependent AMPK-p38 MAPK pathway in C2C12 skeletal muscle cells. J Mol Endocrinol. 2015;54(3):251-62.

271. Hida K, Wada J, Zhang H, Hiragushi K, Tsuchiyama Y, Shikata K, et al. Identification of genes specifically expressed in the accumulated visceral adipose tissue of OLETF rats. J Lipid Res. 2000;41(10):1615-22.

272. Hida K, Wada J, Eguchi J, Zhang H, Baba M, Seida A, et al. Visceral adipose tissue-derived serine protease inhibitor: A unique insulin-sensitizing adipocytokine in obesity. Proceedings of the National Academy of Sciences of the United States of America. 2005;102(30):10610-5.

273. Heiker JT, Klöting N, Kovacs P, Kuettner EB, Sträter N, Schultz S, et al. Vaspin inhibits kallikrein 7 by serpin mechanism. Cellular and Molecular Life Sciences. 2013;70(14):2569-83.

274. Klöting N, Kovacs P, Kern M, Heiker JT, Fasshauer M, Schön MR, et al. Central vaspin administration acutely reduces food intake and has sustained blood glucose-lowering effects. Diabetologia. 2011;54(7):1819-23.

275. Nakatsuka A, Wada J, Iseda I, Teshigawara S, Higashio K, Murakami K, et al. Vaspin Is an Adipokine Ameliorating ER Stress in Obesity as a Ligand for Cell-Surface GRP78/MTJ-1 Complex. Diabetes. 2012;61(11):2823-32.

276. Klöting N, Berndt J, Kralisch S, Kovacs P, Fasshauer M, Schön MR, et al. Vaspin gene expression in human adipose tissue: Association with obesity and type 2 diabetes. Biochemical and Biophysical Research Communications. 2006;339(1):430-6.

277. Schultz S, Saalbach A, Heiker John T, Meier R, Zellmann T, Simon Jan C, et al. Proteolytic activation of prochemerin by kallikrein 7 breaks an ionic linkage and results in C-terminal rearrangement. Biochemical Journal. 2013;452(2):271-80.

278. Aust G, Richter O, Rohm S, Kerner C, Hauss J, Kloting N, et al. Vaspin serum concentrations in patients with carotid stenosis. Atherosclerosis. 2009;204(1):262-6.

279. Jian W, Peng W, Xiao S, Li H, Jin J, Qin L, et al. Role of Serum Vaspin in Progression of Type 2 Diabetes: A 2-Year Cohort Study. PLOS ONE. 2014;9(4):e94763.

280. Teshigawara S, Wada J, Hida K, Nakatsuka A, Eguchi J, Murakami K, et al. Serum Vaspin Concentrations Are Closely Related to Insulin Resistance, and rs77060950 at SERPINA12 Genetically Defines Distinct Group with Higher Serum Levels in Japanese Population. The Journal of Clinical Endocrinology & Metabolism. 2012;97(7):E1202-E7.

281. Youn BS, Kloting N, Kratzsch J, Lee N, Park JW, Song ES, et al. Serum vaspin concentrations in human obesity and type 2 diabetes. Diabetes. 2008;57(2):372-7.

282. Badman MK, Pissios P, Kennedy AR, Koukos G, Flier JS, Maratos-Flier E. Hepatic Fibroblast Growth Factor 21 Is Regulated by PPARα and Is a Key Mediator of Hepatic Lipid Metabolism in Ketotic States. Cell Metabolism. 2007;5(6):426-37.

283. Badman MK, Koester A, Flier JS, Kharitonenkov A, Maratos-Flier E. Fibroblast Growth Factor 21-Deficient Mice Demonstrate Impaired Adaptation to Ketosis. Endocrinology. 2009;150(11):4931-40.

284. So WY, Leung PS. Fibroblast Growth Factor 21 As an Emerging Therapeutic Target for Type 2 Diabetes Mellitus. Medicinal Research Reviews. 2016;36(4):672-704.

285. Zhang X, Yeung DCY, Karpisek M, Stejskal D, Zhou Z-G, Liu F, et al. Serum FGF21 Levels Are Increased in Obesity and Are Independently Associated With the Metabolic Syndrome in Humans. Diabetes. 2008;57(5):1246.

286. Semba RD, Sun K, Egan JM, Crasto C, Carlson OD, Ferrucci L. Relationship of Serum Fibroblast Growth Factor 21 with Abnormal Glucose Metabolism and Insulin Resistance: The Baltimore Longitudinal Study of Aging. The Journal of Clinical Endocrinology & Metabolism. 2012;97(4):1375-82.

287. Reinehr T, Woelfle J, Wunsch R, Roth CL. Fibroblast Growth Factor 21 (FGF-21) and Its Relation to Obesity, Metabolic Syndrome, and Nonalcoholic Fatty Liver in Children: A Longitudinal Analysis. The Journal of Clinical Endocrinology & Metabolism. 2012;97(6):2143-50.

288. Chavez AO, Molina-Carrion M, Abdul-Ghani MA, Folli F, DeFronzo RA, Tripathy D. Circulating Fibroblast Growth Factor-21 Is Elevated in Impaired Glucose Tolerance and Type 2 Diabetes and Correlates With Muscle and Hepatic Insulin Resistance. Diabetes Care. 2009;32(8):1542.

289. Lin Z, Tian H, Lam KS, Lin S, Hoo RC, Konishi M, et al. Adiponectin mediates the metabolic effects of FGF21 on glucose homeostasis and insulin sensitivity in mice. Cell Metab. 2013;17(5):779-89.

290. Sarruf DA, Thaler JP, Morton GJ, German J, Fischer JD, Ogimoto K, et al. Fibroblast growth factor 21 action in the brain increases energy expenditure and insulin sensitivity in obese rats. Diabetes. 2010;59(7):1817-24.

291. Kharitonenkov A, Wroblewski VJ, Koester A, Chen Y-F, Clutinger CK, Tigno XT, et al. The Metabolic State of Diabetic Monkeys Is Regulated by Fibroblast Growth Factor-21. Endocrinology. 2007;148(2):774-81.

292. Thompson WC, Zhou Y, Talukdar S, Musante CJ. PF-05231023, a long-acting FGF21 analogue, decreases body weight by reduction of food intake in non-human primates. Journal of pharmacokinetics and pharmacodynamics. 2016;43(4):411-25.

293. Talukdar S, Zhou Y, Li D, Rossulek M, Dong J, Somayaji V, et al. A Long-Acting FGF21 Molecule, PF-05231023, Decreases Body Weight and Improves Lipid Profile in Non-human Primates and Type 2 Diabetic Subjects. Cell Metab. 2016;23(3):427-40.

294. Gaich G, Chien JY, Fu H, Glass LC, Deeg MA, Holland WL, et al. The effects of LY2405319, an FGF21 analog, in obese human subjects with type 2 diabetes. Cell Metab. 2013;18(3):333-40.

295. Kim JH, Bae KH, Choi YK, Go Y, Choe M, Jeon YH, et al. Fibroblast growth factor 21 analogue LY2405319 lowers blood glucose in streptozotocin-induced insulin-deficient diabetic mice by restoring brown adipose tissue function. Diabetes Obes Metab. 2015;17(2):161-9.

296. Lee JH, Kang YE, Chang JY, Park KC, Kim HW, Kim JT, et al. An engineered FGF21 variant, LY2405319, can prevent non-alcoholic steatohepatitis by enhancing hepatic mitochondrial function. Am J Transl Res. 2016;8(11):4750-63.

297. Degirolamo C, Sabba C, Moschetta A. Therapeutic potential of the endocrine fibroblast growth factors FGF19, FGF21 and FGF23. Nature reviews Drug discovery. 2016;15(1):51-69.

298. Kolumam G, Chen MZ, Tong R, Zavala-Solorio J, Kates L, van Bruggen N, et al. Sustained Brown Fat Stimulation and Insulin Sensitization by a Humanized Bispecific Antibody Agonist for Fibroblast Growth Factor Receptor 1/betaKlotho Complex. EBioMedicine. 2015;2(7):730-43.

299. Mashili FL, Austin RL, Deshmukh AS, Fritz T, Caidahl K, Bergdahl K, et al. Direct effects of FGF21 on glucose uptake in human skeletal muscle: implications for type 2 diabetes and obesity. Diabetes/Metabolism Research and Reviews. 2011;27(3):286-97.

300. Lee MS, Choi S-E, Ha ES, An S-Y, Kim TH, Han SJ, et al. Fibroblast growth factor-21 protects human skeletal muscle myotubes from palmitate-induced insulin resistance by inhibiting stress kinase and NF-κB. Metabolism. 2012;61(8):1142-51.

301. Cuevas-Ramos D, Mehta R, Aguilar-Salinas CA. Fibroblast Growth Factor 21 and Browning of White Adipose Tissue. Front Physiol. 2019;10:37.

302. De Henau O, Degroot G-N, Imbault V, Robert V, De Poorter C, McHeik S, et al. Signaling Properties of Chemerin Receptors CMKLR1, GPR1 and CCRL2. PLOS ONE. 2016;11(10):e0164179.

303. Wittamer V, Franssen J-D, Vulcano M, Mirjolet J-F, Le Poul E, Migeotte I, et al. Specific Recruitment of Antigen-presenting Cells by Chemerin, a Novel Processed Ligand from Human Inflammatory Fluids. The Journal of Experimental Medicine. 2003;198(7):977.

304. Goralski KB, McCarthy TC, Hanniman EA, Zabel BA, Butcher EC, Parlee SD, et al. Chemerin, a novel adipokine that regulates adipogenesis and adipocyte metabolism. J Biol Chem. 2007;282(38):28175-88.

305. Roh SG, Song SH, Choi KC, Katoh K, Wittamer V, Parmentier M, et al. Chemerin--a new adipokine that modulates adipogenesis via its own receptor. Biochem Biophys Res Commun. 2007;362(4):1013-8.

306. Zylla S, Pietzner M, Kuhn JP, Volzke H, Dorr M, Nauck M, et al. Serum chemerin is associated with inflammatory and metabolic parameters-results of a population-based study. Obesity (Silver Spring). 2017;25(2):468-75.

307. Li Y, Shi B, Li S. Association between Serum Chemerin Concentrations and Clinical Indices in Obesity or Metabolic Syndrome: A Meta-Analysis. PLOS ONE. 2014;9(12):e113915.

308. Sell H, Divoux A, Poitou C, Basdevant A, Bouillot JL, Bedossa P, et al. Chemerin correlates with markers for fatty liver in morbidly obese patients and strongly decreases after weight loss induced by bariatric surgery. J Clin Endocrinol Metab. 2010;95(6):2892-6.

309. Sell H, Laurencikiene J, Taube A, Eckardt K, Cramer A, Horrighs A, et al. Chemerin Is a Novel Adipocyte-Derived Factor Inducing Insulin Resistance in Primary Human Skeletal Muscle Cells. Diabetes. 2009;58(12):2731-40.

310. Becker M, Rabe K, Lebherz C, Zugwurst J, Göke B, Parhofer KG, et al. Expression of Human Chemerin Induces Insulin Resistance in the Skeletal Muscle but Does Not Affect Weight, Lipid Levels, and Atherosclerosis in LDL Receptor Knockout Mice on High-Fat Diet. Diabetes. 2010;59(11):2898-903.

311. Ernst MC, Issa M, Goralski KB, Sinal CJ. Chemerin Exacerbates Glucose Intolerance in Mouse Models of Obesity and Diabetes. Endocrinology. 2010;151(5):1998-2007.

312. Takahashi M, Okimura Y, Iguchi G, Nishizawa H, Yamamoto M, Suda K, et al. Chemerin regulates β-cell function in mice. Scientific Reports. 2011;1:123.

313. Huang Z, Xie X. [Chemerin induces insulin resistance in C2C12 cells through nuclear factor-kappaB pathway-mediated inflammatory reaction]. Xi bao yu fen zi mian yi xue za zhi = Chinese journal of cellular and molecular immunology. 2015;31(6):725-9.

314. Sell H, Laurencikiene J, Taube A, Eckardt K, Cramer A, Horrighs A, et al. Chemerin is a novel adipocyte-derived factor inducing insulin resistance in primary human skeletal muscle cells. Diabetes. 2009;58(12):2731-40.

315. Wang Y, Sul HS. Ectodomain Shedding of Preadipocyte Factor 1 (Pref-1) by Tumor Necrosis Factor Alpha Converting Enzyme (TACE) and Inhibition of Adipocyte Differentiation. Molecular and Cellular Biology. 2006;26(14):5421-35.

316. Chacon MR, Miranda M, Jensen CH, Fernandez-Real JM, Vilarrasa N, Gutierrez C, et al. Human serum levels of fetal antigen 1 (FA1/Dlk1) increase with obesity, are negatively associated with insulin sensitivity and modulate inflammation in vitro. Int J Obes. 2008;32(7):1122-9.

317. Kavalkova P, Touskova V, Roubicek T, Trachta P, Urbanova M, Drapalova J, et al. Serum preadipocyte factor-1 concentrations in females with obesity and type 2 diabetes mellitus: the influence of very low calorie diet, acute hyperinsulinemia, and fenofibrate treatment. Hormone and metabolic research = Hormon- und Stoffwechselforschung = Hormones et metabolisme. 2013;45(11):820-6.

318. Moon YS, Smas CM, Lee K, Villena JA, Kim KH, Yun EJ, et al. Mice lacking paternally expressed Pref-1/Dlk1 display growth retardation and accelerated adiposity. Mol Cell Biol. 2002;22(15):5585-92.

319. Villena JA, Kim KH, Sul HS. Pref-1 and ADSF/resistin: two secreted factors inhibiting adipose tissue development. Hormone and metabolic research = Hormon- und Stoffwechselforschung = Hormones et metabolisme. 2002;34(11-12):664-70.

320. Villena JA, Choi CS, Wang Y, Kim S, Hwang Y-J, Kim Y-B, et al. Resistance to High-Fat Diet–Induced Obesity but Exacerbated Insulin Resistance in Mice Overexpressing Preadipocyte Factor-1 (Pref-1): A New Model of Partial Lipodystrophy. Diabetes. 2008;57(12):3258-66.

321. Abdallah BM, Beck-Nielsen H, Gaster M. FA1 Induces Pro-Inflammatory and Anti-Adipogenic Pathways/Markers in Human Myotubes Established from Lean, Obese, and Type 2 Diabetic Subjects but Not Insulin Resistance. Frontiers in Endocrinology. 2013;4:45.

322. Miyamae T, Marinov AD, Sowders D, Wilson DC, Devlin J, Boudreau R, et al. Follistatin-Like Protein-1 Is a Novel Proinflammatory Molecule. The Journal of Immunology. 2006;177(7):4758-62.

323. Fan N, Sun H, Wang Y, Wang Y, Zhang L, Xia Z, et al. Follistatin-Like 1: A Potential Mediator of Inflammation in Obesity. Mediators of Inflammation. 2013;2013:752519.

324. Wu Y, Zhou S, Smas CM. Downregulated Expression of the Secreted Glycoprotein Follistatin-like 1 (Fstl1) is a Robust Hallmark of Preadipocyte to Adipocyte Conversion. Mechanisms of development. 2010;127(3-4):183-202.

325. Gorgens SW, Raschke S, Holven KB, Jensen J, Eckardt K, Eckel J. Regulation of follistatin-like protein 1 expression and secretion in primary human skeletal muscle cells. Archives of physiology and biochemistry. 2013;119(2):75-80.

326. Shen Y, Zhao Y, Yuan L, Yi W, Zhao R, Yi Q, et al. SPARC is over-expressed in adipose tissues of diet-induced obese rats and causes insulin resistance in 3T3-L1 adipocytes. Acta histochemica. 2014;116(1):158-66.

327. Chavey C, Boucher J, Monthouël-Kartmann M-N, Sage EH, Castan-Laurell I, Valet P, et al. Regulation of Secreted Protein Acidic and Rich in Cysteine during Adipose Conversion and Adipose Tissue Hyperplasia. Obesity. 2006;14(11):1890-7.

328. Kos K, Wong S, Tan B, Gummesson A, Jernas M, Franck N, et al. Regulation of the fibrosis and angiogenesis promoter SPARC/osteonectin in human adipose tissue by weight change, leptin, insulin, and glucose. Diabetes. 2009;58(8):1780-8.

329. Xu L, Ping F, Yin J, Xiao X, Xiang H, Ballantyne CM, et al. Elevated Plasma SPARC Levels Are Associated with Insulin Resistance, Dyslipidemia, and Inflammation in Gestational Diabetes Mellitus. PLOS ONE. 2013;8(12):e81615.

330. Wolf RM, Steele KE, Peterson LA, Magnuson TH, Schweitzer MA, Wong GW. Lower Circulating C1q/TNF-Related Protein-3 (CTRP3) Levels Are Associated with Obesity: A Cross-Sectional Study. PLOS ONE. 2015;10(7):e0133955.

331. Deng W, Li C, Zhang Y, Zhao J, Yang M, Tian M, et al. Serum C1q/TNF-related protein-3 (CTRP3) levels are decreased in obesity and hypertension and are negatively correlated with parameters of insulin resistance. Diabetol Metab Syndr. 2015;7:33.

332. Weigert J, Neumeier M, Schäffler A, Fleck M, Schölmerich J, Schütz C, et al. The adiponectin paralog CORS-26 has anti-inflammatory properties and is produced by human monocytic cells. FEBS Letters. 2005;579(25):5565-70.

333. Kopp A, Bala M, Buechler C, Falk W, Gross P, Neumeier M, et al. C1q/TNF-related protein-3 represents a novel and endogenous lipopolysaccharide antagonist of the adipose tissue. Endocrinology. 2010;151(11):5267-78.

334. Tsuji S, Uehori J, Matsumoto M, Suzuki Y, Matsuhisa A, Toyoshima K, et al. Human intelectin is a novel soluble lectin that recognizes galactofuranose in carbohydrate chains of bacterial cell wall. J Biol Chem. 2001;276(26):23456-63.

335. de Souza Batista CM, Yang RZ, Lee MJ, Glynn NM, Yu DZ, Pray J, et al. Omentin plasma levels and gene expression are decreased in obesity. Diabetes. 2007;56(6):1655-61.

336. Pan HY, Guo L, Li Q. Changes of serum omentin-1 levels in normal subjects and in patients with impaired glucose regulation and with newly diagnosed and untreated type 2 diabetes. Diabetes research and clinical practice. 2010;88(1):29-33.

337. Tan BK, Adya R, Farhatullah S, Lewandowski KC, O'Hare P, Lehnert H, et al. Omentin-1, a Novel Adipokine, Is Decreased in Overweight Insulin-Resistant Women With Polycystic Ovary Syndrome. Diabetes. 2008;57(4):801.

338. Yang RZ, Lee MJ, Hu H, Pray J, Wu HB, Hansen BC, et al. Identification of omentin as a novel depot-specific adipokine in human adipose tissue: possible role in modulating insulin action. Am J Physiol Endocrinol Metab. 2006;290(6):E1253-61.

339. Lee JT, Huang Z, Pan K, Zhang HJ, Woo CW, Xu A, et al. Adipose-derived lipocalin 14 alleviates hyperglycaemia by suppressing both adipocyte glycerol efflux and hepatic gluconeogenesis in mice. Diabetologia. 2016;59(3):604-13.

340. Considine RV, Sinha MK, Heiman ML, Kriauciunas A, Stephens TW, Nyce MR, et al. Serum immunoreactive-leptin concentrations in normal-weight and obese humans. N Engl J Med. 1996;334(5):292-5.

341. Yaspelkis BB, 3rd, Davis JR, Saberi M, Smith TL, Jazayeri R, Singh M, et al. Leptin administration improves skeletal muscle insulin responsiveness in diet-induced insulin-resistant rats. Am J Physiol Endocrinol Metab. 2001;280(1):E130-42.

342. Doh KO, Park JO, Kim YW, Park SY, Jeong JH, Jeon JR, et al. Effect of leptin on insulin resistance of muscle--direct or indirect? Physiological research. 2006;55(4):413-9.

343. Bates SH, Gardiner JV, Jones RB, Bloom SR, Bailey CJ. Acute stimulation of glucose uptake by leptin in l6 muscle cells. Hormone and metabolic research = Hormon- und Stoffwechselforschung = Hormones et metabolisme. 2002;34(3):111-5.

344. Fang X, Fetros J, Dadson KE, Xu A, Sweeney G. Leptin prevents the metabolic effects of adiponectin in L6 myotubes. Diabetologia. 2009;52(10):2190-200.

345. Jiang Y, Lu L, Hu Y, Li Q, An C, Yu X, et al. Resistin Induces Hypertension and Insulin Resistance in Mice via a TLR4-Dependent Pathway. Sci Rep. 2016;6:22193.

346. Muse ED, Obici S, Bhanot S, Monia BP, McKay RA, Rajala MW, et al. Role of resistin in diet-induced hepatic insulin resistance. Journal of Clinical Investigation. 2004;114(2):232-9.

347. Haider DG, Schindler K, Schaller G, Prager G, Wolzt M, Ludvik B. Increased Plasma Visfatin Concentrations in Morbidly Obese Subjects Are Reduced after Gastric Banding. The Journal of Clinical Endocrinology & Metabolism. 2006;91(4):1578-81.

348. Berndt J, Klöting N, Kralisch S, Kovacs P, Fasshauer M, Schön MR, et al. Plasma Visfatin Concentrations and Fat Depot–Specific mRNA Expression in Humans. Diabetes. 2005;54(10):2911-6.

349. Retnakaran R, Youn BS, Liu Y, Hanley AJ, Lee NS, Park JW, et al. Correlation of circulating full-length visfatin (PBEF/NAMPT) with metabolic parameters in subjects with and without diabetes: a cross-sectional study. Clinical endocrinology. 2008;69(6):885-93.

350. Harasim E, Chabowski A, Gorski J. Lack of downstream insulin-mimetic effects of visfatin/eNAMPT on glucose and fatty acid metabolism in skeletal muscles. Acta physiologica (Oxford, England). 2011;202(1):21-8.

351. Chakaroun R, Raschpichler M, Kloting N, Oberbach A, Flehmig G, Kern M, et al. Effects of weight loss and exercise on chemerin serum concentrations and adipose tissue expression in human obesity. Metabolism. 2012;61(5):706-14.

352. Deng W, Li C, Zhang Y, Zhao J, Yang M, Tian M, et al. Serum C1q/TNF-related protein-3 (CTRP3) levels are decreased in obesity and hypertension and are negatively correlated with parameters of insulin resistance. Diabetology & Metabolic Syndrome. 2015;7(1):33.

353. Wagner RM, Sivagnanam K, Clark WA, Peterson JM. Divergent relationship of circulating CTRP3 levels between obesity and gender: a cross-sectional study. PeerJ. 2016;4:e2573.

354. Peterson JM, Wei Z, Wong GW. C1q/TNF-related protein-3 (CTRP3), a novel adipokine that regulates hepatic glucose output. J Biol Chem. 2010;285(51):39691-701.

355. Peterson JM, Seldin MM, Wei Z, Aja S, Wong GW. CTRP3 attenuates diet-induced hepatic steatosis by regulating triglyceride metabolism. American Journal of Physiology - Gastrointestinal and Liver Physiology. 2013;305(3):G214-G24.

356. Li X, Jiang L, Yang M, Wu YW, Sun JZ, Sun SX. CTRP3 improves the insulin sensitivity of 3T3-L1 adipocytes by inhibiting inflammation and ameliorating insulin signalling transduction. Endokrynol Pol. 2014;65(4):252-8.

357. Graham TE, Yang Q, Blüher M, Hammarstedt A, Ciaraldi TP, Henry RR, et al. Retinol-Binding Protein 4 and Insulin Resistance in Lean, Obese, and Diabetic Subjects. New England Journal of Medicine. 2006;354(24):2552-63.

358. Yang Q, Graham TE, Mody N, Preitner F, Peroni OD, Zabolotny JM, et al. Serum retinol binding protein 4 contributes to insulin resistance in obesity and type 2 diabetes. Nature. 2005;436(7049):356-62.

359. Zemany L, Bhanot S, Peroni OD, Murray SF, Moraes-Vieira PM, Castoldi A, et al. Transthyretin Antisense Oligonucleotides Lower Circulating RBP4 Levels and Improve Insulin Sensitivity in Obese Mice. Diabetes. 2015;64(5):1603-14.

360. Fan N, Sun H, Wang Y, Wang Y, Zhang L, Xia Z, et al. Follistatin-like 1: a potential mediator of inflammation in obesity. Mediators Inflamm. 2013;2013:752519.

361. CĂToi AF, Suciu Ş, PÂRvu AE, CopĂEscu C, Galea RF, Buzoianu AD, et al. Increased chemerin and decreased omentin-1 levels in morbidly obese patients are correlated with insulin resistance, oxidative stress and chronic inflammation. Clujul Medical. 2014;87(1):19-26.

362. Jialal I, Devaraj S, Kaur H, Adams-Huet B, Bremer AA. Increased Chemerin and Decreased Omentin-1 in Both Adipose Tissue and Plasma in Nascent Metabolic Syndrome. The Journal of Clinical Endocrinology & Metabolism. 2013;98(3):E514-E7.

363. Berman LJ, Weigensberg MJ, Spruijt-Metz D. Physical activity is related to insulin sensitivity in children and adolescents, independent of adiposity: a review of the literature. Diabetes Metab Res Rev. 2012;28(5):395-408.

364. Wei M, Gibbons LW, Mitchell TL, Kampert JB, Lee CD, Blair SN. The association between cardiorespiratory fitness and impaired fasting glucose and type 2 diabetes mellitus in men. Ann Intern Med. 1999;130(2):89-96.

365. Conn VS, Koopman RJ, Ruppar TM, Phillips LJ, Mehr DR, Hafdahl AR. Insulin Sensitivity Following Exercise Interventions: Systematic Review and Meta-Analysis of Outcomes Among Healthy Adults. J Prim Care Community Health. 2014;5(3):211-22.

366. Bird SR, Hawley JA. Update on the effects of physical activity on insulin sensitivity in humans. BMJ Open Sport Exerc Med. 2016;2(1):e000143.

367. Roberts CK, Little JP, Thyfault JP. Modification of insulin sensitivity and glycemic control by activity and exercise. Med Sci Sports Exerc. 2013;45(10):1868-77.

368. Motahari-Tabari N, Ahmad Shirvani M, Shirzad EAM, Yousefi-Abdolmaleki E, Teimourzadeh M. The effect of 8 weeks aerobic exercise on insulin resistance in type 2 diabetes: a randomized clinical trial. Glob J Health Sci. 2014;7(1):115-21.

369. Many G, Hurtado ME, Tanner C, Houmard J, Gordish-Dressman H, Park JJ, et al. Moderate-intensity aerobic training program improves insulin sensitivity and inflammatory markers in a pilot study of morbidly obese minority teens. Pediatr Exerc Sci. 2013;25(1):12-26.

370. Reichkendler MH, Rosenkilde M, Auerbach PL, Agerschou J, Nielsen MB, Kjaer A, et al. Only minor additional metabolic health benefits of high as opposed to moderate dose physical exercise in young, moderately overweight men. Obesity (Silver Spring). 2014;22(5):1220-32.

371. Sogaard D, Lund MT, Scheuer CM, Dehlbaek MS, Dideriksen SG, Abildskov CV, et al. High-intensity interval training improves insulin sensitivity in older individuals. Acta Physiol (Oxf). 2018;222(4):e13009.

372. Gallo-Villegas J, Aristizabal JC, Estrada M, Valbuena LH, Narvaez-Sanchez R, Osorio J, et al. Efficacy of high-intensity, low-volume interval training compared to continuous aerobic training on insulin resistance, skeletal muscle structure and function in adults with metabolic syndrome: study protocol for a randomized controlled clinical trial (Intraining-MET). Trials. 2018;19(1):144.

373. Gillen JB, Martin BJ, MacInnis MJ, Skelly LE, Tarnopolsky MA, Gibala MJ. Twelve Weeks of Sprint Interval Training Improves Indices of Cardiometabolic Health Similar to Traditional Endurance Training despite a Five-Fold Lower Exercise Volume and Time Commitment. PLoS One. 2016;11(4):e0154075.

374. Whyte LJ, Ferguson C, Wilson J, Scott RA, Gill JM. Effects of single bout of very high-intensity exercise on metabolic health biomarkers in overweight/obese sedentary men. Metabolism. 2013;62(2):212-9.

375. Pesta DH, Goncalves RLS, Madiraju AK, Strasser B, Sparks LM. Resistance training to improve type 2 diabetes: working toward a prescription for the future. Nutr Metab (Lond). 2017;14:24.

376. Strasser B, Pesta D. Resistance training for diabetes prevention and therapy: experimental findings and molecular mechanisms. Biomed Res Int. 2013;2013:805217.

377. Inoue DS, De Mello MT, Foschini D, Lira FS, De Piano Ganen A, Da Silveira Campos RM, et al. Linear and undulating periodized strength plus aerobic training promote similar benefits and lead to improvement of insulin resistance on obese adolescents. J Diabetes Complications. 2015;29(2):258-64.

378. AminiLari Z, Fararouei M, Amanat S, Sinaei E, Dianatinasab S, AminiLari M, et al. The Effect of 12 Weeks Aerobic, Resistance, and Combined Exercises on Omentin-1 Levels and Insulin Resistance among Type 2 Diabetic Middle-Aged Women. Diabetes Metab J. 2017;41(3):205-12.

379. Van Proeyen K, Szlufcik K, Nielens H, Pelgrim K, Deldicque L, Hesselink M, et al. Training in the fasted state improves glucose tolerance during fat-rich diet. J Physiol. 2010;588(Pt 21):4289-302.

380. Taylor HL, Wu CL, Chen YC, Wang PG, Gonzalez JT, Betts JA. Post-Exercise Carbohydrate-Energy Replacement Attenuates Insulin Sensitivity and Glucose Tolerance the Following Morning in Healthy Adults. Nutrients. 2018;10(2).

381. Stuart CA, South MA, Lee ML, McCurry MP, Howell ME, Ramsey MW, et al. Insulin responsiveness in metabolic syndrome after eight weeks of cycle training. Med Sci Sports Exerc. 2013;45(11):2021-9.

382. Stuart CA, Howell ME, Baker JD, Dykes RJ, Duffourc MM, Ramsey MW, et al. Cycle training increased GLUT4 and activation of mammalian target of rapamycin in fast twitch muscle fibers. Med Sci Sports Exerc. 2010;42(1):96-106.

383. Holten MK, Zacho M, Gaster M, Juel C, Wojtaszewski JF, Dela F. Strength training increases insulin-mediated glucose uptake, GLUT4 content, and insulin signaling in skeletal muscle in patients with type 2 diabetes. Diabetes. 2004;53(2):294-305.

384. Prior SJ, Blumenthal JB, Katzel LI, Goldberg AP, Ryan AS. Increased skeletal muscle capillarization after aerobic exercise training and weight loss improves insulin sensitivity in adults with IGT. Diabetes Care. 2014;37(5):1469-75.

385. Rattigan S, Wallis MG, Youd JM, Clark MG. Exercise training improves insulin-mediated capillary recruitment in association with glucose uptake in rat hindlimb. Diabetes. 2001;50(12):2659-65.

386. Prior SJ, Goldberg AP, Ortmeyer HK, Chin ER, Chen D, Blumenthal JB, et al. Increased Skeletal Muscle Capillarization Independently Enhances Insulin Sensitivity in Older Adults After Exercise Training and Detraining. Diabetes. 2015;64(10):3386-95.

387. Malin SK, Solomon TP, Blaszczak A, Finnegan S, Filion J, Kirwan JP. Pancreatic beta-cell function increases in a linear dose-response manner following exercise training in adults with prediabetes. Am J Physiol Endocrinol Metab. 2013;305(10):E1248-54.

388. Madsen SM, Thorup AC, Overgaard K, Jeppesen PB. High Intensity Interval Training Improves Glycaemic Control and Pancreatic beta Cell Function of Type 2 Diabetes Patients. PLoS One. 2015;10(8):e0133286.

389. O'Leary MF, Wallace GR, Bennett AJ, Tsintzas K, Jones SW. IL-15 promotes human myogenesis and mitigates the detrimental effects of TNFalpha on myotube development. Sci Rep. 2017;7(1):12997.

390. Crossland H, Smith K, Atherton PJ, Wilkinson DJ. A novel puromycin decorporation method to quantify skeletal muscle protein breakdown: A proof-of-concept study. Biochem Biophys Res Commun. 2017;494(3-4):608-14.

391. Batsis JA, Villareal DT. Sarcopenic obesity in older adults: aetiology, epidemiology and treatment strategies. Nat Rev Endocrinol. 2018;14(9):513-37.

392. Yaffe D, Saxel O. Serial passaging and differentiation of myogenic cells isolated from dystrophic mouse muscle. Nature. 1977;270(5639):725-7.

393. Yaffe D. Retention of differentiation potentialities during prolonged cultivation of myogenic cells. Proc Natl Acad Sci U S A. 1968;61(2):477-83.

394. Nikoulina SE, Ciaraldi TP, Carter L, Mudaliar S, Park KS, Henry RR. Impaired muscle glycogen synthase in type 2 diabetes is associated with diminished phosphatidylinositol 3-kinase activation. J Clin Endocrinol Metab. 2001;86(9):4307-14.

395. Bouzakri K, Roques M, Gual P, Espinosa S, Guebre-Egziabher F, Riou JP, et al. Reduced activation of phosphatidylinositol-3 kinase and increased serine 636 phosphorylation of insulin receptor substrate-1 in primary culture of skeletal muscle cells from patients with type 2 diabetes. Diabetes. 2003;52(6):1319-25.

396. Cozzone D, Frojdo S, Disse E, Debard C, Laville M, Pirola L, et al. Isoform-specific defects of insulin stimulation of Akt/protein kinase B (PKB) in skeletal muscle cells from type 2 diabetic patients. Diabetologia. 2008;51(3):512-21.

397. McIntyre EA, Halse R, Yeaman SJ, Walker M. Cultured muscle cells from insulin-resistant type 2 diabetes patients have impaired insulin, but normal 5-amino-4-imidazolecarboxamide riboside-stimulated, glucose uptake. J Clin Endocrinol Metab. 2004;89(7):3440-8.

398. Gaster M. Metabolic flexibility is conserved in diabetic myotubes. J Lipid Res. 2007;48(1):207-17.

399. Andrikopoulos S, Proietto J. The biochemical basis of increased hepatic glucose production in a mouse model of type 2 (non-insulin-dependent) diabetes mellitus. Diabetologia. 1995;38(12):1389-96.

400. Song S, Andrikopoulos S, Filippis C, Thorburn AW, Khan D, Proietto J. Mechanism of fat-induced hepatic gluconeogenesis: effect of metformin. Am J Physiol Endocrinol Metab. 2001;281(2):E275-82.

401. Magnusson I, Rothman DL, Katz LD, Shulman RG, Shulman GI. Increased rate of gluconeogenesis in type II diabetes mellitus. A 13C nuclear magnetic resonance study. J Clin Invest. 1992;90(4):1323-7.

402. Puhakainen I, Koivisto VA, Yki-Jarvinen H. Lipolysis and gluconeogenesis from glycerol are increased in patients with noninsulin-dependent diabetes mellitus. J Clin Endocrinol Metab. 1992;75(3):789-94.

403. Nurjhan N, Consoli A, Gerich J. Increased lipolysis and its consequences on gluconeogenesis in non-insulin-dependent diabetes mellitus. J Clin Invest. 1992;89(1):169-75.

404. Zhang Y, Xie Z, Zhou G, Zhang H, Lu J, Zhang WJ. Fructose-1,6-bisphosphatase regulates glucose-stimulated insulin secretion of mouse pancreatic beta-cells. Endocrinology. 2010;151(10):4688-95.

405. van Poelje PD, Potter SC, Chandramouli VC, Landau BR, Dang Q, Erion MD. Inhibition of fructose 1,6-bisphosphatase reduces excessive endogenous glucose production and attenuates hyperglycemia in Zucker diabetic fatty rats. Diabetes. 2006;55(6):1747-54.

406. Kaur R, Dahiya L, Kumar M. Fructose-1,6-bisphosphatase inhibitors: A new valid approach for management of type 2 diabetes mellitus. Eur J Med Chem. 2017;141:473-505.

407. Hunter RW, Hughey CC, Lantier L, Sundelin EI, Peggie M, Zeqiraj E, et al. Metformin reduces liver glucose production by inhibition of fructose-1-6-bisphosphatase. Nat Med. 2018;24(9):1395-406.

408. Peiris AN, Struve MF, Mueller RA, Lee MB, Kissebah AH. Glucose metabolism in obesity: influence of body fat distribution. J Clin Endocrinol Metab. 1988;67(4):760-7.

409. Dash S, Sano H, Rochford JJ, Semple RK, Yeo G, Hyden CS, et al. A truncation mutation in TBC1D4 in a family with acanthosis nigricans and postprandial hyperinsulinemia. Proc Natl Acad Sci U S A. 2009;106(23):9350-5.

410. Huang X, Vaag A, Hansson M, Groop L. Down-regulation of insulin receptor substrates (IRS)-1 and IRS-2 and Src homologous and collagen-like protein Shc gene expression by insulin in skeletal muscle is not associated with insulin resistance or type 2 diabetes. J Clin Endocrinol Metab. 2002;87(1):255-9.

411. Draznin B. Molecular mechanisms of insulin resistance: serine phosphorylation of insulin receptor substrate-1 and increased expression of p85alpha: the two sides of a coin. Diabetes. 2006;55(8):2392-7.

412. Gaster M. Insulin resistance and the mitochondrial link. Lessons from cultured human myotubes. Biochim Biophys Acta. 2007;1772(7):755-65.

413. Nicholson T, Church C, Baker DJ, Jones SW. The role of adipokines in skeletal muscle inflammation and insulin sensitivity. J Inflamm (Lond). 2018;15:9.

414. Ciaraldi TP, Ryan AJ, Mudaliar SR, Henry RR. Altered Myokine Secretion Is an Intrinsic Property of Skeletal Muscle in Type 2 Diabetes. PLoS One. 2016;11(7):e0158209.

415. Jiang LQ, Duque-Guimaraes DE, Machado UF, Zierath JR, Krook A. Altered response of skeletal muscle to IL-6 in type 2 diabetic patients. Diabetes. 2013;62(2):355-61.

416. Pedersen BK, Febbraio MA. Muscle as an endocrine organ: focus on muscle-derived interleukin-6. Physiol Rev. 2008;88(4):1379-406.

417. Steensberg A, Keller C, Starkie RL, Osada T, Febbraio MA, Pedersen BK. IL-6 and TNF-alpha expression in, and release from, contracting human skeletal muscle. Am J Physiol Endocrinol Metab. 2002;283(6):E1272-8.

418. Steensberg A, van Hall G, Osada T, Sacchetti M, Saltin B, Klarlund Pedersen B. Production of interleukin-6 in contracting human skeletal muscles can account for the exercise-induced increase in plasma interleukin-6. J Physiol. 2000;529 Pt 1:237-42.

419. Carey AL, Steinberg GR, Macaulay SL, Thomas WG, Holmes AG, Ramm G, et al. Interleukin-6 increases insulin-stimulated glucose disposal in humans and glucose uptake and fatty acid oxidation in vitro via AMP-activated protein kinase. Diabetes. 2006;55(10):2688-97.

420. Nieto-Vazquez I, Fernandez-Veledo S, de Alvaro C, Lorenzo M. Dual role of interleukin-6 in regulating insulin sensitivity in murine skeletal muscle. Diabetes. 2008;57(12):3211-21.

421. Shoda H, Nagafuchi Y, Tsuchida Y, Sakurai K, Sumitomo S, Fujio K, et al. Increased serum concentrations of IL-1 beta, IL-21 and Th17 cells in overweight patients with rheumatoid arthritis. Arthritis Res Ther. 2017;19(1):111.

422. Varma V, Yao-Borengasser A, Rasouli N, Nolen GT, Phanavanh B, Starks T, et al. Muscle inflammatory response and insulin resistance: synergistic interaction between macrophages and fatty acids leads to impaired insulin action. Am J Physiol Endocrinol Metab. 2009;296(6):E1300-10.

423. Khan IM, Perrard XY, Brunner G, Lui H, Sparks LM, Smith SR, et al. Intermuscular and perimuscular fat expansion in obesity correlates with skeletal muscle T cell and macrophage infiltration and insulin resistance. Int J Obes (Lond). 2015;39(11):1607-18.

424. Fink LN, Costford SR, Lee YS, Jensen TE, Bilan PJ, Oberbach A, et al. Pro-inflammatory macrophages increase in skeletal muscle of high fat-fed mice and correlate with metabolic risk markers in humans. Obesity (Silver Spring). 2014;22(3):747-57.

425. Nisr RB, Shah DS, Ganley IG, Hundal HS. Proinflammatory NFkB signalling promotes mitochondrial dysfunction in skeletal muscle in response to cellular fuel overloading. Cell Mol Life Sci. 2019.

426. Shibouta Y, Suzuki N, Shino A, Matsumoto H, Terashita Z, Kondo K, et al. Pathophysiological role of endothelin in acute renal failure. Life Sci. 1990;46(22):1611-8.

427. Hungness ES, Luo GJ, Pritts TA, Sun X, Robb BW, Hershko D, et al. Transcription factors C/EBP-beta and -delta regulate IL-6 production in IL-1beta-stimulated human enterocytes. J Cell Physiol. 2002;192(1):64-70.

428. Mesinovic J, Zengin A, De Courten B, Ebeling PR, Scott D. Sarcopenia and type 2 diabetes mellitus: a bidirectional relationship. Diabetes Metab Syndr Obes. 2019;12:1057-72.

429. Allen DL, Cleary AS, Speaker KJ, Lindsay SF, Uyenishi J, Reed JM, et al. Myostatin, activin receptor IIb, and follistatin-like-3 gene expression are altered in adipose tissue and skeletal muscle of obese mice. Am J Physiol Endocrinol Metab. 2008;294(5):E918-27.

430. Hittel DS, Berggren JR, Shearer J, Boyle K, Houmard JA. Increased secretion and expression of myostatin in skeletal muscle from extremely obese women. Diabetes. 2009;58(1):30-8.

431. Milan G, Dalla Nora E, Pilon C, Pagano C, Granzotto M, Manco M, et al. Changes in muscle myostatin expression in obese subjects after weight loss. J Clin Endocrinol Metab. 2004;89(6):2724-7.

432. Roth SM, Martel GF, Ferrell RE, Metter EJ, Hurley BF, Rogers MA. Myostatin gene expression is reduced in humans with heavy-resistance strength training: a brief communication. Exp Biol Med (Maywood). 2003;228(6):706-9.

433. Hittel DS, Axelson M, Sarna N, Shearer J, Huffman KM, Kraus WE. Myostatin decreases with aerobic exercise and associates with insulin resistance. Med Sci Sports Exerc. 2010;42(11):2023-9.

434. Lin J, Arnold HB, Della-Fera MA, Azain MJ, Hartzell DL, Baile CA. Myostatin knockout in mice increases myogenesis and decreases adipogenesis. Biochem Biophys Res Commun. 2002;291(3):701-6.

435. Allen DL, Cleary AS, Hanson AM, Lindsay SF, Reed JM. CCAAT/enhancer binding protein-delta expression is increased in fast skeletal muscle by food deprivation and regulates myostatin transcription in vitro. Am J Physiol Regul Integr Comp Physiol. 2010;299(6):R1592-601.

436. Marchildon F, Lala N, Li G, St-Louis C, Lamothe D, Keller C, et al. CCAAT/enhancer binding protein beta is expressed in satellite cells and controls myogenesis. Stem Cells. 2012;30(12):2619-30.

437. Wilkes JJ, Lloyd DJ, Gekakis N. Loss-of-function mutation in myostatin reduces tumor necrosis factor alpha production and protects liver against obesity-induced insulin resistance. Diabetes. 2009;58(5):1133-43.

438. Dong J, Dong Y, Dong Y, Chen F, Mitch WE, Zhang L. Inhibition of myostatin in mice improves insulin sensitivity via irisin-mediated cross talk between muscle and adipose tissues. Int J Obes (Lond). 2016;40(3):434-42.

439. Tarum J, Folkesson M, Atherton PJ, Kadi F. Electrical pulse stimulation: an in vitro exercise model for the induction of human skeletal muscle cell hypertrophy. A proof-of-concept study. Exp Physiol. 2017;102(11):1405-13.

440. Feng YZ, Nikolic N, Bakke SS, Kase ET, Guderud K, Hjelmesaeth J, et al. Myotubes from lean and severely obese subjects with and without type 2 diabetes respond differently to an in vitro model of exercise. Am J Physiol Cell Physiol. 2015;308(7):C548-56.

441. Park S, Turner KD, Zheng D, Brault JJ, Zou K, Chaves AB, et al. Electrical pulse stimulation induces differential responses in insulin action in myotubes from severely obese individuals. J Physiol. 2019;597(2):449-66.

442. Sarabia V, Lam L, Burdett E, Leiter LA, Klip A. Glucose transport in human skeletal muscle cells in culture. Stimulation by insulin and metformin. J Clin Invest. 1992;90(4):1386-95.

443. Aas V, Torbla S, Andersen MH, Jensen J, Rustan AC. Electrical stimulation improves insulin responses in a human skeletal muscle cell model of hyperglycemia. Ann N Y Acad Sci. 2002;967:506-15.

444. James DE, Jenkins AB, Kraegen EW. Heterogeneity of insulin action in individual muscles in vivo: euglycemic clamp studies in rats. Am J Physiol. 1985;248(5 Pt 1):E567-74.

445. Huang C, Somwar R, Patel N, Niu W, Torok D, Klip A. Sustained exposure of L6 myotubes to high glucose and insulin decreases insulin-stimulated GLUT4 translocation but upregulates GLUT4 activity. Diabetes. 2002;51(7):2090-8.

446. Bettadapur A, Suh GC, Geisse NA, Wang ER, Hua C, Huber HA, et al. Prolonged Culture of Aligned Skeletal Myotubes on Micromolded Gelatin Hydrogels. Sci Rep. 2016;6:28855.

447. Evers-van Gogh IJ, Alex S, Stienstra R, Brenkman AB, Kersten S, Kalkhoven E. Electric Pulse Stimulation of Myotubes as an In Vitro Exercise Model: Cell-Mediated and Non-Cell-Mediated Effects. Sci Rep. 2015;5:10944.

448. O'Leary MF, Wallace GR, Davis ET, Murphy DP, Nicholson T, Bennett AJ, et al. Obese subcutaneous adipose tissue impairs human myogenesis, particularly in old skeletal muscle, via resistin-mediated activation of NFkappaB. Sci Rep. 2018;8(1):15360.

449. Fantuzzi G. Adipose tissue, adipokines, and inflammation. J Allergy Clin Immunol. 2005;115(5):911-9; quiz 20.

450. Hida K, Wada J, Eguchi J, Zhang H, Baba M, Seida A, et al. Visceral adipose tissue-derived serine protease inhibitor: a unique insulin-sensitizing adipocytokine in obesity. Proc Natl Acad Sci U S A. 2005;102(30):10610-5.

451. Heiker JT, Kloting N, Kovacs P, Kuettner EB, Strater N, Schultz S, et al. Vaspin inhibits kallikrein 7 by serpin mechanism. Cell Mol Life Sci. 2013;70(14):2569-83.

452. Shaker OG, Sadik NA. Vaspin gene in rat adipose tissue: relation to obesity-induced insulin resistance. Mol Cell Biochem. 2013;373(1-2):229-39.

453. Kloting N, Berndt J, Kralisch S, Kovacs P, Fasshauer M, Schon MR, et al. Vaspin gene expression in human adipose tissue: association with obesity and type 2 diabetes. Biochem Biophys Res Commun. 2006;339(1):430-6.

454. Edgar R, Domrachev M, Lash AE. Gene Expression Omnibus: NCBI gene expression and hybridization array data repository. Nucleic Acids Res. 2002;30(1):207-10.

455. Ibrahim DM, Mohamed NR, Fouad TA, Soliman AF. Short-Term Impact of Laparoscopic Sleeve Gastrectomy on Serum Cartonectin and Vaspin Levels in Obese Subjects. Obes Surg. 2018;28(10):3237-45.

456. Breitfeld J, Wiele N, Gutsmann B, Stumvoll M, Bluher M, Scholz M, et al. Circulating Adipokine VASPIN Is Associated with Serum Lipid Profiles in Humans. Lipids. 2019;54(4):203-10.

457. Esteghamati A, Noshad S, Mousavizadeh M, Zandieh A, Nakhjavani M. Association of vaspin with metabolic syndrome: the pivotal role of insulin resistance. Diabetes Metab J. 2014;38(2):143-9.

458. Seeger J, Ziegelmeier M, Bachmann A, Lossner U, Kratzsch J, Bluher M, et al. Serum levels of the adipokine vaspin in relation to metabolic and renal parameters. J Clin Endocrinol Metab. 2008;93(1):247-51.

459. Fuente-Martin E, Argente-Arizon P, Ros P, Argente J, Chowen JA. Sex differences in adipose tissue: It is not only a question of quantity and distribution. Adipocyte. 2013;2(3):128-34.

460. White UA, Tchoukalova YD. Sex dimorphism and depot differences in adipose tissue function. Biochim Biophys Acta. 2014;1842(3):377-92.

461. Kotani K, Tokunaga K, Fujioka S, Kobatake T, Keno Y, Yoshida S, et al. Sexual dimorphism of age-related changes in whole-body fat distribution in the obese. Int J Obes Relat Metab Disord. 1994;18(4):207-2.

462. Beigh SH, Jain S. Prevalence of metabolic syndrome and gender differences. Bioinformation. 2012;8(13):613-6.

463. Li C, Engstrom G, Hedblad B, Calling S, Berglund G, Janzon L. Sex differences in the relationships between BMI, WHR and incidence of cardiovascular disease: a population-based cohort study. Int J Obes (Lond). 2006;30(12):1775-81.

464. Holliday KL, McWilliams DF, Maciewicz RA, Muir KR, Zhang W, Doherty M. Lifetime body mass index, other anthropometric measures of obesity and risk of knee or hip osteoarthritis in the GOAL case-control study. Osteoarthritis Cartilage. 2011;19(1):37-43.

465. Aibara D, Matsuo K, Yamano S, Matsusue K. Insulin induces expression of the hepatic vaspin gene. Endocr J. 2019.

466. Aibara D, Matsuo K, Yamano S, Matsusue K. Vaspin is a novel target gene of hepatic CCAAT-enhancer-binding protein. Gene. 2019:144113.

467. Liu S, Li X, Wu Y, Duan R, Zhang J, Du F, et al. Effects of vaspin on pancreatic beta cell secretion via PI3K/Akt and NF-kappaB signaling pathways. PLoS One. 2017;12(12):e0189722.

468. Liu P, Li G, Wu J, Zhou X, Wang L, Han W, et al. Vaspin promotes 3T3-L1 preadipocyte differentiation. Exp Biol Med (Maywood). 2015;240(11):1520-7.

469. Sun N, Wang H, Wang L. Vaspin alleviates dysfunction of endothelial progenitor cells induced by high glucose via PI3K/Akt/eNOS pathway. Int J Clin Exp Pathol. 2015;8(1):482-9.

470. Liu S, Duan R, Wu Y, Du F, Zhang J, Li X, et al. Effects of Vaspin on Insulin Resistance in Rats and Underlying Mechanisms. Sci Rep. 2018;8(1):13542.

471. Nakatsuka A, Wada J, Iseda I, Teshigawara S, Higashio K, Murakami K, et al. Vaspin is an adipokine ameliorating ER stress in obesity as a ligand for cell-surface GRP78/MTJ-1 complex. Diabetes. 2012;61(11):2823-32.

472. Dugani CB, Klip A. Glucose transporter 4: cycling, compartments and controversies. EMBO Rep. 2005;6(12):1137-42.

473. Maria Z, Campolo AR, Lacombe VA. Diabetes Alters the Expression and Translocation of the Insulin-Sensitive Glucose Transporters 4 and 8 in the Atria. PLoS One. 2015;10(12):e0146033.

474. dos Santos JM, Benite-Ribeiro SA, Queiroz G, Duarte JA. The effect of age on glucose uptake and GLUT1 and GLUT4 expression in rat skeletal muscle. Cell Biochem Funct. 2012;30(3):191-7.

475. Kahn BB, Pedersen O. Suppression of GLUT4 expression in skeletal muscle of rats that are obese from high fat feeding but not from high carbohydrate feeding or genetic obesity. Endocrinology. 1993;132(1):13-22.

476. McGee SL, van Denderen BJ, Howlett KF, Mollica J, Schertzer JD, Kemp BE, et al. AMP-activated protein kinase regulates GLUT4 transcription by phosphorylating histone deacetylase 5. Diabetes. 2008;57(4):860-7.

477. Niu W, Huang C, Nawaz Z, Levy M, Somwar R, Li D, et al. Maturation of the regulation of GLUT4 activity by p38 MAPK during L6 cell myogenesis. J Biol Chem. 2003;278(20):17953-62.

478. Montessuit C, Rosenblatt-Velin N, Papageorgiou I, Campos L, Pellieux C, Palma T, et al. Regulation of glucose transporter expression in cardiac myocytes: p38 MAPK is a strong inducer of GLUT4. Cardiovasc Res. 2004;64(1):94-104.

479. Montell E, Turini M, Marotta M, Roberts M, Noe V, Ciudad CJ, et al. DAG accumulation from saturated fatty acids desensitizes insulin stimulation of glucose uptake in muscle cells. Am J Physiol Endocrinol Metab. 2001;280(2):E229-37.

480. Al-Khalili L, Chibalin AV, Kannisto K, Zhang BB, Permert J, Holman GD, et al. Insulin action in cultured human skeletal muscle cells during differentiation: assessment of cell surface GLUT4 and GLUT1 content. Cell Mol Life Sci. 2003;60(5):991-8.

481. Aas V, Kase ET, Solberg R, Jensen J, Rustan AC. Chronic hyperglycaemia promotes lipogenesis and triacylglycerol accumulation in human skeletal muscle cells. Diabetologia. 2004;47(8):1452-61.

482. Chowdhury HH, Jevsek M, Kreft M, Mars T, Zorec R, Grubic Z. Insulin-induced exocytosis in single, in vitro innervated human muscle fibres: a new approach. Pflugers Arch. 2005;450(2):131-5.

483. Jensen EB, Zheng D, Russell RA, Bassel-Duby R, Williams RS, Olson AL, et al. Regulation of GLUT4 expression in denervated skeletal muscle. Am J Physiol Regul Integr Comp Physiol. 2009;296(6):R1820-8.

484. Lee AS. The ER chaperone and signaling regulator GRP78/BiP as a monitor of endoplasmic reticulum stress. Methods. 2005;35(4):373-81.

485. Matsuo K, Gray MJ, Yang DY, Srivastava SA, Tripathi PB, Sonoda LA, et al. The endoplasmic reticulum stress marker, glucose-regulated protein-78 (GRP78) in visceral adipocytes predicts endometrial cancer progression and patient survival. Gynecol Oncol. 2013;128(3):552-9.

486. Li X. Endoplasmic reticulum stress regulates inflammation in adipocyte of obese rats via toll-like receptors 4 signaling. Iran J Basic Med Sci. 2018;21(5):502-7.

487. Khadir A, Kavalakatt S, Abubaker J, Cherian P, Madhu D, Al-Khairi I, et al. Physical exercise alleviates ER stress in obese humans through reduction in the expression and release of GRP78 chaperone. Metabolism. 2016;65(9):1409-20.

488. Yilmaz E. Endoplasmic Reticulum Stress and Obesity. Adv Exp Med Biol. 2017;960:261-76.

489. Kawasaki N, Asada R, Saito A, Kanemoto S, Imaizumi K. Obesity-induced endoplasmic reticulum stress causes chronic inflammation in adipose tissue. Sci Rep. 2012;2:799.

490. Zhang Y, Liu R, Ni M, Gill P, Lee AS. Cell surface relocalization of the endoplasmic reticulum chaperone and unfolded protein response regulator GRP78/BiP. J Biol Chem. 2010;285(20):15065-75.

491. Hessvik NP, Llorente A. Current knowledge on exosome biogenesis and release. Cell Mol Life Sci. 2018;75(2):193-208.

492. Kowal J, Tkach M, Thery C. Biogenesis and secretion of exosomes. Curr Opin Cell Biol. 2014;29:116-25.

493. Whitham M, Parker BL, Friedrichsen M, Hingst JR, Hjorth M, Hughes WE, et al. Extracellular Vesicles Provide a Means for Tissue Crosstalk during Exercise. Cell Metab. 2018;27(1):237-51 e4.

494. Malloci M, Perdomo L, Veerasamy M, Andriantsitohaina R, Simard G, Martinez MC. Extracellular Vesicles: Mechanisms in Human Health and Disease. Antioxid Redox Signal. 2019;30(6):813-56.

495. Gustafson D, Veitch S, Fish JE. Extracellular Vesicles as Protagonists of Diabetic Cardiovascular Pathology. Frontiers in Cardiovascular Medicine. 2017;4(71).

496. Fasshauer M, Bluher M. Adipokines in health and disease. Trends Pharmacol Sci. 2015;36(7):461-70.

497. Kranendonk ME, Visseren FL, van Balkom BW, Nolte-'t Hoen EN, van Herwaarden JA, de Jager W, et al. Human adipocyte extracellular vesicles in reciprocal signaling between adipocytes and macrophages. Obesity (Silver Spring). 2014;22(5):1296-308.

498. Thomou T, Mori MA, Dreyfuss JM, Konishi M, Sakaguchi M, Wolfrum C, et al. Adipose-derived circulating miRNAs regulate gene expression in other tissues. Nature. 2017;542(7642):450-5.

499. Liu T, Zhang L, Joo D, Sun SC. NF-kappaB signaling in inflammation. Signal Transduct Target Ther. 2017;2.

500. Eguchi A, Lazic M, Armando AM, Phillips SA, Katebian R, Maraka S, et al. Circulating adipocyte-derived extracellular vesicles are novel markers of metabolic stress. J Mol Med (Berl). 2016;94(11):1241-53.

501. Stepanian A, Bourguignat L, Hennou S, Coupaye M, Hajage D, Salomon L, et al. Microparticle increase in severe obesity: not related to metabolic syndrome and unchanged after massive weight loss. Obesity (Silver Spring). 2013;21(11):2236-43.

502. Agouni A, Lagrue-Lak-Hal AH, Ducluzeau PH, Mostefai HA, Draunet-Busson C, Leftheriotis G, et al. Endothelial dysfunction caused by circulating microparticles from patients with metabolic syndrome. Am J Pathol. 2008;173(4):1210-9.

503. Kobayashi Y, Eguchi A, Tempaku M, Honda T, Togashi K, Iwasa M, et al. Circulating extracellular vesicles are associated with lipid and insulin metabolism. Am J Physiol Endocrinol Metab. 2018;315(4):E574-E82.

504. Filipe V, Hawe A, Jiskoot W. Critical evaluation of Nanoparticle Tracking Analysis (NTA) by NanoSight for the measurement of nanoparticles and protein aggregates. Pharm Res. 2010;27(5):796-810.

505. Bachurski D, Schuldner M, Nguyen PH, Malz A, Reiners KS, Grenzi PC, et al. Extracellular vesicle measurements with nanoparticle tracking analysis - An accuracy and repeatability comparison between NanoSight NS300 and ZetaView. J Extracell Vesicles. 2019;8(1):1596016.

506. Nolan JP, Duggan E. Analysis of Individual Extracellular Vesicles by Flow Cytometry. Methods in molecular biology (Clifton, NJ). 2018;1678:79-92.

507. Andreu Z, Yáñez-Mó M. Tetraspanins in extracellular vesicle formation and function. Frontiers in immunology. 2014;5:442-.

508. Nishimura S, Manabe I, Nagai R. Adipose tissue inflammation in obesity and metabolic syndrome. Discov Med. 2009;8(41):55-60.

509. Willms E, Cabanas C, Mager I, Wood MJA, Vader P. Extracellular Vesicle Heterogeneity: Subpopulations, Isolation Techniques, and Diverse Functions in Cancer Progression. Front Immunol. 2018;9:738.

510. Rana S, Yue S, Stadel D, Zoller M. Toward tailored exosomes: the exosomal tetraspanin web contributes to target cell selection. Int J Biochem Cell Biol. 2012;44(9):1574-84.

511. Chairoungdua A, Smith DL, Pochard P, Hull M, Caplan MJ. Exosome release of beta-catenin: a novel mechanism that antagonizes Wnt signaling. J Cell Biol. 2010;190(6):1079-91.

512. Brzozowski JS, Bond DR, Jankowski H, Goldie BJ, Burchell R, Naudin C, et al. Extracellular vesicles with altered tetraspanin CD9 and CD151 levels confer increased prostate cell motility and invasion. Sci Rep. 2018;8(1):8822.

513. Deng ZB, Poliakov A, Hardy RW, Clements R, Liu C, Liu Y, et al. Adipose tissue exosome-like vesicles mediate activation of macrophage-induced insulin resistance. Diabetes. 2009;58(11):2498-505.

514. Sato Y, Ohshima T. The expression of mRNA of proinflammatory cytokines during skin wound healing in mice: a preliminary study for forensic wound age estimation (II). Int J Legal Med. 2000;113(3):140-5.

515. Willoughby DS, McFarlin B, Bois C. Interleukin-6 expression after repeated bouts of eccentric exercise. Int J Sports Med. 2003;24(1):15-21.

516. Sell H, Eckardt K, Taube A, Tews D, Gurgui M, Van Echten-Deckert G, et al. Skeletal muscle insulin resistance induced by adipocyte-conditioned medium: underlying mechanisms and reversibility. Am J Physiol Endocrinol Metab. 2008;294(6):E1070-7.

517. Kranendonk ME, Visseren FL, van Herwaarden JA, Nolte-'t Hoen EN, de Jager W, Wauben MH, et al. Effect of extracellular vesicles of human adipose tissue on insulin signaling in liver and muscle cells. Obesity (Silver Spring). 2014;22(10):2216-23.

518. Anand S, Samuel M, Kumar S, Mathivanan S. Ticket to a bubble ride: Cargo sorting into exosomes and extracellular vesicles. Biochim Biophys Acta Proteins Proteom. 2019.

519. Mancuso P. The role of adipokines in chronic inflammation. Immunotargets Ther. 2016;5:47-56.

520. Jacobsen SC, Brons C, Bork-Jensen J, Ribel-Madsen R, Yang B, Lara E, et al. Effects of short-term high-fat overfeeding on genome-wide DNA methylation in the skeletal muscle of healthy young men. Diabetologia. 2012;55(12):3341-9.

521. Seaborne RA, Strauss J, Cocks M, Shepherd S, O'Brien TD, van Someren KA, et al. Human Skeletal Muscle Possesses an Epigenetic Memory of Hypertrophy. Sci Rep. 2018;8(1):1898.

522. Gensous N, Bacalini MG, Franceschi C, Meskers CGM, Maier AB, Garagnani P. Age-Related DNA Methylation Changes: Potential Impact on Skeletal Muscle Aging in Humans. Front Physiol. 2019;10:996.

523. Davegardh C, Broholm C, Perfilyev A, Henriksen T, Garcia-Calzon S, Peijs L, et al. Abnormal epigenetic changes during differentiation of human skeletal muscle stem cells from obese subjects. BMC medicine. 2017;15(1):39.

524. Davegardh C, Hall Wedin E, Broholm C, Henriksen TI, Pedersen M, Pedersen BK, et al. Sex influences DNA methylation and gene expression in human skeletal muscle myoblasts and myotubes. Stem Cell Res Ther. 2019;10(1):26.

525. Melo SA, Luecke LB, Kahlert C, Fernandez AF, Gammon ST, Kaye J, et al. Glypican-1 identifies cancer exosomes and detects early pancreatic cancer. Nature. 2015;523(7559):177-82.

526. Lane RE, Korbie D, Hill MM, Trau M. Extracellular vesicles as circulating cancer biomarkers: opportunities and challenges. Clin Transl Med. 2018;7(1):14.

527. Hallberg SJ, Gershuni VM, Hazbun TL, Athinarayanan SJ. Reversing Type 2 Diabetes: A Narrative Review of the Evidence. Nutrients. 2019;11(4).

528. Saslow LR, Daubenmier JJ, Moskowitz JT, Kim S, Murphy EJ, Phinney SD, et al. Twelve-month outcomes of a randomized trial of a moderate-carbohydrate versus very low-carbohydrate diet in overweight adults with type 2 diabetes mellitus or prediabetes. Nutr Diabetes. 2017;7(12):304.

529. Stern L, Iqbal N, Seshadri P, Chicano KL, Daily DA, McGrory J, et al. The effects of low-carbohydrate versus conventional weight loss diets in severely obese adults: one-year follow-up of a randomized trial. Ann Intern Med. 2004;140(10):778-85.

530. Bauman WA, Schwartz E, Rose HG, Eisenstein HN, Johnson DW. Early and long-term effects of acute caloric deprivation in obese diabetic patients. Am J Med. 1988;85(1):38-46.

531. Hughes TA, Gwynne JT, Switzer BR, Herbst C, White G. Effects of caloric restriction and weight loss on glycemic control, insulin release and resistance, and atherosclerotic risk in obese patients with type II diabetes mellitus. Am J Med. 1984;77(1):7-17.

532. Snel M, Jonker JT, Hammer S, Kerpershoek G, Lamb HJ, Meinders AE, et al. Long-term beneficial effect of a 16-week very low calorie diet on pericardial fat in obese type 2 diabetes mellitus patients. Obesity (Silver Spring). 2012;20(8):1572-6.

533. Daly ME, Paisey R, Paisey R, Millward BA, Eccles C, Williams K, et al. Short-term effects of severe dietary carbohydrate-restriction advice in Type 2 diabetes--a randomized controlled trial. Diabet Med. 2006;23(1):15-20.

534. Bhatt AA, Choudhari PK, Mahajan RR, Sayyad MG, Pratyush DD, Hasan I, et al. Effect of a Low-Calorie Diet on Restoration of Normoglycemia in Obese subjects with Type 2 Diabetes. Indian J Endocrinol Metab. 2017;21(5):776-80.

Appendix

Gene of interest	Manufacturer	Species	Primer/ probe sequence
Calpain 1	Applied Biosystems UK	Human	**Forward:** 5'- CATGGAGACTATTGGCTTCGC -3' **Reverse:** 5'- GAGACGCATTGGCCAGGA -3'
Calpain 2	Applied Biosystems UK	Human	**Forward:** 5'- GCACACCATCGGCTTTGG -3' **Reverse:** 5'- CCCGGAGGTTGATGAAGGT -3'
FBP1	Applied Biosystems UK	Human	**Forward:** 5'GGCCGCACGTGGAATG-3' **Reverse:** 5'- TTGAACGGCAAGAACTTGATGT-3'
FOXO3	Applied Biosystems UK	Human	**Forward:** 5'- CGGCTCACTCTGTCCCAGAT -3' **Reverse:** 5'- TGTCGCCCTTATCCTTGAAGTAG -3'
GAPDH	Primer Design	Human	Proprietary
GRP78	Applied Biosystems	Human	**Forward:** 5'GGCCGCACGTGGAATG-3' **Reverse:** 5'- TTGAACGGCAAGAACTTGATGT-3'
GSK3B	Applied Biosystems UK	Human	**Forward:** 5'GGCCGCACGTGGAATG-3' **Reverse:** 5'- TTGAACGGCAAGAACTTGATGT-3'
LDLR	Applied Biosystems UK	Human	**Forward:** 5'GGCCGCACGTGGAATG-3' **Reverse:** 5'- TTGAACGGCAAGAACTTGATGT-3'
MAFbx	Primer Design	Human	**Forward:** 5'AACTCAAATACAAAATAGGACGCTTT -3' **Reverse:** 5'- CCTTCGCTTCTCAAAACAAAC -3'
mTOR	Applied Biosystems UK	Human	**Forward**: 5'- AGGCCGCATTGTCTCTATCAA -3' **Reverse:** 5'- GCAGTAAATGCAGGTAGTCATCCA -3'
MuRF-1	Primer Design	Human	**Forward:** 5'- GACGCCCTGAGCCATT -3' **Reverse:** 5'- CCTCTTCCTGATCTTCTTCTTCAAT -3'
MyoD	Primer Design	Human	**Forward**: 5'- CGCCTGAGCAAAGTAAATGAG -3' **Reverse:** 5'- GCCCTCGATATAGCGGATG -3'
SLC2A4 (GLUT4)	Primerdesign	Human	**Forward:** 5'-ATGGCTGTGGCTGGTTTCT- **Reverse:** 5'-AGCAGGAGGACCGCAAATA-3'
TBC1D4	Applied Biosystems UK	Human	**Forward:** 5'GGCCGCACGTGGAATG-3' **Reverse:** 5'- TTGAACGGCAAGAACTTGATGT-3'
Vaspin	Applied Biosystems	Human	**Forward:** 5'-GGG AGC CTT GGC ATG ATG **Reverse:** 5'-AGC AAA GGC AAG GGC AGA T-3'
Vaspin	Thermo fisher	Mouse	**Probe:** Proprietary
GRP78	Thermofisher	Mouse	**Probe** Proprietary
Vaspin	Thermo fisher	Rat	**Probe:** Proprietary
GRP78	Thermofisher	Rat	**Probe** Proprietary

Appendix 1. Primer sequences used for qRT-PCR.

Housekeeping	Insulin & Receptors	PI3Kinase Signalling	PI3 Kinase Target Genes	Insulin Signalling Target Genes	Metabolism	Other
18S	Insulin receptor	AKT1	GLUT4	CEBPA	ACACA	ENPP1
GAPDH	IRS1	AKT2	UCP1	CEBPB	ACOX1	PTPN1
B Actin	IRS2	AKT3	G6PC	FOS	FASN	PREX1
	IRS4	MTOR	BCL2L1	JUN	FBP1	lin28a
	SORBS1	EIF2B1	PCK2		PPARdelta	
	PPP1CA	GSK3A	HK2		PPARgamma	
		GSK3B	SREBF1		EIF4EBP1	
		PDPK1			LDLR	
		PIK3CA				
		PRKCG				
		PRKCZ				
		FOXO1				
		AS160				
		Rac1				
		PGC1 alpha				
		Lactate dehydrogenase				

Appendix 2. Genes on microfluidics cards.

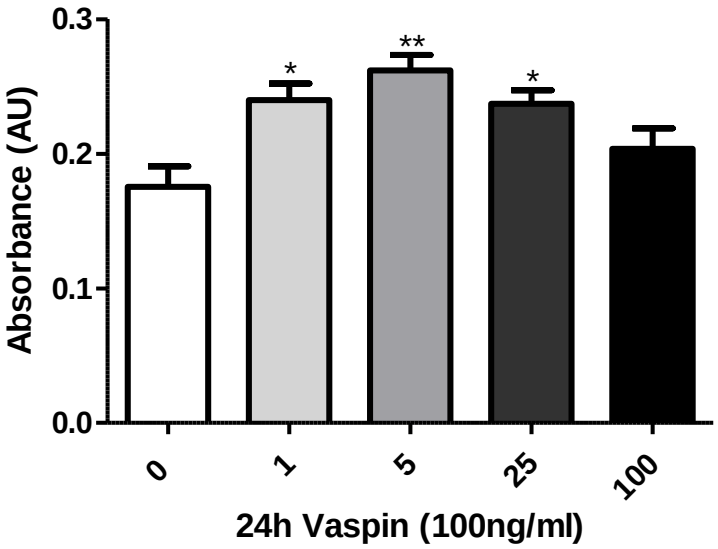

Appendix 3. Effect of Vaspin stimulation on primary human myoblast proliferation as determined by MTS assay. N=5 biological replicates from one patient. Data are presented as mean ± SEM. * ($p<0.05$) ** ($p<0.01$) denotes a significant increase in absorbance from control as determined by Dunnetts's post-hoc tests following 1 way ANOVA.